Towards Rapid Label-free Enrichment of Specific Stem Cell Populations for Autologous Cell Therapies

Alice Rae Philipson

Submitted in accordance with the requirements for the degree of
Tissue Engineering and Regenerative Medicine – Innovation in Medical and Biological Engineering

The University of Leeds
School of Mechanical Engineering

December 2019

The candidate confirms that the work submitted is her own and that appropriate credit has been given where reference has been made to the work of others.

Acknowledgements

I would like to express my deepest gratitude to Prof. Christoph Wälti, Prof. Jennifer Kirkham, Prof. Michael McPherson and Dr. Chris Wood for their incredible expertise and unyielding support in the completion of this work. Their time, patience and positivity over the past four years has been hugely appreciated and I cannot express how grateful I am.

I would like to thank Dr. Christian Tiede and the BioScreening and Technology group for the extensive training in phage display and protein production, Dr. Michal Szymonik and Dr. Rajan Sharma for their invaluable advice and experience, and Prof. Peter Giannoudis for his involvement in making this work possible.

I would like to extend my thanks to my wonderful colleagues in the Bioelectronics research group, in the Oral Biology department and in the Institute of Medical and Biological Engineering, with special thanks to Africa Smith De Diego without whom this four years would not have been the same.

Finally I would like to thank my unbelievably supportive family, partner and friends who encouraged me to take this opportunity and have been there for me every step of the way.

Abstract

Autologous mesenchymal stem cell (MSC) therapies have huge potential in addressing clinical challenges for otherwise intractable diseases. Label-free, intra-operative separation and enrichment of MSC subpopulations would provide a step change in delivery of such therapies. The long term goal of this research is to use binding proteins to provide a surface with switchable affinity, coupled with microfluidics to selectively bind and subsequently collect released cells. The specific aim of this thesis was to take the first steps towards achieving this goal, by identifying the most suitable binding proteins for cell capture and release in a prototype device and determining the feasibility of cell enrichment from complex clinical samples such as bone marrow aspirate.

A prototype device was developed exploiting the cell surface marker CD271 to select for MSCs. Affimer binding proteins and a commercially available antibody were investigated for specific cell capture and release. Specificity for CD271+ cells was demonstrated via flow cytometry using two different cell types. CD271 binding proteins were immobilised to a low-fouling substrate in a microfluidic channel and known mixtures of the two cell populations used to demonstrate specific cell capture. Increased flow rates allowed for bound cells to be released, collected and analysed, providing evidence that cells remained viable and minimally manipulated after enrichment. Clinical samples of bone marrow aspirate were then used in the same way and the results compared to gold standard methods of cell sorting.

Results showed that the percentage of CD271+ cells selected from bone marrow mononuclear cell populations using the prototype device was similar to results obtained using established cell sorting methodologies. This work demonstrated that affinity capture via antibody technology, together with a surface designed to provide a controlled release mechanism, offers a high-throughput, minimally manipulative approach to select and enrich MSC populations for therapeutic applications.

Table of Contents

List of Tables

List of Figures

List of Abbreviations

MSC	Mesenchymal stem cell
BMAC	Bone marrow aspirate concentrate
SCI	Spinal cord injury
ALS	Amyotrophic lateral sclerosis
GvHD	Graft versus host disease
MMP	Matrix metalloproteinases
SDF-1	Stromal-derived factor 1
CXCR4	C-X-C chemokine receptor 4
HGF	Hepatocyte growth factor
GFP	Green fluorescent protein
BM-MSC	Bone marrow-derived mesenchymal stem cell
AT-MSC	Adipose tissue-derived mesenchymal stem cell
UC-MSC	Umbilical cord-derived mesenchymal stem cell
DGC	Density gradient centrifugation
HSC	Hematopoietic stem cell
MACS	Magnetic-activated cell sorting
FACS	Fluorescence-activated cell sorting
BM-MNC	Bone marrow mononuclear cell
DEP	Dielectrophoresis
FFF	Field flow fractionation
RNA	Ribonucleic acid
DNA	Deoxyribonucleic acid
SELEX	Systematic evolution of ligands by exponential enrichment
ssDNA	Single-stranded deoxyribonucleic acid
RT-PCR	Reverse transcription polymerase chain reaction
PCR	Polymerase chain reaction
FDA	Food and Drug Administration
hESC	Human embryonic stem cell

ISCT	International Society for Cellular Therapy
Ig	Immunoglobulin
CFU-F	Colony-forming unit fibroblast
mRNA	Messenger ribonucleic acid
VCAM-1	Vascular cell adhesion molecule-1
VLA-4	Very late antigen-4
HSC70	Heat shock cognate 70
HME	Hematopoietic microenvironment
SSEA-4	Stage-specific embryonic antigen-4
SUSD2	Sushi domain containing 2
TNAP	Tissue non-specific alkaline phosphatase
BSTG	BioScreening and Technology Group
E. coli	*Escherichia coli*
FBS	Foetal bovine serum
DPSC	Dental pulp stromal cell
MEM	Minimal Essential Medium
P/S	Penicillin streptomycin solution
EDTA	Ethylenediaminetetraacetic acid
DMEM	Dulbecco’s Modified Eagle Medium
SPR	Surface plasmon resonance
SAM	Self-assembled monolayer
EDC	1-ethyl-3-(3-dimethylaminopropyl)carbodiimide).HCl
NHS	N-hydroxysuccinimide
ELISA	Enzyme-linked immunosorbent assay
HRP	Horseradish peroxidase
TMB	3,3',5,5'-tetramethylbenzidine
IPTG	Isopropyl-β-D-thiogalactoside
IMAC	Immobilised metal affinity chromatography
Ni-NTA	Nickel-nitrilotriacetic acid
SDS	Sodium dodecyl sulphate

SDS-PAGE	Sodium dodecyl sulphate polyacrylamide gel electrophoresis
IMEMS	Ion mobility enabled mass spectrometer
DMSO	Dimethylsulphoxide
PBS	Phosphate-buffered saline
PBST	Phosphate-buffered saline containing 0.1% Tween 20
ySUMO	Yeast small ubiquitin-like modifier
RT	Room temperature
LB	Lysogeny broth
Carb	Carbenicillin
PEG	Polyethylene glycol
NaCl	Sodium chloride
DTT	Dithiothreitol
TCEP	Tris(2-carboxyethyl)phosphine
PE	Phycoerythrin
SEM	Standard error of the mean
NDM1	New Delhi metallo-beta-lactamase 1
BCA	Bicinchoninic acid
FITC	Fluorescein isothiocyanate
PDMS	Polydimethylsiloxane
MES	2-(N-morpholino)ethanesulfonic acid
ALP	Alkaline phosphatase
BCIP	5-bromo-4-chloro-3-indolyl phosphate
NBT	Nitro blue tetrazolium
BSA	Bovine serum albumin
PTFE	Polytetrafluoroethylene
7-AAD	7-amino-actinomycin D
dsDNA	Double-stranded deoxyribonucleic acid
CTC	Circulating tumour cell
EpCAM	Epithelial cell adhesion molecule
PI	Propidium iodide

DNase I	Deoxyribonuclease I
CPC	Circulating plasma cell
AT-SVF	Adipose tissue stromal vascular fraction
SAW-DEP	Surface acoustic wave-dielectrophoresis

Chapter 1: Introduction

Over the last two decades there has been an overwhelming volume of research in respect of mesenchymal stem cells (MSCs) and their therapeutic potential. This has led to an increasing number of clinical trials involving MSC therapies addressing treatment of clinically intractable diseases such as cardiovascular disease, neurodegenerative diseases, spinal cord injury, musculoskeletal diseases, immune diseases and autoimmune diseases (1). Although the safety of MSC therapies is now widely accepted, their efficacy is still under much debate and the translation of MSC therapies to commercial products has been slow.

One of the reasons for the slow rate of translation, and inconsistent clinical results, is the challenge involved in harvesting a therapeutic population of cells that are present at very small percentages among other cell types in the body. MSCs are reported to be present in the range of 1 in 10,000 to 1 in 100,000 cells in bone marrow mononuclear cell populations (BM-MNCs)(2), and 1000s of MSCs are thought to be required for effective cell therapies (3-5). Currently MSCs are enriched by their adherence to plastic, and culture-expanded to gain a larger number of cells for therapeutic use. This results in the use of a heterogeneous population of cells with unknown properties (6), and could be the reason that the efficacy of MSC-based therapies has been variable and not yet been proven. Furthermore, there are risks of contamination and phenotypic changes during cell culture (7), as well as the processes being time-consuming and expensive.

Novel MSC enrichment technologies have the potential to change the way MSC therapies are delivered leading to more reliable and reproducible results to potentially demonstrate therapeutic efficacy. There is a clinical need to enrich a high purity population of cells with known properties, using a high-throughput technology and at low cost. Moreover, the cells must be minimally manipulated (biological characteristics not altered) during the enrichment process to ensure a high level of safety and reduce the regulatory requirements for translation. This thesis will describe the development of an MSC enrichment device which takes advantage of the beneficial properties of microfluidic technology and uses a high resolution affinity-capture based mechanism for cell enrichment. The device has been designed for intraoperative use with a patient's own cells (autologous cells) therefore reducing both the risk of bio-contamination and the risk of immune rejection. Thus, this device has the potential to overcome the limitations associated with current MSC enrichment technologies and provide a high purity population of clinically beneficial cells for immediate use in autologous cell therapies.

This thesis will begin by introducing MSCs and reviewing the most recent clinical trials using MSC therapy. The therapeutic mechanisms of MSCs will be discussed and the main barriers to translation highlighted in more detail. A review of cell enrichment technologies used traditionally will demonstrate the limitations of these technologies regarding MSC enrichment, and emerging novel technologies will help inform this research project further. Finally, MSC surface antigens will be evaluated with regards to their ability to select a clinically beneficial population of cells. This information is required for the affinity-based cell capture in this work.

Following a review of the literature, the overall project aim and specific objectives will be described in Chapter 3, as well as chapter outlines for the subsequent chapters.

Chapter 2: Literature review

2.1 Introduction to MSCs

MSCs were first reported by Friedenstein and colleagues in 1970 (8), who demonstrated the isolation of clonogenic, proliferating fibroblastic cells from bone marrow and their ability to differentiate into bones and osteocytes. Their work was expanded upon in the next two decades and in 1999, Pittenger *et al.* (2) described the isolation, expansion and characterisation of multipotent human MSCs establishing chondrogenic, adipogenic and osteogenic lineages. Since then MSCs have been shown to differentiate into many other cell types including cardiomyocytes (9), endothelial cells (10), pancreatic islet cells (11) and neuron-like cells (12) and this multipotency was thought of as the basis of their therapeutic potential. However as the field of MSC research progresses, it has been found that the differentiation potential of MSCs is likely to have minimal impact on tissue regeneration and the more prominent therapeutic mechanisms are related to the paracrine mechanisms and immunomodulatory properties of MSCs (1, 13-15)(Section 2.3).

The regenerative properties of MSCs have been demonstrated when applied to a wide range of clinically intractable diseases through *in vitro* and *in vivo* pre-clinical studies (1). This has led to an increasing number of clinical trials for MSC therapies over the last 15 years (Figure 2.1). Adult MSCs are an attractive cell source for therapies since they avoid the ethical and safety issues associated with embryonic and induced pluripotent stem cells. Moreover, they are relatively easy to harvest from many different tissues in the body through minimally invasive techniques. The therapeutic potential of MSCs is potentially wide-reaching, which is reflected in the broad range of disease areas where MSC therapies are being investigated. Section 2.2 reviews the latest results from clinical trials in some of the most widely investigated conditions.

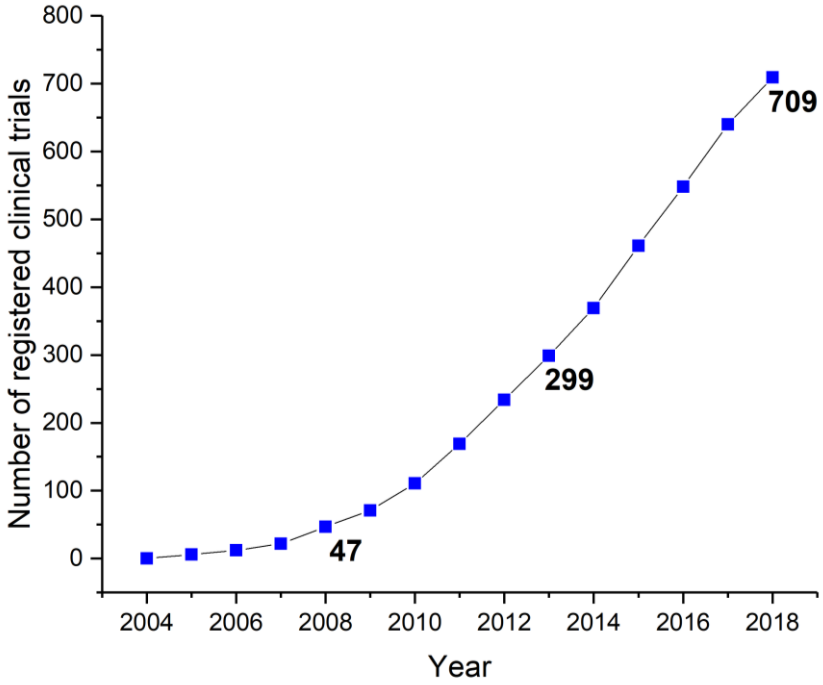

Figure 2.1 The increasing number of registered clinical trials using MSCs

A search of ClinicalTrials.gov from 01/01/2004 to 01/01/2019 using the search term of 'mesenchymal stem cells' was used to extract the above data which represents registered clinical trials globally.

2.2 The therapeutic potential of MSCs

A brief review of the current status of MSC therapies is included in this section, with a particular focus on the processing of MSCs prior to treatment, and the different treatment strategies that have been employed. Figure 2.2 shows a summary of some of the conditions where MSCs have the potential to provide therapeutic intervention.

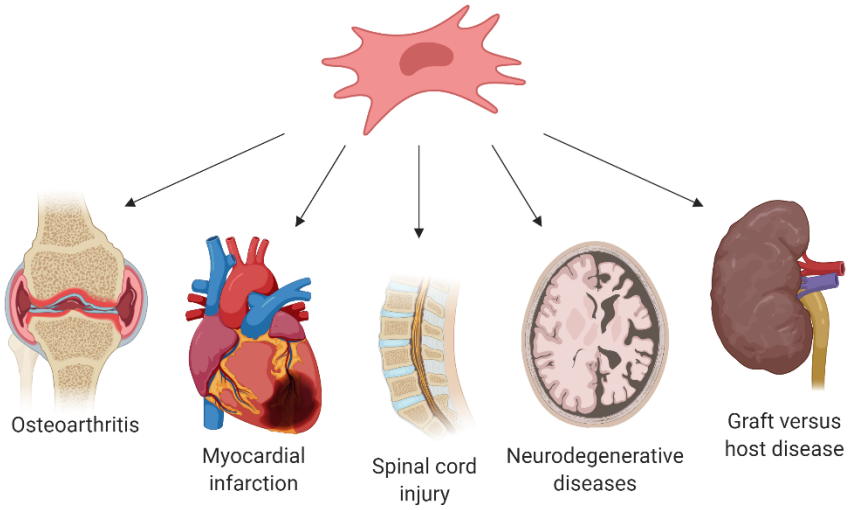

Figure 2.2 The potential therapeutic applications of MSCs

Examples of the different conditions where MSC therapies have been applied. This diagram was created with BioRender.com.

2.2.1 Musculoskeletal applications of MSC therapies

Approximately one in three people worldwide live with a chronic, painful musculoskeletal condition (16), accounting for the greatest proportion of persistent pain across all geographies and ages (17). Although musculoskeletal conditions affect people of all ages, the prevalence of conditions increases with age (16) and by 2050, the number of people aged 65 and over is expected to reach nearly 2.1 billion (18). There are huge concerns for the social and economic impact of an ageing population and therefore new treatments for age-related conditions is a global priority. Musculoskeletal diseases have therefore become one of the primary focuses for MSC therapy and Sections 2.2.1.1 and 2.2.1.2 discuss the progress of MSC therapies for bone and cartilage regeneration respectively – two of the leading areas of research.

2.2.1.1 MSC therapy for bone regeneration

MSCs have been widely investigated for the treatment of non-union bone fractures due to the important role of MSCs in the natural bone healing process (13). In the normal bone healing process, resident stromal, stem and progenitor cells work together with pro-inflammatory and anti-inflammatory immune cells as well as circulating blood cells to coordinate complex cell signalling which leads to the regeneration of new bone (19). However, where injuries result in large bone defects, the normal bone healing process may not be sufficient and therapeutic intervention is required.

Various MSC-based strategies have been explored for this purpose, including systemic injection of MSCs (20), direct injection to the injury site (21, 22) and injection with pre-fabricated or injectable scaffold materials (23-25). Horwitz *et al.* (1999)(26) reported positive outcomes for the treatment of osteogenesis imperfecta by intravenous injection of un-manipulated bone marrow in three children, including an increase in total body bone mineral content due to the increased growth velocity and lower frequency of bone fractures. Despite this, there are reservations regarding the intravenous injection of MSCs since it has been reported that many of the cells become trapped in the lungs (27). Alternatively, MSCs have been injected by arterial delivery and there are studies which show this is a more effective route of administration (28-30). Unfortunately, there are still safety concerns surrounding the dose and velocity of injections due to changes in cerebral blood flow which increase the risk of stroke development (31).

More favourably, local injection of MSCs overcomes some of the drawbacks discussed above. This method was first introduced over 20 years ago where Connolly *et al.* (1991)(32) used autologous bone marrow injection to stimulate healing in 18 out of 20 non-union tibial fracture patients. However little was known about the number or concentration of cells required for bone union. More recently this knowledge gap was addressed by Hernigou *et al.* (2005)(3), who related the number of MSCs in concentrated aspirate samples to the clinical healing of non-union tibial fractures. It was found that bone union was achieved in 53 out of 60 patients and where bone union had not occurred, the number of MSCs injected had been significantly lower than where treatment had been successful. They proposed that a graft requires more than 1000 MSCs per mL in order to be successful, with approximately 20 mL of bone marrow graft injected into each fracture site. This in turn suggests concentration of aspirate is essential since they found that there were on average only 600 MSCs per mL in bone marrow aspirate samples that were not concentrated.

Finally, tissue engineering approaches utilising a variety of natural and synthetic biomaterials have been investigated for their therapeutic potential. These methods have the advantage of controlling the delivery of MSCs and the potential to enhance bone regeneration via the co-delivery of osteoinductive growth factors (13). Park *et al.* (2011)(23) highlighted the benefits of using a calcium phosphate cement mixed with alginate to increase cell viability, proliferation and osteogenic differentiation of MSCs *in vitro*, whilst Kim *et al.* (2007)(25) used a scaffold made from acrylated hyaluronic acid to deliver MSCs and bone morphogenic protein-2 to rat calvarial defects *in vivo.* They found that there was the most mature bone formation in this treatment group compared to four control groups.

Although many pre-clinical studies have claimed to show the efficacy of MSC therapy for bone regeneration, published results from registered national and international clinical trials are lacking (13). A review carried out by Oryan *et al.* (2017)(13) stated that of 16 registered trials to treat long bone defects with MSCs, three treatment categories could be established; trials that used direct injection of MSCs without *in vitro* expansion (4 in total), trials that used direct injection of expanded MSCs (5 in total) and trials that used MSCs with bone substitutes (8 in total). However, of all of these trials only one trial in the last category had published results. Here, Liebergall *et al.* (2013)(33) used immunoselected MSCs (see Section 2.5.1.4) combined with platelet-rich plasma and demineralised bone matrix to treat 24 patients with tibial fractures. It was found that the treatment reduced the healing period by approximately 40 days compared to no intervention, however it was not possible to elucidate which factor/factors of the combined treatment contributed to the improved outcome.

There are more published results available for the treatment of oral and craniofacial bone repair using MSCs - the majority of which report positive outcomes (34-38). Three of these studies use MSCs concentrated by a 'bone marrow aspirate concentration' system (BMAC-Kit; Harvest Technologies Corporation)(36-38)(see Section 2.5.1.2), one used bone marrow aspirate with no concentration (35) and the final study used cells enriched for MSCs in a bioreactor (34). The only study to report no difference between MSC treatment and control treatments was carried out using cells expanded in normal tissue culture conditions (39).

At this point it is deemed too soon to advocate MSC therapy for bone regeneration due to the lack of published clinical trials and controversies in results (13). The major barriers to translation are reported to be the limited number of MSCs available for implantation (therefore often requiring *in vitro* expansion), the heterogeneity in the quality of MSCs from different donors and the lack of standardisation in procedures (40).

2.2.1.2 MSC therapy for cartilage regeneration

Unlike bone defects, cartilage defects have very limited ability to self-repair due to the avascular and aneural nature of cartilage tissue (41, 42). Cartilage loss can occur as a consequence of traumatic injury or through chronic degeneration which eventually leads to decreased mobility and can frequently progress to osteoarthritis – one of the most common musculoskeletal disorders and the 11th cause of disability in the world (43, 44). Current surgical interventions for cartilage damage include bone marrow stimulation, mosaicplasty and autologous

chondrocyte implantation, however there are inherent complications with such procedures, for example; donor site morbidity, high costs and the need for two operations (41, 45). Furthermore, for the treatment of osteoarthritis these interventions are restricted to the repair of focal defects and there are no treatments available for the global pathology of osteoarthritis (46). The innate ability of MSCs to differentiate into chondrocytes, as well as their immunomodulatory and inflammatory properties, provides an alternative therapeutic approach for the treatment of cartilage defects as well as related diseases such as osteoarthritis.

Similarly to bone regeneration strategies, both cell therapy (direct injection of MSCs) and tissue engineering approaches (cell-scaffold combinations) have been investigated for cartilage repair. A systematic review of all *in vitro*, pre-clinical and clinical studies of MSC therapy for cartilage repair was carried out by Goldberg and colleagues (2017)(42), who found that the majority of pre-clinical studies (85%) used tissue engineering approaches rather than direct injection. In clinical trials, MSCs were delivered in a suspension with various different co-stimulators either through arthroscopic implantation, open surgery or intra-articular injection. The review concluded that there was a lack of continuity between *in vitro*, pre-clinical and clinical studies and that the efficacy of MSC treatments was yet to be established.

In a review of MSC therapy for the treatment of osteoarthritis, Freitag *et al.* (2016)(46) highlighted the clinical results from two methods of therapy – MSC scaffold transplantation techniques and MSC injectable techniques. Using a scaffold transplantation technique, Wakitani *et al.* (1994)(47) demonstrated that culture-expanded adherent MSCs embedded in a collagen gel and transplanted into rabbit knee articular cartilage defects resulted in some hyaline-like cartilage formation, however there was no significant difference between the cell-transplanted group and the cell-free control group. Nejadnik *et al*. (2010)(48) compared autologous chondrocyte repair to the use of autologous MSCs (both cell types expanded in culture prior to transplantation) in 72 age-matched patients and found that BMSCs were as effective as chondrocytes for articular cartilage repair and had the advantages of one less knee surgery, reduced costs and minimised donor-site morbidity. Using an injectable technique, Emadedin *et al.* (2012)(49) used intra-articular injection of passage-2 MSCs to treat six patients with osteoarthritis of the knee. They found that six months post-injection, pain was reduced and walking distance was improved, however they proposed that repeat injections may have been more beneficial.

Whilst the methods of treatment vary, so does the cell dosage in each case. In an *in vitro* study, it was found that hyaluronic acid hydrogels with higher cell

seeding density (60 million cells/mL) produced constructs with improved biomechanical properties compared to lower cell seeding densities (20 million cells/mL)(50). In a pre-clinical study, MSCs embedded in a collagen gel were transplanted into cartilage defects in rabbit knees and it was found that a cell seeding density of 50 million cells/mL resulted in significantly more cartilage matrix production than a cell seeding density of 1 million cells/mL (51). However, there is a need for caution in using high cell seeding densities associated with higher metabolic demands and the limited capacity for oxygen, carbon dioxide and other nutrients to diffuse within a graft (52).

Whilst the safety of MSC treatment appears promising, the efficacy of treatments remains unclear due to the myriad of different strategies explored. What is clear, is the need for a single-stage procedure to avoid expensive, time-consuming and potentially harmful *in vitro* expansion of cells requiring a two stage procedure (42).

2.2.2 MSC therapy for cardiovascular diseases

Cardiovascular diseases are a leading cause of death in the world and are formally recognised by the United Nations as a major concern for global health (53). In 2015, there were an estimated 422.7 million cases of cardiovascular disease globally and 17.92 million deaths (53). As with musculoskeletal diseases, the risk of cardiovascular disease increases with age and therefore the implications of an ageing population must be addressed. Adult heart tissue has an inability to replace cells lost due to disease and MSC therapy has the potential to promote regeneration. Although cardiac cell-based therapies have shown limited cardiomyocyte differentiation capacity and poor long-term engraftment *in vivo* (14), there has been therapeutic benefit established via their paracrine mechanisms (see Section 2.3.3).

Evidence to support the safety and efficacy of MSC therapy for cardiac regeneration has been collected via a number of independent clinical studies (54-58). A randomised placebo-controlled trial showed that intra-myocardial injections of culture-expanded MSCs improved myocardial function in patients with ischaemic heart failure compared to phosphate buffered saline injections (54). Another clinical trial investigated the use of *in vitro* lineage-directed cardiopoietic stem cells derived from MSCs (and obtained from bone marrow aspirate) to treat advanced heart failure (55). It was found that intra-myocardial injection of cardiopoietic stem cells led to left ventricular reverse modelling – a marker of improved outcome in patients with advanced heart failure.

Interestingly, a phase I and phase II randomised, blinded and placebo-controlled trial with 65 patients with ischaemic cardiomyopathy compared both culture-expanded MSCs and MSCs derived from the concentration of whole bone

marrow, with placebo controls (58). It was found that trans-endocardial stem cell injection with MSCs derived from either method were safe and both resulted in some improved outcomes compared to placebo controls. However there were some measured outcomes that were only significantly improved for culture-expanded MSCs rather than MSCs concentrated from bone marrow aspirate suggesting MSCs isolated by density gradient centrifugation (see Section 2.5.1.2) were inferior to culture-expanded MSCs (see Section 2.5.1.1).

The majority of MSC therapies used in clinical studies for cardiac regeneration appear to utilise culture-expanded MSCs. Although these have provided a promising outlook, the expansion of cells *in vitro* requires expensive and time-consuming procedures which more sophisticated isolation methods could avoid.

2.2.3 MSC therapy for neurological diseases

Neurological disorders are a large cause of disability and death worldwide. A systematic analysis for the Global Burden of Disease Study 2015 showed that the burden of neurological diseases had increased substantially over the previous 25 years due to population ageing (59). It is predicted that the number of patients who will need neurological care will continue to grow in the coming decades. In addition, spinal cord injury (SCI) caused by traumatic events causes a substantial financial burden on health care systems due to the need for high-level acute care in the short term and associated secondary complications in the long term (60). Traffic accidents have been found to be the most common cause of SCI however falls in the elderly population are the second most common cause.

For neurodegenerative diseases such as Alzheimer's disease, Parkinson's disease, Huntingdon's disease, amyotrophic lateral sclerosis (ALS) and multiple system atrophy, cumulative data has suggested common cellular and molecular pathological mechanisms (61). MSC transplantation in models of these diseases has improved survival rates, reduced pathology and rescued cognitive function decline. The proposed mechanisms for improvement include neuroprotection by secretion of neurotrophic factors, induction of neurogenesis, modulation of inflammation and prevention of misfolded protein aggregation (61).

In terms of clinical trials, the majority reported to date have been early phase trials focussing on the demonstration of safety. For the treatment of multiple sclerosis and ALS, Karussis *et al.* (2010)(62) reported that intrathecal and intravenous injections of culture-expanded MSCs in 34 patients had no major adverse effects and elicited immunomodulatory effects. Similar trials for the treatment of ALS also confirmed the safety and possible benefits of MSC injections with pending phase II results (63-65). For the treatment of ischaemic stroke Lee *et al.* (2010)(66) carried out a long-term (5-year) assessment of 16 patients receiving intravenous

injection of culture-expanded MSCs compared to a control group. It was concluded that the MSC therapy was safe with no significant side effects whilst also showing some clinical improvement. In a randomised trial including 33 patients with multiple system atrophy, the intra-arterial and intravenous injection of culture-expanded MSCs (2 doses of 40 million cells) reported no serious adverse effects and led to decreased deterioration compared to a placebo group (67).

Similarly, the secretion of neuroprotective cytokines such as vascular endothelial growth factor, glial-cell-line-derived neurotrophic factor and brain-derived neurotrophic factor can increase neural regeneration, strengthen axon growth and revive damaged neurons in SCI (68). A systematic review carried out by Xu *et al.* (2019)(68) assessed the safety and efficacy of MSCs in treating SCI patients and found 11 studies that met the inclusion criteria. Meta-analysis of the 11 studies showed that some sensory functions were significantly improved by MSC transplantation, however, there was no significant difference found in motor functions. In contrast, locomotor improvements have been reported in animal models using MSC transplantation (69, 70). There were no serious or permanent adverse effects reported from the 11 studies.

MSC therapy for neurological diseases and SCI is in the early stages of clinical assessment but has so far been shown to be safe and has demonstrated some therapeutic effect. Similar to MSC therapies explored for cardiovascular disease, MSCs have been expanded *in vitro* in many of the clinical trials to date.

2.2.4 MSC therapy for other diseases

Although the main disease areas being targeted for potential treatment with MSCs have been discussed above, there are many other examples of where stem cell therapy has produced encouraging results in clinical studies. For example, in the treatment of graft versus host disease (GvHD), a prominent case study in 2004 showed donor MSCs expanded in culture and injected intravenously into a patient with acute GvHD (and unresponsive to all other therapy) had a rapid healing effect. This case study sparked the quick succession of numerous other studies including two large multicentre phase II trials also demonstrating remarkable efficacy (71, 72). MSC therapy has also been found to be safe and effective for digestive system disorders including liver disease (73), inflammatory bowel diseases (Crohn’s disease (74) and ulcerative colitis (75)) and coeliac disease (76). In particular, a related illness of Crohn’s disease - perianal fistulas - was successfully addressed by Dietz *et al.* (2017)(77), where 83% of patients had complete clinical healing six months after implantation of MSCs in a bioabsorbable matrix.

2.2.5 Summary of MSC therapeutic potential demonstrated in clinical trials to date

In conclusion, in the last two decades there has been a vast amount of *in vitro*, pre-clinical and clinical research into the safety and efficacy of MSC therapies. This brief review has focussed on the results of registered clinical trials in some of the most prevalent disease areas. The safety of MSCs has been confirmed with no serious or permanent adverse effects reported in any of the clinical trials reviewed. However, there appears to be controversial results regarding the efficacy of MSCs across the majority of conditions investigated. Although the outlook remains promising it is clear that there are limitations to current methodologies. These limitations and challenges are discussed in more detail in Section 2.4 - including the clinical need for the development of novel cell enrichment technologies. In addition, although the therapeutic mechanisms of MSCs are not completely understood, some key themes have been recognised which are outlined in Section 2.3. Isolation of MSC subpopulations with higher purities would help elucidate these specific mechanisms further and provides another motivation for the development of novel enrichment technologies.

2.3 Potential therapeutic mechanisms of MSCs

It is thought unlikely that there is a uniform MSC therapeutic mechanism for all disease states, however, there are common attributes that have been identified in many *in vitro* and *in vivo* studies that are likely to contribute to the beneficial effects of MSC therapies. The identified mechanisms are described below and summarised in Figure 2.3.

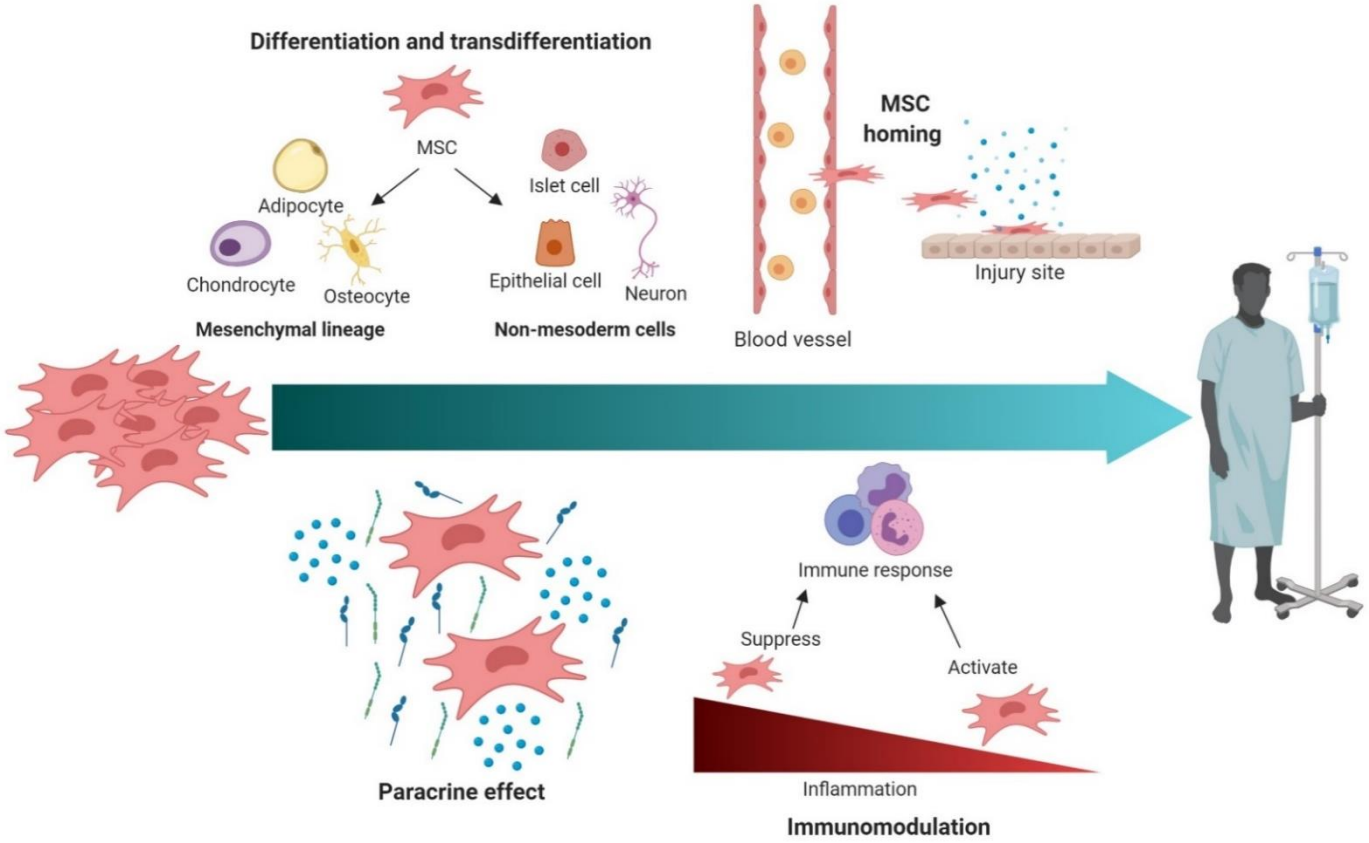

Figure 2.3 The proposed therapeutic mechanisms of MSCs

The differentiation potential, homing capabilities, paracrine effects and immunomodulatory behaviour of MSCs have been identified as therapeutic mechanisms in *in vitro* and *in vivo* studies. This diagram was created with BioRender.com and adapted from (78).

2.3.1 Homing efficiency of MSCs

When MSCs are injected systemically they have the ability to home to damaged tissues exhibiting inflammation (79, 80). This homing mechanism has been shown to involve important cell trafficking-related molecules such as chemokines, adhesion molecules and matrix metalloproteinases (MMPs)(1). Of these, some key mediators have been identified; the stromal-derived factor 1 (SDF-1)/C-X-C chemokine receptor type 4 (CXCR4) axis and the hepatocyte growth factor (HGF)/MET proto-oncogene (c-MET) receptor tyrosine kinase axis (81, 82). SDF-1 and HGF are upregulated at sites of tissue damage and the results of an *in vitro* study carried out by Bo-Ra Son *et al.* (2006)(81) indicated that these factors along with MMPs could be involved in the migration of MSCs. Further *in vivo* evidence was reported by Kitaori *et al.* (2009)(83), where it was shown that SDF-1/CXCR4 signalling was crucial for the recruitment of MSCs to a fracture site in a mouse model.

In order for MSCs to reach damaged tissue, they must be able to transmigrate the endothelial barrier (84). Schmidt *et al.* (2006)(84) found that by direct cell-cell contacts, MSCs integrated into the endothelial wall of capillary vessels and could fully pass the endothelial barrier within 30 minutes of perfusion in an isolated heart. It was found by Rüster *et al.* (2006)(85) that the ability to interact with endothelial cells involved MSCs engaging vascular cell adhesion molecule-1 (VCAM-1) and very late antigen-4 (VLA-4). It has also been demonstrated that inflammatory cytokines such as transforming growth factor β1, interleukin 1β and tumour necrosis factor-α (TNF- α) promoted invasion and migration of MSCs through the extracellular matrix by up-regulation of MMP activity (86).

The molecules described above are proposed to drive the migration of MSCs however the precise mechanisms are not fully understood (78). Moreover, many intravenously administered MSCs become trapped in the lungs and do not reach the damaged tissue (87, 88).

2.3.2 Differentiation potential of MSCs

While the multipotent potential of MSCs has been largely documented *in vitro* and *in vivo*, there is accumulating evidence that their contribution to tissue regeneration is largely via indirect mechanisms rather than the direct replacement of lost tissue (1, 13, 78). Nevertheless, there are reports that describe the differentiation of transplanted MSCs in models of injury; Sasaki *et al.* (2008)(89) injected MSCs derived from green fluorescent protein (GFP) transgenic mice intravenously into back skin-injured mice and found GFP-positive cells associated with specific markers for keratinocytes, endothelial cells and pericytes

at the site of the wound – demonstrating the transdifferentation of injected MSCs as well as their homing efficiency. Li *et al.* (2010)(90) investigated the differentiation characteristics of MSCs transplanted into a mouse model of renal tubular injury. They reported that MSCs were able to differentiate toward renal tubular epithelium and contributed to the maintenance of structural integrity during the repair process. In contrast, Oryan *et al.* (2017)(13) suggested that MSCs indirectly contribute to cell differentiation (in the case of bone regeneration) via an MSC-mediated reduction in TNF-α, which inhibits osteoblast differentiation (91).

It has been proposed that in order to benefit from MSC differentiation, local administration of cells or administration with a scaffold material is the preferred method (78). This is due to reports that systemically injected MSCs are likely to be trapped in the lungs and other tissues (88, 92) as discussed in Section 2.3.1.

2.3.3 Paracrine effects of MSCs

It is becoming more widely acknowledged that the therapeutic effects of MSCs are largely attributable to their ability to secrete a wide variety of cytokines, chemokines and growth factors (78). Once MSCs have migrated to damaged tissues, they interact with local stimuli such as inflammatory cytokines, ligands of Toll-like receptors and hypoxia, which signals MSCs to secrete molecules mediating processes such as angiogenesis and the prevention of cell apoptosis (1). It was found that the release of vascular endothelial growth factor and fibroblast growth factor 2 – both promotors of angiogenesis - was increased when MSCs were exposed to the stimulants TNF-α, endotoxin and hypoxia (93). An increase in angiogenic factors could improve regional blood flow at a site of injury as well as stimulating autocrine mechanisms (93). Xu *et al.* (2007)(94) found that MSCs exhibited an anti-apoptotic effect mediated by the release of interleukin-6 when in direct contact with lymphocytes.

A multitude of other proteins that are upregulated by MSC paracrine mechanisms have been identified, including; Toll-like receptor 2/6 (95), transforming growth factor-β1 (96), interleukin-8, monocyte chemotactic protein-1, MMPs, pentraxin 3 and cathepsin L (97), however, the majority of studies have been carried out *in vitro*. It is therefore necessary to systematically examine the MSC secretome *in vivo* to further inform MSC therapies (98).

2.3.4 Immunomodulatory behaviour of MSCs

The unique immunomodulatory behaviour of MSCs was first shown by Liechty *et al.* (2000)(99) when human MSCs were transplanted into foetal sheep early in gestation before and after the expected development of immunological

competence. They found that there was long-term engraftment of MSCs even after the development of immunological competence. It has since been found that MSCs have the ability to inhibit the activation and proliferation of T cells, B cells, dendritic cells, macrophages and natural killer cells (100, 101). The underlying mechanisms of suppression are linked with inflammatory stimuli such as nitric oxide, indoleamine 2,3, dioxygenase, prostaglandin E2, tumour necrosis factor-inducible gene 6 protein, chemokine ligand 2 and programmed death ligand 1 via stimulation of inflammatory cytokines such as interferon-γ, TNF-α and interleukin-1 (1).

As well as the inhibition of immune cells, MSCs also preferentially activate T-cell subsets with regulatory activity (Tregs) and maintain the capability of Tregs to suppress self-reactive T-effector responses (78, 102). This means that even short-lived MSCs could have long lasting effects on immunoregulation. These immunomodulatory properties have important implications for the treatment of autoimmune diseases and GvHD (Section 2.2.4).

Furthermore, it has emerged that not only can MSCs negatively modulate a high-inflammation environment but if the levels of inflammatory cytokines are low, MSCs stimulate cells of the immune system to release proinflammatory molecules and promote host defence (98). Monocytes arriving at an inflammatory environment can develop into M1 macrophages or M2 macrophages depending on microenvironmental cues (103). The M1 macrophages release proinflammatory cytokines stimulating local inflammation. This demonstrates that MSCs and macrophages have dynamic regulatory feedback and can switch between proinflammatory and anti-inflammatory activities to create a loop that prevents excessive tissue damage and promotes repair (103).

2.4 Clinical challenges of MSC therapy

The large amount of research into MSCs and their therapeutic mechanisms has led to an increasing number of clinical trials using MSCs over the last 15 years (see Figure 2.1). However, there are still only a handful of therapies available commercially for clinical use and none are FDA-approved (104). Osiris Therapeutics (United States) completed the first major industry-sponsored phase III trial of allogeneic bone marrow-derived MSCs for treatment of GvHD in 2009 (105). The product – Prochymal – did not result in a significantly different benefit compared to a placebo treatment. However, subset analysis revealed that children were more responsive than adults and this led to market approval for Prochymal in Canada to treat children with acute GvHD. A similar allogeneic MSC product for treatment of GvHD is approved for use in Japan (TEMCELL).

The first MSC-based product approved for use in Europe was in 2018 to treat Crohn's-related anal fistulas (105). The product - Alofisel - contains expanded human allogeneic MSCs extracted from adipose tissue. Two further MSC-based products are CARTISTEM and HeartSheet approved for use in Japan and South Korea respectively (104). CARTISTEM uses allogeneic umbilical cord-derived MSCs for the treatment of knee cartilage defects and HeartSheet uses cultured autologous skeletal myoblast cells for treatment of severe heart failure. Currently these are the only commercially available MSC-based products.

This slow rate of translation is also reflected in the data used to create Figure 2.1. If the number of clinical trials is categorised by study phase, it becomes clear that the majority of studies are in early phase I/phase I or phase II, and that this trend has not changed over the past 15 years (Figure 2.4). There has been a slight increase in the percentage of clinical trials in Phase I in the last 15 years but a slight decline in the number of clinical trials in Phase II/Phase III. A small number of clinical trials have reached Phase IV in the last five years compared with none in the first 10 years. Altogether this data confirms that there is a hurdle between demonstrating the safety of MSC therapies and demonstrating the efficacy. Some of the key barriers to translation are discussed in Sections 2.4.1 and 2.4.2.

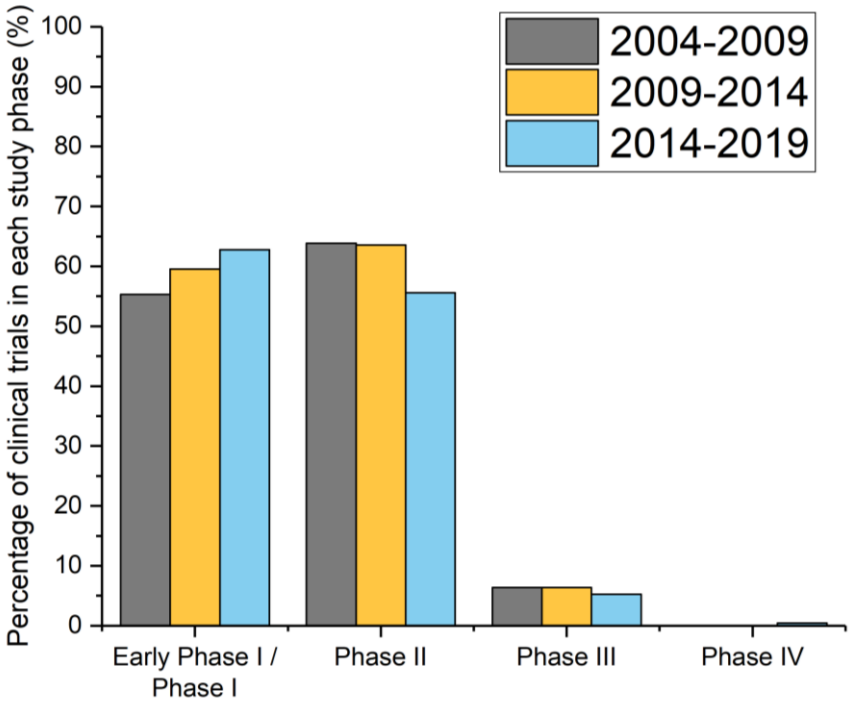

Figure 2.4 The percentage of registered clinical trials involving MSCs in each study phase

This global data was extracted from ClinicalTrials.gov using a search term of 'mesenchymal stem cells' and filtered by year and phase of study.

2.4.1 The lack of standardisation in MSC pre-clinical research and clinical trials for MSC therapy

One of the reasons that efficacy has not yet been proven for many MSC therapies is the lack of standardisation between clinical trials and different research groups in the field. Following a review of published results from clinical trials (Section 2.2), it is evident that there is no clear consensus on the most appropriate therapeutic strategy for MSCs, including the source of MSCs, the delivery method and what constitutes a beneficial dose of cells. This means that there is a lack of evidence behind each individual strategy. Although these limitations are common across all disease areas, it is likely that these factors will ultimately be application-specific and there must be a concerted effort to design more large, multicentre studies using standardised protocols.

In terms of sources of MSCs, bone marrow-derived MSCs (BM-MSCs) have been most commonly used (106), however, MSCs are found throughout the body and the best source for therapies remains unclear (46). Bone marrow has been traditionally used since it can be relatively easily accessed using already available tools (from bone marrow transplantation procedures) however, adipose tissue-derived MSCs (AT-MSCs) and umbilical cord-derived MSCs (UC-MSCs) have

been found to be promising alternative sources that can be harvested through less invasive procedures (107). In a comparison of all three sources, Kern *et al.* (2006)(107) found that UC-MSCs had a higher proliferation capacity whereas AT-MSCs contained the highest frequency of MSCs. Despite this, UC-MSCs were not as reliably sourced as AT-MSCs and BM-MSCs. MSCs have also been isolated from dental pulp tissue (108), skeletal muscle tissue (109), and amniotic fluid (110).

A further debate concerns whether MSCs should be allogeneic or autologous for clinical therapies. MSCs are immunosuppressive with low immunogenicity and thus can avoid eliciting immune responses in recipients (111)(Section 2.3.4). They also have the advantage of being available as 'off-the-shelf' products which is favourable in terms of time, cost and quality assurance. It is noted that of the handful of commercially available products, all but one utilises allogeneic MSCs. Despite this, there are reports that allogeneic MSCs are not fully immune privileged and without immunosuppressive therapy can cause an immune response and graft rejection (112-114). A safer approach to MSC therapy is to use autologous cells where there is no possibility of immune rejection and no need for immunosuppressive therapies. Perhaps the reason that autologous cell therapies are lagging behind allogeneic cell therapies, is due to the lack of adequate technology available for autologous cell processing – the focus of this research project.

2.4.2 Inadequate isolation methods for MSCs

In the majority of clinical trials to date, the processing of cells prior to therapy has been via MSC isolation methods which have a number of limitations. In almost all of the clinical trials reviewed, cells were expanded *in vitro* to enrich a therapeutic population with sufficient cell numbers. There are a number of issues associated with the *in vitro* expansion of cells; first and foremost, the enrichment of MSCs based on their adherence to tissue-culture plastic yields a highly heterogeneous population (6). This means that large cell numbers are required since not all cells will be therapeutic in nature. Moreover, it could be the reason why the efficacy of treatments in clinical trials has been inconsistent - different culture methods yield different populations of cells with unknown properties. In addition, *in vitro* expansion requires Good Manufacturing Practices (115), is time-consuming (often taking weeks to acquire sufficient cell numbers) and costly. Finally, it has been shown that culturing MSCs *in vitro* – with growth factors - can change their characteristics, such as their becoming more susceptible to apoptosis and loss of clonogenic potential (7).

Enrichment of MSC populations for therapies is necessary since MSCs are present at 0.001–0.01% of mononuclear cells in bone marrow aspirates (2). Enriching MSCs by their adherence to tissue-culture plastic has been the most commonly adopted method, however techniques have also been used to concentrate the mononuclear cell fraction of bone marrow aspirate using density gradient centrifugation (Section 2.5.1.2). Unfortunately these methods also yield a heterogeneous population of cells, with low numbers of MSCs, resulting in many of the same limitations as culture-expanded cells. In one clinical trial, MSCs were isolated by immunoselection (33)(Section 2.5.1.4) providing a population of MSCs with higher purity. However no comparison was made with MSCs isolated by alternative techniques and therefore this study did not confirm whether this technique resulted in a greater therapeutic effect. There are also concerns with the safety of current immunoselection procedures (discussed in Section 2.5.1.4) and controversy over the specific identity of MSCs (discussed in Section 2.6.1) which further limit this study.

There are inherent issues with the isolation techniques currently available for MSC processing prior to therapeutic applications and both Diogo *et al*. (2012)(6), and Zhu *et al.* (2013)(116), described the development of novel stem cell isolation and bioprocessing techniques as a crucial factor for the success of stem cell therapies. In Section 2.5, current MSC enrichment methods are reviewed in more detail as well as some of the emerging methods which have informed this research project.

2.5 Introduction to cell sorting methods for MSC enrichment

In this section, conventional methods of cell sorting will be discussed as well as their limitations in respect of MSC therapies. Following this there will be a review of the most promising future directions in this field.

2.5.1 Traditional cell sorting methods for MSC enrichment

2.5.1.1 Cell-culture based enrichment of MSCs

MSCs can be enriched from different tissues in the body based on their preferential adherence to plastic. This mainly eliminates haematopoietic cells since they are non-adherent and can be discarded during medium exchange (6, 117). However, some non-mesenchymal stem cells (stromal cells which do not conform to the current formal criteria – see Section 2.6.1) also adhere to the tissue culture plastic leading to a heterogeneous and undefined population of

cells. Steps have been taken to increase the purity of MSC populations during *in vitro* expansion, for example, using differential trypsinization and selective medium during cell culture; differential trypsinization is where MSCs are released from the tissue culture plastic during short incubation times but other cell types are not (117), and using different compositions of cell culture medium can favour the proliferation of various stem cells over other cell types (116). Unfortunately, there is no standardised conditioned medium for MSC culture due to the lack of a comprehensive list of conditioned medium components (118). Factors such as the glucose concentration, serum concentration, amino acids, inorganic salts and vitamins can affect the proliferation, morphology, clonogenicity and differentiation potential of isolated cells (118, 119). Although these techniques may increase the homogeneity of populations, enrichment by preferential adherence is unlikely to produce a pure population of MSCs for cell therapies.

Moreover, there are several additional issues associated with the *in vitro* expansion of MSCs which are discussed in Section 2.4.2. Namely the requirement for Good Manufacturing Practices, the timely processes involved, the risk of contamination during cell culture and the high costs associated. The logistical aspects for large-scale manufacturing of cell therapies which require *in vitro* expansion are a huge challenge and barrier to translation.

2.5.1.2 Density gradient centrifugation (DGC) for MSC enrichment

Density gradient centrifugation (DGC) is one of the simplest methods of cell enrichment. A density gradient is established longitudinally in a test tube and the cell sample is added to the top (116). When the solution is centrifuged, cells with higher density cross the interface between the two layers and sediment at the bottom whilst cells that have a lower density settle at the interface (6).

This method is commonly used to isolate mononuclear cells from bone marrow using a Ficoll-Paque density gradient (6)(Figure 2.5), however this technique has extremely low resolution and yields low numbers of MSCs (106). The resulting population is heterogeneous consisting of differentially matured B-cells, T-cells and monocytes as well as the more rare progenitor cells which includes haematopoietic stem cells and MSCs (120). DGC can be used as a preparative step for a higher resolution technique such as magnetic-activated cell sorting (MACS) or fluorescent-activated cell sorting (FACS)(Sections 2.5.1.3 and 2.5.1.4), although this has also been found to considerably reduce the yield of bone marrow mononuclear cells (BM-MNCs) and therefore MSCs, with nearly 75% loss of mononuclear cells using Ficoll-Paque DGC (120). In a separate study, it was found that red blood cell lysis of 6 mL of bone marrow aspirate

yielded the same number of MSCs as Ficoll-Paque DGC of 60 mL of bone marrow aspirate, suggesting that red blood cell lysis is a superior method to isolate mononuclear cells (121), although the higher volume of aspirate could also affect the mononuclear cell count independently from the isolation method.

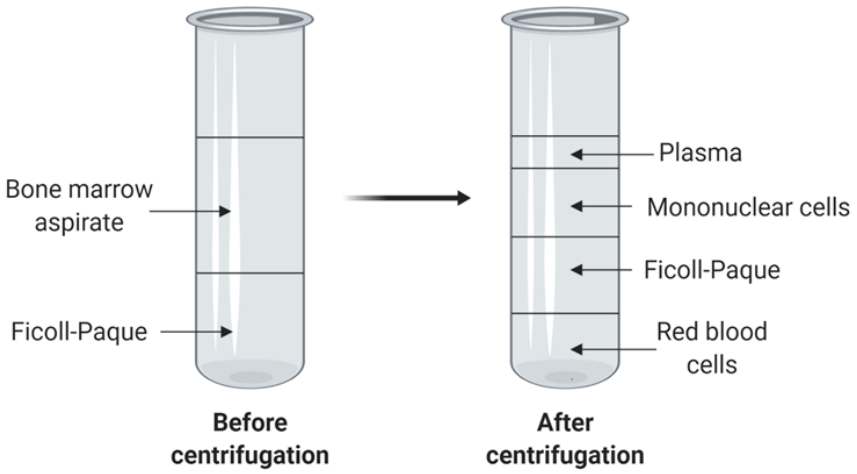

Figure 2.5 Density gradient centrifugation (DGC) for the isolation of mononuclear cells from bone marrow aspirate

Bone marrow mononuclear cells are commonly isolated from bone marrow aspirate using a Ficoll-Paque density gradient. The left-hand side shows the density gradient solution and cell sample before centrifugation, and the right-hand side shows the solutions after centrifugation where the cells have been separated according to their density. This diagram was created with BioRender.com.

An intraoperative bone marrow aspirate concentrate (BMAC) device (SmartPReP®2) has been developed which concentrates bone marrow total nucleated cells (122). The BMAC device was found to have a superior performance to other bone marrow aspirate concentration systems (BioCUE® and MAGELLAN®) in terms of the number and concentration of MSCs after centrifugation (123), and cells isolated from the BMAC device were also shown to have comparable functional activity to Ficoll-Paque DGC isolated cells and achieved a greater yield (122). However, no comparison to higher resolution techniques such as immunoselected cells has been made.

Furthermore, it was found that contaminating cells in heterogeneous populations isolated by DGC compromised the therapeutic effect of MSCs (124, 125), and factors such as the centrifugation speed and washing buffers could impair the functionality and recovery of mononuclear cells (126). Mouquet *et al.* (2011)(125) found that 37% of rabbit BM-MNCs were apoptotic after Ficoll-Paque DGC and

the presence of apoptotic cells among mononuclear cells reduced the efficacy of cardiac cell therapy after myocardial infarction. Assmus *et al.* (2010)(124) reported how contaminating red blood cells affected the functionality of BM-MNCs in a dose-dependent manner and the degree of contamination was a determining factor of the extent of recovery in patients with acute myocardial infarction. Finally, van Beem *et al.* (2008)(126) studied the effects of different DGC protocols and found that lower centrifugation speeds resulted in lower mononuclear cell recovery, and washing buffer without human serum albumin and heparin resulted in lower mononuclear cell recovery and impaired function measured by clonogenic capacity.

DGC has a number of associated issues and although a simple method of enrichment, it is far from an ideal method. To attain high purity MSC populations, higher resolution techniques have been developed based on antibody labelling of specific antigens – described in Sections 2.5.1.3 and 2.5.1.4.

2.5.1.3 Fluorescence activated cell sorting (FACS) for MSC enrichment

Fluorescence-activated cell sorting (FACS or flow cytometry) relies on the specific labelling of antigen markers with fluorescently tagged monoclonal antibodies (6). Cells are labelled in a mixed suspension and analysed using a flow cytometer; inside the flow cytometer cells are drawn into a stream created by a surrounding sheath of isotonic fluid that creates laminar flow (127). This allows single cell analysis and is the basis of the high resolution of this technique. At an ‘interrogation point’, a laser is used to excite the fluorescent molecules to a higher energy state and upon returning to their resting states, the fluorochromes emit light energy at higher wavelengths. The use of multiple fluorochromes with similar excitation wavelengths but different emission wavelengths, allows several cell antigens to be detected simultaneously (127). The light signals are detected by photomultiplier tubes and converted to digital outputs for analysis.

To sort cells using this technique, after laser excitation the single cells are separated into small droplets using mechanical vibration (6). The droplets pass through an electrical charging ring where a charge is placed on the droplet according to the fluorescence of the cell inside. The droplets then flow parallel to electromagnets and are deflected into collection tubes according to their charge (Figure 2.6).

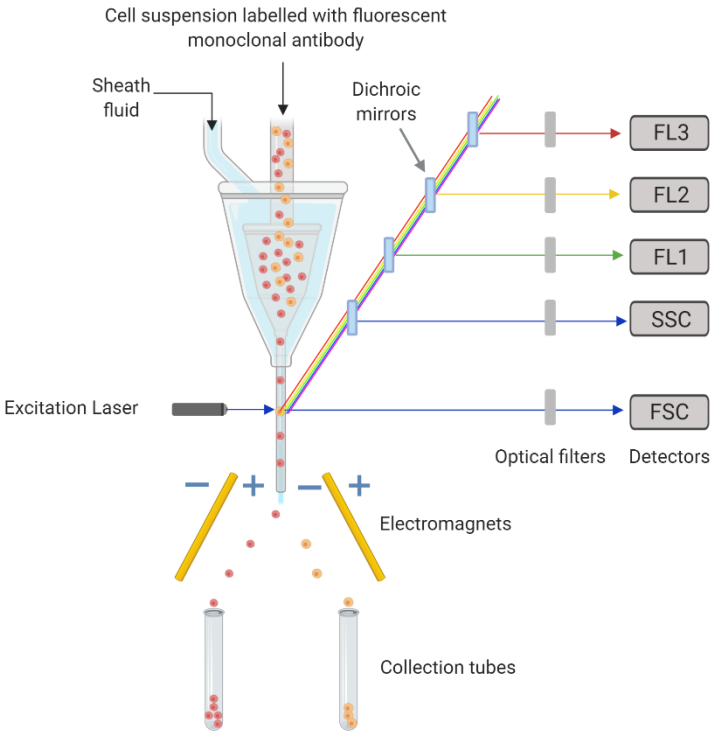

Figure 2.6 Fluorescence-activated cell sorting (FACS)

A sheath fluid creates laminar flow so that cells pass individually through a laser beam. Fluorescently labelled cells are excited by the laser and the emitted light is detected. Mechanical vibration then causes the flow to separate into small droplets which become charged according to the fluorescence of the cell inside. Droplets are then deflected by electromagnets into separate collection tubes based on their different charges. This diagram was created with BioRender.com.

There is no doubt that FACS results in high purity cell separations due to the highly specific nature of monoclonal antibodies and the single cell analysis employed, however, this technique has limited capacity for point-of-care clinical applications and is much more widely used as an analytical and diagnostics tool. The reasons for this are as follows; firstly, the technique is limited by the time taken for high purity separations, although the single cell analysis has a relatively high throughput (5000 – 25,000 cells per second (128)), a large number of cells must be analysed for rare populations, and processing times are typically between three and six hours including pre-processing steps for immunostaining (6). The fact the cells are labelled with an antibody conjugated to a fluorophore is also undesirable for clinical applications since the labels remain attached to the cells post-separation. In addition, the cells are at risk of contamination during processing and experience high shear stress during the procedure which could lead to cell damage (6, 128). Finally, the equipment is large, very expensive, and requires skilled technicians to operate.

2.5.1.4 Magnetic activated cell sorting (MACS) for MSC enrichment

Magnetic-activated cell sorting (MACS) is a trademark name (Miltenyi Biotec, Germany) for immunoselection using magnetic nanoparticles conjugated to monoclonal antibodies (6). The nanoparticles are approximately 50 nm in diameter and are biologically (as far as we know) and optically inert which has led to MACS beads becoming the gold standard for magnetic cell separation (129). The beads are mixed with cells in suspension, then passed through a column in a magnetic field. Cells bound to the antibody binders - conjugated to the magnetic beads - are retained in the column whilst unbound cells are eluted. The magnet is then removed so that bound cells can be collected (Figure 2.7). The columns are filled with a matrix of ferromagnetic steel-wool or iron-spheres which focus the magnetic field lines towards their surface inducing strong magnetic field gradients (129). Once the magnetic field is removed, the ferromagnetic matrix can no longer retain the bound cells and labelled cells can be collected.

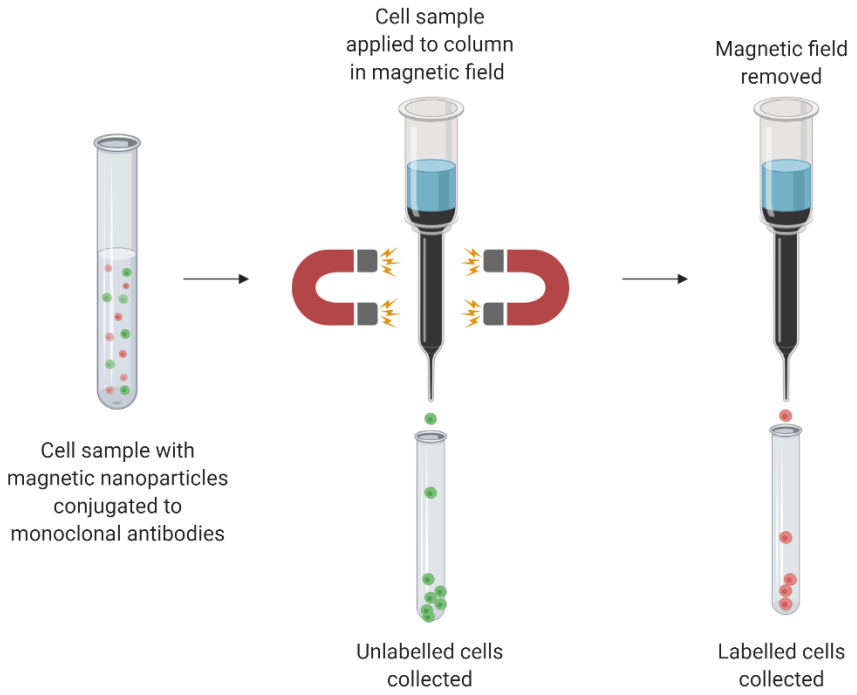

Figure 2.7 Magnetic-activated cell sorting (MACS)

Magnetic nanoparticles (MACS beads) conjugated to antibodies that recognise specific antigens on the surface of the desired cells, are incubated with a cell suspension prior to their application to a MACS column in a strong magnetic field. The unlabelled cells elute from the column and are collected. The magnetic field is then removed enabling the labelled cells to be collected. This diagram was created with BioRender.com

Compared to FACS, MACS is easier to use, achieves higher throughput and comparable purity (after two consecutive cycles)(6, 130). Despite this, the throughput and purity depends on a number of factors including the starting population of cells and the particular MACS instrument and reagents used. Instruments are available for automatic processing of up to eight samples simultaneously (autoMACS™ Pro) and a closed and automated CE-certified system (CliniMACS® Plus) has been developed to process up to 1.2 x 10^{11} cells in one sterile run. However, the CliniMACS system is only approved for limited therapeutic applications and many of the reagents are intended for *in vitro* use only (129, 131). Multiple parameter MACS is possible by the enzymatic removal of magnetic beads after the initial step of isolation (MACS-MultiSort)(128), however this would inherently lead to longer processing times and higher costs.

For MSC enrichment, the clinical-scale isolation of a subset of MSCs (CD271+) has been demonstrated using CliniMACS CD271 GMP MicroBeads (132), however this product is for research use and *in vitro* cell processing only. One of the reasons for this could be the major concern of interference caused by

magnetic beads in the purified population (116). Moreover the equipment and reagents are expensive and there is no information regarding the length of the full procedure. Although MACS is currently leading the way on cell enrichment, the main drawback is the fact that cells are labelled with magnetic nanoparticles and monoclonal antibodies which remain attached to the cell surface or are internalised through endocytosis after enrichment. This limitation is the motivation for developing minimally manipulative and intraoperative cell enrichment technologies for autologous MSC therapies.

An additional limitation of both MACS and FACS for MSC enrichment is the lack of consensus on the most appropriate biomarkers for MSC isolation. A review of MSC surface markers used to enrich therapeutic populations of MSCs is included in Section 2.6, however it is believed that there is no single marker for the isolation of a pure population of MSCs.

2.5.2 Emerging cell sorting methods for MSC enrichment

The most frequently used cell sorting methods for MSC enrichment in clinical trials and/or used as standard practice for research purposes have been discussed in Section 2.5.1. In this section, methods that are currently being developed for MSC enrichment are reviewed including some of the most pioneering work to date.

2.5.2.1 Microfluidic methods for MSC enrichment

There has been a methodological shift away from macroscale technologies towards microscale technologies due to a number of beneficial properties these systems encompass, including; laminar flow, easy integration with mechanical, electrical and optical systems and low-cost fabrication (133). In addition, microfluidic systems can be under continuous operation in a closed system to prevent contamination. With regard to an intraoperative cell enrichment technology, a microfluidic device would have further benefits such as a small size - increasing portability, and the relatively low cost of fabrication would be favourable for a single use device essential for clinical applications.

As a result of advances in microfluidic technologies, traditional macroscale methods of cell sorting such as FACS and MACS have been developed as microscale technologies (μFACS and μMACS). A μMACS device was developed by Adams *et al.* (2008)(134) with multi-target capabilities. The device incorporated microfabricated ferromagnetic strips to generate large magnetic field gradients within a microchannel. Two different magnetic tags had distinct

magnetisation and radius properties which caused labelled targets to be deflected at the corresponding ferromagnetic strips into different outlets. The net amplitude and direction of the force experienced by the target was governed by the sum of the fluidic drag and the magnetophoretic force. For successful deflection, the magnetophoretic force was required to exceed the fluidic drag component and since the balance of the forces has a non-linear dependence on the radius, the different magnetisation and radius of the magnetic tags allowed for multitarget sorting.

This method achieved high purity and high throughput separations but was only capable of isolating targets such as bacteria, viruses and molecules with sizes smaller or comparable to the magnetic tag. This is because for larger targets (such as mammalian cells), the net amplitude and direction of the magnetophoretic force would no longer exceed the fluidic drag component and therefore additional adaptions to the method would be required. As well as this, this method still has many of the same limitations as macroscale MACS – including the requirement of labelling which is still present post-separation.

Droplet microfluidics was used to analyse periosteal cells containing MSCs at different stages of osteogenic lineage commitment in a μFACS style device (135). Using fluorescent-conjugated antibodies against alkaline phosphatase and STRO-1 (prospective markers of MSCs – see Section 2.6.2), three distinct cell phenotypes were identified and enumerated using a microfluidic channel and optical detection system. At this stage the device was not able to sort the cells based on their signal and was used for identification and analysis purposes only. Baret *et al.* (2009)(136) achieved cell sorting in a μFACS device using a pulse of high-voltage alternating current to cause chosen droplets to deflect into a separate outlet by dielectrophoresis. This device was however limited to a low throughput of 2000 droplets per second and has not yet demonstrated separation using mammalian cells.

Although harnessing some of the more advantageous aspects of microfluidics, the inherent issue of cell labelling remains relevant to these microfluidic technologies. To overcome these, an effort has been made to develop label-free microfluidic techniques using dielectrophoresis and field flow fractionation - described in Sections 2.5.2.2 and 2.5.2.3 respectively.

2.5.2.2 Dielectrophoresis (DEP) for MSC enrichment

Dielectophoresis (DEP) has the ability to sort cells based on their polarisability, which is determined by properties such as their size and shape, membrane integrity and morphology, cytoplasm conductivity and nucleus-cytoplasm volume

ratio (137). Cells exposed to an electric field experience mechanical forces due to the induced electric charges at interfaces such as the cell membrane and structural components inside the cell. The induced charges are small however, and since they are non-uniform in nature they produce an electric dipole moment in the cell. In a non-uniform electric field, the polarised cell experiences an electric field gradient causing the cell to move relative to its surroundings. Depending on the polarity of the induced dipole moment, the cell will either move towards regions of high electric field gradient (positive DEP) or regions of low electric field gradient (negative DEP)(Figure 2.8). The highest field gradients occur at the electrode edges which results in the trapping of cells experiencing positive DEP whilst the cells experiencing negative DEP can be removed using fluid flow.

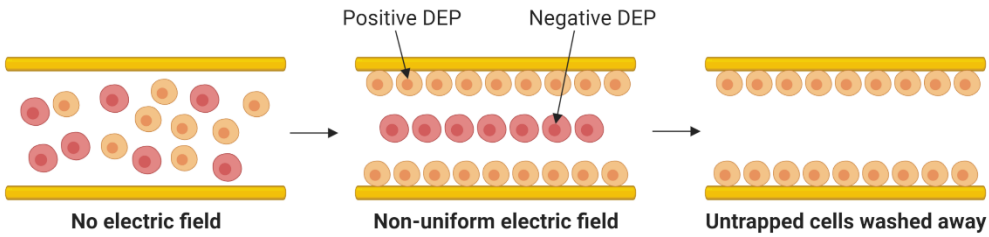

Figure 2.8 Dielectrophoresis (DEP) for cell separation

Cells experience positive or negative dielectrophoresis according to the polarity of the induced dipole moment in a non-uniform electric field. If a cell is more polarisable than the surrounding medium, it will move towards regions of high electric field gradient (at the electrodes) and if a cell is less polarisable than the surrounding medium it will move to regions of low electric field gradient (away from the electrodes). Cells that are not trapped at the electrodes can be washed away using fluid flow. This diagram was created with BioRender.com.

The DEP force experienced by a cell is dependent upon the Clausius-Mossotti factor which in turn is frequency dependent (138). Where the direction of the DEP force is independent of the applied voltage, the relative polarisability of the cells and the suspending medium can be manipulated by controlling the frequency of the applied electric field. For cell separation, the key is to find an operating frequency where the desired cell type experiences a different DEP force to the undesired cell types. This has been demonstrated a handful of times using cell lines derived from bone marrow stem cells (139), and to separate MSCs from differentiated cells (140, 141), however these studies use a maximum of three different cell types and separation from native BM-MNC populations has yet to be achieved. It is therefore unknown whether the dielectric properties of MSCs

will be sufficiently different to distinguish MSCs from all the other cell types present in BM-MNCs.

Furthermore, the purities of cell populations enriched using DEP are often low and contaminated with unwanted cell types (116). Song *et al.* (2015)(141) used a DEP device to separate MSCs from differentiated osteoblasts and reported that purity could be increased from 50 % to ~80 %, however, this was at a low flow rate (1.8 µL/min) and did not use clinically relevant populations. Yoshioka *et al.* (2018)(139) used a DEP device to separate two bone marrow-derived cell lines with distinct DEP properties and observed similar purities (~80 %), however, there was very low cell recovery (~30 %) which would not be appropriate for capturing rare MSC populations.

Currently DEP technologies are not sophisticated enough to enrich MSC populations from clinical samples with high purity. Moreover, cell damage is unavoidable for cells experiencing positive DEP (118) and problems can arise due to electrode fouling. In addition, when cells are kept in physiologically relevant medium with high conductivity, DEP can cause joule heating and electrochemical reactions to occur causing further concerns for cell viability.

2.5.2.3 Field flow fractionation (FFF) for MSC enrichment

Another cell separation method based only on physical parameters is field flow fractionation (FFF). This method relies on differences in cell morphology and biophysical differences such as cell mass, charge, size, density, shape and rigidity (6). Separation is achieved by combining laminar flow with an external perpendicular field applied to the channel (142)(Figure 2.9). Different fields have been applied to FFF including gravitational, centrifugal sedimentation and dielectrophoretic which in turn determines the distinguishing properties used for separation. According to the particular physical property or properties, cells are distributed differently in the flow profile leading to different elution times.

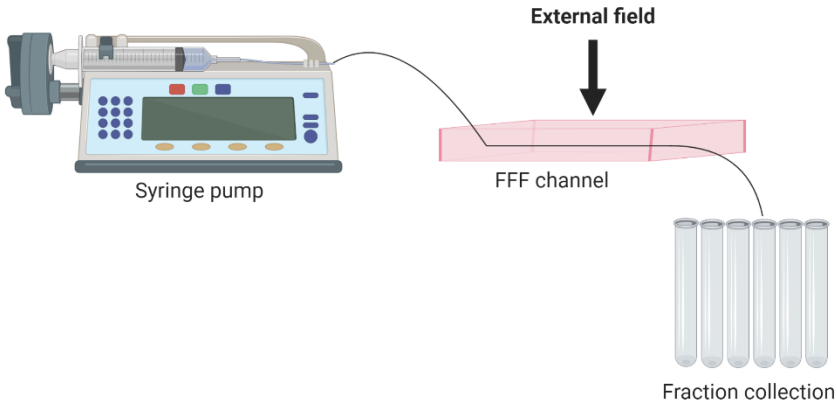

Figure 2.9 A field flow fractionation (FFF) device

FFF combines laminar flow with an external field applied perpendicular to a channel and cells elute from the channel in different fractions based on their physical properties. The type of external field applied determines which cell properties the elution times depend upon. Different external fields have been used in FFF including gravitational, centrifugal sedimentation and dielectrophoretic. This diagram was created with BioRender.com and adapted from (143).

There are only two examples of where FFF has been applied for the enrichment of MSCs; one using gravitational FFF (144) and another using DEP-FFF (145). The simpler device of the two - which uses gravitational FFF - was able to isolate populations of cells with MSC morphology from different sources, as well as enrich adipogenic progenitor cells from adipose tissue (144). However the purity of populations were not reported nor any further analysis of the cells post-enrichment. The second example used a more sophisticated DEP-FFF device and enriched NG2-postive cells (a marker for stromal/pericyte cells) from a starting population of less than 2% in adipose tissue to 28% after enrichment in the device, achieving a 14-fold enrichment but still a relatively low overall purity (145).

Similarly to the previously discussed physical-based methods, FFF has low resolution leading to low purity populations. Another limitation of FFF is the inherently low throughput of the technique, typically processing less than one million cells per run (146).

2.5.2.4 Other microfluidic label-free cell sorting techniques for MSC enrichment

There are a handful of examples where label-free microfluidic methods have been applied for MSC enrichment based simply on the different sizes of cells. Lee *et*

al. (2018)(147) used a spiral-shaped inertial microfluidic sorter to isolate MSCs from mouse bone marrow samples based on their larger size compared to other mouse bone marrow-derived cells. This method accomplished reasonable recoveries and enrichment but with low purities (~13%). Wu *et al.* (2009)(148) used a louver-array microstructure to enrich human amniotic fluid stem cells in which the smaller sized stem cells could flow through the gaps in the array whereas larger endothelial cells could not. High separation efficiencies were reported at 97% for two consecutive separations or 83% for one separation, however this was at low flow rates and no analysis was carried out on the cells post-enrichment. Finally, Jung *et al.* (2015)(149) used hydrodynamic filtration to isolate three subpopulations of human MSCs based on their different sizes. The smallest sized cells (<25 μM) were separated with the highest purity (reported at 100%) and demonstrated specific surface markers of MSCs, however the throughput of the device was not described.

There are a number of other microfluidic cell sorting techniques based on: microscale filters, deterministic lateral displacement, magnetophoresis, acoustophoresis and aqueous two-phase systems (150), however none of these have yet been applied for MSC enrichment. This is likely to be due to the fact that these label-free techniques potentially lack the specificity and high resolution required to enrich high purity populations. In light of this, the next section will introduce alternative affinity-capture based techniques for MSC enrichment.

2.5.3 Affinity-capture based systems for MSC enrichment

Affinity-capture based methods have the advantage of high specificity whilst avoiding external labelling of target cells. The principle of affinity-capture based methods is the use of highly specific binding molecules attached to a solid substrate to allow for specific cell capture and release. The most traditional binding molecule is an antibody – previously discussed in Sections 2.5.1.3 and 2.5.1.4, where their use in FACS and MACS allows for high resolution cell separations via solution-based methods. However, over the past 30 years alternative non-antibody binding molecules (referred to as aptamers) have been developed which can hold some advantages over conventional antibody technology. Binding molecules that have the potential to be used as specific capture molecules in a cell enrichment device are reviewed in the following sections.

2.5.3.1 Aptamers as cell capture molecules for MSC enrichment

RNA, DNA or peptide molecules with high specificity and binding affinity towards a target molecule are described as aptamers (151). Aptamers are selected using *in vitro* screening techniques such as the systematic evolution of ligands by exponential enrichment (SELEX) and phage display.

SELEX is a technique used to screen large libraries of combinatorial RNA or ssDNA against a target molecule. RNA or ssDNA binders are eluted from the target molecule and reverse transcription polymerase chain reaction (RT-PCR) or PCR amplification is used to enrich a pool of target-specific binders. The process is repeated multiple times to result in highly specific aptamers which can be used for therapeutic applications (Figure 2.10). Phage display is an analogous technique to screen large libraries of peptide aptamers and is described in more detail in Chapter 5: Section 5.1.1.

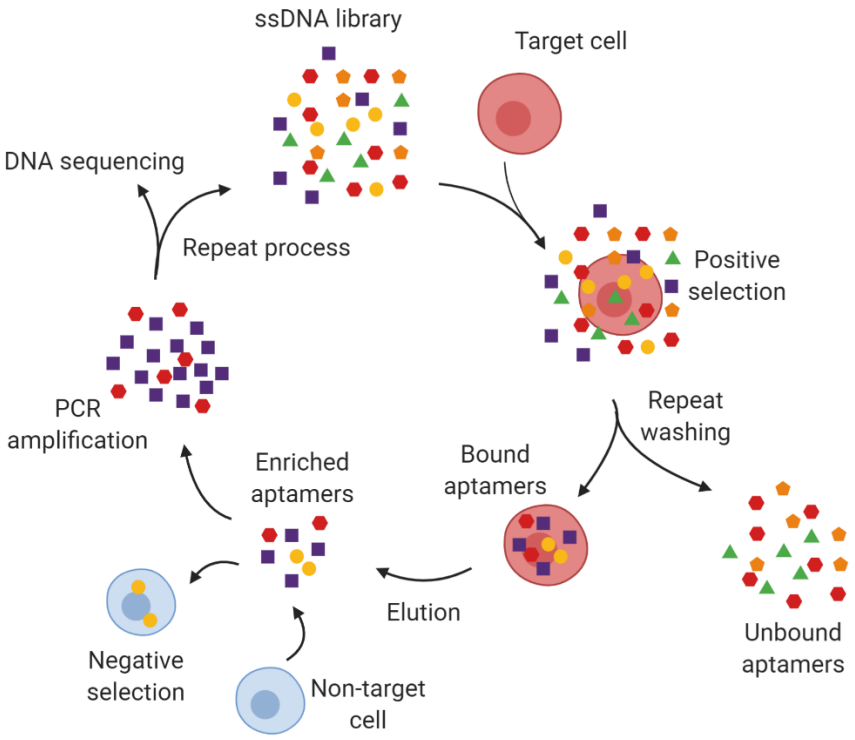

Figure 2.10 Systematic evolution of ligands by exponential enrichment (SELEX)

A ssDNA or RNA library is incubated with a target cell and unbound aptamers are washed away. Bound aptamers are eluted and can be further enriched with negative selection with non-target cells. Enriched aptamers are amplified using polymerase chain reaction (PCR)(or reverse transcription-PCR in the case of RNA) and the process is repeated multiple times to identify highly specific aptamers for target cells. This diagram was created with BioRender.com and adapted from (118).

Aptamers are proposed to have advantages over antibodies for affinity-based cell capture, for example; they have uniform activity independent from batch synthesis, unlimited shelf-life and reversible heat-induced aptamer denaturation (151). Furthermore, there is opportunity to modify aptamers post-selection to enhance binding affinity and reduce non-specific binding.

The therapeutic use of aptamers has been explored for a wide variety of applications with some treatments already FDA-approved (152). On the other hand, there has been limited investigation of the therapeutic use of aptamers for MSC enrichment, and the only example is presented by Guo *et al.* (2006)(153) who explored the use of DNA aptamers for the isolation and surface immobilisation of MSCs from porcine bone marrow. Using SELEX, and monitoring the enrichment of specific cell-binding aptamers using flow cytometry, 36 clones were obtained and analysed. After initial analysis, one clone was

chosen for further characterisation demonstrating specific binding to porcine MSCs compared to human MSCs and a mouse cell line. The aptamer was biotinylated which enabled bound cells to be ‘fished out’ by anti-biotin microbeads and characterised post-enrichment. Aptamer-sorted cells proliferated and showed adipogenic and osteogenic differentiation whereas cells isolated by plastic adherence and cultured in the same conditions did not. Finally, biotinylated aptamer could be immobilised onto a surface and was shown to trap MSCs from an agitated cell suspension.

This pioneering work demonstrates the efficacy of aptamers for cell enrichment applications, however, it requires further development to become a feasible platform for intraoperative clinical application. For example, aptamers must be isolated against human MSCs rather than porcine MSCs and the cells must be able to be released from the aptamer coated surface. In this case, the groups long term goal was to create an aptamer-coated scaffold for bone tissue engineering and therefore cell release would not have been a priority.

In more recent work, a DNA aptamer was selected that was specific for human embryonic stem cells (hESCs) and could enrich hESCs from a mixture of human foreskin fibroblasts using biotinylated aptamer and streptavidin-labelled magnetic beads (154). The authors were also able to identify that the aptamer was binding to alkaline phosphatase expressed on the cells. This aptamer was then later implemented in a tissue engineering approach for osteochondral defect repair demonstrating the ability to recruit a higher number of MSCs to a scaffold with aptamer incorporated compared to a scaffold with no aptamer (155). Moreover, the aptamer scaffold was used in a full thickness rat osteochondral defect and displayed superior healing to a scaffold without aptamer. This study demonstrates the efficacy of aptamers in regenerative medicine and presents the opportunity for their implementation in an MSC enrichment technology.

2.5.3.2 Affimers as cell capture molecules for MSC enrichment

Peptide aptamers - “Affimers” - were first introduced as “Adhirons” in 2014 by the BioScreening Technology Group (BSTG) at the University of Leeds (156), and later referred to as Affimer proteins. Affimer proteins have the potential to be used as binding molecules in an affinity-capture based device with some advantages over traditional antibodies. For example, Affimers are easy to express in *E. coli* - therefore avoiding the use of animals and mammalian cell culture, and they do not contain cysteine residues - allowing the site-directed introduction of a cysteine for site-specific coupling of biotin/fluorescent labels to enhance their utility. Furthermore, for use as a binding molecule in an affinity-capture based device,

they have the advantage of being approximately ten times smaller than antibodies allowing increased packing density on a solid substrate, and they have tuneable affinity due to the ability to change the properties of selected Affimers via affinity maturation or mutagenesis. The affinity of binding molecules is a critical factor in this application since the cells need to be released from the solid substrate after capture.

Peptide aptamers such as Affimers consist of a short amino acid sequence embedded within a small and very stable protein backbone referred to as a scaffold (157). The conformational constraint applied by the scaffold stabilises the insert loop and can increase the binding affinity to a specific ligand by as much as 1000 times compared to free peptide (157). In search of a highly stable protein scaffold for Affimer proteins, the consensus design concept was used to generate a scaffold based on a consensus sequence of plant-derived phytocystatins. This ensured that a scaffold with desirable properties such as a small size, monomeric, high solubility, and high stability - without the need for disulphide bonds and glycosylation - was generated for aptamer peptide presentation. Within the protein scaffold two loops of nine randomised amino acid positions were introduced to create an Affimer phage display library comprising of 1.3×10^{10} clones. The X-ray crystal structure of the Affimer scaffold is shown in Figure 2.11.

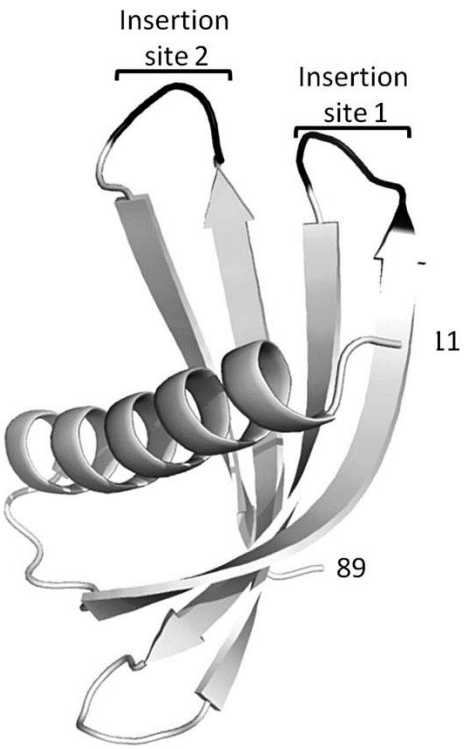

Figure 2.11 X-ray crystal structure of the Affimer scaffold

The Affimer scaffold has a single alpha helix, four anti-parallel β strands and two loops of nine randomised amino acid positions (insertion sites) for library production. Residues 1-10 and 90-92 are not visible in the structure and are presumed to be disordered. The X-ray crystal structure is shown here at 1.75 Å resolution. This image was taken from (156).

In 2017, Tiede *et al.* (158) presented some of the outcomes of over 350 successful screens of the Affimer library, including; Affimer binders selected against homologous protein family members – with the purpose to increase the understanding of intracellular signalling pathways, Affimers used as affinity histochemistry reagents with high sensitivity, Affimers capable of blocking the biological function of specific receptors, and Affimers for *in vivo* rapid imaging of tumours. Moreover, in 2016 Sharma *et al.* (159) reported the use of Affimers in an electrochemical impedance biosensor for detection of human interleukin-8 (IL-8). This application is the most relevant to this thesis since the biosensor consisted of Affimer proteins immobilised to a solid substrate used as capture molecules – the same intention as binding cell surface molecules in this work, however for whole cell capture.

2.5.3.3 Antibodies as cell capture molecules for MSC enrichment

Despite aptamers presenting a promising opportunity for use as specific cell capture molecules, the concept relies on the selection and identification of

suitable aptamers during *in vitro* screening of a target. In the case that an appropriate binding molecule cannot be identified for the intended application, antibodies provide a long-established method of specific antigen binding which could be utilised in an affinity-capture based device and are commercially available.

Antibodies specific to a particular antigen are produced by mature B lymphocytes when an antigen is recognised as being foreign (160). The antibodies are released into the bloodstream and specifically bind with the foreign molecule allowing the immune system to eliminate the molecule from the system. Antibodies are immunoglobulins (Igs) which in their monomeric form are glycoproteins with a molecular weight of approximately 150 kDa (160). The basic structure of the monomer is a Y-shape which consists of four polypeptide chains – two heavy chains and two light chains connected by disulphide bonds (Figure 2.12).

Antibodies have dual functions, antigen binding and biological activity mediation. The different functions are carried out by different parts of the antibody; the fragment antigen binding (Fab fragment) contains the antigen binding site and the fragment crystallisable region (Fc region) can activate the immune system. The Fc region contains protein sequences common to all Igs as well as determinants unique to the individual classes (IgA, IgD, IgE, IgM and IgG), and are referred to as constant regions since they do not vary significantly among different Ig molecules within the same class. The Fab portion contains both heavy and light chains where one heavy and one light chain combine to form the specific antigen binding site of the antibody. The two heavy chains and the two light chains are identical in any given antibody meaning there are two identical antigen binding sites.

Antibody technology has been successfully employed for MSC enrichment using solution-based methods - FACS and MACS (Sections 2.5.1.3 and 2.5.1.4), and could provide a suitable capture molecule in an affinity-capture based method of cell enrichment.

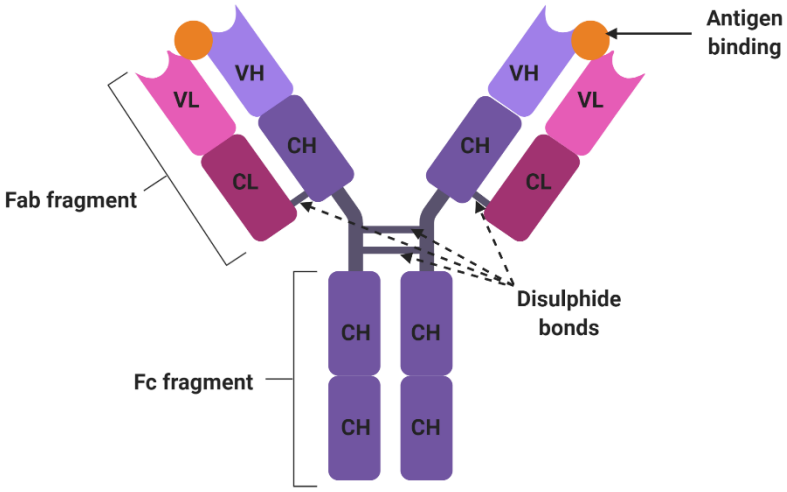

Figure 2.12 Structure of an antibody binding molecule

An antibody has a Y-shaped structure which consists of four polypeptide chains – two heavy chains and two light chains connected by disulphide bonds. The Fc fragment is known as the constant region since it does not significantly vary between immunoglobulin molecules within the same immunoglobulin class. The Fab fragment is made up of light chains and heavy chains, and one light chain and one heavy chain combine to make a specific antigen binding site. CH=heavy chain constant region, VH=heavy chain variable region, CL=light chain constant region, VL=light chain variable region. This diagram was created with Biorender.com and adapted from (160).

2.5.4 Summary of cell sorting methods for MSC enrichment

In reviewing the limitations of conventional cell enrichment technologies, as well as evaluating the most promising technologies currently in development, the work to be carried out in this thesis will investigate the use of an affinity-capture based microfluidic device to enrich a subset of MSCs with therapeutic potential. By taking the advantageous aspects of microfluidic technologies and combining these with the high resolution of an affinity-capture based approach - without the need for extrinsic labelling, this project will develop a novel MSC enrichment device. Furthermore, alternative binding molecules (Affimers - Section 2.5.3.2) as well as commercially available antibodies (Section 2.5.3.3) will be explored as binding molecules to optimise cell capture and release in the device. In order to exploit specific antigen binding technology, an appropriate MSC surface molecule (antigen) must be identified and utilised. In the next section, the specific criteria and nomenclature for MSCs will be discussed, and the most promising surface markers for MSC enrichment reviewed.

2.6 MSC surface antigens for affinity-based cell capture

In advance of reviewing the different MSC surface antigens, it is first necessary to discuss MSC nomenclature and the impact that differing MSC terminology has had on stem cell research - including attempts to standardise definitions and criteria such as specific surface molecule (antigen) expression.

2.6.1 MSC nomenclature and specific surface antigen criteria

MSCs were officially named as mesenchymal stem cells over 25 years ago by US biologist Arnold Caplan (161). This was based on their capacity to be induced to form a variety of mesodermal phenotypes and tissues *in vitro* (162). The term has since been used in over 700 clinical trials (see Figure 2.1) and in more than 32,000 Medline-indexed articles (163). Despite this, MSCs have also been described in numerous other ways, for example; marrow stromal cells, multipotent stromal cells, mesodermal stem cells and mesenchymal stromal cells. The lack of a clear definition has resulted in inconsistencies and ambiguities in stem cell research (163, 164).

Prompted by this, in 2005, the International Society for Cellular Therapy (ISCT) published a position statement for clarification of the nomenclature of MSCs (165). Here it was advised that the term “multipotent mesenchymal stromal cell” should be used for plastic-adherent cells and the term “mesenchymal stem cell” should be reserved for cells that demonstrate stem cell activity defined by clearly stated criteria. The ISCT criteria for MSCs was published in 2006 as follows (164):

- Adherence to plastic
- Specific surface antigen expression (see Table 2.1)
- Multipotent differentiation potential

Table 2.1 ISCT minimal criteria for the specific surface antigen expression of MSCs

POSITIVE (≥ 95%)	NEGATIVE (≤ 2%)
CD105	CD45
CD73	CD34
CD90	CD14 or CD11b
	CD79α or CD19
	HLA-DR

The specific antigen expression criteria ensures there is a lack of expression of haematopoietic antigen that would likely be found in MSC cultures. This includes markers for leukocytes, haematopoietic progenitors, endothelial cells, monocytes and macrophages. The multipotent differentiation potential refers to trilineage differentiation to osteoblasts, adipocytes and chondroblasts under standard *in vitro* differentiating conditions.

Despite these recommendations, the term mesenchymal stem cell is still widely used without observation of the criteria and assays commonly used to evaluate a cell's 'stemness' can be easily misinterpreted (163). Furthermore, as the number of MSC sources increases it has been shown that the gene expression patterns, proteome and functionality of MSCs differs in accordance with their source and no general assumptions can be made between different populations (166).

To date, misperception still exists and in 2017, Caplan suggested that his original nomenclature was misleading and a term such as medicinal signalling cell would be more appropriate (162). He proposed that since the main *in vivo* function of MSCs is not their multipotency, they should not be deemed a stem cell. However this shift in nomenclature is disputed by others in the field concerned that it could heighten assumptions of broad therapeutic use that have not yet been proven (163). It has been suggested that in order to make important advancements in the field of stem cell research, it will be crucial to rigorously control the use of the term MSC and stop its use as an umbrella term for multiple different cell types (163).

With respect to the work carried out in this thesis, one specific cell surface antigen will be used to demonstrate the proof-of-concept of an affinity-capture based microfluidic device to enrich a subset of cells with therapeutic potential. It is noted

that the surface antigens defined by the ISCT do not uniquely identify MSCs and were proposed alongside the functional criteria to best recognise MSCs in line with current knowledge (164). However, these markers are also expressed on many other stromal cells including fibroblasts (166), meaning that they would not be suitable candidates for use as a single MSC marker in this project. Alternative MSC surface molecules have been proposed which could provide a more suitable candidate marker. The efficacy of these markers to be used to enrich a therapeutic population of cells is reviewed in the following section.

2.6.2 Alternative MSC surface molecules (antigens)

In 2014, Lv *et al.* (167) published a review of human MSC surface markers in which four molecules were highlighted as the most commonly used markers to select for MSCs. These four markers are the focus of this next section.

2.6.2.1 STRO-1 selection of MSCs

In 1991, Simmons *et al.* (168) described the generation and specificity of a murine IgM monoclonal antibody termed STRO-1 according to its reactivity with bone marrow stromal elements *in vitro* and *in vivo*. They found that STRO-1+/glycophorin A- cells were enriched 100-fold for colony-forming unit-fibroblast (CFU-F) – an assay used to determine the clonogenic potential of cells and therefore assess the proportion of MSCs in a population. Glycophorin A is a marker associated with erythroid cells and since the majority of STRO-1+ cells co-expressed glycophorin A, they found it was necessary to deplete glycophorin A+ cells to enrich CFU-F.

Psaltis *et al.* (2010)(169) used STRO-1 as a single marker for MSC isolation (without depletion of glycophorin A) and compared the activity of STRO-1+ immunoselected mesenchymal precursor cells (STRO-1-MPC) to cells isolated by plastic adherence (PA-MSC). They found that STRO-1-MPC had greater clonogenicity, proliferative capacity, multilineage differentiation potential and mRNA expression of MSC-related transcripts than PA-MSC. Furthermore, conditioned medium from STRO-1-MPC had greater paracrine activity with respect to cardiac cell proliferation and migration, and endothelial migration and tube formation – demonstrating the cardiovascular regenerative potential of STRO-1-MPC.

Gronthos *et al.* (2003)(170) reported a CFU-F enrichment factor of approximately 5000-fold using STRO-1 in combination with vascular cell adhesion molecule-1 (VCAM-1/CD106) to isolate a minor subpopulation of STRO-1+ selected cells

(1.4 ± 0.3%) which equated to 0.02% of the total BM-MNC population. Cells immunoselected for STRO-1+/VCAM-1+ were also used by Martens *et al.* (2006)(171), in an athymic rat model of acute myocardial infarction which resulted in a dose-dependent induction of arteriogenesis and vascular network formation.

Despite the fact that STRO-1 has been recognised as the 'best-known MSC marker' (172, 173), the molecular identity of the antigen remains elusive (174). It has been suggested that STRO-1 is an endothelial antigen and that its expression in MSCs is induced during *in vitro* culture only (175). This finding is supported by Lee *et al.* (2009)(176) who found that STRO-1 expression increased over 9 days in culture with no initial analysis of an un-cultured population. However it has also been proposed that STRO-1 binds to cell surface heat shock cognate 70 (HSC70/HSPA8) and that additional investigation of this molecule could provide further insight into MSC biology (174).

The practicality of using STRO-1 as an MSC marker for therapeutic applications is limited; it has been found that STRO-1 is not universally expressed in all MSC sources (167), for example there was no expression found in MSCs derived from adipose tissue (177) and umbilical cord matrix (178) - two promising alternative MSC sources to bone marrow. Moreover, the use of STRO-1 as a sole marker would yield an erythroid-contaminated population due to the high percentage (>95%) of STRO-1 cells which co-express glycophorin A (167, 168).

2.6.2.2 CD271 selection of MSCs

CD271 - also named low-affinity nerve growth factor receptor (LNGFR) - is a receptor for neurotrophins which stimulate neuronal cells to survive and differentiate (167). In 2002, Quirici *et al.* (179) found that positive selection using anti-CD271 antibodies isolated a homogenous and multipotent population of cells. They found that CFU-F for CD271+ cells were increased more than 60-fold compared with cells isolated by density gradient centrifugation and no residual CFU-F activity was observed in the CD271- fraction of cells. Furthermore, the CD271+ cells had greater capacity to give rise to adipocyte colonies and displayed increased calcium accumulation in their extracellular matrices after osteogenic differentiation compared to cells isolated by plastic adherence or negative selection of CD45-/glycophorin A- cells.

Since then, Jones *et al.* (2002-2019)(180-186) have published a considerable amount of work regarding a subset of MSCs with phenotype CD271bright/CD45low i.e. high expression of the CD271 antigen and low expression of the CD45 antigen. They demonstrated that there was a significant correlation between the frequency of CFU-F and CD271bright/CD45low cells (180, 184), and that these cells expressed other classic markers of MSCs

including CD73, CD105, CD90, CD106 and alkaline phosphatase (184, 185). They suggested that the enumeration of cells of this phenotype could be used as an indicator of bone marrow sample quality (181) and would be suitable for intra-operative quality control of bone marrow aspirates (180). The work of Jones and colleagues has focused on the identification of MSCs *in vivo* and has found that CD271 is the most differentially expressed marker on MSCs compared to other marrow cell populations (186).

Further evidence supports the concept that CD271+ cells are a therapeutic cell population; Kuci *et al.* (2010)(187) reported their immunosuppressive and haematopoietic engraftment-promoting properties of immunoselected CD271+ cells and Hermida-Gómez *et al*. (2011)(188) reported the involvement of immunoselected CD271+ cells in spontaneous cartilage repair, and the superior quality of chondral repair using this subset of cells. Flores-Torales *et al.* (2010)(189) proposed CD271 as a sole marker for isolating MSCs from fresh samples of bone marrow. In their study, it was found that the percentage of CD271+ cells from 25 donors was significantly correlated with the percentage of CD90+/CD105+/CD45-/CD34-/CD79- cells, markers defined by the ISCT criteria though not inclusive of all specified markers (Section 2.6.1)

Altogether these observations have resulted in the commercialisation of CD271 as a preferred marker for the purification of a homogenous population of cells that contains all bone marrow MSC activity (186, 190). Despite this, similar to STRO-1, CD271 is not a universal marker for MSCs and although CD271+ cells can be isolated from bone marrow and adipose tissue (191), expression was absent in umbilical cord matrix (192) and other sources (167). Furthermore, the necessity to exclude hematopoietic cells (CD34+ and CD45+ cells) prevents CD271 alone from being used to isolate a pure population of therapeutic cells (179, 193).

2.6.2.3 CD146 selection of MSCs

CD146 – also named melanoma cell adhesion molecule (MCAM) - is a cell adhesion protein involved in vascular endothelial cell activity and angiogenesis (167). CD146 expression on MSCs has been correlated to an increased capacity for multipotent differentiation (194), where Russell and colleagues (2010) determined that the tripotent clones expressed higher levels of CD146 than their unipotent counterparts. In addition to this, Sacchetti *et al.* (2007)(195) found that CD146 distinguished bone marrow MSCs from other osteogenic cell strains and was expressed at high levels on CFU-F but was expressed at decreased levels in non-clonal cultures, where mature osteoblastic cells were present. Furthermore, when CD45- cells were selected for CD146 by FACS, CFU-Fs were

enriched more than 800-fold from BM-MNC and ~80 % of CFU-F were recovered in this fraction.

In addition to the clonogenic and multipotent potential of CD146+ cells, Sacchetti *et al.* (2007)(195) demonstrated that CD146+ cells were capable of transferring the haematopoietic microenvironment (HME) to heterotopic sites *in vivo* – revealing functional relationships between the establishment of the HME, progenitor cells in bone marrow and angiogenesis. Before this, relatively little was known about the role that BM-MSCs play in the HME, which is crucial for the regulation and maintenance of haematopoiesis (193). Tormin *et al.* (2011)(193) were then able to provide a greater insight into these relationships with their analysis of co-stained CD146 and CD271 BM-MNCs. In this study it was found that all assayable CFU-Fs were highly and exclusively enriched not only in the CD146+/CD271+ fractions of lineage-depleted cells but also in the CD146-/CD271+ fraction of cells. They found that the differences in CD146 expression correlated with *in situ* localisation of cells and were able to identify a CD146-/CD271+ phenotype for bone-lining cells and a CD146+/CD271+ phenotype for cells located in perivascular regions.

Following this work, Maijenbrug *et al.* (2012)(196) investigated the effects of ageing on these two subpopulations – CD146+/CD271+ and CD146-/CD271+. They found that CD146 expression decreased with age and the main population in adults was CD146-/CD271+ and the main population in paediatric and foetal bone marrow was CD146+/CD271+. This is important to note when considering the application of cell therapies; patients requiring cell therapies could be of any age and therefore a marker that decreases in expression with age would not be suitable unless the relationship was consistent and well defined.

2.6.2.4 Stage-specific embryonic antigen-4 (SSEA-4) selection of MSCs

Stage-specific embryonic antigen-4 (SSEA-4) is an early embryonic glycolipid antigen commonly used as a marker for undifferentiated pluripotent human embryonic stem cells. In 2007, Gang *et al.* (197) proposed that SSEA-4 could also identify an adult mesenchymal stem cell population. They found that approximately 2–4% of human bone marrow cells expressed SSEA-4 and that its expression gradually increased in culture. They also found that when SSEA-4 was used for the prospective isolation of MSCs, SSEA-4+ cells adhered to plastic and formed a homogenous cell monolayer whereas SSEA-4- cells failed to grow. SSEA-4+ cells demonstrated trilineage differentiation potential however no assessment of their clonogenic capacity was reported.

Beyond this work there is little evidence to support SSEA-4 as a reliable MSC surface marker. Zeddou *et al.* (2010)(192) reported the expression of SSEA-4 on MSCs cultured from bone marrow but not umbilical cord matrix, whereas others have reported no SSEA-4 expression on bone marrow cells (193, 198). Notably, there has been no direct comparison of the multipotency and clonogenicity of SSEA-4+ cells compared to cells isolated by plastic adherence or by other molecules (167).

2.6.2.5 Other proposed markers for the selection of MSCs

In addition to the markers discussed above, there have been various other markers used to isolate clonogenic MSCs from BM; including α6-integrin (CD49f) in combination with podocalyxin-like protein (PODXL)(199), stage specific antigen-3 (SSEA-3) in combination with CD105 (200) and CD200 (201). Furthermore, in search of unique MSC markers, research groups have reported molecules that are expressed only on MSCs compared to other marrow cells, such as the neural ganglioside GD2 (202). In further support of the perivascular niche of bone marrow derived MSCs, the pericyte marker 3G5 has been found to be expressed on adherent colony-forming cells (203) and STRO-1 selected cells (204).

Various research has highlighted alternative or additional markers associated with the CD271+ subpopulation of MSCs; Sivasubramaniyan *et al.* (2013)(205) found that the type I integral membrane protein Sushi domain containing 2 (SUSD2) was exclusively expressed on CD271+/CD45- cells and isolation of SUSD2+ cells enriched CFU-F approximately 70-fold. They propose that the W5C5 antibody - which reacts with SUSD2 - could provide a highly specific method for the isolation of BM-MSCs.

Using CD56-specific 39D5 and MSCA-1-specific W8B2 monoclonal antibodies, Battula *et al.* (2009)(206) showed that these reagents were selectively expressed on CD271+ cells and no other bone marrow cells. CD271+/CD56+ and CD271+/MSCA-1+ subpopulations co-expressed established MSC markers and gave rise to CFU-F providing a more specific subset of cells for autologous cell therapies. It must also be noted that the MSCA-1 antigen has been found to be identical to tissue non-specific alkaline phosphatase (TNAP)(207) and TNAP is also thought of as a marker of MSCs. TNAP has been long known as a marker for mineralising cells, however it has also been found that TNAP activity within progenitor cells induces adipocyte and neuron differentiation as well as immunomodulation (208).

2.6.2.6 Summary of alternative MSC surface antigens for MSC selection

Similarly to other properties of MSC, the determination of their specific surface antigen expression has been confounded by a lack of standardisation in the field. Analysis of surface markers has often been acquired after *in vitro* culture which can change the expression of markers according to the cell culture reagents (209) and confluence of cells (176). In addition, different cell sources have been used which further confuse the literature.

While it is still considered that there is no consensus on a single surface molecule to identify MSCs (167), this thesis will focus on the utility of the CD271 antigen as a marker to enrich a therapeutic subpopulation of MSCs from bone marrow aspirate. There has been independent evidence from several research groups that CD271 antibodies can isolate a population of cells from bone marrow which are enriched for CFU-F and demonstrate trilineage differentiation potential. Moreover, CD271 has been shown to be expressed on freshly isolated bone marrow cells which is of crucial concern for this project since the aim is to develop a cell enrichment technology for intraoperative use with no *in vitro* expansion of cells prior to therapy. Finally, unlike STRO-1, the CD271 antigen has been identified, which means CD271 recombinant protein is available to buy – a factor that must be considered for the experiments carried out in this project.

2.7 Summary and considerations for proposed research

In consideration of all the literature, this research project proposes to design and fabricate a microfluidics-based device, with a cell capture surface based on affinity capture, to enrich a subset of CD271+ MSCs from clinical samples of bone marrow aspirate. Controlled flow will allow unbound cells to be washed away resulting in an enriched population of cells for potential use in autologous cell therapies. Mechanisms to release and collect the enriched cells will be explored including investigating pH change and increased fluid flow. In Section 2.5.3.1, the advantages of aptamers for use in specific cell capture were briefly discussed, and in Section 2.5.3.2 peptide aptamers named Affimers were introduced as alternative non-antibody binding proteins. Affimers, as well as commercially available antibodies, will be explored as capture molecules for CD271-expressing cells in the proposed microfluidic device.

Chapter 3: Introduction to research project

This chapter will describe the specific research aim and objectives of this project and outline the results reported in each of the following chapters of work.

3.1 Research aim

The long-term goal of this research is to produce a cell sorting device that will enrich specific cells from clinically relevant samples within intraoperative times and without the need for extrinsic labelling. This would therefore be commensurate with the criteria for minimal manipulation for use in autologous cell therapies. The aim of the research described in this thesis was to develop a prototype microfluidic device for affinity-based capture of CD271+ cells and assess the feasibility of using the device for enriching cells from clinical bone marrow aspirates.

3.2 Research objectives

3.2.1 Objective 1

To screen Affimer libraries in order to identify CD271-specific binding proteins and to investigate their potential use as capture molecules for CD271+ cells

The efficacy of CD271 as a biomarker to be used in order to enrich a therapeutic population of MSCs was described in Section 2.6.2.2. The use of novel peptide aptamers (“Affimers”) as non-antibody protein binding proteins was described in Section 2.5.3.2. The first objective of this research project was to use the *in vitro* screening technique of phage display to select for CD271-specific binding proteins from the Affimer libraries. The specificity of selected Affimers to CD271 would then be investigated and compared to commercially available antibodies with the intention of immobilising the most appropriate binding protein to a solid substrate in a microfluidic channel for specific cell capture (Objective 2).

3.2.2 Objective 2

To design and fabricate a prototype microfluidic device capable of specific capture and release of CD271+ cells

The clinical need for novel MSC enrichment methods was described in Section 2.4.2. The benefits of microfluidic technologies were described in Section 2.5.2.1.

The second objective of this research project was to design and fabricate a prototype microfluidic device with affinity-based capture of CD271+ cells. The device would be designed to overcome the limitations of current MSC enrichment technologies to achieve enrichment with: high specificity, minimal manipulation, no extrinsic labelling of cells and within intraoperative timeframes.

3.2.3 Objective 3

To evaluate the feasibility of specific capture of CD271+ cells from clinical samples of bone marrow aspirate using a prototype microfluidic device

The third objective of this research project was to investigate the CD271+ population of cells in clinical samples of bone marrow aspirate and evaluate the feasibility of enriching the CD271+ subpopulation using the prototype microfluidic device. The efficacy of the device will be compared to current 'gold standard' cell sorting methods - MACS and FACS - and assessed against the required criteria for novel MSC enrichment technologies.

3.3 Chapter outlines

3.3.1 Chapter 4

Chapter 4 describes the materials and methods common to all chapters in this thesis, whereas materials and methods exclusive to one chapter are described in the relevant chapter.

3.3.2 Chapter 5

Chapter 5 describes the results from phage display screening of human recombinant CD271 protein. Three candidate Affimer proteins from the phage display screening were produced and purified and their binding to CD271 recombinant protein characterised using enzyme linked immunosorbent assays and surface plasmon resonance. One Affimer protein was investigated for specific capture of CD271+ cells from dental pulp stromal cells and a CD271+ cell line, assessed via flow cytometry. The specificity of Affimer proteins was compared to a commercially available CD271 antibody and the most suitable binding protein investigated for specific cell capture in a prototype microfluidic device.

3.3.3 Chapter 6

Chapter 6 describes the design, fabrication and optimisation of a prototype microfluidic device. The device was fabricated using soft lithography techniques and specific cell capture and release optimised using a CD271+ cell line and CD271- cells. Analysis of the cells post-enrichment was carried out to assess the viability, proliferation and manipulation (in terms of cell labelling) of enriched cells compared to control cells which had not been enriched in the microfluidic device. The device was also compared to current methods of MSC enrichment – MACS and FACS – in terms of specificity and cell recovery.

3.3.4 Chapter 7

Chapter 7 describes the use of conventional cell enrichment technologies (MACS and FACS) to enrich and characterise a subpopulation of CD271+ cells from clinical samples containing BM-MNCs. Once critical information such as the percentage and number of CD271+ cells was established, the enrichment of CD271+ cells from clinical samples using the prototype device was assessed. The performance of the device was compared to MACS and FACS and evaluated against the criteria required for a novel MSC enrichment technology.

3.3.5 Chapter 8

Chapter 8 discusses the different factors that must be considered for future work and summarises the thesis conclusions.

Chapter 4: Material and Methods

This Chapter will detail the general materials and methods used throughout this thesis. Materials and methods that are specific to only one chapter are detailed in the appropriate chapter of work.

4.1 Cell culture

Cell culture refers to the *in vitro* expansion of cells either harvested directly from the tissue or derived from an established cell line. Cells harvested directly from tissue are known as primary cells, they are cultured until they reach confluence (i.e. occupy all available space in a tissue culture flask) and then subcultured (i.e. passaged) into a new tissue culture flask to allow more room for growth. Cells derived from primary sources have a finite life span before they lose their ability to proliferate. Established cell lines are immortalised through a process called transformation, these cells have the ability to proliferate indefinitely and are known as continuous cell lines (210).

Different cell types require different culture conditions, however, the culture vessel will inevitably contain; a medium that supplies essential nutrients, antibiotics to prevent infection and serum (usually foetal bovine serum, FBS) that provides various hormones, growth and adhesion factors, lipids and minerals (211). Culture vessels are usually kept at 37 °C and at pH 7.4. The growth medium controls the pH by incorporating a bicarbonate based buffer system and the percentage of CO_2 in air is controlled exogenously. All cell culture is maintained in a sterile environment and handled using aseptic technique.

4.1.1 Dental pulp stromal cell (DPSC) culture

Dental pulp stromal cells (DPSCs) were used for flow cytometry experiments to assess whether Affimer proteins bound to CD271+ cells. DPSCs were harvested from extracted third molars obtained with consent through the Leeds School of Dentistry Skeletal Tissues Research Tissue Bank (Dental Research Ethics Committee approval 160916/AP/211). Cells were received cryopreserved at passage 2.

Cells were thawed and resuspended in Minimum Essential Medium (MEM) - Alpha Eagle with Earle’s BSS (Lonza, BE12-169F) supplemented with 10% FBS (Sigma Aldrich, F7524), 1% L-glutamine (200 mM, Sigma, G7513) and 1% penicillin streptomycin solution (P/S, Sigma, P4458). Cultures were incubated at

37 °C, 5% CO_2 and passaged when 80-90% confluent. Cells were detached from culture flasks by addition of 3-5 mL trypsin-EDTA solution (Sigma, T4049). Cells from passages 3 to 5 were used for all experiments.

4.1.2 SH-SY5Y cell culture

SH-SY5Y neuroblastoma cells, which constitutively express CD271, were used to assess whether Affimer proteins bound to CD271+ cells and to optimise cell capture and release in a prototype microfluidic device. SH-SY5Y cells were kindly donated by the Faculty of Biological Sciences (University of Leeds) and received cryopreserved at passage 13. The cells were originally provided to the Faculty of Biological Sciences by Dr. J. A. Sim (University of Manchester, Manchester, UK).

Cells were thawed and resuspended in Dulbecco's Modified Eagle Medium:F12 (DMEM:F12, Lonza, BE12-719F) supplemented with 10% FBS and 1% P/S solution. Cultures were incubated at 37 °C, 5% CO_2 and passaged when 80-90% confluent. Cells were detached from culture flasks by addition of 3-5 mL trypsin-EDTA solution. Cells were used up to passage 30.

4.1.3 Fibroblast cell culture

Human fibroblast cells were used as CD271- cells during the optimisation of specific cell capture in a prototype microfluidic device. Primary dermal fibroblasts from normal adults were purchased from ATCC (PCS-201-012). The cells were thawed and re-suspended in DMEM - high glucose cell culture medium (Sigma, D5671) supplemented with 10% FBS (Sigma Aldrich, F7524), 1% L-Glutamine (200 mM, Sigma, G7513) and 1% P/S solution (Sigma, P4458). Cultures were incubated at 37 °C, 5% CO_2 and passaged when 80-90% confluent. Cells were detached from culture flasks by addition of 3-5 mL trypsin-EDTA solution (Sigma, T4049). Cells were used up to passage 10.

4.2 Surface plasmon resonance (SPR)

Surface plasmon resonance (SPR) is a label-free, non-destructive method to characterise ligand binding. The technique involves immobilising a ligand to a metal film (usually gold) which is placed at the interface of two dielectric media (212)(Figure 4.1). Medium 1 is a prism which has a higher refractive index (n_1), and medium 2 is the analyte solution which has a lower refractive index (n_2). When a plane-polarised light beam hits the prism, the light is bent towards the

plane of the interface when moving from medium 1 to medium 2. Total internal reflection can be achieved by adjusting the incident angle (θ) so it is greater than the critical angle (θ_C)(where $\sin(\theta_C)=n_2/n_1$). Under total internal reflection conditions, evanescent waves are formed in the lower refractive index medium (n_2).

Surface plasmons are electromagnetic waves confined to the metal-dielectric interface. The surface plasmons can be excited by the evanescent wave and this phenomenon is termed surface plasmon resonance (SPR). The magnitude of the wave is related to the dielectric constant of medium 2 and when surface plasmon resonance occurs, the intensity of the reflected light decreases sharply. Adsorption and desorption on the gold surface i.e. analyte association and dissociation, changes the refractive index of medium 2 near the metal-dielectric interface therefore changing the angle required for resonance.

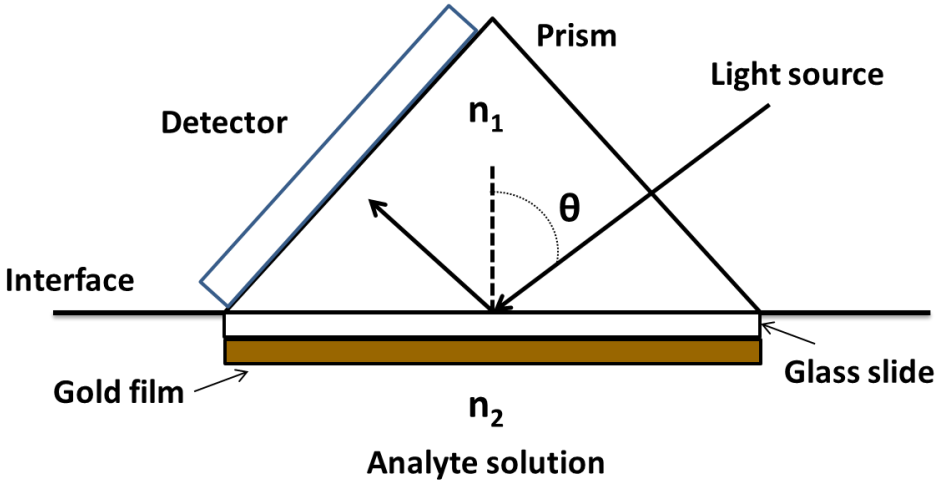

Figure 4.1 Surface plasmon resonance (SPR) schematic

Total internal reflection occurs when the incident angle (θ) is greater than the critical angle (θ_C)(where $\sin(\theta_C)=n_2/n_1$). This causes evanescent waves to form in the analyte solution which has a lower refractive index than the prism ($n_1 > n_2$). Evanescent waves cause surface plasmons at the interface to become excited, termed surface plasmon resonance (SPR). Association and dissociation of analyte causes a change in the refractive index of the analyte solution (n_2) which changes the angle required for SPR.

SPR is an analogous system to the desired method of cell capture within a microfluidic cell enrichment device, making it an ideal method to assess CD271 protein binding to selected Affimer proteins (Section 5.2.10). SPR analysis was also used during the development of the prototype device to assess whole cell

binding to a functionalised surface (Section 6.2.2). The specific protocols for these experiments are described in the respective sections.

4.3 Self-assembled monolayers (SAMs)

Self-assembled monolayers (SAMs) contain a head group, a backbone and a specific terminal group (213). The head group guides the self-assembly process linking the hydrocarbon chain to the surface through a strong bond. The hydrocarbon chains form a packed monolayer through inter-molecular interactions such as van der Waals, and the specific terminal group allows different molecules such as proteins to be anchored to the monolayer.

To create a non-fouling surface for specific cell capture in this work, a polyethylene glycol (PEG) monolayer terminated with a carboxylic acid group (HS-C11-(EG)6-OCH2-COOH, ProChima Surfaces TH 003-m11.n6) was formed on gold-coated surfaces (used for specific cell capture) prior to functionalisation. A non-fouling surface was required to help prevent non-specific adsorption of unwanted cell types in the device, and PEG monolayers are commonly used for this purpose (214).

4.4 Crosslinking chemistry for the immobilisation of proteins to a solid surface

For the work in this thesis, 1-ethyl-3-(3-dimethylaminopropyl)carbodiimide).HCl (EDC) and *N*-hydroxysuccinimide (NHS) crosslinking chemistry was used to immobilise proteins to various different surfaces, including; a CM5 substrate (GE Healthcare, Chapter 5: Section 5.2.10), a gold-coated glass disk (Xantec Bioanalytics, Chapter 6: Section 6.2.2) - both for SPR analysis - and a gold-coated substrate in the prototype microfluidic device (Chapter 6: Section 6.2.3 and 6.2.5). A CM5 substrate has a carboxymethylated dextran matrix attached to a gold surface, whereas the gold-coated substrates were first coated with a SAM terminated with a carboxylic acid group. Carbodiimide compounds are commonly used for labelling or crosslinking to carboxylic acids, and EDC is water soluble so allows for aqueous crosslinking (215).

The crosslinking reaction mechanism is summarised as follows; EDC reacts with carboxylic acid groups on the surface to create an unstable intermediate, NHS is added to form a stable amine-reactive ester which allows for efficient conjugation of primary amines at a physiological pH (Figure 4.2).

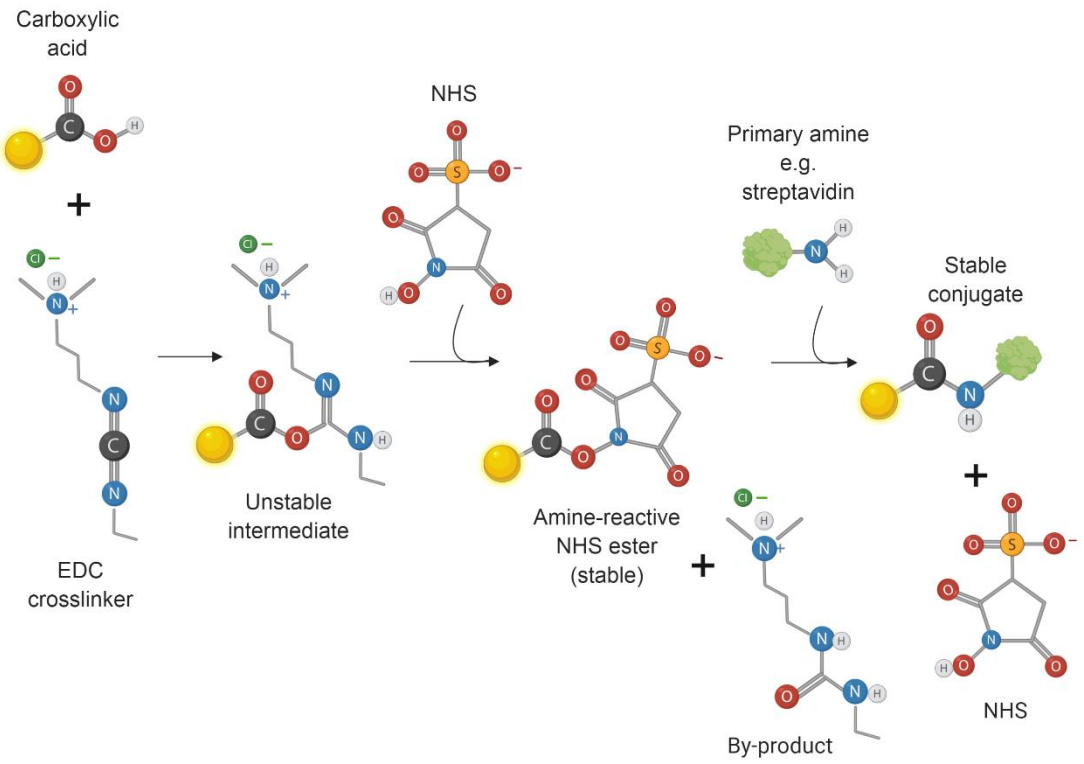

Figure 4.2 EDC crosslinking reaction mechanism

EDC reacts with carboxylic acid groups to form an unstable intermediate. NHS is added to form a more stable amine-reactive ester which reacts with primary amines at physiological pH. This diagram was created with BioRender.com.

4.5 Analysis of flow cytometry data using CytExpert software

CytExpert software was used to analyse all flow cytometry data recorded in this thesis. With the exception of viability testing (Chapter 6: Section 6.3.6), single cells were gated on the occasion of each analysis in order to exclude cellular debris and doublets which could lead to false positive results. An example of the gating strategy is shown in Figure 4.3 for the analysis of SH-SY5Y cells used during the optimisation of cell capture and release in a prototype microfluidic device (Chapter 6: Section 6.3.2).

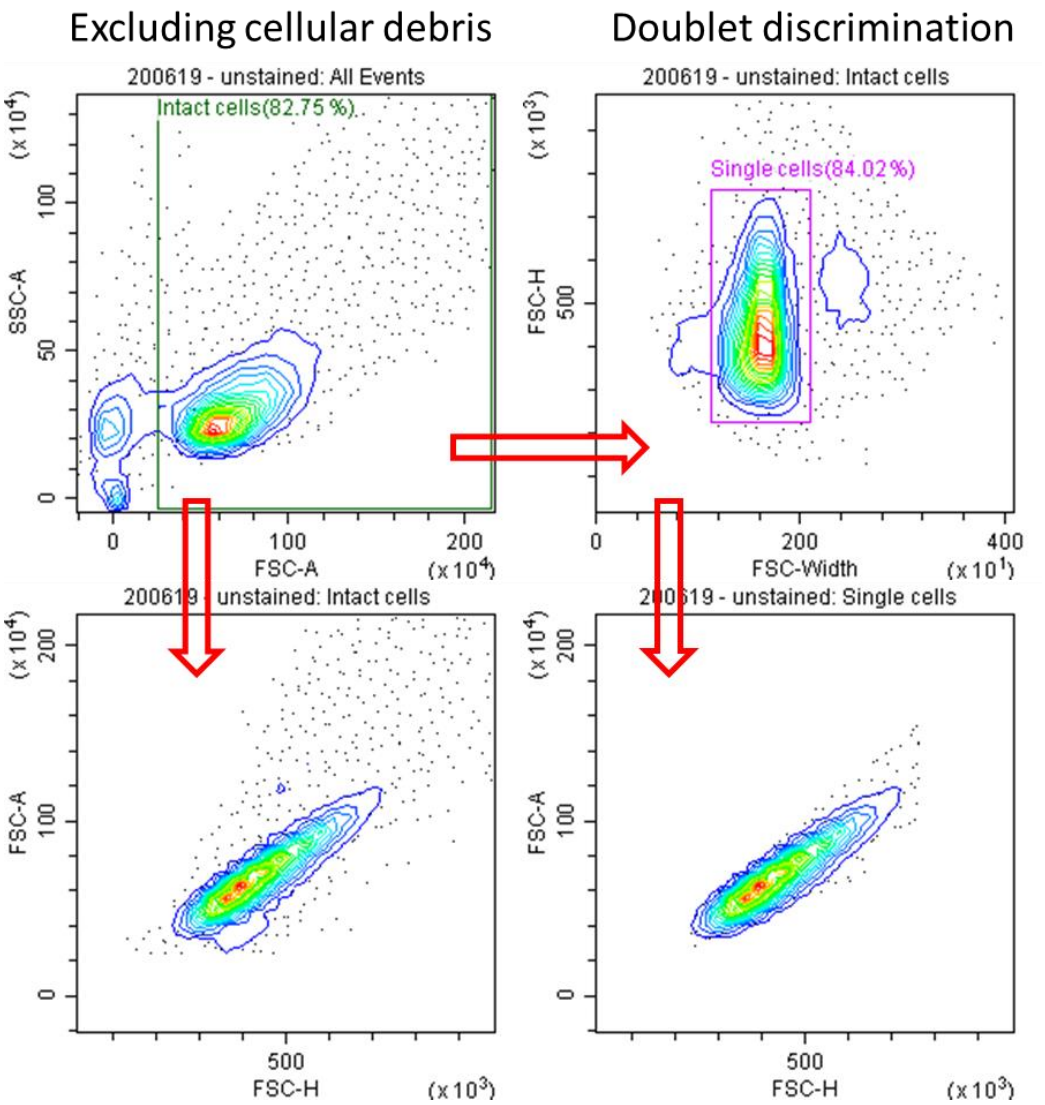

Figure 4.3 Flow cytometry gating strategy for single cells

For all flow cytometry data excluding viability testing, single cells were gated; first, intact cells were gated to exclude cellular debris (top left panel), then single cells were gated to exclude doublets (top right panel). The bottom panels show a comparison of intact cells (bottom left panel) and single cells (bottom right panel) on a forward scatter area against forward scatter height contour plot. Contour plots indicate the density of cells using contour lines and different colours; in CytExpert software, red indicates the area of highest cell density in the centre of the plot and dark blue indicates the areas of lower cell density at the edges of the plot. This example shows the gating of SH-SY5Y single cells used during the optimisation of cell capture and release in a prototype microfluidic device.

4.6 Statistical analysis

All statistical analysis was carried out using IBM SPSS Statistics 25 software. The Shapiro Wilk test of normality was used to assess the distribution of replicates, and if the replicates were normally distributed an independent samples t-test was

used to compare means. If the replicates were not normally distributed, a Mann Whitney U test was used to compare means. For the experiments carried out in Chapter 5, the n value represents the number of technical replicates carried out in each experiment. In Chapters 6 and 7, a minimum of three biological replicates were carried out for each experiment (each replicate carried out on a different day using a different device). In addition, in Chapter 7 where donor samples are used, bone marrow mononuclear cells from multiple donors were combined for each experiment and the n value represents the number of replicates carried out on different days with different donor samples (unless otherwise specified).

Chapter 5:
Identification of suitable binding proteins for the capture of CD271+ cells

5.1 Introduction

To address Objective 1 (Section 3.2.1), this chapter of work aimed to identify a suitable binding protein for the capture of CD271+ cells in a cell enrichment device.

Affimer proteins were selected against human CD271 recombinant protein using phage display (Section 5.3.1), and target-specific clones identified by phage enzyme-linked immunosorbent assay (phage ELISA, Section 5.3.1.4) and DNA sequencing (Section 5.3.1.5). Once target-specific clones were identified, the unique insert sequences were sub-cloned into an *E. coli* expression vector and produced in *E. coli* cells (Section 5.3.2). Affimer proteins were purified and their binding to CD271 protein assessed using ELISA and SPR (Section 5.3.3). Finally, Affimer proteins displaying specific binding to CD271 recombinant protein were investigated for their specific binding to CD271+ cells present in DPSC populations and SH-SY5Y neuroblastoma cells (CD271+ cell line)(Section 5.3.4).

The following sections will detail the processes involved in phage display selection of target-specific Affimers and the production and purification of Affimer proteins.

5.1.1 Phage display

Phage display is a powerful *in vitro* screening technique used to identify ligands for proteins and other macromolecules (216). A filamentous bacteriophage can display polypeptide or protein sequences as fusion coat proteins on the phage surface. This can be used to create libraries of up to 10^{10} different variants (217). The phage phenotype and genotype are physically linked such that the gene encoding the displayed molecule is packed within the same virion as a single-stranded DNA, meaning that identical phage particles will be obtained from the same *E Coli*. clone.

Phage display was used in this work to identify potential ligands for CD271 protein expressed on MSCs. The phage display library was created by the BioScreening and Technology Group (BSTG) at the University of Leeds, and is based on a consensus phytocystatin sequence, modified and truncated for use as a non-antibody protein scaffold now referred to as an Affimer (formerly an “Adhiron”)

(156). Briefly, the coding region of the Affimer scaffold was cloned between NheI and NotI restriction sites in a phagemid vector which allowed the production of an Affimer/truncated-pIII fusion coat protein in ER2738 suppressor cells for phage display. The library was constructed by splice overlap extension of two PCR products to introduce two nine-amino acid variable regions (see Chapter 2: Section 2.5.3.2, Figure 2.11), estimated to contain ~1.3 x 10^{10} independent clones. A small subsection of the library contained only one variable loop region (158).

Phage display relies on multiple cycles of biopanning to select highly specific ligands against target molecules. Figure 5.1 shows a typical biopanning cycle; the target protein is immobilized on a solid substrate, the phage display library is incubated with the immobilized target, unbound phage are washed away and bound phage are eluted and amplified in bacteria ready for the next selection round. In this work, the target protein was biotinylated prior to phage display biopanning facilitating immobilisation to biotin-binding solid substrates. In each biopanning round the biotin-binding substrate was changed to minimise non-specific binding. After three biopanning rounds, the binding activity of bound phage was tested in a phage ELISA (see Section 5.1.2).

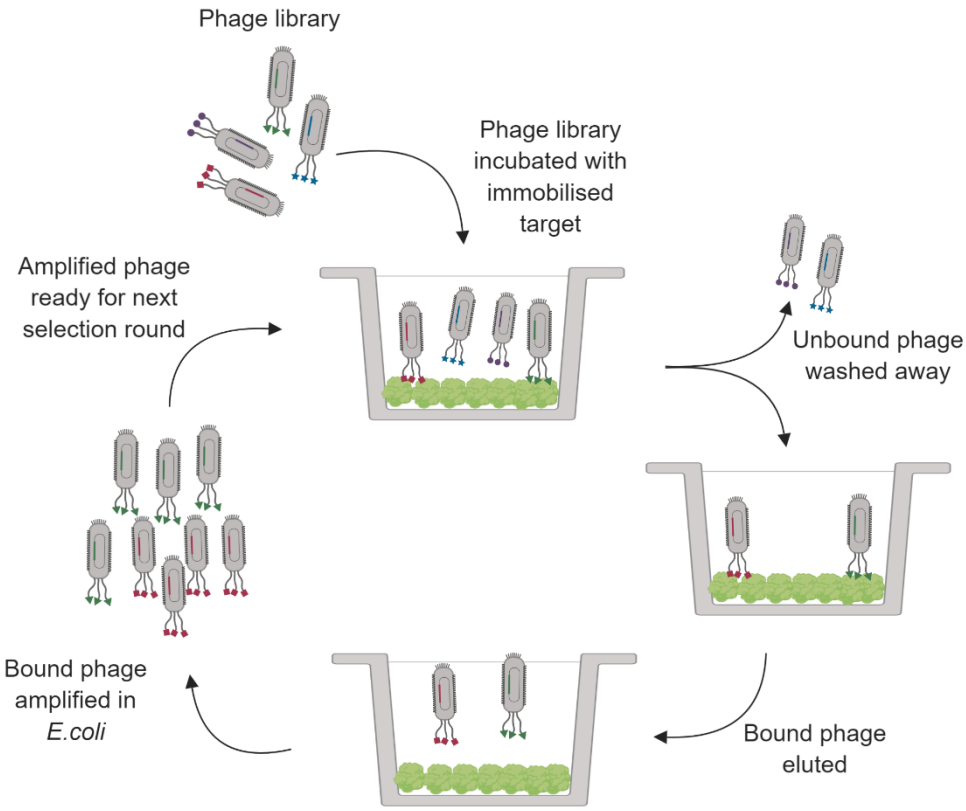

Figure 5.1 Schematic illustrating phage display biopanning

The phage library is incubated with an immobilised target and unbound phage are washed away. Bound phage are eluted and amplified in *E. coli* cells ready for the next biopanning round. Typically three or four rounds of biopanning are carried out in order to enrich target-specific ligands with the desired binding behaviour. This diagram was created with BioRender.com.

5.1.2 Enzyme-linked immunosorbent assay (ELISA)

An enzyme-linked immunosorbent assay (ELISA) is a plate-based assay which enables the quantification of substances such as proteins, peptides and hormones (218). There are various formats an ELISA can be carried out in however the principle remains the same - an antigen is immobilised to a plate and recognised by, and then complexed with, an antigen-specific antibody conjugated to an enzyme. The enzyme activity can be detected by reaction with a substrate that produces a measurable product. The enzyme used for detection in this work was horseradish peroxidase (HRP) which reacts with 3,3',5,5'-tetramethylbenzidine (TMB) substrate to produce a soluble blue product measured at 620 nm. ELISAs were used in this study for two purposes; to check that proteins were successfully biotinylated, and to assess the binding activity of different clones isolated by phage display. The different ELISA formats used in the work in this chapter are outlined below.

5.1.2.1 Direct ELISA to check for biotinylation

The ELISA format used to check the successful biotinylation of proteins was a direct ELISA. The biotinylated protein was directly adsorbed onto the well plate and a streptavidin-HRP conjugate was used for detection (Figure 5.2). This detection strategy takes advantage of the well-known avidin-biotin interaction, which is the strongest non-covalent interaction known (219). A streptavidin molecule can bind up to four biotin molecules making it an ideal approach for the detection of bound molecules.

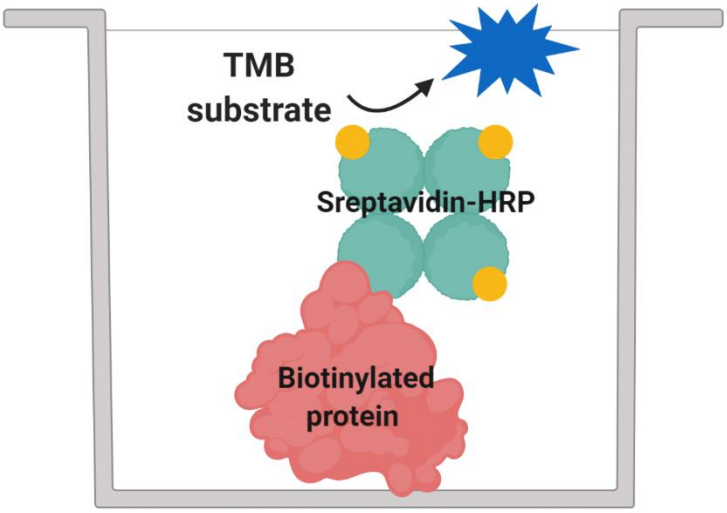

Figure 5.2 Direct ELISA format for detecting biotinylated protein

In the direct ELISA format, a protein is directly adsorbed onto a solid substrate and complexed with a primary antibody conjugated to an enzyme. In this case, the protein is biotinylated and streptavidin is used instead of a primary antibody, which is conjugated to HRP and detected via reaction with TMB substrate. This diagram was created with BioRender.com.

5.1.2.2 Sandwich ELISA to assess binding behaviour of individual clones

A phage ELISA was carried out to assess the binding behaviour of clones selected by phage display biopanning. The format of the phage ELISA was a “sandwich” ELISA with indirect detection. The wells were coated with streptavidin as a capture molecule for the biotinylated target protein and bound phage was detected via an anti-phage-HRP antibody (Figure 5.3).

Sandwich ELISAs were also carried out to assess the binding behaviour of purified Affimer proteins - streptavidin was again used as a capture molecule and HRP-conjugated secondary antibodies were used as detection molecules.

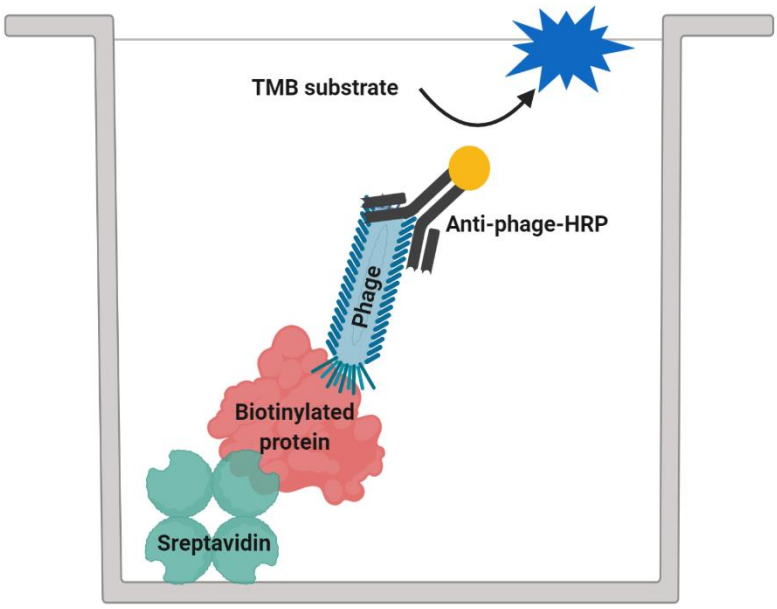

Figure 5.3 Sandwich ELISA format for assessing phage binding behaviour to target protein

In a sandwich ELISA, a capture molecule is used to immobilise the antigen to a solid substrate. In this case, streptavidin was used to capture biotinylated proteins. Bound phage was detected via an anti-phage-HRP secondary antibody and HRP activity measured using TMB substrate. This diagram was created with BioRender.com

5.1.3 DNA sequencing

DNA sequencing is the process of determining the nucleotide sequence of a piece of DNA. This is commonly carried out by Sanger sequencing, where the target DNA is first copied many times making fragments of different lengths. At the end of each fragment is a dideoxy nucleotide which terminates the chain and is marked with a particular colour of dye depending on the nucleic base (A, T, C or G)(220). The dye at the end of each fragment can be detected and produces a chromatogram where the DNA sequence can be read from the peaks.

To identify the phage display clones responsible for specific binding in the phage ELISA, clones were sent to an external facility for DNA sequencing. DNA sequencing was also carried out after DNA sub-cloning (Section 5.1.4.2) to confirm the correct Affimer sequence had been cloned.

5.1.4 Recombinant protein production and purification methods

Recombinant proteins are widely used throughout biological and biomedical sciences and the technology of their production and purification is now relatively simple (221). Despite this, different proteins require different protocols and these must be optimised for each individual protein. The strategy used for Affimer protein production and purification has been previously optimised by the BSTG and is outlined in Figure 5.4. In the following section, the individual techniques involved are described.

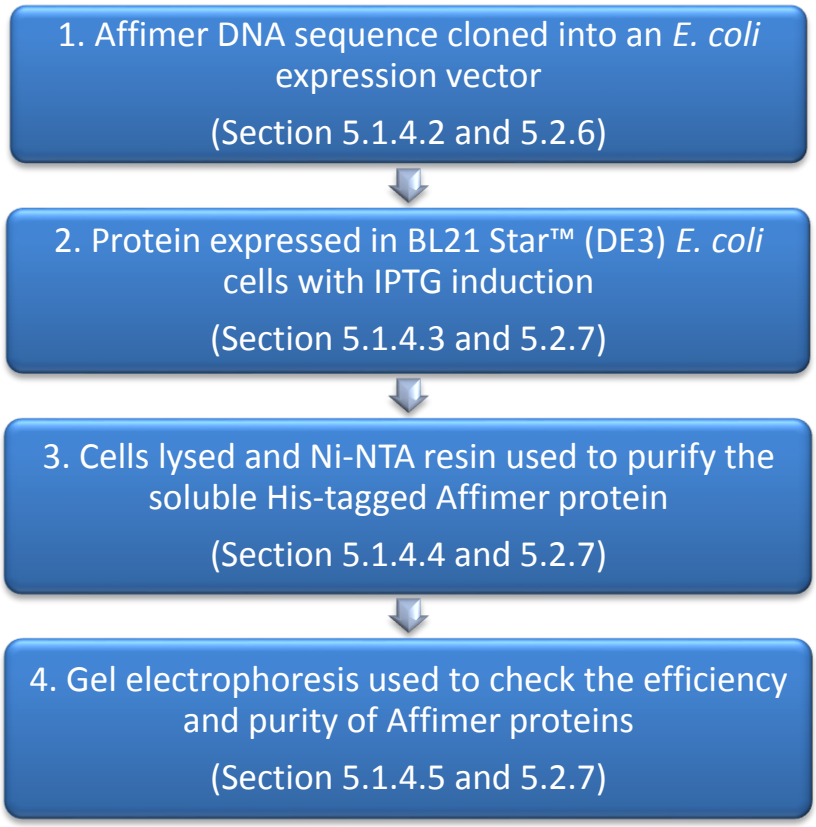

Figure 5.4 Affimer protein production and purification overview

5.1.4.1 Polymerase Chain Reaction (PCR)

Affimer insert sequences are amplified prior to DNA sub-cloning using the polymerase chain reaction (PCR). PCR is based on the ability of DNA polymerase to synthesize DNA complementary to a template strand (222).

Briefly, a DNA template that contains the target sequence is heated to a high temperature to denature the DNA strands. A primer sequence (complementary to the target sequence) is required to provide the starting point for DNA polymerase and nucleotide bases are added to provide the ‘building blocks’ for

new DNA strands. The temperature is lowered to enable the DNA primers to attach to the template DNA, then raised again for the polymerase to make new strands of DNA. Through repeated cycles, thousands to millions of DNA copies are generated (223).

5.1.4.2 DNA sub-cloning

Recombinant DNA technology is the process of joining two or more DNA segments to generate a single molecule capable of autonomous replication in a given host (224). In the case of DNA sub-cloning, a previously cloned DNA segment is the insert sequence, cloned into a plasmid or bacteriophage cloning vector.

Figure 5.5 shows a schematic of a basic sub-cloning protocol; both insert DNA and vector DNA are treated with restriction endonucleases and purified using agarose or polyacrylamide gel electrophoresis (Section 5.1.4.5). The digested components are combined and treated with DNA ligase, then introduced into competent *E. coli* cells. An antibiotic resistance gene in the plasmid allows transformants to be identified by using the appropriate antibiotic in cell cultures.

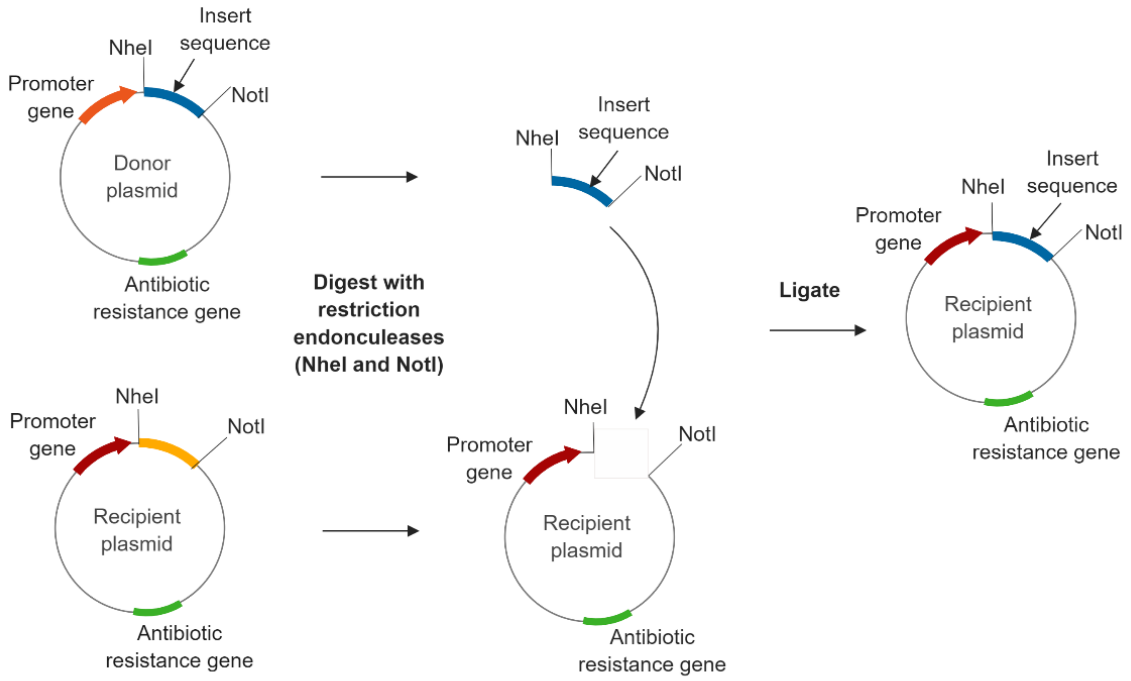

Figure 5.5 DNA sub-cloning schematic

A basic protocol for DNA sub-cloning involves digesting both donor plasmid and recipient plasmid with restriction endonucleases and ligating the digested products. An antibiotic resistance gene is included so that transformants can be selected. This diagram was created with BioRender.com

5.1.4.3 Protein expression in *E. coli* cells

E. coli as an expression host is fast, inexpensive and useful in many cases of protein production (221). For Affimer protein production, the BL21 Star™ (DE3) *E. coli* strain is commonly used which is compatible with the T7 *lac*O promoter system. Affimer proteins are produced as fusions to an N-terminal hexahistidine affinity tag which enables purification via immobilised metal affinity chromatography (Section 5.1.4.4).

Using a T7 system, protein expression is induced using isopropyl-β-D-thiogalactoside (IPTG) which triggers transcription of the lac operon. Cells are grown to high densities and IPTG is added at mid-to-late log phase of growth to achieve maximal yields. A low temperature (25 °C) is used during induction so that recombinant proteins remain soluble.

5.1.4.4 Protein purification using immobilised metal affinity chromatography (IMAC)

Once the recombinant protein has been expressed in *E. coli* cells, it is extracted by cell lysis. The lysis buffer contains a cocktail of enzymes and protease inhibitors to break down the cell wall, and has a relatively high ionic strength to promote protein solubility and stability. The soluble protein can then be purified using immobilised metal affinity chromatography (IMAC). This process uses a resin such as nickel-nitrilotriacetic acid (Ni-NTA)(for His-tagged proteins) where the histidine residues bind to the nickel ions whilst other proteins can be washed away. The His-tagged protein can be eluted using an elution buffer with a high concentration of imidazole (300 mM) which competes for binding to the nickel resin. Wash buffers contain a low concentration of imidazole (20 mM) to elute weakly bound contaminants.

5.1.4.5 Polyacrylamide and agarose gel electrophoresis

Gel electrophoresis is a method used to separate mixtures of DNA, RNA or proteins according to their molecular size (225). An electrical field is applied such that one end of the gel is positively charged and the other is negatively charged. Molecules move through the gel according to their size and charge with smaller molecules travelling at a faster speed. DNA and RNA are negatively charged molecules and are therefore pulled towards the positive end of the gel. However proteins may not carry an appropriate negative charge and are mixed with a detergent – sodium dodecyl sulphate (SDS) - beforehand. This causes the proteins to unfold and have a negative charge proportional to the polypeptide chain length.

Typically DNA and RNA fragments are separated on agarose gels and proteins on SDS polyacrylamide (SDS-PAGE) gels. A DNA-binding dye is used in the agarose gel solution which can be visualised under UV light. Coomassie blue is used to stain SDS-PAGE gels where the intensity of the bands is usually proportional to the amount of protein, providing a semi-quantitative method.

5.1.5 Mass spectrometry

Mass spectrometry measures the mass to charge ratio (*m/z*) of ions and can be used for a number of applications including proteomics. For this work, mass spectrometry was used to determine the mass of an Affimer protein before and after reaction with biotin-maleimide (Section 5.2.9).

In mass spectrometry, samples are loaded into a mass spectrometer, vaporised, and ionised by an ion source. The mass spectrometer used in this case was an ion mobility enabled mass spectrometer (IMEMS) which uses Travelling Wave Ion Mobility. In an IMEMS, ions move through a buffer-filled guide where their charge determines the magnitude of the interaction with the buffer gas, which affects the mobility of the ions (226). The ions are therefore separated, and then detected.

5.2 Materials and Methods

5.2.1 Biotinylation of phage display target: CD271-His recombinant protein

The target protein was biotinylated prior to phage display biopanning to facilitate immobilisation to biotin-binding substrates.

Human CD271-His recombinant protein was purchased from Sino Biological (13184-H08H) and biotinylated according to a protocol previously optimised by the BSTG. Protocols optimised by the BSTG were used throughout phage display screening (Section 5.2.3), for DNA sub-cloning (Section 5.2.6), and for Affimer protein production and purification (Section 5.2.7).

A 10 mM solution of EZ-Link® NHS-SS biotin (Thermo Scientific, 21441) in dimethylsulphoxide (DMSO, Sigma-Aldrich, D8418) was prepared and 0.64 µL incubated with CD271-His recombinant protein (0.2 mg/mL, 130 µL) for 1 h at RT. The amount of biotin solution used was proportional to the molecular weight of the protein (45-60 kDa). To remove excess biotin, Zeba Spin Desalting Columns, 7K MWCO (Thermo Scientific, 89882) were used according to the manufacturer's instructions. An equal volume of 80% glycerol was added to the biotinylated protein and stored at -20 °C.

5.2.2 Direct ELISA to determine biotinylation of target protein

A direct ELISA (Section 5.1.2.1) was carried out to check that the target protein had been successfully biotinylated.

Phosphate-buffered saline (PBS) was aliquoted into Nunc-Immuno™ MaxiSorp™ strips (Thermo Scientific, 469949, 50 µL per well) and biotinylated CD271-His protein was added in different volumes (1 µL and 0.01 µL) to two wells. Two additional wells contained PBS only. The wells were incubated at 4 °C overnight then washed 3x with 300 µL PBST (PBS containing 0.1% Tween 20)

on a plate washer (TECAN HydroFlex). Wells were blocked with 10x Blocking Buffer (Sigma, B6429, 250 µL per well) and incubated for 3 h at 37 °C before washing was repeated (3x 300 µL PBST). High sensitivity streptavidin-HRP (Thermo Scientific, 21130) was diluted 1:1000 in 2x Blocking Buffer (10x Blocking Buffer diluted in PBST) and 50 µL was added to each well. After 1 h incubation on a vibrating platform shaker (Heidolph VIBRAMAX 100; speed setting 3) the plate was washed 6x (300 µL PBST) and 50 µL TMB substrate (SeramunBlau® fast TMB substrate solution, Seramun, S-001-TMB) added per well. The colour was allowed to develop for 5 min and the absorbance was measured at 620 nm.

5.2.3 Phage display screening of target protein: biotinylated CD271-His recombinant protein

Two phage display screens of biotinylated CD271-His protein were carried out using two slightly different protocols. The first protocol included overnight washing with the aim to wash away any weakly bound or non-specifically bound phage (**protocol 1**). The second protocol eliminated the overnight washing steps in order to capture clones with weaker affinity to the target protein (**protocol 2**). The second protocol also eluted bound phage to investigate change in pH as a possible release mechanism in the final cell enrichment application.

In the first phage display screen, a yeast small ubiquitin-like modifier (ySUMO) protein was screened alongside CD271-His protein as a positive control known to produce hits from the Affimer library (156). In the second phage display screen, a tubulin protein was used as a positive control (158). In both screens, the first biopanning round was carried out on streptavidin-coated wells, the second on streptavidin-coated magnetic beads, and the third on NeutrAvidin-coated wells. The solid substrate was changed in each biopanning round to reduce non-specific binding.

5.2.3.1 First biopanning round

Streptavidin coated (high binding capacity) 8-well strips (Thermo Scientific, 15501) were blocked with 2x Blocking Buffer (250 µL per well) and incubated overnight at 37 °C. The phage display library (40 µL) was diluted 1 in 10 with 2x Blocking Buffer and pre-panned in the pre-blocked wells for 2 h on a vibrating platform shaker at RT. The phage were moved to a new pre-blocked well every 40 min. Pre-panning was carried out to reduce non-specific binding to the streptavidin-coated wells. At the same time, biotinylated target was immobilised to a pre-blocked streptavidin-coated well by incubating for 2 h on a vibrating platform shaker at RT.

Immobilised target protein was washed 3x with PBST (300 µL per well) on a plate washer. The pre-panned phage was added to the target wells and incubated for 2 h on a shaker (125 rpm). The plate was washed 27x with PBST (300 µL per well) to wash away unbound phage. Bound phage were eluted by addition of glycine-HCl (0.2 M, 100 µL, pH 2.2) for 10 min at RT, then neutralised with tris-HCl (1 M, 15 µL, pH 9.1) and incubated with ER2738 *E. coli* cells in 2TY media[1] (8 mL, A_{600} ~0.6). Any bound phage remaining in the target well was eluted with addition of triethylamine (Sigma-Aldrich, T0886, 1 mM in PBS, 100 µL, pH 10.75) for 6 min at RT, neutralised with tris-HCl (1 M, 50 µL, pH 7) and added to the ER2738 *E. coli* cell culture.

The cell culture was incubated for 1 h at 37 °C shaking at low speed (90 rpm). Phage-infected ER2738 cells (1 µL – representing 100 - 250 colony forming units) were plated on a LB carb plate (lysogeny broth agar plates containing 100 µg/mL carbenicillin) and incubated overnight at 37 °C. The remaining cells were centrifuged at 3000 g for 5 min then plated on a LB carb plate and incubated overnight at 37 °C.

Colonies on the 1 µL plate were counted and the total number of colony forming units per 8 mL cell culture was calculated. The plate containing the remaining cells was scraped and diluted in 2TY carb (2TY media containing 100 µg/mL carbenicillin) to make 8 mL cultures (A_{600}=0.2). Cell cultures were incubated for 1 h at 37 °C, 230 rpm. M13K07 helper phage (0.32 µL, titre ca. 10^{14}/mL) was added and incubated for a further 30 min at 37 °C, 90 rpm. Kanamycin (25 mg/mL, 16 µL) was added and incubated overnight at 25 °C, 170 rpm.

The phage-infected cultures were centrifuged at 3500 g for 10 min. The phage-containing supernatant was transferred to a fresh tube and a small aliquot was taken for the second biopanning round. Polyethylene glycol-sodium chloride (PEG-NaCl) precipitation solution (2 mL, 20% (w/v) PEG 8000, 2.5 M NaCl) was added to the remaining supernatant and incubated overnight at 4 °C. The precipitated phage was centrifuged at 4,816 g for 30 min, the pellet resuspended in TE buffer[2] (320 µL) and stored at 4 °C.

5.2.3.2 Second biopanning round

Streptavidin beads (Dynabeads® MyOne™ streptavidin T1, 10 mg/mL, Invitrogen, 656.01/656.02, 20 µL) were washed 2x in PBST and blocked using 2x Blocking Buffer (100 µL) overnight on a Stuart SB2 fixed speed rotator (20 rpm). The beads were centrifuged at 800 g for 1 min and immobilised on a magnet. The

[1] 2TY media (per litre): 10 g yeast extract, 16 g tryptone, 5 g sodium chloride
[2] TE buffer: 10 mM Tris, 1 mM EDTA, pH 8.0

phage-containing supernatant from the first biopanning round was blocked with 10x Blocking Buffer (60 µL) and pre-panned on the pre-blocked streptavidin beads for 2 h on the fixed speed rotator. At the same time, biotinylated target (10 µL) was added to pre-blocked beads with 2x Blocking Buffer (300 µL) and incubated for 2 h on the rotator to immobilise the target protein.

The beads with immobilised protein were centrifuged at 1000 g for 1 min, placed on a magnet and washed 3x in 2x Blocking Buffer (1 mL). The beads with pre-panned phage were centrifuged at 1000 g for 1 min and placed on a magnet so that the supernatant containing the pre-panned phage could be removed and added to the immobilised target. The pre-panned phage and the beads with immobilised target were mixed and transferred to pre-blocked wells of a deep well 96 plate (Thermo Scientific, 95040450).

For protocol 1: A pre-programmed protocol “Phage_Display_Competition” (see Appendix A: KingFisher Flex Protocol “Phage_Display_Competition”) was used on the KingFisher Flex (an automated system for handling magnetic beads). At the end of the protocol, the beads were released into PBS (100 µL) and transferred into Protein LoBind Tubes. The wells were washed with PBST with 20% glycerol (200 µL) and added to the tubes to a total volume of 1 mL. The tubes were incubated for 24 h on a rotator with 1x buffer change. The samples were centrifuged at 800 g for 30 s then transferred to a pre-blocked deep well 96 well plate. A second pre-programmed protocol “Phage_Display_Wash_Elute” (see Appendix B: KingFisher Flex Protocol "Phage_Display_Wash_Elute") was used on the Kingfisher Flex to elute the phage into glycine-HCl and triethylamine as in the first biopanning round.

For protocol 2: A pre-programmed protocol “Phage_Display_Standard” (see Appendix C: KingFisher Flex Protocol “Phage_Display_Standard”) was used on the KingFisher Flex. At the end of the protocol the beads were released into glycine-HCl, then triethylamine, and neutralised with tris-HCl as in the first biopanning round. No overnight washing was carried out.

For both protocols, once the bound phage had been eluted, samples were treated in the same way as the first biopanning round; incubation with ER2738 *E. coli* cells (8 mL cultures), plated on LB carb plates overnight and phage prepared for the third biopanning round using M13K07 helper phage.

5.2.3.3 Third biopanning round

NeutrAvidin Coated (HBC) 8-well strips (Thermo Scientific, 15508) were blocked with 2x Blocking Buffer (250 µL) and incubated overnight at 37 °C. Phage containing supernatant (220 µL) from the second biopanning round was pre-panned in the pre-blocked wells for 4 h at RT, shaking (Heidolph VIBRAMAX 100;

speed setting 3). The pre-panned phage was moved to a new well every hour. At the same time, biotinylated target (10 µL) was incubated in a pre-blocked well for immobilisation.

The immobilised target and a blank negative control well (also pre-blocked) were washed 3x with PBST (300 µL per well) on a plate washer. Pre-panned phage (100 µL) and 10x Blocking Buffer (40 µL) were added to the target well and the negative control well, and incubated for 1 h on a shaker. Wells were washed 27x with PBST (300 µL per well) on a plate washer.

For protocol 1: PBST with 20% glycerol (250 µL) was added and incubated shaking overnight with 1x buffer change. Wells were washed 27x with PBST (300 µL per well) on a plate washer. The bound phage was eluted as previously described and added to ER2738 cell cultures.

For protocol 2: No overnight washing was carried out. Bound phage were eluted at pH 9, pH 7, pH 5 and using the standard protocol with pH 2.2 and pH 10.75 (Section 5.2.3.1). Each elution was neutralised with tris-HCl (1 M, pH 7, 50 µL) and added to separate ER2738 cell cultures.

For both protocols, after 1 h amplification in *E. coli* cells (5 mL cultures), a range of volumes (0.1 µL, 1 µL, 10 µL) were plated on LB carb plates and incubated overnight at 37 °C. Ten microlitres of cell suspension containing phage eluted from the negative well was also plated for comparison.

5.2.4 Phage ELISA to assess the binding behaviour of individual clones

A sandwich ELISA (section 5.1.2.2) was carried out to investigate the binding behaviour of individual clones from the final round of phage display biopanning.

Colonies from the final round of biopanning were picked and grown in a 96-well V-bottom deep well plate in 2TY carb (200 µL per well) overnight at 27 °C, shaking (750 rpm, Heidolph incubator 1000 and Titramax 1000). The overnight culture (10 µL) was transferred to fresh 2TY carb (200 µL) and incubated for 1 hour at 37 °C, 1200 rpm. M13K07 helper phage (titre ca. 10^{14}/mL) was diluted 1:1000 in 2TY carb and added (10 µL per well) to the fresh cultures. The cultures were incubated for 30 min at 400 rpm. Kanamycin stock (25 mg/mL) was diluted 1:20 in 2TY carb and added at 10 µL per well to the phage-infected cultures. The cultures were incubated overnight at RT and 750 rpm.

Streptavidin in PBS (2.5 µg/mL) was aliquoted (50 µL per well) into F96 Maxisorp Nunc-immuno plates (Thermo Scientific, 442404) and incubated overnight at

4 °C. The plates were blocked with 3x Blocking Buffer (100 µL per well) and incubated overnight at 37 °C. The plates were washed 1x with PBST (300 µL per well) on a plate washer. Biotinylated target protein was diluted 1:100 in 2x Blocking Buffer and aliquoted (50 µL per well) in one half of the plate and 2x Blocking Buffer (50 µL per well) was incubated in the second half of the plate (negative control wells). The plates were incubated for 2 h at room temperature, 300 rpm, then washed 1x with PBST (300 µL per well).

The phage-infected cultures were centrifuged at 3500 g for 5 min. The phage-containing supernatant was added (40 µL per well) with 10x Blocking Buffer (10 µL per well) to one well with biotinylated target and one negative control well. The plate was incubated for 1 hour at RT and 300 rpm. After 1x wash with PBST (300 µL per well), anti-Fd-Bacteriophage-HRP (Seramun Diagnostica GmbH, A-020-1-HRP) was diluted 1:1000 in 2x Blocking Buffer and added at 50 µL per well. The plate was incubated for 1 h at 300 rpm and washed 6x with PBST (300 µL per well). TMB substrate (Seramun, S-001-TMB) was aliquoted at 50 µL per well and the colour developed for 5 min. The absorbance was measured at 620 nm on a microplate reader.

5.2.5 DNA sequencing of individual clones from the phage ELISA

Clones that demonstrated target-specific binding in the phage ELISA were sent to an external facility for DNA sequencing (Section 5.1.3).

Phage-infected cultures (1 µL) prepared for the phage ELISA were transferred to 2TY carb (4 mL) and grown overnight at 37 °C at 230 rpm. The cells were centrifuged at 4700 g for 15 min and the plasmid DNA extracted and purified using a QIAprep Spin Miniprep Kit (QIAGEN, 27106) according to the manufacturer's instructions. The DNA was eluted in 50 µL purified water and sent to Genewiz for sequencing (15 µL at 100 ng/µL).

5.2.6 Sub-cloning of unique DNA sequences

Unique DNA sequences were subcloned (Section 5.1.4.2) from the pDHis phagemid vector to a pET11a expression vector for Affimer protein production and purification.

The pET11a plasmid was digested with NheI and NotI restriction enzymes; pET11a plasmid (50 µg), sterile deionised water (150 µL), CutSmart™ Buffer (50 µL, supplied with NEB restriction enzymes), NheI-HF™ (25 µL, NEB, R3131S) and NotI-HF™ (25 µL, NEB, R3189S) were mixed and incubated for 6 h at

37 °C. The total volume was divided between four tubes and Antartic Phosphatase Reaction Buffer (14 µL, 10x, NEB, B0289S) and Antartic Phosphatase (1 µL, 5000 units/mL, NEB, M0289S) were added and incubated for 15 min at 37 °C. The tubes were incubated at 65 °C for 5 min to heat inactivate the Antartic Phosphatase. A 10x Orange G Loading Dye (14 µL, 30% Glycerol; 0.2% Orange G; H_2O) was added and the digested vector separated on a 0.7% agarose gel. The digested vector was extracted from the gel using a FastGene Gel Extraction/PCR kit (FastGene, FG-91302) according to the manufacturer's instructions. The vector DNA was stored at -20 °C.

DNA sequences from the phagemid vector were amplified using PCR (Section 5.1.4.1); sterile water (14.3 µL), 5x Phusion HF Buffer (5 µL, supplied with Phusion DNA polymerase), dNTP Mix (25 mM, MP Biomedicals, NTPMX255), DMSO (0.75 µL, supplied with Phusion DNA polymerase), Forward Primer (5' – ATGGCTAGCAACTCCCTGGAAATCGAAG, 10 µM, 2 µL), Reverse Primer (5' – TTACTAATGCGGCCGCACAAGCGTCACCAACCGGTTTG, 10 µM, 2 µL), Phusion High-Fidelity DNA Polymerase (0.25 µL, Thermo Scientific, F-530) and template DNA (phagemid vector, 0.5 µL, 100 ng/µL) were mixed. The PCR thermocycling conditions are shown in Table 5.1. DpnI (0.5 µL, NEB, R0176) was added to each PCR tube and incubated for 1 h at 37 °C. The amplified DNA was purified using a FastGene Gel Extraction/PCR kit according to the manufacturer's instructions and eluted in 50 µL sterile water.

Table 5.1 PCR thermocycling conditions

Cycle step	Temperature (°C)	Time	Cycles
Initial denaturation	98	30 s	1
Denaturation	98	20 s	30
Annealing	54	20 s	
Extension	72	20 s	
Final extension	72	10 min	1
Hold	4	Hold	

The PCR-amplified DNA sequences were digested with the same restriction enzymes as the pET11a vector. Sterile water (3.5 µL), CutSmart™ Buffer (6 µL), NheI-HF™ (0.25 µL) and NotI-HF™ (0.25 µL) were added and incubated at 37 °C overnight. The digest products were purified using a FastGene Gel

Extraction/PCR kit according to the manufacturer's instructions. The insert DNA was separated on a 2% agarose gel and stored at -20 °C.

Digested insert DNA was ligated with digested pET11a vector DNA; 10x T4 DNA ligase buffer (supplied with T4 DNA ligase), vector DNA (75 ng), insert DNA (25 ng), sterile water (14 µL) and T4 DNA ligase (1 µL, NEB, M0202) were incubated at RT overnight. A ligation reaction was also set up with no insert DNA as a negative control. The ligation reactions were transformed into XL1-Blue supercompetent cells (Agilent Technologies, 200236), plated on LB carb plates and incubated overnight at 37 °C.

Single colonies were picked and grown in 4 mL 2TY carb overnight at 37 °C, 230 rpm. The cultures were centrifuged at 4816 g for 15 min and the plasmid DNA extracted using QIAprep Spin Miniprep Kit (QIAGEN, 27106) according to the manufacturer's instructions. Aliquots (15 µL, 100 ng/µL) of each DNA sample were sent for DNA sequencing (Genewiz) to ensure the correct sequence had been sub-cloned into the pET11a vector.

5.2.7 Affimer protein production and purification

Once it had been confirmed that the intended sequence had been sub-cloned into the pET11a vector, Affimer protein was produced and purified as described below.

The DNA sequences were transformed into BL21 Star™ (DE3) chemically competent *E. coli* cells (Life Technologies, C6010-03), plated on LB carb plates and incubated overnight at 37 °C. A single colony was picked from each plate and grown up in 2TY carb (7 mL) at 37 °C, 230 rpm for 5 h. The starter culture (5 mL) was transferred to pre-warmed 2TY carb (400 mL) and grown to OD_{600} ~0.8. The cultures were induced with IPTG (200 µL, 1 M) and incubated overnight at 25 °C and 150 rpm. Cells were harvested by centrifugation at 4816 g for 15 min. The cell pellets were resuspended in a 1:50 ratio (of original culture volume) in lysis buffer[3] (to a total volume of 8 mL) supplemented with Lysozyme® (80 µL, Sigma-aldrich, L6876-1G), Triton™ X-100 (80 µL, Sigma-aldrich, X100), Benzonase® Nuclease, Purity >99% (3.2 µL, Novagen®, 70664) and Halt protease inhibitor cocktail, EDTA-free (100X, 80 µL, Thermo Scientific, 78439). The cells were incubated for 20 min on a fixed speed rotator. Non-specific proteins were denatured in a water bath at 50 °C for 20 min. Cell debris was

[3] Lysis buffer: 50 mM NaH_2PO_4, 300 mM NaCl, 20 mM imidazole, 10% glycerol, pH 7.4

removed by centrifugation at 4816 g for 20 min. Further centrifugation at 12 000 g for 20 min removed any remaining cell debris and insoluble proteins.

Amintra Ni-NTA resin (800 µL, Expedeon, ANN0100/ANN0025) was washed in wash buffer[4] (5 mL) by centrifugation at 1000 g for 1 min. The soluble protein fractions were incubated with the resin for 1 h on a fixed speed rotator. The resin was washed several times (>5) by centrifugation at 1000 g for 1 min, then transferred to an equilibrated Pierce Centrifuge Column (Thermo Scientific, 89897). The resin was washed on the column in wash buffer until the A_{280} reading (measured with a NanoDrop Lite Spectrophotometer) was consistently <0.09. The Affimer was eluted from the column in elution buffer[5] (1 mL elutions) until no more protein was present.

The insoluble protein fraction, soluble protein fraction, unbound protein, first wash, final wash and elutions were separated on a SDS-PAGE (15%) gel. The Affimers were dialysed into PBS, 5% glycerol, 1 mM dithiothreitol (DTT) and stored at -80 °C.

5.2.8 Sandwich ELISA to investigate Affimer protein binding to CD271-Fc recombinant protein

A sandwich ELISA (Section 5.1.2.2) was carried out to investigate the binding behaviour of the purified Affimer proteins. Since both the Affimer proteins and the CD271 recombinant protein had a His tag, detection via an anti-His tag antibody was not possible. To resolve this, a second CD271 recombinant protein was purchased from Sino Biological (13184-H02H-50), which was fused with the Fc region of human IgG1. The CD271-Fc protein was biotinylated in the same way as the CD271-His protein (Section 5.2.1) to allow immobilisation to a streptavidin-coated ELISA plate.

Streptavidin-coated plates were prepared and blocked as previously described (Section 5.2.4). Biotinylated CD271-Fc protein was diluted 1:100 in 2x Blocking Buffer and aliquoted at 50 µL per well for positive wells, whilst negative wells contained 2x Blocking Buffer only. The plate was incubated for 1 h on a vibrating platform shaker and washed 1x in PBST (300 µL per well). Affimers were added (10 µg/mL, 50 µL per well) and incubated for 1 h on a vibrating platform shaker. The plate was washed 1x with PBST (300 µL per well) and Anti-6X His tag® antibody-HRP (50 µL per well, Abcam, ab1187) was added 1:1000 in 2x Blocking

[4] Wash buffer: 50 mM NaH_2PO_4, 500 mM NaCl, 20 mM imidazole, pH 7.4
[5] Elution buffer: 50 mM NaH_2PO_4, 500 mM NaCl, 300 mM imidazole, 20% glycerol, pH 7.4

Buffer. The plate was incubated for 1 h on a vibrating platform shaker. After 10x washes with PBST (300 µL per well), TMB (50 µL per well) was added and developed for 5 min. Absorbance was measured at 620 nm.

5.2.9 Biotinylation of Affimer proteins

Affimer insert sequences were expressed in an Affimer scaffold with a C-terminal cysteine to allow for site-specific labelling. A fraction of the purified Affimers were labelled with biotin to allow immobilisation to a streptavidin-coated substrate.

Immobilised tris(2-carboxyethyl)phosphine (TCEP) disulphide-reducing gel (150 µL, Thermo Scientific, 77712) was washed 3x with PBS containing 1 mM EDTA (300 µL). PBS containing 50 mM EDTA (4 µL) and Affimer (150 µL, 0.5 mg/mL) were added to the gel and incubated on a fixed speed rotator for 1 h. The gel was discarded and the Affimer molecules (with reduced cysteine's,130 µL) were reacted with biotin malemide (Sigma-Aldrich, B1267, 6 µL, 2 mM) for 2 h at RT. Zeba Spin Desalting Columns, 7K MWCO (Thermo Scientific, 89882) were used to remove any excess biotin according to the manufacturer's instructions. An equal volume of 80 % glycerol (130 µL) was added and the Affimers were stored at -20 °C. A direct ELISA was carried out to check biotinylation (Section 5.2.2) as well as mass spectrometry analysis (Section 5.1.5).

5.2.10 Surface plasmon resonance analysis of Affimers binding to CD271 recombinant protein

Surface plasmon resonance (SPR, Section 4.2) was used to characterise Affimer protein binding to CD271 recombinant protein, including the specificity and affinity of binding interactions.

A 4-channel BIACORE 3000 instrument and BIACORE 3000 control software were used to collect data. The first set of experiments was carried out using a carboxymethylated dextran substrate where both CD271 recombinant proteins (CD271-His and CD271-Fc), and a negative control protein were immobilised to the substrate via crosslinking chemistry (Section 4.4). pH scouting was carried out prior to binding assays to find the pH at which proteins were immobilised to the sensor surface most efficiently.

5.2.10.1 Assessing the appropriate pH for protein immobilisation to a CM5 sensor substrate (pH scouting)

The sensor substrate CM5 (GE Healthcare Life Sciences, BR100399) was docked and running buffer (0.1 M sodium acetate, pH 5.6) injected over all four flow cells. Target protein (15 µL at a concentration of 5 µg/mL) was injected in different pH buffers at 5 µL/min and the response units recorded before and after the injection. The pH range investigated included pH 7.4 (PBS), pH 5.6 (running buffer - 0.1M sodium acetate), pH 5.5, pH 5.0 and pH 4.5 (all 10 mM sodium acetate buffers). This range was chosen because efficient pre-concentration of the protein at the sensor surface requires the pH to lie between the pk_a of the surface and the isoelectric point of the protein. Between each buffer, a high salt wash (1 M NaCl, 15 µL) was injected to regenerate the substrate surface. The immobilisation buffer was chosen based on the increase in response units whilst minimising the compromise on biological pH. An example of pH scouting for CD271-Fc protein is shown in Figure 5.6 where pH 5.0 was chosen for immobilisation.

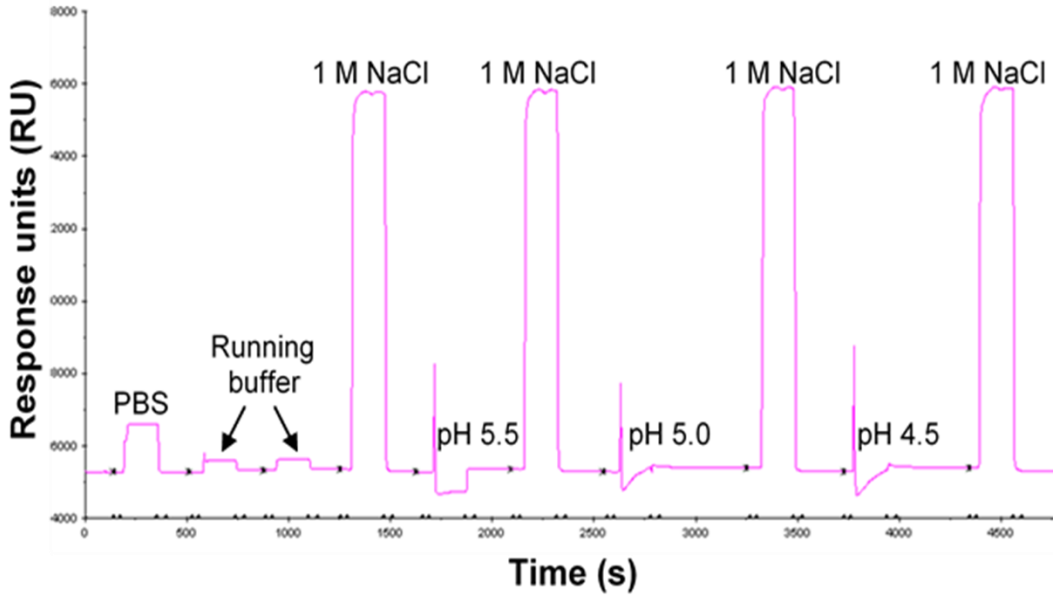

Figure 5.6 SPR Sensogram showing pH scouting for CD271-Fc recombinant protein

pH scouting was carried out to assess the efficiency of protein immobilisation at different pHs. CD271-Fc recombinant protein (5 µg/mL) was injected at 5 µL/min in PBS (pH 7.4), running buffer (0.1 M sodium acetate, pH 5.6), 10 mM sodium acetate, pH 5.5, 10 mM sodium acetate, pH 5.0 and 10 mM sodium acetate, pH 4.5. A high salt solution wash (1 M NaCl) was carried out between each immobilisation to regenerate the substrate surface. pH 5.0 was considered the best compromise between efficiency and biological pH, however the protein concentration was increased to 10 µg/mL for binding assays.

5.2.10.2 Protein immobilisation to a CM5 sensor substrate

Proteins were immobilised to a CM5 sensor substrate using EDC and NHS crosslinking chemistry (Section 4.4).

A mock immobilisation was carried out on flow cell 1 where no protein was immobilised. TNAP recombinant protein (His tag)(TNAP-His, Sino Biological, 10440-H08H-50) was immobilised on flow cell 2 as a negative control, CD271-His protein was immobilised on flow cell 3 and CD271-Fc protein was immobilised on flow cell 4. The flow rate was set to 5 µL/min. An NHS aliquot and an EDC aliquot (supplied with Amine Coupling Kit, GE Healthcare Life Sciences, BR100050) were mixed together in equal amounts (70 µL total) and injected to activate the sensor surface. The target protein was injected in the pre-determined buffer until the desired amount of units were immobilised (~10x the molecular weight of the protein). Unreacted protein was washed off the surface by a high salt solution (5 µL, 1 M NaCl) and unreacted sites were capped using ethanolamine hydrochloride (35 µL, 1.0 M, supplied with the Amine Coupling Kit,

GE Healthcare Life Sciences, BR100050). An example immobilisation of CD271-His protein is shown in Figure 5.7.

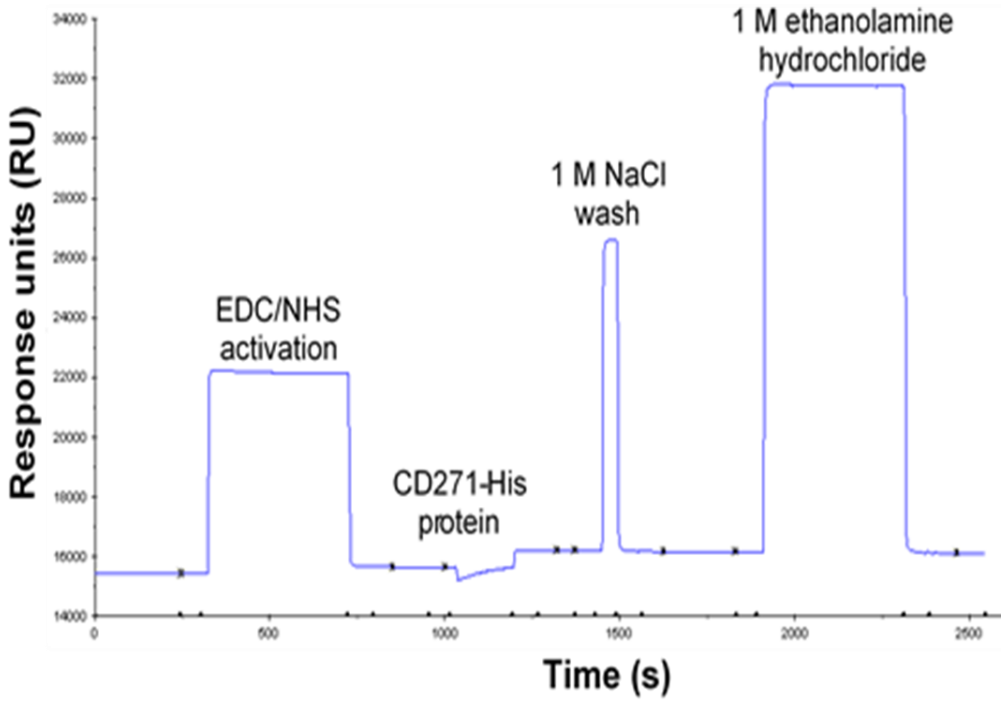

Figure 5.7 SPR sensogram showing the immobilisation of CD271-His recombinant protein to a CM5 sensor substrate

Proteins were immobilised onto a CM5 sensor substrate via NHS/EDC crosslinking chemistry. In the above example, CD271-His protein (10 µg/mL) was injected over the activated surface at 5 µL/min until the desired amount of protein was immobilised (~10x the molecular weight of the protein). A high salt solution wash (1 M NaCl) was carried out to wash away unreacted material and 1 M ethanolamine hydrochloride was injected to cap unreacted sites. 257.4 units of CD271-His were immobilised in the example above.

5.2.10.3 SPR binding assays

For the binding assays, Affimer protein was dialysed into PBS and injected in two-fold concentration steps from 25 nM to 400 nM over all four flow cells. An automated method was used with 3 minute injections at 50 µL/min with running buffer of PBS with 0.1% Tween 20.

A second sensor substrate CM5 was assembled for a further experiment. The same procedure of pH scouting and immobilisation was carried out with the following proteins immobilised; flow cell 1 had no protein immobilised, flow cell 2 had CD45-Fc protein (Sino Biological, 10086-H02H) immobilised as a negative control, flow cell 3 had CD271-Fc protein immobilised in reducing conditions (5

mM DTT in the immobilisation buffer) and flow cell 4 had CD271-Fc immobilised in non-reducing conditions (no DTT in the immobilisation buffer). The Affimers were injected over all four flow cells in two-fold concentration steps beginning at 3.125 nM and increasing to 50 nM for 6 min at 50 µL/min. The running buffer was PBS with 0.1% Tween 20.

BIAevaluation software was used to analyse data and overlay curves from all four flow cells. For all experiments, the baseline was normalised before any injections and the sensogram from flow cell 1 (or a non-binding flow cell) subtracted from all other curves to minimise refractive index effects. BIAevaluation software was also used to carry out kinetic analysis of binding curves to find the equilibrium binding constant of Affimer and target protein interactions.

5.2.11 Sandwich ELISA to investigate CD271 binding to Affimers when tethered to a solid substrate

In a cell enrichment device, Affimers would be tethered to a solid substrate for cell capture. To investigate binding in this format, a sandwich ELISA (Section 5.1.2.2) with biotinylated Affimers tethered to a streptavidin-coated ELISA plate, was carried out.

Streptavidin-coated plates were prepared and blocked as previously described (Section 5.2.4). Biotinylated Affimer (10 µg/mL in 2x Blocking Buffer) was added to positive wells, whilst negative wells contained 2x Blocking Buffer only. The plate was incubated for 1 h at RT on a shaker (300 rpm). After 1x PBST wash (300 µL per well), CD271-Fc protein was added at 50 µL per well (1:100 in 2x Blocking Buffer). The concentration of CD271-Fc protein was not determined due to the small amount of reagent available. The plate was incubated for 1 h at RT with shaking (300 rpm) and washed 1x with PBST (300 µL per well). Mouse monoclonal anti-human IgG Fc antibody (Abcam, ab31925) was added at 50 µL per well (1:10000 in 2x Blocking Buffer) and incubated for 1 h at RT with shaking (300 rpm). The plate was washed 1x with PBST (300 µL per well) and rabbit anti-mouse immunoglobulins/HRP (Dako, P0260) were added at 50 µL per well (1:1000 in 2x Blocking Buffer) for 1 h, RT, shaking (300 rpm). The plate was washed 10x with PBST (300 µL per well) and TMB substrate added (50 µL per well). The absorbance was measured at 620 nm.

5.2.12 Flow cytometry analysis of Affimer proteins binding to CD271+ cells

Flow cytometry (see Chapter 2: Section 2.5.1.3) was used to compare CD271 antibody and CD271 Affimer protein binding to CD271+ cells. CD271 Affimer protein and CD271 antibody were titrated to find the optimum concentration for cell labelling. IgG1-PE isotype-matched control antibody (BD BioSciences, 555749) was used at the same concentration as CD271-PE antibody, and a control of unlabelled cells was analysed alongside all samples.

Cells were detached from culture flasks using trypsin-EDTA solution (3-5 mL). The cell suspension was counted using a haemocytometer and diluted to a concentration of 5 x 10^6 cells/mL in FACS buffer[6]. Aliquots (100 µL) were dispensed into Falcon™ round-bottom polypropylene tubes (FACS tubes, Corning, 352063) and Affimer protein added to different tubes at 20 µg/mL, 10 µg/mL, 5 µg/mL and 2.5 µg/mL. Human CD271 phycoerythrin-conjugated antibody (CD271-PE, Miltenyi Biotec,130-113-983) was added to different tubes at the manufacturer's recommended working concentration (0.5 µg/mL), 0.25 µg/mL and 0.125 µg/mL. Cells were incubated in the dark at 4 °C for 30 min.

Cells were washed by adding 2 mL FACS buffer and centrifuging at 300 g for 5 min. For indirect Affimer protein labelling, a secondary antibody was used for fluorescent detection. Streptavidin Alexa Fluor 488 conjugate (Thermo Scientific, S-11223) was added (1 µg/mL) and incubated in the dark at 4 °C for 30 min. Washing was repeated and samples were resuspended in 350 µL FACS buffer for analysis.

A CytoFLEX S Flow Cytometer was used to record data. A minimum of 10,000 events were collected for each experiment and analysed using CytExpert software (see Chapter 4: Section 4.5)

5.2.13 Magnetic-activated cell sorting of CD271+ cells

CD271+ cells were pre-enriched prior to flow cytometry analysis using MACS (see Chapter 2: Section 2.5.1.4). A CD271 MicroBead kit was purchased from Miltenyi Biotec (130-099-023) and used according to the manufacturer's instructions (227), summarised below.

Cells were detached from culture flasks using trypsin-EDTA solution (3-5 mL). The cell suspension was counted using a haemocytometer and re-suspended in

[6] FACS buffer: PBS (Lonza, 17-516F) 0.5% bovine serum albumin (BSA, Sigma Aldrich, A9647) and 0.05% sodium azide, filter sterilised (0.22 µm)

60 µL MACS buffer[7] per 10^7 cells. CD271 MicroBeads and FcR Blocking Reagent (40 µL each per 10^7 cells) were added, mixed and incubated for 15 min at 4 °C. Cells were washed by adding 2 mL MACS buffer per 10^7 cells and centrifuged at 300 g for 10 min. Cells were resuspended in 500 µL MACS buffer per 10^8 cells.

A LS column (Miltenyi Biotec, 130-042-401) was placed in the magnetic field of a MACS separator. The column was prepared by rinsing with 3 mL MACS buffer before the cell suspension was applied. The column was washed with 3x 3 mL MACS buffer. The flow-through containing unbound cells were collected and counted using a haemocytometer. The column was removed from the magnetic field, 5 mL of MACS buffer added, and a plunger (supplied with the LS column) was used to flush out bound cells. Bound cells were counted using a haemocytometer.

Bound and unbound cells were labelled with CD271-PE antibody, IgG1-PE isotype-matched control antibody and Affimer protein at the pre-determined concentrations from Section 5.2.12. The different populations were analysed using a flow cytometer as described in Section 5.2.12.

5.2.14 Fluorescent labelling of Affimer proteins for flow cytometry experiments

Affimer proteins were labelled with Alexa Fluor 647 C_2 maleimide (Thermofisher Scientific, A20347) for direct detection in flow cytometry experiments. This was carried out using the same labelling method as for the biotinylation of Affimer proteins (Section 5.2.9), using the C-terminal cysteine for site-specific labelling. Labelling was carried out directly after purification (Section 5.2.7).

Fluorescently-labelled Affimer proteins were separated on an SDS-PAGE gel (Section 5.1.4.5) alongside unlabelled Affimer proteins with known concentration. The intensity of the bands of Affimer proteins with known concentration was plotted and used to estimate the concentration of the fluorescently-labelled Affimers.

The fluorescently-labelled Affimers were titrated for flow cytometry analysis using the same protocol as Section 5.2.12. Once an appropriate working concentration had been defined, fluorescently-labelled Affimer protein labelling was compared to antibody labelling also described in Section 5.2.12.

---

[7] MACS buffer: PBS (Lonza, 17-516F), 2 mM EDTA (Sigma Aldrich, E7889), 0.5% BSA (Sigma Aldrich, A9647), filter sterilised

5.3 Results and Discussion

5.3.1 Phage display selection of CD271-specific Affimer proteins

A commercial source of CD271-His recombinant protein was purchased for phage display screening. Screening was carried out in collaboration with the BSTG established at the University of Leeds in 2010. Two Affimer libraries were screened in total; one with a single variable loop region and the other with two variable loop regions (see Section 5.1.1), the two libraries were mixed and screened at the same time.

The aim of phage display screening was to identify Affimer proteins which were highly specific towards CD271 protein, and thus able to act as capture molecules for MSCs in a microfluidic device. Various Affimer proteins were used as controls during the experiments described in this chapter. All control Affimer proteins were selected according to published data demonstrating target-specific binding.

5.3.1.1 Biotinylation of phage display target: CD271-His recombinant protein

The commercially sourced CD271-His recombinant protein was biotinylated using EZ-Link™ Sulfo-NHS-SS-Biotin (Section 5.2.1). This was to facilitate the immobilisation of the target protein to streptavidin/NeutrAvidin-coated wells and beads for phage display screening. An ELISA indicated that the biotinylation had been successful (Figure 5.8); wells that had been coated with the biotinylated protein reacted with streptavidin-HRP and TMB substrate to produce a soluble blue reaction product whereas wells where no protein was present remained clear. This provided reassurance that the target protein would be bound to streptavidin/NeutrAvidin-coated substrates during the phage display protocol.

Figure 5.8 ELISA results showing that CD271-His recombinant protein was successfully biotinylated

An ELISA was carried out to see if the protein had been successfully biotinylated. Wells A and B were coated with biotinylated CD271 protein, wells C and D were coated with Blocking Buffer only. The blue reaction product is produced when TMB substrate reacts with streptavidin-HRP which has bound to biotin. The results shown here indicate that the protein was successfully biotinylated. In wells A and B, 1 µL and 0.01 µL of biotinylated CD271 protein were added to 50 µL PBS respectively. The concentration of biotinylated CD271 protein was not calculated due to the limited sample available.

5.3.1.2 Phage display screening of biotinylated CD271 recombinant protein using a protocol with additional washing steps

Two protocols of phage display screening were explored – a protocol with additional washing steps and a protocol with less stringent washing. Initially, a protocol with additional washes was used to isolate only the highest affinity binders. A ySUMO protein was screened alongside CD271 protein as it is known to produce positive hits from the Affimer libraries (156).

After three rounds of biopanning, bound phage particles were eluted from wells coated with the target protein and wells with no target protein. The eluted phage were amplified in ER2738 *E. coli* cells and a range of volumes (0.1 µL, 1 µL, 10 µL) were plated on LB carb plates overnight (Section 5.2.3.3). Colony-forming units were counted the following day to estimate the success of the screening process. If a large amplification in clone numbers is observed between negative and positive plates, it is more likely that phage particles have bound specifically to the target protein. The number of colonies on the CD271 positive plate was 19 times greater than from the CD271 negative plate. The number of colonies on the ySUMO positive plate was >4000 times greater than from the ySUMO negative plate (Table 5.2). This was an early indication that fewer specific binders had been isolated for the CD271 target compared to the ySUMO target.

Table 5.2 The number of colony-forming units per 5 mL culture after three rounds of phage display biopanning

After three rounds of phage display biopanning, bound phage particles were eluted from target protein wells (positive wells) and no-protein wells (negative wells) and amplified in ER2738 *E. coli* cells. After one hour, the cell suspensions were plated on LB carb plates in a range of volumes (0.1 µL, 1 µL, 10 µL) and colonies were counted on the following day. The number of colony-forming units per 5 mL of cells was calculated for both positive and negative wells, where colony-forming units on the negative plate represent non-specific binding. The greater the amplification between negative and positive plates, the more likely it is that target-specific Affimer clones have been selected. ySUMO protein was screened alongside CD271 as it is known to produce positive hits from the Affimer library (156).

Target protein	Colony-forming units/5 mL cells (10^2)	
	Positive plate	**Negative plate**
CD271	4500	240
ySUMO	240000	55

5.3.1.3 Phage display screening of biotinylated CD271 recombinant protein using a protocol with less stringent washing

The second protocol offered the opportunity to isolate weaker binders, this was important since for a cell enrichment application using positive selection, the cells need to be released from the binding protein after capture. Additionally, using this protocol, the bound phage were eluted to investigate pH change as a possible cell release mechanism.

Table 5.3 details the number of colony-forming units on positive plates compared to negative plates for the elutions at different pH values. During this biopanning method, a tubulin protein was screened alongside CD271-His recombinant protein as a positive control (158). For CD271-His recombinant protein, the amplification between negative and positive plates was >20 times. For the tubulin protein, amplification was >100 times. The difference between positive and negative plates for CD271 protein was similar to the first phage display screen (around 20 times greater), suggesting that the number of specific clones identified from both screens would be similar. The difference between positive and negative plates for tubulin protein was around 5 times greater than for CD271 protein suggesting that the number of specific clones identified for CD271 protein would be less than the number of specific clones identified for tubulin protein.

The majority of clones from the CD271 biopanning were eluted using the standard elution protocol – addition of 0.2 M glycine-HCl pH 2.2 then 1 mM triethylamine

pH 10.75. However, there were also clones eluted at pH 9.0, 7.0 and 5.0 signifying pH change could be a possible cell release mechanism.

Table 5.3 The number of colony-forming units per 5 mL culture after three rounds of phage display standard biopanning with elutions at different pH values

After three rounds of phage display biopanning, bound phage particles were eluted from the target protein wells (positive wells) and no protein wells (negative wells), using different pH buffers, and amplified in ER2738 *E. coli* cells. After one hour, the cell suspensions were plated on LB carb plates in a range of volumes (0.1 µL, 1 µL, 10 µL) and colonies were counted on the following day. The number of colony-forming units per 5 mL of cells was calculated for both positive and negative wells where colony-forming units on the negative plate represent non-specific binding. The greater the amplification between negative and positive plates, the more likely it is that target-specific Affimer clones have been selected. Tubulin protein was screened alongside CD271 as it is known to produce positive hits from the Affimer libraries (158).

Target protein	pH elution	Colony-forming units/5 mL cells (10^2)	
		Positive plate	Negative plate
CD271	9.00	730	370
	7.00	770	
	5.00	3100	
	2.20 and 10.75	> 8000	
Tubulin	2.20 and 10.75	19000	170

5.3.1.4 Determining the specificity of individual clones via phage ELISA

Individual clones from the positive colony plates (thought to be positive hits as these cells were infected with bound phage) were randomly selected for subsequent analysis by phage ELISA (Section 5.2.4). Clones were picked, cultured and infected with helper phage to produce phage particles. The phage ELISA format mimics the phage display selection process by immobilising the biotinylated target protein onto a streptavidin-coated well. Phage from each individual clone were then added both to a well coated with target protein (positive well) and a well with no protein (negative well). Bound phage were detected using a HRP-conjugated anti-phage antibody.

For the first screening protocol, 92 clones from the CD271 positive plate were analysed, alongside four clones from the ySUMO positive control plate. Figure 5.9 shows that only eight of these 92 clones demonstrated target-specific binding in the phage ELISA. This can be seen by a larger absorbance value detected in the positive well versus the negative well i.e. phage binding to wells coated with target-protein but not to wells with no protein. The four clones from the ySUMO screen also demonstrated target-specific binding.

For the second screening protocol, 24 clones from each pH elution were analysed, alongside four clones from the tubulin positive control plate. Figure 5.10 shows that nine CD271 clones demonstrated target-specific binding. Interestingly, the majority of these (seven out of the nine clones) were eluted at pH 9, with one additional clone eluted at pH 7 and one at pH 5, confirming that pH change could potentially be used as a cell release mechanism. The four positive control clones all demonstrated tubulin-specific binding.

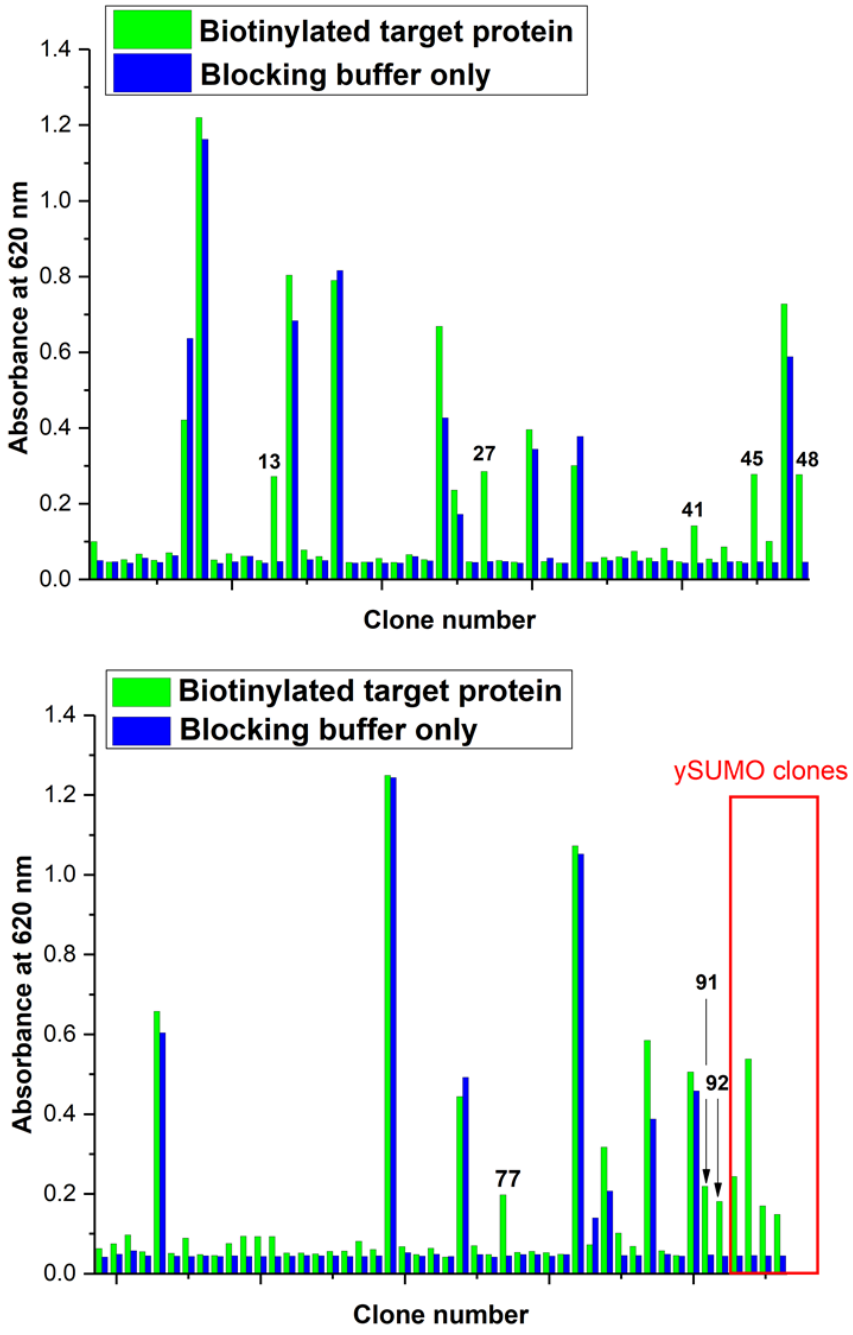

Figure 5.9 Phage ELISA results of clones from the first phage display screen

Phage ELISA results of 92 CD271 clones selected after three rounds of phage display biopanning. A larger absorbance value of the target protein-coated well (green) compared to the no-protein well (blue) indicates that the clone bound specifically to the target protein. Upper panel: CD271 clones 1-48, lower panel: CD271 clones 49-92 and ySUMO clones 1-4 (positive controls). CD271 clones 13, 27, 41, 45, 48, 77, 91 and 92 were investigated further.

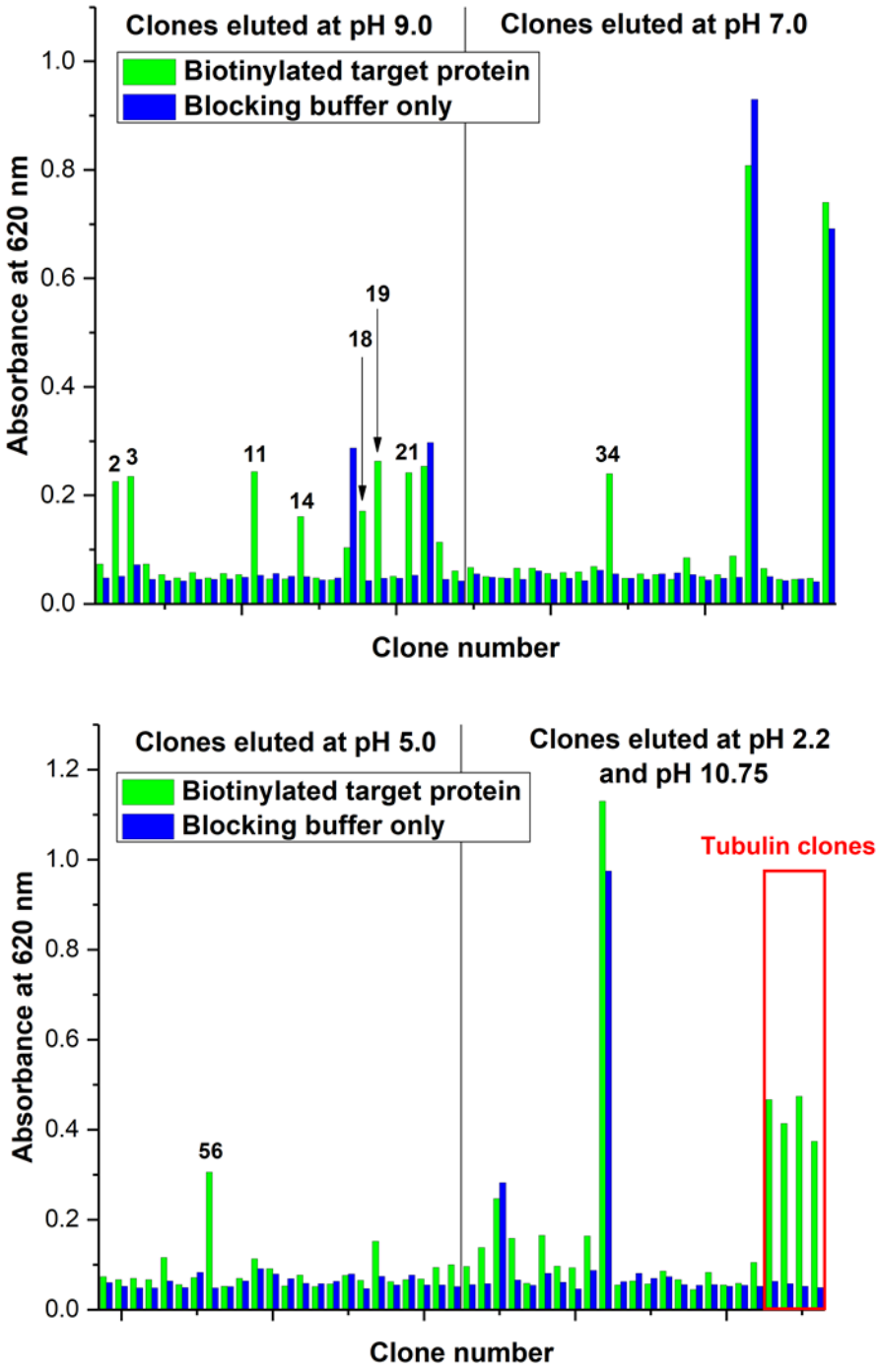

Figure 5.10 Phage ELISA results of clones from the second phage display screen eluted at different pH values

Phage ELISA results of 92 clones selected after three rounds of phage display biopanning and eluted using different pH buffers. A larger absorbance value of the target protein-coated well (green) compared to the no protein well (blue) indicates the clone binds specifically to the target protein. Upper panel: CD271 clones 1-48, lower panel: CD271 clones 49-92 and tubulin clones 1-4 (positive controls, also eluted at pH 2.2 and 10.75). CD271 clones 2, 3, 11, 14, 18, 19, 21, 34 and 56 were investigated further.

5.3.1.5 DNA sequencing of clones indicating CD271-specific binding

The clones that demonstrated target-specific binding were sent for DNA sequencing. Table 5.4 shows the unique Affimer insert sequences for the variable loop regions. Three unique sequences were identified; one from the first phage display screen and two from the second phage display screen. One sequence (CD271-1) was from the Affimer library with one variable loop region and two sequences (CD271-2 and CD271-3) were from the Affimer library with two variable loop regions.

Table 5.4 Affimer variable loop sequences for clones identified in phage ELISAs

Individual clones which showed specific binding in the phage ELISAs were sent for DNA sequencing. All clones from the first phage display screen were from the two-loop Affimer library and were identical (CD271-3). Two unique sequences were found from second phage display screen, one from the two-loop Affimer library (CD271-2) and one from the single-loop Affimer library (CD271-1).

Affimer sequence ID	Frequency of sequence	Loop 1 sequence	Loop 2 sequence
CD271-1	1 (from second screen)	HGHWPFLDQ	–
CD271-2	8 (from second screen)	SGHWPFDHH	GLHAELRMM
CD271-3	8 (from first screen)	SQPLEFNWW	TWQYYRKLN

5.3.2 Producing and purifying Affimer proteins

The three unique Affimer sequences CD271-1, CD271-2 and CD271-3 were sub-cloned from the phagemid vector into a bacterial expression vector (Sections 5.1.4.2 and 5.2.6), and Affimer proteins were recombinantly produced and purified (Sections 5.1.4 and 5.2.7). This was to enable more extensive characterisation of their binding to the target protein, and subsequently, cells expressing the target protein (Section 5.3.3).

5.3.2.1 DNA sub-cloning of Affimer insert sequences

The insert DNA from the pDHis phagemid vector was sub-cloned into a pET11a expression vector. The insert DNA was amplified from the phagemid vector using PCR (Section 5.1.4.1 and 5.2.6), and both the insert DNA and the pET11a vector DNA were digested with NotI and NheI restriction enzymes to allow ligation of the compatible ends. Figure 5.11 shows the digested insert DNA separated on a 2% agarose gel. The Affimer insert DNA is expected to be around 300 base pairs which was confirmed by comparison to a DNA ladder.

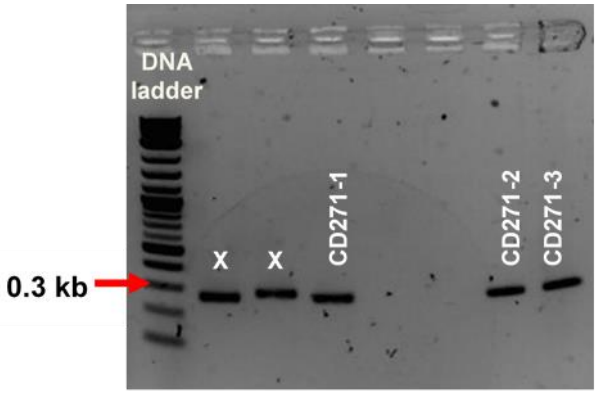

Figure 5.11 Agarose gel (2%) showing Affimer double-digested insert DNA

Insert DNA was double-digested with restriction enzymes in preparation for ligation into an expression vector. The double-digested insert DNA was run on a 2% agarose gel and compared to a DNA ladder. Wells marked with an X were DNA sequences sub-cloned at the same time as CD271-1, CD271-2 and CD271-3 but not discussed in this thesis. All insert DNA was approximately 0.3 kilobases (kb) which is the expected number of base pairs for Affimer insert DNA.

Following ligation reactions (Section 5.2.6), the ligated samples were introduced into XL1-Blue supercompetent cells by bacterial transformation and samples were incubated overnight on LB carb plates at 37 °C. A negative ligation reaction with no insert DNA was set up as a control and no colonies grew. In comparison, colonies grew for all three insert DNA ligations. Single colonies were picked and the plasmid DNA extracted using a miniprep kit (Section 5.2.6). DNA sequencing of the isolated plasmids confirmed the correct Affimer sequences had been sub-cloned into the pET11a vector.

5.3.2.2 Protein production and purification of Affimer proteins

Affimer proteins were recombinantly produced and purified as described in Section 5.2.7. Following cell lysis and centrifugation, soluble His-tagged Affimer proteins were eluted from a Ni-NTA column using a buffer containing a high concentration (300 mM) of imidazole. Aliquots of the insoluble, soluble, unbound, first wash and final wash were taken to analyse on a 15% SDS-PAGE gel (Section 5.1.4.5), along with aliquots of each of the 1 mL elution samples (Figure 5.12). From the gel images it can be seen that the Affimer proteins were of the expected size (~13 kDa) with some dimers present in Affimers CD271-1 and CD271-2. Dimers can form due to the C-terminal cysteine residue on the Affimer scaffold contributing to the formation of disulphide bridges.

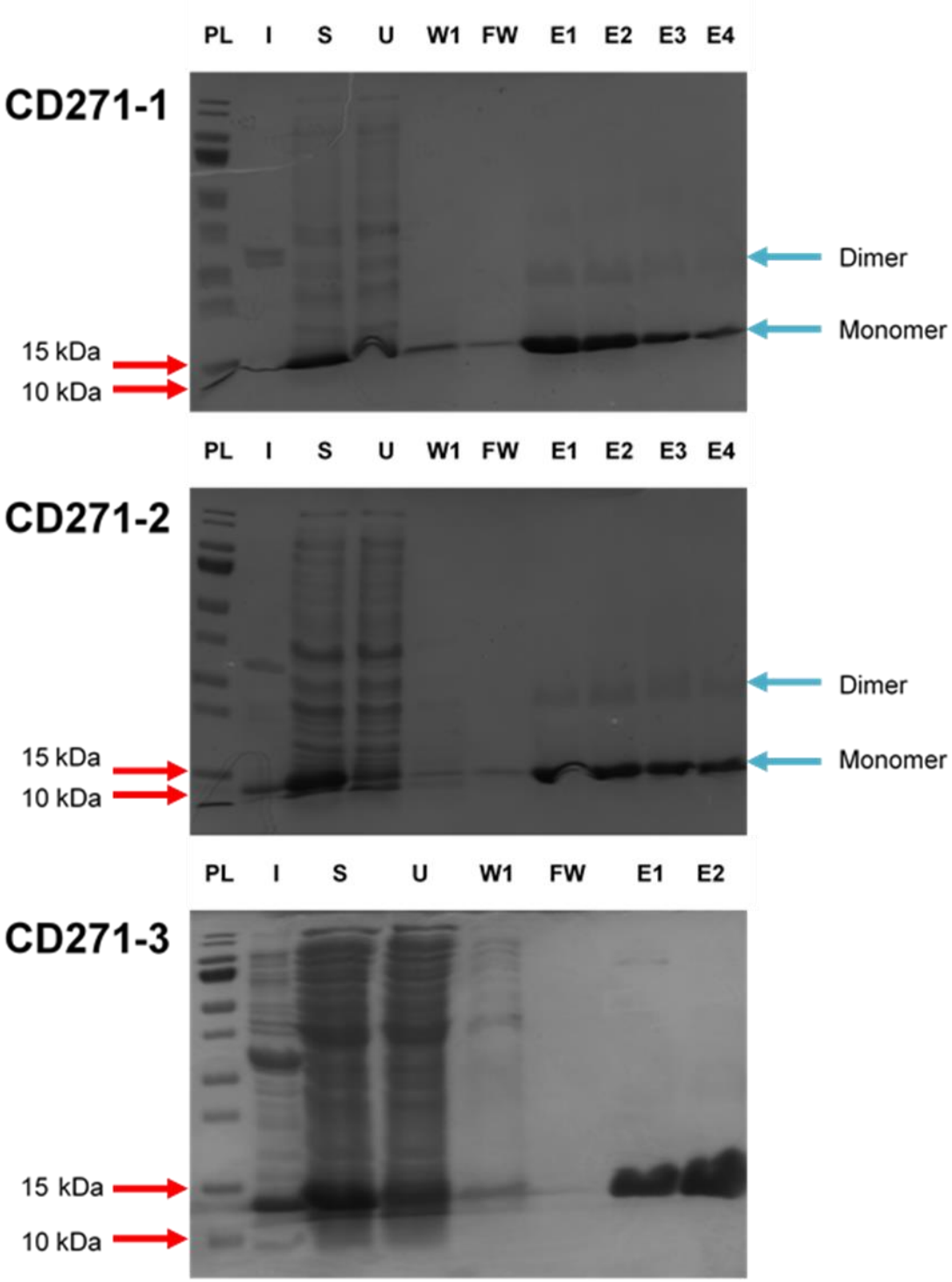

Figure 5.12 SDS-PAGE gels (15%) of purified Affimer proteins

Affimer proteins were purified using a Ni-NTA column and eluted in 1 mL fractions. The Affimer proteins were of the expected mass (~13 kDa) with some dimers present in CD271-1 and CD271-2. PL is a protein ladder (Thermofisher Scientific, 26616), I is the insoluble fraction, S is the soluble fraction, U is the unbound fraction, W1 is the first wash, FW is the final wash and E1 - E4 are respective elutions. All gels were stained with Coomassie blue.

5.3.3 Characterisation of Affimer-CD271 protein binding

Once the Affimer proteins had been purified, more extensive characterisation of Affimer binding to CD271 could be carried out. The two main methods used for characterisation were ELISA (Section 5.2.8 and 5.2.11) and SPR (Section 5.2.10). In order to carry out a sandwich ELISA (Section 5.1.2.2), a new CD271 recombinant protein was bought with an Fc tag rather than a His tag (Sino Biological, 13184-H02H). The DNA sequence encoding the CD271 extracellular domain was fused with the Fc region of human IgG1 at the C-terminus. The secreted recombinant protein is a disulphide–linked homodimeric protein. Using a CD271-Fc protein allowed detection via the His tag on the Affimer scaffold without interference from a His tag on the CD271 recombinant protein.

5.3.3.1 Biotinylation of CD271-Fc recombinant protein for characterisation assays

The CD271-Fc recombinant protein was biotinylated for immobilisation to a streptavidin coated surface as described in the phage ELISA (Section 5.2.4). The protein was biotinylated in the same way as the CD271-His recombinant protein (Section 5.2.1) and a direct ELISA (Section 5.1.2.1) showed successful biotinylation (Figure 5.13).

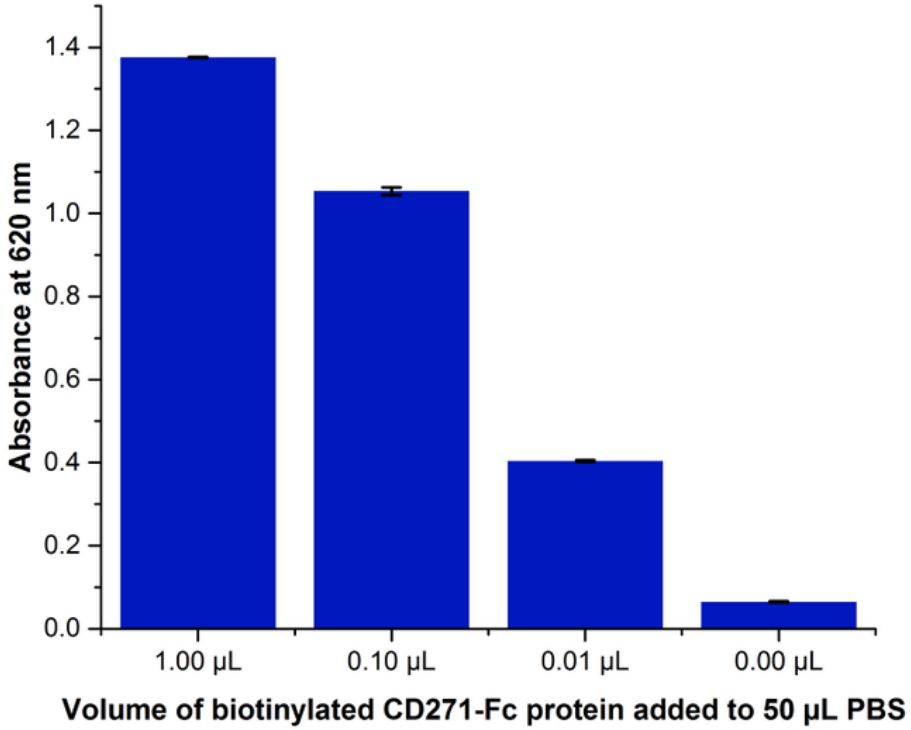

Figure 5.13 ELISA showing the successful biotinylation of CD271-Fc recombinant protein

An ELISA was carried out to see if the CD271-Fc recombinant protein had been successfully biotinylated. Different volumes of biotinylated CD271-Fc recombinant protein were added to 50 µL PBS and reacted with a streptavidin-HRP conjugate and TMB substrate. The protein showed strong absorbance at 620 nm indicating biotin was present, and the absorbance value decreased as the quantity of protein decreased. The concentration of the biotinylated CD271 protein was not measured due to the limited sample volume. Bars represent the mean result ± standard error of the mean (SEM), n=2 technical replicates.

5.3.3.2 Sandwich ELISA to investigate Affimer protein binding to CD271-Fc recombinant protein

It was important to check that the purified Affimer proteins demonstrated the same specific binding behaviour to CD271 protein as was observed by phage ELISA. This was achieved by carrying out a sandwich ELISA (Section 5.1.2.2) in the same format as the phage ELISA (Section 5.2.4) – wells were first coated with streptavidin, then coated with biotinylated CD271 protein and bound Affimer proteins were detected via an anti-His tag antibody. A GFP-18 Affimer was used as a negative control against biotinylated CD271 protein whilst a NDM1-21 Affimer was used as a positive control against its own biotinylated target protein New Delhi metallo-beta-lactamase 1 (NDM1).

Figure 5.14 indicates that Affimers CD271-1 and CD271-2 demonstrated specific binding comparable to the positive control, however Affimer CD271-3 did not demonstrate any specific binding. Although a small amount of binding was observed for the negative control, it was of significantly smaller magnitude than the observed specific binding (for normally distributed data).

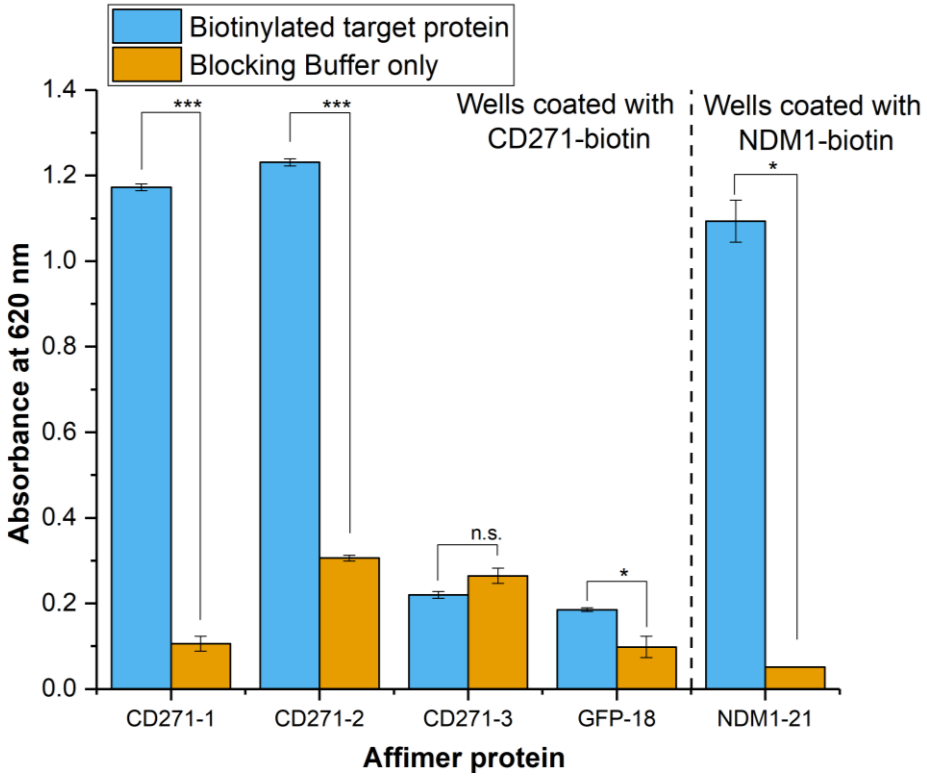

Figure 5.14 Sandwich ELISA showing Affimers CD271-1 and CD271-2 bound to CD271-Fc recombinant protein

A sandwich ELISA was carried out to investigate if purified Affimer proteins bound to their target protein. Affimer proteins CD271-1 and CD271-2 showed a large difference in absorbance between the wells coated with biotinylated target protein (CD271) and the wells coated with Blocking Buffer only and were taken forward for further investigation (***$p<0.00001$). CD271-3 Affimer was not taken forward for further investigation (n.s.=not significant). GFP-18 Affimer was used as a negative control and NDM1-21 Affimer used as a positive control (*$p<0.05$). Statistical analysis was carried out by an independent t-test for normally distributed data (CD271-1, CD271-2, CD271-3 and GFP-18 replicates). Statistical analysis was carried out by Mann-Whitney U test for NDM1-21 replicates since data was not normally distributed according to the Shapiro Wilk test of normality. Bars represent the mean result ± SEM, n=3 technical replicates.

5.3.3.3 Biotinylation of CD271-1 and CD271-2 Affimer proteins for characterisation assays

Affimers CD271-1 and CD271-2 were biotinylated so that the Affimer proteins could be immobilised to a streptavidin surface. Binding in this format was crucial since in a cell capture device the Affimers would be immobilised to a solid substrate. Affimers were biotinylated via their C-terminal cysteine residue using biotin-malemide (Section 5.2.9). As before, a direct ELISA (Section 5.1.2.1) showed that both Affimers were successfully biotinylated (Figure 5.15).

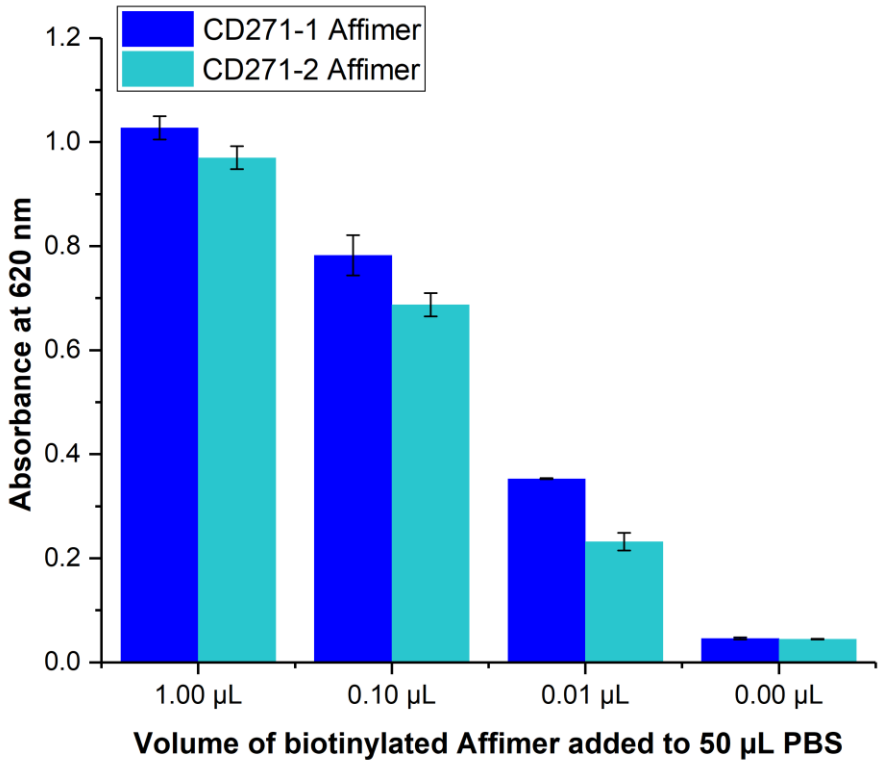

Figure 5.15 ELISA results showing the successful biotinylation of CD271-1 and CD271-2 Affimer proteins

Different volumes of biotinylated CD271-1 and CD271-2 Affimer proteins were added to 50 µL PBS and reacted with a streptavidin-HRP conjugate and TMB substrate. The proteins both showed strong absorbance at 620 nm indicating biotin was present. The absorbance value decreased as the volume added decreased. The concentration of the biotinylated Affimer proteins was measured via bicinchoninic acid (BCA) assay at a later date (CD271-1: 9 µM, CD271-2: 6 µM). Bars represent the mean value ± SEM, n=2 technical replicates.

Additionally, the Affimers were analysed before and after biotinylation by mass spectrometry, and the masses compared with the calculated mass from their amino acid sequences. Good agreement was seen between the calculated masses and the mass spectrometry results and the mass spectrometry results again confirmed the addition of biotin-malemide (see Table 5.5).

Table 5.5 Mass spectrometry results of biotinylated Affimer proteins

The Affimer proteins were analysed via mass spectrometry before and after biotinylation to verify the addition of biotin-malemide (451.54 Da). The expected masses of the proteins were also calculated from the amino acid sequence of the Affimer proteins. There was good agreement between the calculated masses and the mass spectrometry results and the results confirmed the successful biotinylation of Affimers CD271-1 and CD271-2.

Affimer protein	Calculated mass from sequence (Da)	Mass spectrometry result (Da)
CD271-1	11608.08	11606.43
CD271-2	12359.02	12357.82
Biotinylated CD271-1	12058.62	12059.30
Biotinylated CD271-2	12809.56	12810.25

5.3.3.4 Sandwich ELISA to investigate whether CD271-Fc recombinant protein bound to biotinylated Affimers when tethered to a solid substrate

With reassurance that the Affimers were biotinylated, a sandwich ELISA was carried out in the format analogous to cell capture in a microfluidic device. Wells were coated with streptavidin, then with biotinylated Affimer protein. Human CD271-Fc protein was added and after washing, bound target was detected via anti-human IgG antibody and anti-mouse IgG HRP antibodies. A biotinylated ToxinB-18 Affimer was used as a negative control as well as a human CD45-Fc recombinant protein in place of human CD271-Fc recombinant protein.

Figure 5.16 shows that only Affimer CD271-1 showed a strong absorbance in the sandwich ELISA meaning that CD271-Fc protein was bound. None of the negative controls showed any specific binding, nor did Affimer CD271-2.

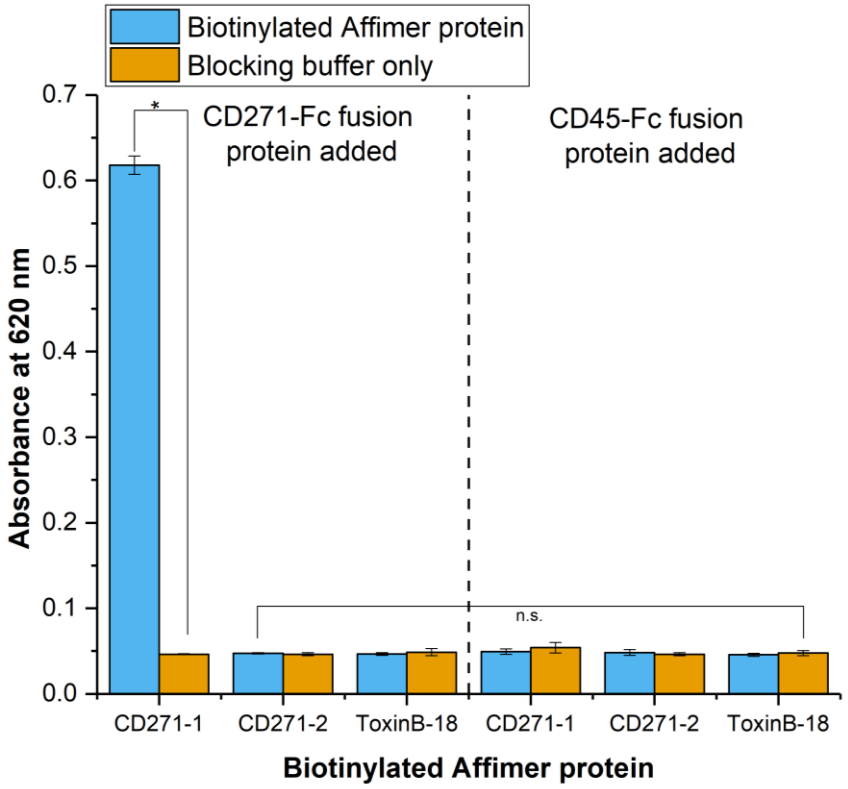

Figure 5.16 Sandwich ELISA results showing that CD271-Fc recombinant protein bound to CD271-1 Affimer when it was tethered to a solid substrate

A sandwich ELISA was carried out to investigate if CD271-Fc recombinant protein bound to biotinylated Affimer proteins when they were tethered to a solid substrate (representative of cell capture within a cell separation device). There was a significantly larger absorbance value when CD271-Fc recombinant protein was added to a well coated with biotinylated CD271-1 Affimer protein compared to a well coated with Blocking Buffer only (*$p<0.05$). There was no significant difference between the positive and negative wells for CD271-2 Affimer protein or ToxinB-18 Affimer protein (negative control). CD45 (Fc tag) recombinant protein was also used as a negative control and no significant differences between positive and negative wells were observed. Statistical analysis was carried out by Mann Whitney U test since data was not normally distributed according to the Shapiro Wilk test of normality. Bars represent the mean value ± SEM, n=3 technical replicates.

5.3.3.5 SPR analysis of Affimer CD271-1 binding to CD271 recombinant protein

Next, the binding of Affimer CD271-1 was investigated using SPR (Sections 4.2 and 5.2.10). A dextran CM5 substrate was used to covalently immobilise CD271 protein via amine coupling (Section 4.4), and the CD271-1 Affimer was injected

into the flow cell at a range of concentrations. The SPR was carried out in this format since there was a limited amount of CD271 protein available, and only a small amount of protein is required for immobilisation compared to the amount required for multiple analyte injections. pH scouting was carried out prior to immobilisation to find the optimal pH for protein attachment to the surface (Section 5.2.10.1). Binding was detected by a change in the surface plasmon resonance and recorded as a sensogram in response units (RUs).

There were four flow cells in total, the first flow cell was used as a reference cell with no protein immobilised. The second flow cell contained the originally screened CD271 protein (CD271-His recombinant protein) and the third flow cell contained the CD271-Fc recombinant protein used in the ELISA characterisation assays (Section 5.2.8). The final flow cell was immobilised with TNAP-His recombinant protein as a negative control.

Figure 5.17 shows that Affimer CD271-1 displayed specific binding to the flow cells containing immobilised CD271 protein. It was however observed that Affimer CD271-1 showed a larger response to the CD271-Fc recombinant protein compared to the CD271-His recombinant protein, requiring further investigation (see below). Additionally, it was found that as the concentration of CD271-1 Affimer injected was increased, the binding curves reached a maximum response and then began to dissociate during the injection period. It was hypothesised that the dissociation during the analyte injection could be caused by aggregation of the Affimers at higher concentrations.

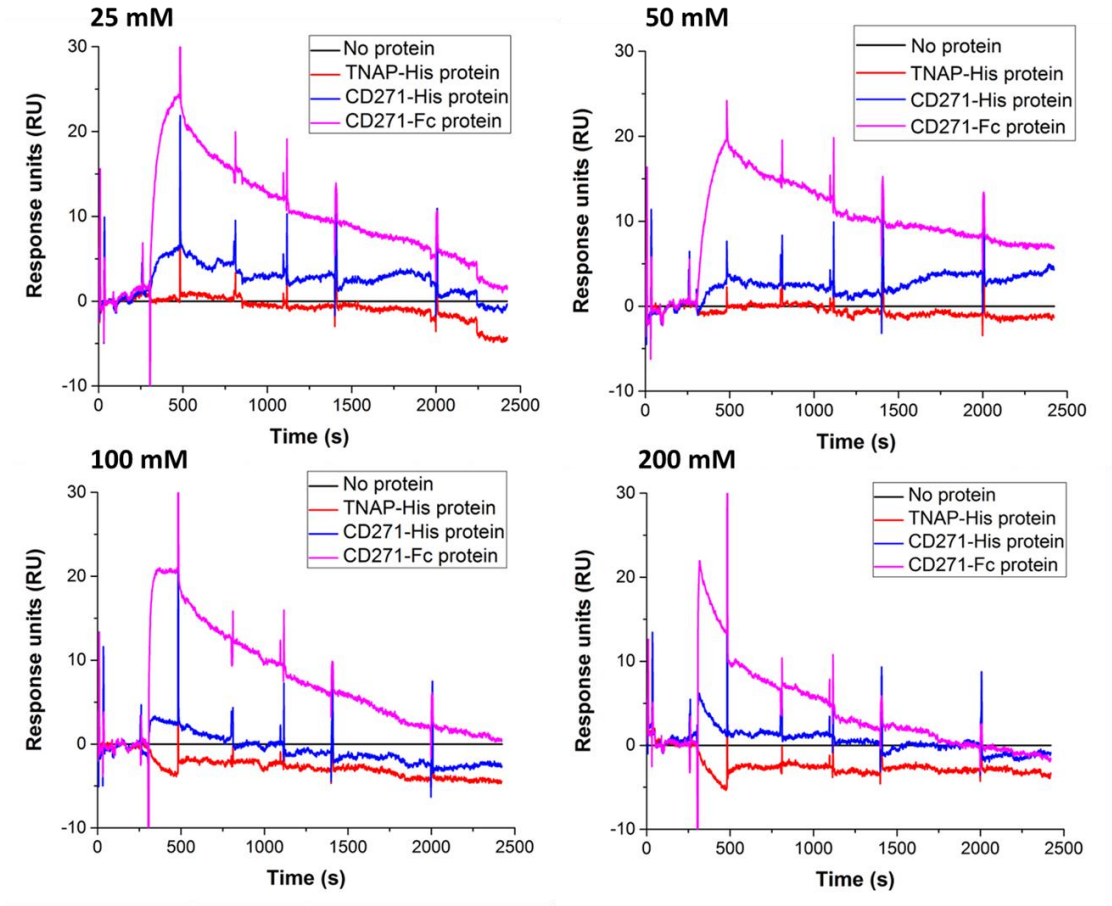

Figure 5.17 SPR sensograms showing CD271-1 Affimer protein binding specifically to CD271 recombinant protein

CD271-Fc recombinant protein (pink), CD271-His recombinant protein (blue) and TNAP-His recombinant protein (red) were immobilised to a CM5 substrate. A reference cell had no protein immobilised (black) and was subtracted from all other flow cells to minimise refractive index effects. CD271-1 Affimer proteins were injected for 180 s at 50 µL/min at the concentrations indicated.

To further investigate the specific binding of Affimer CD271-1, a second CM5 substrate was functionalised. In this experiment, the aim was to further explore the larger binding response observed for the CD271-Fc protein compared to the CD271-His protein. To do this, a CD45-Fc protein was immobilised in one flow cell to ensure that the Affimer was not binding to the Fc portion of the protein. In addition, the CD271-Fc protein was immobilised under reducing conditions (with 5 mM DTT added to the immobilisation buffer) as well as non-reducing conditions (no DTT added to immobilisation buffer) to assess whether binding was preferable due to the homodimeric form of the CD271-Fc protein compared to the monomeric form of the CD271-His protein. As previously, one flow cell was used as a reference cell with no protein immobilised. The Affimer was injected at a

lower concentration range to avoid aggregation of Affimers at high concentrations.

The data gathered from this additional experiment (shown in Figure 5.18) confirms that CD271-1 Affimer binds specifically to the CD271 antigen rather than the Fc portion of the protein. Further to this, there was no difference in the binding behaviour of Affimer CD271-1 to CD271-Fc protein in reducing conditions compared to non-reducing conditions. This suggests that there was another reason for the greater response to the CD271-Fc protein, such as a difference in the quality of the target proteins.

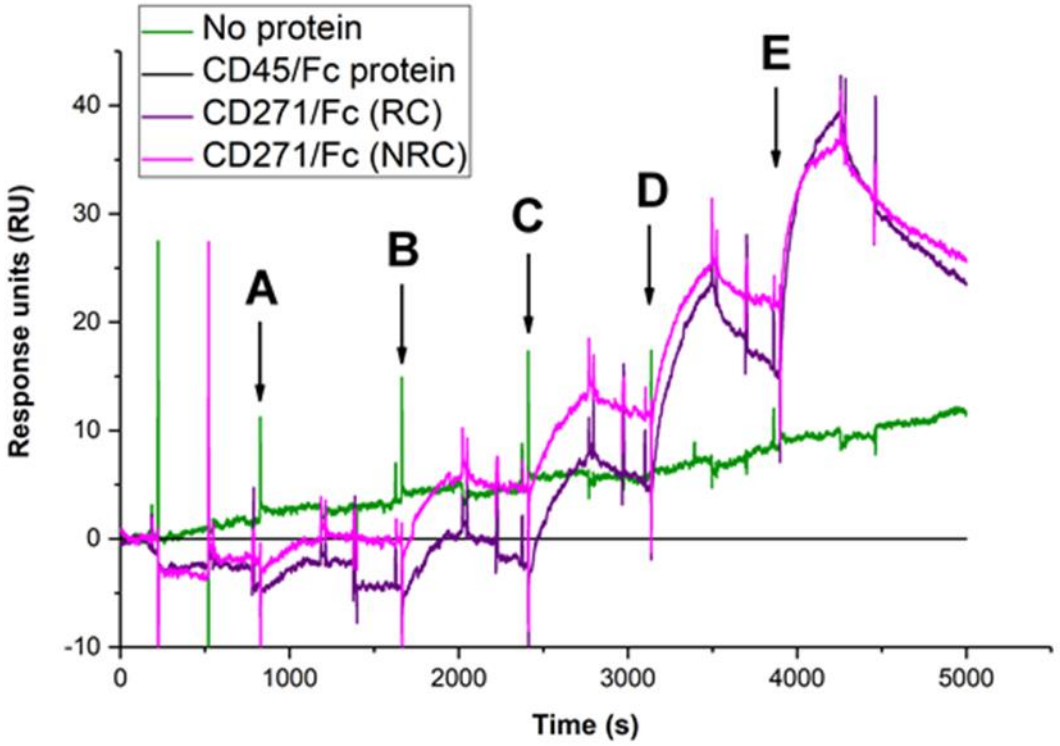

Figure 5.18 SPR sensogram showing CD271-1 Affimer protein binding specifically to CD271 recombinant protein in reducing and non-reducing conditions

A second CM5 substrate was immobilised with CD271-Fc recombinant protein in non-reducing conditions (NRC, pink), CD271-Fc recombinant protein in reducing conditions (RC, purple) and CD45-Fc recombinant protein in non-reducing conditions (black). A reference cell had no protein immobilised (green). The reference cell had a drifting baseline so the cell with CD45-Fc recombinant protein immobilised was subtracted from all other flow cells to minimise refractive index effects (no binding was observed to CD45-Fc recombinant protein). The black arrows represent where CD271-1 Affimer was injected at increasing concentrations: A – 3.125 nM, B – 6.25 nM, C – 12.5 nM, D – 25 nM, E – 50 nM. CD271-1 Affimer was injected for 360 s at 50 µL/min.

To determine the approximate affinity of the binding interaction between CD271-1 Affimer and CD271-Fc protein, BIAevaluation software was used to perform a kinetic fitting to the binding curve. The fitting was performed on an individual binding curve rather than a global fit, so must be considered an estimation only.

The kinetic fitting was performed on a curve when 25 nM CD271-1 Affimer had been injected into a flow cell with CD271-Fc protein immobilised (Figure 5.19). The fitting estimated the equilibrium dissociation constant (K_D) to be 10 nM with a small chi squared value indicating a good statistical fit (Table 5.6). The K_D of antibodies is typically in the nanomolar range with high affinity antibodies in the low nanomolar range, and very high affinity antibodies in the picomolar range (228), therefore a K_D of 10 nM is considered to be of high affinity. The optimum affinity of binders in a cell enrichment device must be investigated to ensure cells can be released for subsequent use. However, the affinity of Affimer proteins could be increased or decreased as required using affinity maturation or mutagenesis respectively.

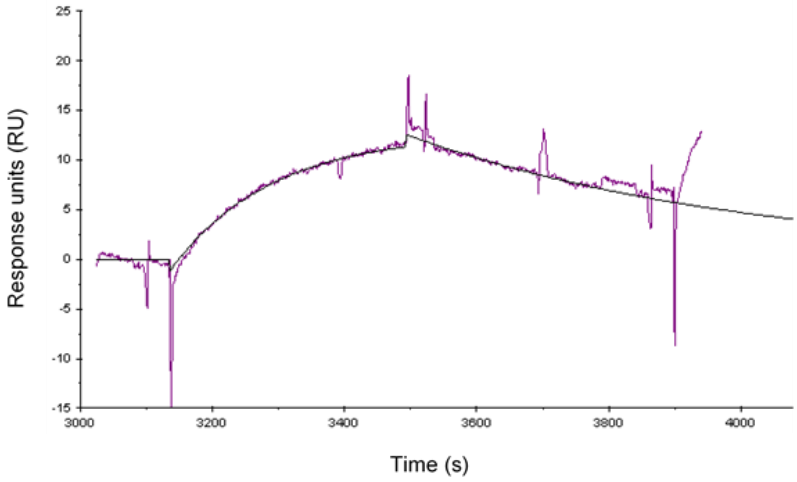

Figure 5.19 Kinetic fitting of Affimer CD271-1 binding to CD271-Fc protein using BIAevaluation software

BIAevaluation software was used to estimate the association and dissociation rate constants for CD271-1 Affimer binding to CD271-Fc recombinant protein. The kinetic fitting was performed on the binding curve where 25 nM CD271-1 Affimer was injected into a flow cell immobilised with CD271-Fc recombinant protein in non-reducing conditions. The chi squared value for the fit was small (see Table 5.6) indicating it was a good statistical fit.

Table 5.6 Calculated constants from BIAevaluation kinetic fitting

The association rate constant, dissociation rate constant and therefore the equilibrium dissociation constant were calculated from the kinetic fitting shown in Figure 5.19. It was found that the equilibrium dissociation constant was 10 nM.

Affimer	Association rate constant (k_a)(M^{-1} s^{-1})	Dissociation rate constant (k_d)(s^{-1})	Equilibrium dissociation constant (K_D)(M)	Chi^2
CD271-1	2×10^5	2×10^{-3}	10×10^{-9}	0.08

5.3.4 Characterisation of Affimer binding to CD271+ cells

The binding of Affimer CD271-1 to CD271+ cells was examined using two different flow cytometry approaches; indirect labelling of biotinylated Affimer protein using a streptavidin Alexa Fluor 488 conjugate (Section 5.2.12), and direct labelling of Affimer protein by Alexa Fluor 647 C_2 maleimide (Section 5.2.14). Affimer binding was compared to antibody binding and was investigated using dental pulp stromal cells (DPSCs) as well as a CD271+ cell line (SH-SY5Y neuroblastoma cells).

5.3.4.1 Antibody and Affimer titrations for flow cytometry analysis using indirectly labelled Affimer

The first stage of characterisation was to carry out antibody and Affimer titrations to investigate the working concentration of both binding molecules. A CD271 antibody conjugated to a phycoerythrin fluorescent dye (CD271-PE) was purchased from Miltenyi Biotec which has a manufacturer's recommended working concentration of 0.5 µg/mL. It was considered that the antibody could be used reliably at lower concentrations and therefore a concentration range of 0.5-0.125 µg/mL was examined. This was the first flow cytometry analysis of Affimers binding to cell surface markers and so the working concentration of Affimers in this application was unknown. The concentration of Affimer used in ELISA characterisation assays provided a starting point.

Figure 5.20 shows that antibody CD271-PE binds to a small percentage of DPSCs compared to an isotype-matched control antibody and unlabelled cells. It also demonstrated that no difference in labelling was observed when the concentration of the antibody was lowered to 0.125 µg/mL. Figure 5.21 shows

that biotinylated Affimer CD271-1 can be used for flow cytometric analysis at lower concentrations than in ELISA assays (2.5 µg/mL compared to 20 µg/mL) without any differences observed in labelling.

Figure 5.21 also shows a comparison of Affimer and antibody binding to DPSCs. The percentage positive for fluorescein isothiocyanate (FITC) labelling (indirect Affimer labelling) was 2.51% and the percentage positive for PE labelling (antibody labelling) was 2.11%. Despite the fact that these two values are close, the percentage of CD271+ cells in a DPSC population is very low, and possibly unreliable to compare antibody and Affimer binding. It was therefore decided to pre-enrich CD271+ cells to gain a larger target population.

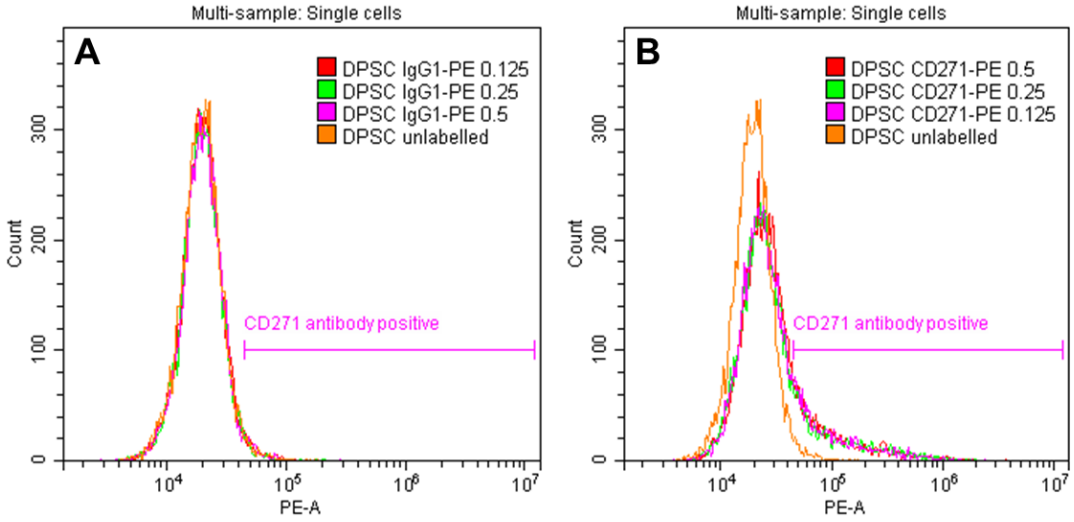

Figure 5.20 Flow cytometry histograms showing that CD271-PE antibody can be used reliably at lower concentrations

CD271-PE antibody (Miltenyi Biotec) and IgG1-PE isotype-matched control antibody (BD Biosciences) were incubated with DPSCs at three different concentrations – 0.5 µg/mL, 0.25 µg/mL and 0.125 µg/mL. Histogram A shows DPSCs incubated with the isotype-matched control antibody compared to unlabelled DPSCs, and histogram B shows DPSCs labelled with CD271-PE antibody compared to unlabelled DPSCs. It was found that the antibodies could be used at the lowest concentration without any effect on the result.

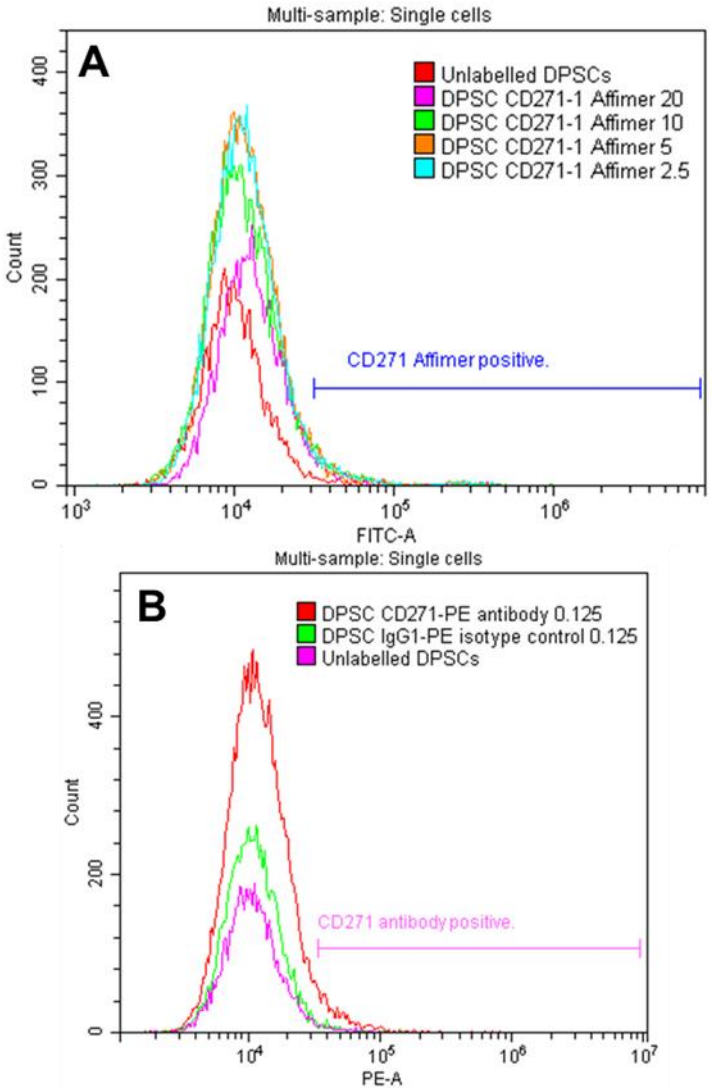

Figure 5.21 Flow cytometry histograms comparing CD271-1 Affimer and CD271 antibody binding to DPSCs

Histogram A shows different concentrations of Affimer CD271-1 binding to DPSCs compared to unlabelled DPSCs (red). In these experiments, biotinylated Affimer was used with a Streptavidin Alexa Fluor 488 conjugate detected in the FITC channel. Histogram B shows the same population of DPSCs incubated with CD271-PE antibody (at the previously determined concentration, red) compared to unlabelled DPSCs (pink), and DPSCs incubated with IgG1-PE (isotype-matched control antibody, green). It was found that the Affimer concentration did not affect cell binding and therefore Affimers could be used at the lowest concentration. It was also determined that the population of CD271+ cells in DPSCs was too low to make an accurate conclusion regarding the comparison of Affimer and antibody binding.

5.3.4.2 MACS enrichment of DPSCs prior to Affimer and antibody comparison using indirectly labelled Affimer

In order to accurately compare Affimer and antibody binding, a larger population of CD271+ cells would be beneficial. To achieve this, DPSCs were pre-enriched for CD271+ cells using CD271 magnetic microbeads (Miltenyi Biotec). After incubation with the microbeads, cells were passed through a column surrounded by a strong magnetic field. CD271+ cells attached to microbeads should be retained in the column while the remaining cells should be washed from the column. The different cell fractions were then analysed by flow cytometry using both CD271 antibody (different clone to CD271 microbeads) and Affimer.

Figure 5.22 compares antibody and Affimer binding to the different cell populations. It can be seen that where antibody was used for labelling (histogram A) a clear enrichment was established in the bound population (contour plot F). However, where Affimer was used for labelling (histogram B), all populations exhibited a small amount of fluorescence and no clear enrichment was seen (contour plot J).

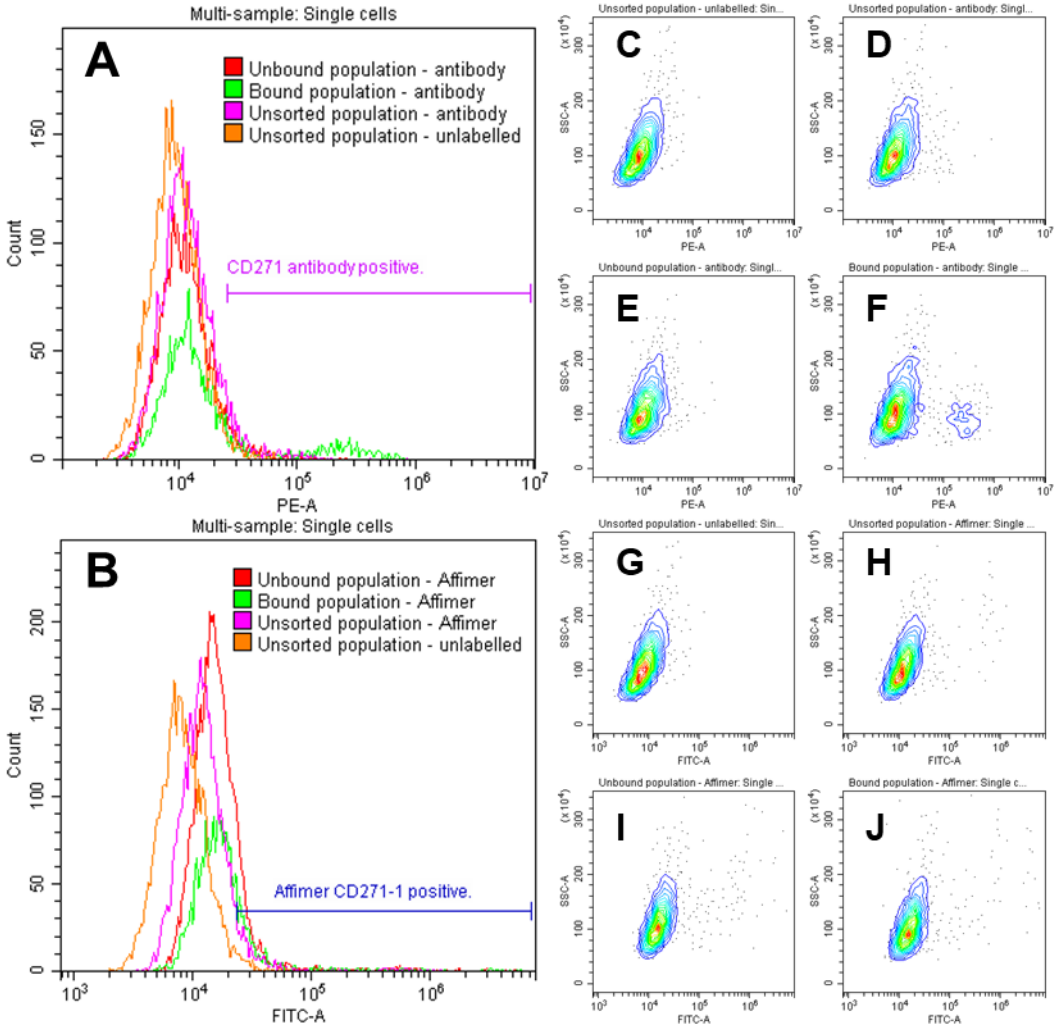

Figure 5.22 Flow cytometry comparison of Affimer and antibody binding to MACS-enriched CD271+ cells from DPSC populations

CD271+ cells were enriched from DPSCs using MACS technology. The eluate from the MACS column (unbound population), the cells retained in the column (bound population) and an unsorted population of cells were each incubated with CD271-PE antibody (histogram A, contour plots C-F: C – unlabelled unsorted population, D – labelled unsorted population, E – labelled unbound population, F – labelled bound population) or biotinylated CD271-1 Affimer (histogram B, contour plots G-J: G – unlabelled unsorted population, H – labelled unsorted population, I – labelled unbound population, J – labelled bound population). The bound population contained an enriched fraction of CD271+ cells identified by the CD271-PE antibody however not by the CD271-1 Affimer.

A further experiment was carried out to troubleshoot the positive fluorescence observed for all populations when labelled with Affimer. In this experiment, a second Affimer was used as a negative control (ToxinB-18 Affimer, shown not to bind to CD271 recombinant protein in ELISA experiments (Section 5.3.3.4)) and the streptavidin Alexa Fluor 488 conjugate alone. The results of this experiment are shown in Figure 5.23.

The antibody bound specifically to a small percentage of the DPSC population (2.88%), consistent with previous antibody labelling. In contrast, both Affimers (CD271-1 and negative control ToxinB-18) and the streptavidin Alexa Fluor 488 conjugate, all displayed positive labelling (6.18% and 5.95% for the ToxinB-18 Affimer and streptavidin Alexa Fluor 488 conjugate respectively, 12.10% for the CD271-1 Affimer).

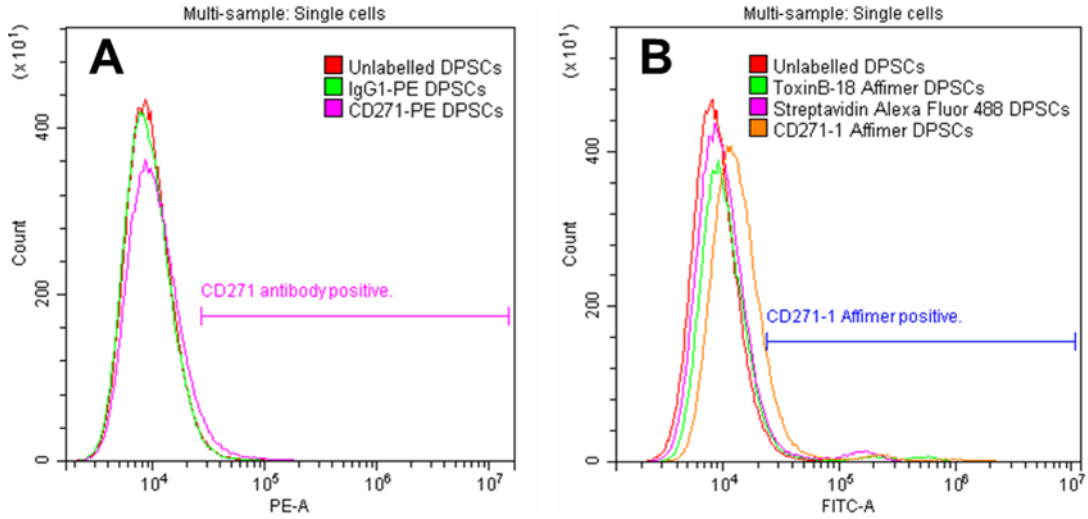

Figure 5.23 Flow cytometry histograms showing extra control experiments carried out to investigate Affimer CD271-1 binding to DPSCs

In histogram A, unseparated DPSCs were incubated with CD271-PE antibody (pink), IgG1-PE isotype-matched control antibody (green) or unlabelled (red). In histogram B, DPSCs were incubated with biotinylated CD271-1 Affimer (orange), biotinylated ToxinB-18 Affimer (negative control, green), streptavidin Alexa fluor 488 conjugate (negative control, pink) or unlabelled (red). A small percentage (2.88%) was CD271 antibody-positive compared to the unlabelled and isotype control. A shift in fluorescence was observed for both negative controls (ToxinB-18 Affimer - 6.18% positive, streptavidin Alexa fluor 488 conjugate - 5.95% positive, compared to unlabelled cells) and a larger percentage of 12.10% positive for CD271-1 Affimer.

5.3.4.3 Direct labelling of CD271-1 Affimer for flow cytometry analysis

In the previous experiments using indirect Affimer labelling, there was a consistently low level of binding observed for all cell populations even when using the secondary antibody (streptavidin Alexa Fluor 488) alone. This suggests that the positive fluorescence observed for cell populations labelled with Affimer could have been artefactual due to non-specific labelling by streptavidin Alexa Fluor 488. Moreover, the CD271-1 Affimer displayed a higher percentage of positive staining when directly compared to a control Affimer and the streptavidin Alexa Fluor 488 alone, suggesting that the CD271-1 Affimer could be displaying specific

binding to the small fraction of DPSCs that were CD271+. To investigate this further and to eliminate the artefactual labelling from the streptavidin Alexa Fluor 488 conjugate, direct fluorescent labelling of Affimer CD271-1 was carried out (Section 5.2.14).

An Alexa Fluor 647 C_2 maleimide was used to fluorescently label Affimer CD271-1 via its C-terminal cysteine residue (same principle as biotinylation, Section 5.2.9). At the same time, a GFP-32 Affimer was fluorescently labelled to use as a negative control. To verify that the Affimers were correctly labelled, and estimate the concentration of the labelled Affimers, samples were separated on a 12% SDS-PAGE gel (Figure 5.24). A dilution series of unlabelled Affimer with known concentration was used alongside samples with unknown concentration.

Imaging of the gels before Coomassie staining indicated that both Affimers were fluorescently labelled. There was dimer present in all samples, however in samples fluorescently labelled, more than 75% of sample had successfully reacted with Alexa Fluor 647 C_2 maleimide, and since dimers were not labelled (disulphide bridges between Affimers prevent reaction with maleimide) it was not judged as a major concern for flow cytometry analysis.

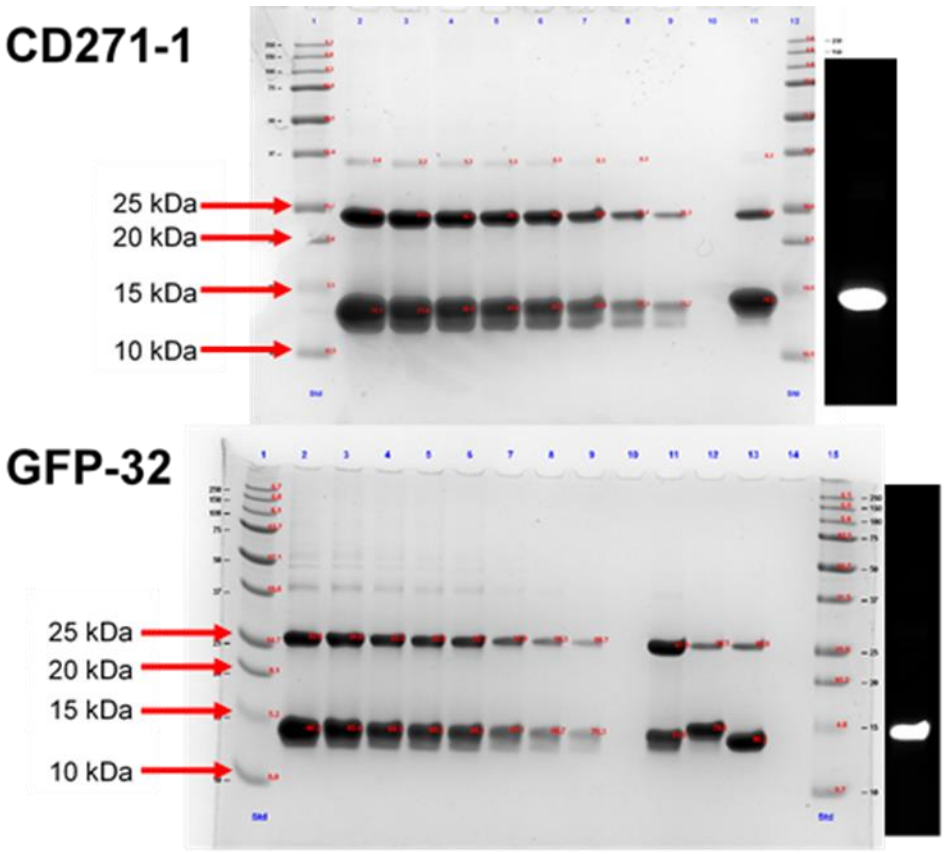

Figure 5.24 SDS-PAGE (12%) gels showing Affimers CD271-1 and GFP-32 labelled with Alexa Fluor 647 C2 maleimide

Affimers CD271-1 and GFP-32 (to be used as a negative control) were conjugated to Alexa Fluor 647 C_2 maleimide via the cysteine residue on the Affimer scaffold. Unlabelled Affimer of known concentration was run as a dilution series to calculate the concentration of the labelled Affimers. For Affimer CD271-1, wells 1 and 12 show protein ladders, wells 2-9 show a dilution of Affimer CD271-1 from 1 mg/mL to 0.05 mg/mL and well 11 shows Affimer CD271-1 conjugated to Alexa Fluor 647 C_2 maleimide. For GFP-32, wells 1 and 15 show protein ladders, wells 2-9 show a dilution series of Affimer GFP-32 from 1 mg/mL to 0.05 mg/mL, well 11 shows GFP-32 Affimer dialysed into PBS (unknown concentration), well 12 shows Affimer GFP-32 conjugated to Alexa Fluor 647 C_2 maleimide and well 13 shows Affimer GFP-32 conjugated to biotin maleimide. On the right-hand side of each gel, an image is shown of the fluorescently labelled Affimers before Coomassie staining. All samples had dimers present however when labelled, >75% of protein was fluorescently labelled monomer.

5.3.4.4 Affimer titrations for flow cytometry analysis using directly labelled Affimer

The fluorescently labelled Affimers were titrated to see the effect of concentration on cell labelling with fluorescently-tagged Affimers. The proportion of cell labelling decreased as the concentration of Affimer decreased suggesting that the cells

interacted non-specifically with the fluorescently-tagged Affimer at high concentrations (Figure 5.25).

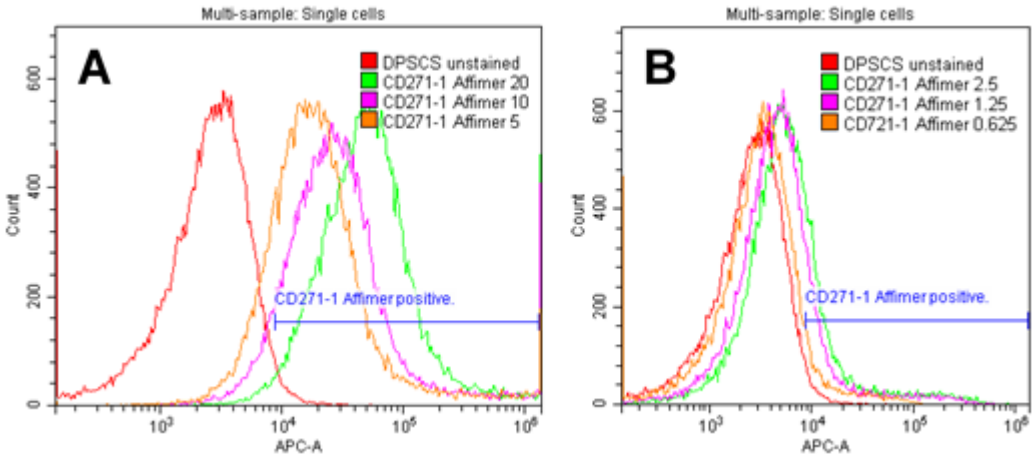

Figure 5.25 Flow cytometry histograms showing fluorescently-tagged CD271-1 Affimer titrations

DPSCs were incubated with different concentrations of fluorescently-tagged CD271-1 Affimer. Histogram A shows unlabelled DPSCs (red) and DPSCs labelled with 20 µg/mL Affimer (green), 10 µg/mL Affimer (pink) and 5 µg/mL Affimer (orange). Histogram B shows unlabelled DPSCs (red) and DPSCs labelled with 2.5 µg/mL Affimer (green), 1.25 µg/mL Affimer (pink) and 0.625 µg/mL Affimer (orange). At higher concentrations of fluorescently-tagged Affimer there was a large shift in fluorescence which reduces as the Affimer concentration was reduced.

Figure 5.26 displays a comparison of directly labelled CD271-1 Affimer (at the lowest concentration tested) with CD271 antibody, and also with a non-specific GFP-32 Affimer at the same concentration. Here it can be seen that although the binding of CD271 antibody and CD271-1 Affimer is similar (3.86% and 5.24% respectively), the positive labelling of GFP-32 Affimer is almost identical to the positive staining of the CD271-1 Affimer (5.29% and 5.24% respectively - Figure 5.26, panel B).

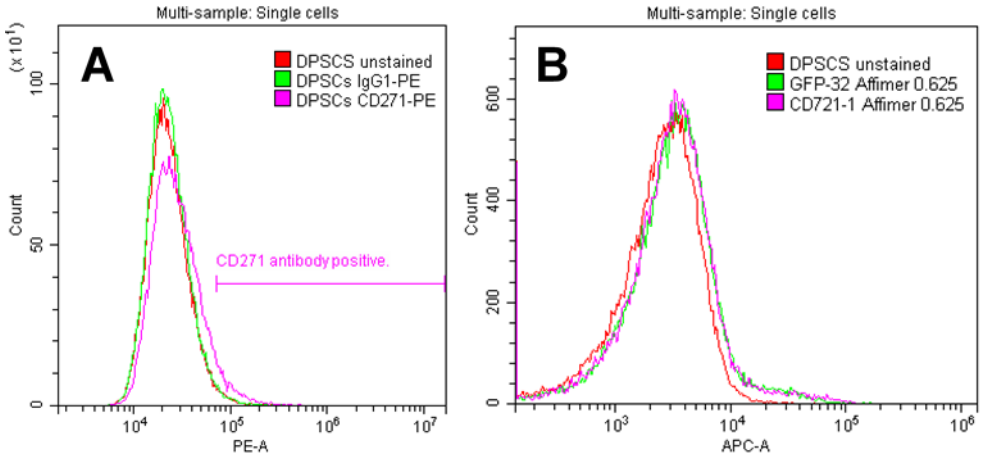

Figure 5.26 Flow cytometry histograms showing fluorescently labelled Affimer and antibody comparison

The same population of DPSCs was incubated with both CD271 antibody and fluorescently labelled CD271-1 Affimer. Histogram A shows DPSCs unlabelled (red), labelled with IgG1-PE (isotype-matched control, green) and labelled with CD271-PE antibody (pink). Histogram B shows DPSCs unlabelled (red), labelled with GFP-32 Affimer (negative control, green) and CD271-1 Affimer (pink). A small positive percentage was observed for cells incubated with CD271 antibody (3.86%). A larger positive percentage was observed for cells incubated with CD271-1 Affimer (5.24%), which was almost identical to the positive percentage observed for a non-specific Affimer (GFP-32, 5.29%).

5.3.4.5 MACS enrichment of DPSCs prior to Affimer and antibody comparison using directly labelled Affimer

It was previously seen that a CD271+ population of cells could be enriched from DPSCs using CD271 microbeads (Figure 5.22) and that this enriched population was more useful in providing conclusive results with respect to antibody and Affimer binding. The same MACS enrichment procedure was carried out and analysed with directly-labelled CD271-1 Affimer and CD271 antibody.

No clear enrichment of CD271+ cells was seen using either the CD271 antibody or the CD271-1 directly-labelled Affimer (Figure 5.27). The bound population after MACS enrichment was less than 300,000 cells and did not appear to be enriched for CD271+ cells when analysed by flow cytometry. The previous MACS enrichment results observed with CD271 antibody labelling were not reproduced. As before, a shift in fluorescence was observed in all populations when labelled with Affimer.

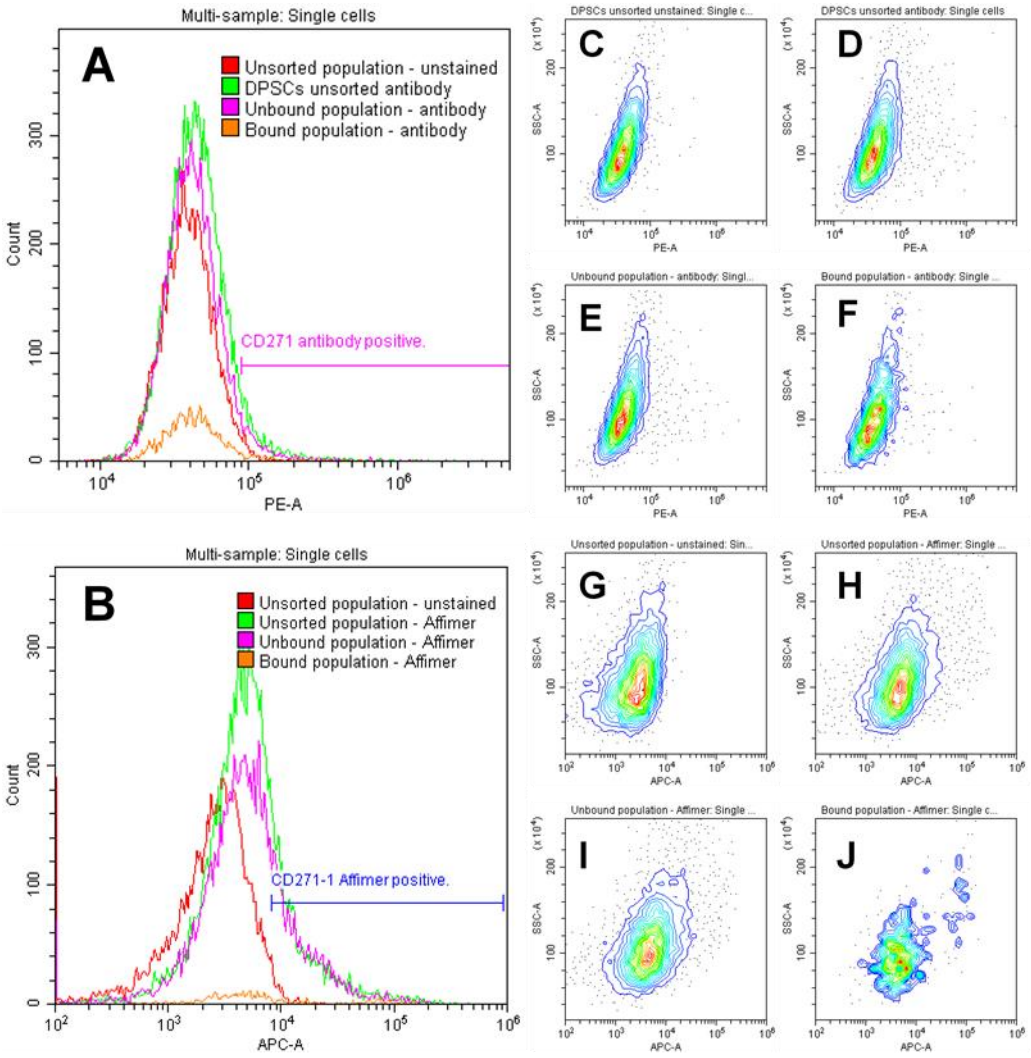

Figure 5.27 Flow cytometry comparison of Affimer and antibody binding to MACS-enriched CD271+ cells using directly labelled Affimer

DPSCs were enriched using MACS technology. The eluate from the MACS column (unbound population), the cells retained in the column (bound population) and an unsorted population of cells were each incubated with CD271-PE antibody (histogram A, contour plots C-F: C – unlabelled unsorted population, D – labelled unsorted population, E – labelled unbound population, F – labelled bound population) or biotinylated CD271-1 Affimer (histogram B, contour plots G-J: G – unlabelled unsorted population, H – labelled unsorted population, I – labelled unbound population, J – labelled bound population). There was no clear enrichment of CD271+ cells seen from either antibody or Affimer labelling.

5.3.4.6 Flow cytometry analysis of CD271-1 Affimer and CD271 antibody binding to SH-SY5Y cells using directly labelled Affimer

When it was found that the CD271+ population of DPSCs could not be consistently enriched, a new strategy was sought to compare antibody and Affimer labelling of CD271+ cells. A search of the literature revealed a

neuroblastoma cell line that constitutively expressed CD271 (229). The cell line – named SH-SY5Y – was obtained and analysed by flow cytometry using both CD271 antibody and CD271-1 Affimer.

The antibody results confirmed the fact that SH-SY5Y cells express CD271 with approximately 80% of the population labelling positive for CD271-PE antibody (Figure 5.28, panel A). The Affimer labelling results for both CD271-1 and GFP-32 were again very similar and not comparable with antibody labelling (approximately 5% and 6% positively labelled respectively, Figure 5.28, panel B). The Affimer labelling suggested a small amount of non-specific binding and was in good agreement with the DPSC flow cytometry data.

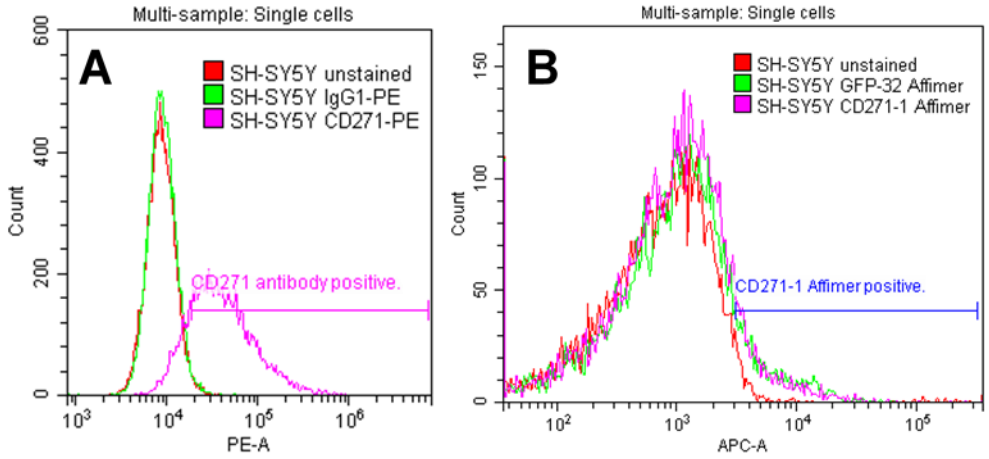

Figure 5.28 Flow cytometry comparison of Affimer and antibody binding to SH-SY5Y cells

SH-SY5Y cells were used to compare Affimer and antibody binding since there is literature evidence that this cell line expresses CD271 (229). Histogram A shows CD271 antibody (pink) binding to SH-SY5Y cells compared to an isotype-matched control antibody (IgG1-PE, green) and unlabelled cells (red). Histogram B shows CD271-1 Affimer (pink) binding to SH-SY5Y cells compared to a non-specific Affimer (GFP-32, green) and unlabelled cells (red). The antibody labelling confirmed that SH-SY5Y cells express CD271 (~80% CD271 antibody positive). The CD271-1 Affimer labelling was similar to the GFP-32 Affimer labelling and only labelled a small percentage of the SH-SY5Y cells (~5-6%).

5.4 Conclusions

In this chapter, human CD271 recombinant protein was screened against Affimer libraries containing approximately 1.3 x 10^{10} independent clones. Two screens were carried out using two different protocols for biopanning. Three unique clones were identified as potential binders to human CD271 protein and were characterised by ELISA and SPR. Following initial characterisation with CD271

recombinant protein, one Affimer (CD271-1) displayed specific binding, with an equilibrium dissociation constant estimated to be 10 nM – comparable to that of a typical antibody. This Affimer was further investigated with cells expressing CD271 protein, and the binding behaviour compared with that of a CD271 antibody. It was found that the Affimer did not display the same binding behaviour as a CD271 antibody. This was compared using two different labelling methods and two different cell types.

There is evidence that suggests the success of phage display screening relies heavily upon the quality of the target protein (158, 230). The phage display screens carried out here only resulted in the identification of three unique clones and this could be due to the quality of the CD271-His recombinant protein that was used. It can be difficult to achieve high quality soluble proteins for membrane proteins with large hydrophobic transmembrane domains, and with extended extracellular regions made up of multiple domains (231), as is the case for CD271. This is because they are often flexible and unstable leading to challenges at all stages of protein production including expression, solubilisation and purification (232). From the initial colony counting it could be seen that the amplification from negative to positive colony plates was not as large as was observed in the case of both positive control proteins. Colony counting is an early indicator of the likeliness that specific binders have been selected.

Additionally, during the characterisation assays the Affimer clones exhibited preferable binding to the CD271-Fc recombinant protein compared with the CD271-His variant. It was hypothesised that this CD271-Fc recombinant protein could be of better quality than the originally screened protein. In previous Affimer library screens it has been found that when several commercial sources of the same protein were screened, only one source selected suitable Affimers (158). To investigate this further a third screen using both proteins – CD271-His and CD271-Fc – was carried out by the BSTG group. The results were consistent with the initial screens where only a handful of unique clones were identified from screening both CD271 proteins – three in total (data not shown). There was some cross reactivity between clones screened against the CD271-His protein with the CD271-Fc protein (and vice versa) however only for two out of three of the unique sequences.

For this research project it was decided not to investigate the newly identified sequences any further. When phage display screening is carried out, it is hoped that a large pool of unique clones will be selected, which are then narrowed down during characterisation, resulting in a handful of appropriate binders for the desired application. Unfortunately, when only a handful of unique clones are selected in the initial stages, it becomes increasingly unlikely that a suitable

binder will be found. It was therefore considered not likely that the third screen would result in a specific binder for CD271+ cells.

There were no further commercial sources of CD271 protein available to buy (at this time), however in future, a different screening strategy could be considered such as whole cell biopanning. By using whole cell biopanning the antigen source is presented to the phage display library in its native conformation along with post-translational modifications (230, 231). This increases the chances of isolating binders appropriate for *in vivo* applications. However, whole cell biopanning can be challenging due to high backgrounds of non-relevant proteins with comparatively low abundance of target protein.

Jones *et al.* (2016)(231) developed a method for whole cell biopanning using transient transfection of the target protein to increase the target antigen density on the cell surface. As well as this, GFP was transiently transfected alongside the target protein to enable cell sorting to select cells with high expression of the target protein. The host cell line was alternated between biopanning rounds to minimise binding to host cell proteins and a low pH wash reduced the enrichment of phage clones bound non-specifically. They found that the method was able to isolate high affinity binders which showed better binding to cells than those isolated from the same library but panned on soluble protein.

Likewise, Crepin *et al*. (2017)(233) used whole-cell biopanning with a synthetic phage display library of nanobodies (single domain antibodies) and successfully isolated nanobodies against follicle-stimulating hormone receptor overexpressed in L-cells. Similarly to Jones *et al.*, a number of modifications were made to decrease non-specific nanobodies present in the final elution fraction. These included two initial depletion steps with wild type L-cells reducing the initial number of phages, and reducing the number of cells used for enrichment. The resulting nanobodies exhibited inhibitory behaviour on follicle-stimulating hormone-dependent cyclic adenosine monophosphate accumulation.

Alfaleh *et al.* (2017)(230) provide a detailed review of studies where different strategies for whole cell biopanning have been optimised. Methods have been developed to screen low numbers of cells - such as a microfluidic phage display system (234), and the use of microselection to target single rare cells amongst a heterogeneous population of cells (235). In addition, strategies have been utilised to further reduce non-specific binding such as the removal of dead cells and cellular debris prior to biopanning (236), as well as the optimisation of temperature and incubation times during biopanning (237, 238). Giordano *et al.* (2001)(239) developed a washing method using differential centrifugation which eliminated the need for repeated washing steps.

Although these studies highlight several novel cell-based biopanning strategies, the success still relies heavily upon the nature of the antigen. For example, Hoogenboom *et al.* (1999)(240) expressed two antigens of interest in Chinese hamster ovary cells but was only able to select receptor specific binders to one of the antigens. Where binders were successfully isolated, the antigen in question is characterised by a large, highly glycosylated immunogenic extracellular domain. In contrast, where binders were not selected, the antigen is characterised by short, heavily glycosylated extracellular loops of approximately 40 amino acids and has low immunogenicity.

The CD271 receptor contains an extracellular domain containing four 40-amino acid repeats followed by a serine/threonine-rich region containing the CD271 antigen (241). Whole cell biopanning for CD271+ cells would require its own optimisation but has the potential to provide binders which would recognise CD271 in its native confirmation on the cell surface membrane rather than to the recombinant protein only.

However, for this research project the priority was to develop a microfluidic cell enrichment device, and during the characterisation of Affimers their binding was compared to a commercially-available CD271 antibody. Reliable and reproducible binding was established with the CD271 antibody providing a suitable candidate binding molecule for cell capture within a cell enrichment device. Although there are potential advantages of using Affimers as cell capture molecules (Chapter 2: Section 2.5.3.2), the antibody provided a good starting point for development of this technology.

The work in this chapter has also established a cell line model which could be used during proof-of-concept stages. Whilst carrying out the initial characterisation of Affimer-target-cell binding, it was found that the percentage of CD271+ cells in a DPSC population was very low and could not be reliably enriched by CD271 microbeads. There are varying reports of CD271 expression of DPSCs found in the literature, Ducret *et al*. (2016)(242) found that 2.4% of the CD31 negative population (to exclude endothelial and leukocytic cells) of dental pulp cells expressed CD271, however this decreased to less than 1% upon *in vitro* expansion. The same pattern was observed by Tomlinson *et al.* (2016)(243), where uncultured dental pulp cells were found to express 1.24 ± 0.46% CD271 but an average expression of 0.2% was found across passages 2 to 4. Pan *et al.* (2016)(244) investigated expression across eight different donors and discovered that CD271 expression ranged from 1.57% to 6.35% (no *in vitro* expansion). Alvarez *et al*. (2015)(245) reported unusually high CD271 expression in passage 4-8 dental pulp cells at 10.6%, however the flow cytometry gating strategies are not detailed in their paper.

Due to the low and varying levels of expression of CD271 on cultured DPSCs, it was decided to carry out experiments during the device development stages using a neuroblastoma cell line where approximately 80% of cells were found to express CD271. Not only is high expression of CD271 an advantage (not requiring any pre-enrichment techniques) but established cell lines grow indefinitely, providing a good supply of cells for experiments. Once proof-of-concept had been shown using an established cell line, clinical utility was investigated using primary cells.

In conclusion, novel binding proteins – Affimers – were investigated for use as cell capture molecules in a cell enrichment device. At this time, no binders were found to be suitable for the application. Instead, an appropriate antibody was found to reliably bind to CD271+ cells and a neuroblastoma cell line was found to express a high percentage of CD271. In Chapter 6, the development of a cell enrichment device will be described using a CD271 antibody as a capture molecule, and the efficacy of the device validated using the neuroblastoma cell line.

Chapter 6:
Developing a prototype microfluidic device for CD271-specific cell capture and release

6.1 Introduction

The aim of the work carried out in this chapter was to design, fabricate and evaluate a prototype microfluidic device capable of specific cell capture and release. In Chapter 5, a CD271 antibody was identified which reliably bound to CD271+ cells and was thus able to act as a capture molecule in a prototype device. A device was designed using Autodesk Fusion360 (Section 6.2.4.1), fabricated and assembled into a prototype device (Sections 6.1.1 and 6.2.4.3) and a series of experiments carried out to evaluate the specificity of cell capture (Section 6.3.2). Once cell capture and release had been optimised (Section 6.3.3), post-enrichment analysis was carried out on cells that had been captured and released in the device to ensure they remained viable (Section 6.3.6 and 6.3.7) and were minimally manipulated during the enrichment procedure (Section 6.3.8).

6.1.1 Soft lithography techniques

Soft lithography refers to a branch of photolithography adapted to process photoresists for the fabrication of microfluidic devices (246), such as the device described in this chapter. Standard photolithography was primarily developed for microelectronics whereas soft lithography is termed as such as it deals with mechanically soft materials. The most widely used material is polydimethylsiloxane (PDMS) since it has low cost, it is biocompatible, and has high durability (247).

In this work, soft lithography techniques were used to fabricate microfluidic channels using a negative mould, where PDMS is poured into the mould, cured and then released from the mould (Figure 6.1). A typical procedure for making a negative mould is outlined in Figure 6.2. The procedure requires a mask and a light source to pattern a photosensitive resist (248). However in this work, a maskless aligner was used which eliminates the need for a mask and directly exposes the pattern onto the resist-covered substrate. The photoresist is spin-coated onto a substrate with the spin speed determining the coat thickness. The photoresist is then pre-baked so that its solvent is evaporated before exposure to UV radiation (an optimum wavelength of 365 nm for SU-8 photoresists). Post-baking is necessary to aid crosslinking of the exposed photoresist before a

developer is applied to dissolve the remainder of the photoresist. A negative mould is the result of the procedure which is then ready for PDMS casting.

Figure 6.1 The process of making PDMS channels using a negative mould

A negative PDMS mould is typically fabricated using photolithography techniques (see Figure 6.2). PDMS is poured into the mould and cured for 24 h at 65 °C. The PDMS can then be released from the mould creating ridges which act as microfluidic channels.

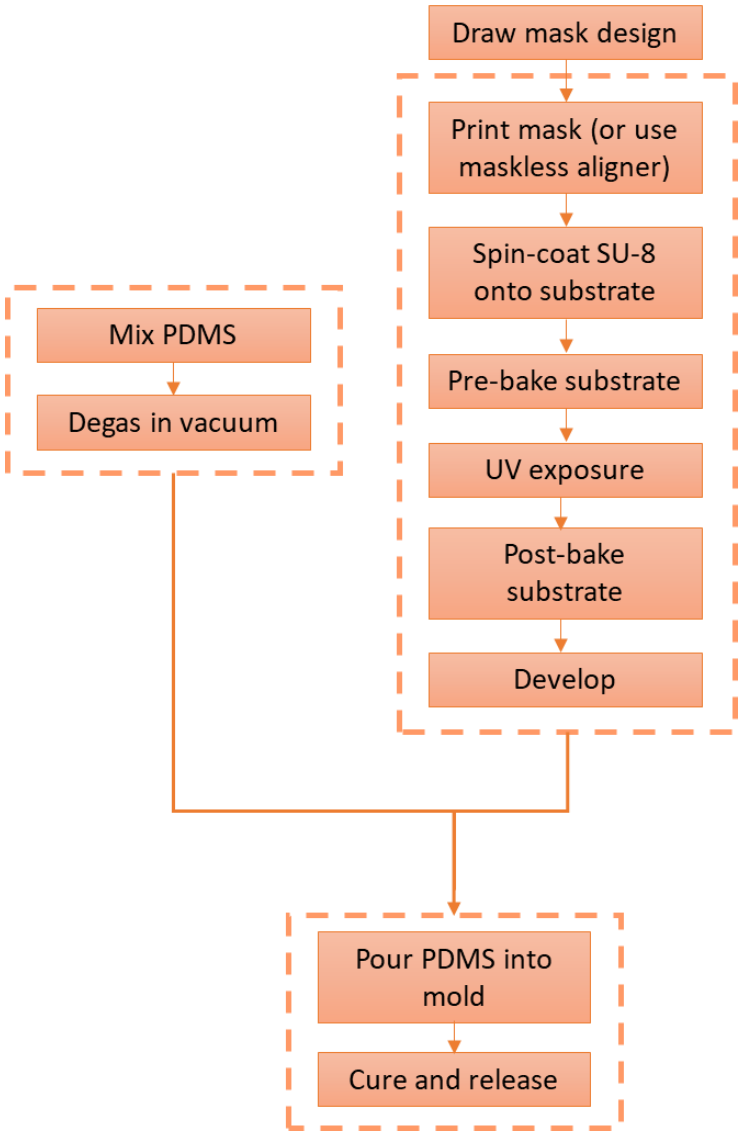

Figure 6.2 A typical photolithography procedure to make a PDMS mould

Flow diagram adapted from (248).

6.2 Materials and Methods

6.2.1 Flow cytometry analysis of the CD271 expression of human dermal fibroblast cells and the CD34 expression of SH-SY5Y cells

Flow cytometry (Chapter 2: Section 2.5.1.3) was used to verify that human dermal fibroblast cells (Section 4.1.3) did not express the CD271 antigen on their cell surface and that SH-SY5Y cells (Section 4.1.2) did not express the CD34 antigen. This information was required to verify the controls used during the experiments described in this chapter.

For the fibroblast cells, the same antibodies and protocol was used as described in Chapter 5: Section 5.2.12. Briefly, CD271-PE antibody (Miltenyi Biotec, 130-091-885) and IgG1-PE isotype-matched control antibody (BD Biosciences, 555749) were incubated with cells in the dark at 4 °C for 30 min. Cells were washed by adding 2 mL FACS buffer and centrifuging at 300 g for 5 min. Cells were re-suspended in 350 µL FACS buffer and analysed using a CytoFLEX S Flow Cytometer.

The same procedure was used for the analysis of SH-SY5Y cells using a CD34-PE antibody (Miltenyi Biotec, 130-113-741).

6.2.2 SPR analysis of CD271+ cells binding to CD271 antibody on a gold surface

Surface plasmon resonance (SPR, Section 4.2) is an established method to characterise protein-protein, DNA-DNA and DNA-protein interactions, however, more recently it has also been used to study whole cell interactions. Ogura *et al.* (2016)(249) published a method to detect the interactions of anti-TNF agents with transmembrane TNF-α on living whole cells, and Mizuguchi *et al.* (250) described a similar technique using epidermal carcinoma A431 cells as an analyte, and immobilised epidermal growth factor as a ligand, with the aim of future applications in drug discovery against membrane receptors on pathological cells. In this work, it was decided to use SPR as an initial method of assessment for the specific cell capture of CD271+ cells on a CD271-antibody functionalised surface - analogous to cell capture in the microfluidic device. Two CD271 antibodies were investigated for specific cell capture, a CD271 antibody conjugated to phycoerythrin dye (CD271-PE, Miltenyi Biotec, 130-091-885, previously shown to bind to CD271+ cells in Chapter 5: Section 5.3.4) and a

CD271 antibody conjugated to biotin (CD271-biotin, Miltenyi Biotec, 130-113-419).

An Autolab ESPIRIT Data Acquisition 4.3 was used for SPR analysis, where antibodies were immobilised on a gold-coated glass disk (Xantec Bioanalytics). The disk was cleaned using the following protocol:

- 10 min sonication in acetone
- Wash in beaker of 100% ethanol
- 10 min sonication in fresh beaker of 100% ethanol
- Wash in fresh beaker of 100% ethanol

and then coated with a monothiol-alkane-PEG self-assembled monolayer (SAM, Section 4.3)(ProChima Surfaces TH 003-m11.n6) terminated with a carboxylic acid group (HS-C11-(EG)6-OCH2-COOH). The disk was incubated in the SAM solution (1 mM in 95% ethanol, 5% acetic acid) for 24 h minimum at RT prior to use. Excess SAM molecules were washed from the disk using 100% ethanol and the disk dried using a nitrogen gun. The glass disk was loaded on to the Autolab ESPIRIT hemi-cylinder using a drop of immersion oil.

The Autolab ESPIRIT has two flow cells which can be run simultaneously with continuous mixing during injections. All injections were carried out such that buffer was injected until the baseline was stable, then the analyte was added whilst measuring and with continuous mixing.

6.2.2.1 Assessing the appropriate pH for protein immobilisation (pH scouting)

pH scouting was carried out to assess a favourable pH for CD271-PE immobilisation. pH 8.0 sodium phosphate buffer was injected into one flow cell and pH 7.0 sodium phosphate buffer was injected into the second flow cell. When the baseline was stable, 5 µg/mL CD271-PE antibody (diluted in the respective buffer) was injected for 6-10 min (until saturation). After the injection, the injection needles were washed, the flow cell drained and fresh buffer injected. The surface was regenerated with 10 mM sodium hydroxide for 2 min before the next two buffers were tested. A pH range of pH 8.0-pH 4.0 was investigated and a compromise of pH 5.0 sodium acetate buffer was selected for CD271-PE immobilisation. Using pH 5.0 sodium acetate buffer resulted in ~50% of the maximum coverage and was closer to biological pH than pH 4.0 - which resulted in a higher coverage (Figure 6.3).

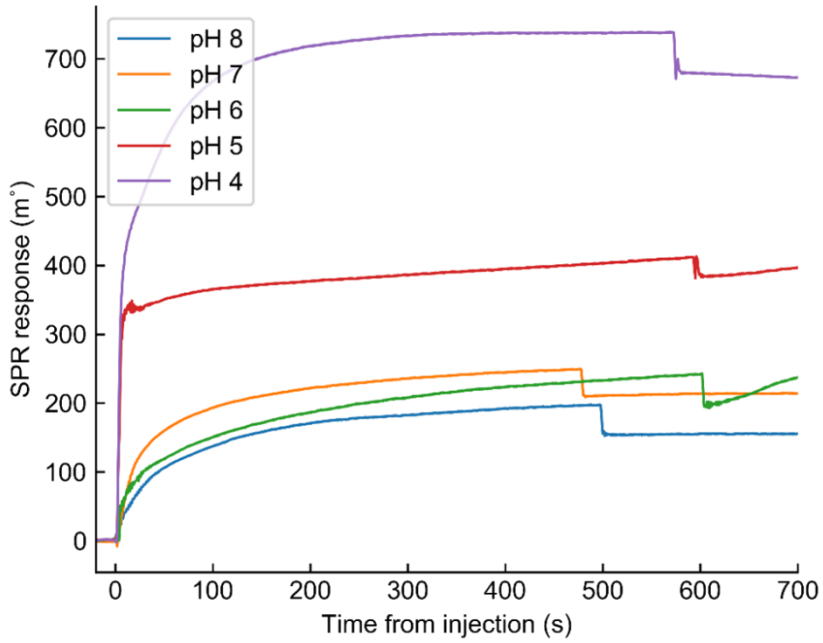

Figure 6.3 pH scouting for the immobilisation of CD271-PE antibody

CD271-PE antibody was immobilised on the SPR disk in buffers of different pH (range pH 8.0 – pH 4.0). Antibody was injected for 6-10 minutes and the antibody loading evaluated. pH 5.0 sodium acetate buffer was selected as the immobilisation buffer for binding assays as a compromise between antibody loading and biological pH.

For the CD271-biotin antibody, streptavidin was first immobilised onto the glass disk at a pH of 5.0 (10 mM sodium acetate buffer) following an online protocol (251), summarised below.

6.2.2.2 Protein immobilisation onto the gold-coated glass disk

For binding assays for both antibodies, the monolayer was first activated using NHS and EDC crosslinking chemistry (see Section 4.4); equal volumes of NHS (GE Healthcare, BR-1000-50, 200 mM) and EDC (GE Healthcare, BR-1000-50, 800 mM) were mixed with an equal volume of 2-(N-morpholino)ethanesulfonic acid (MES) buffer[8]. MES buffer was injected into both channels until the baseline was stable, and then 125 µL of the NHS/EDC solution was injected for 10 min. Between each injection, buffer was injected until the baseline was stable. Sodium acetate buffer (pH 5.0, 10 mM, 50 µL) was injected and when stable, 20 µg/mL CD271-PE antibody (50 µL, final concentration 10 µg/mL) injected until saturation.

[8] MES buffer: MES hydrate (Sigma, M2933), pH 5.5

For the immobilisation of CD271-biotin, 250 µg/mL streptavidin in sodium acetate buffer (50 µL, final concentration 125 µg/mL) was injected for 10 min. After the immobilisation of streptavidin, unreacted sites were capped by injection of 1 M ethanolamine, pH 8.5 (supplied with amine coupling kit, GE Healthcare, BR-1000-50) for 10 min. Finally, CD271-biotin antibody was injected in PBST (20 µg/mL, final concentration 10 µg/mL) until saturation.

6.2.2.3 SPR binding assays to study whole cell interactions

When the antibodies were immobilised, alpha MEM culture medium with 0.005% Tween 20 was injected and used as a running buffer throughout the cell binding assays. For each injection, 75 µL of medium was injected followed by 75 µL of cell suspension. The concentration of cell suspensions started at 3.125×10^5 cells/mL and increased two-fold to a concentration of 2.0×10^7 cells/mL. The SPR signal was measured for 15 min, the needles washed, the flow cell drained and running buffer injected until a stable baseline was achieved.

After the highest cell concentration was injected and a stable baseline established, the pH was increased by injection of glycine-NaOH (80 mM, pH 8.5). The pH was gradually increased to pH 10.0 (in 0.5 steps) until there was no further change in the SPR angle. Between each pH, running buffer (Alpha MEM culture medium with 0.005% Tween 20) was injected until the baseline was stable.

6.2.3 Colorimetry experiment to investigate the immobilisation of CD271 antibody to the channel surface

To ensure that antibody was uniformly present on the channel surface, a colorimetry experiment was carried out on the channel surface substrate. The substrate was a gold-coated glass slide or silicon wafer (see Section 6.2.4.2 for fabrication details), with an adhesion layer of 5 nm titanium and a gold layer of 50 nm – similar to the gold-coated SPR glass disk (Section 6.2.2). From SPR experiments, it was decided to use a CD271-biotin antibody for specific cell capture (see Section 6.3.1.1) which could be detected by an alkaline phosphatase (ALP) conjugated anti-biotin secondary antibody (Miltenyi Biotec, 130-092-612) and reacted with 5-bromo-4-chloro-3-indolyl phosphate (BCIP)/nitro blue tetrazolium (NBT) substrate (Sigma Aldrich, B5655) to produce a blue-purple reaction product which precipitates onto the gold surface (252).

A series of controls was carried out alongside the test condition to ensure the antibody was immobilised via NHS/EDC crosslinking only. Six conditions were tested in total, including a titration of the secondary antibody:

1. Full immobilisation with secondary antibody concentration of 1 µg/mL
2. Full immobilisation with secondary antibody concentration of 0.5 µg/mL
3. Full immobilisation with secondary antibody concentration of 0.1 µg/mL
4. Immobilisation without streptavidin
5. Immobilisation without CD271-biotin antibody
6. Immobilisation without secondary antibody

Two replicates of each condition were carried out.

The same procedure of antibody immobilisation was carried out as for the SPR disk; the gold-coated glass slide was incubated with SAM solution (ProChima Surfaces TH 003-m11.n6, 1 mM in 95% ethanol, 5% acetic acid) at RT for 24 h minimum. The slide was washed with 100% ethanol and dried using a nitrogen gun. The slide was washed with MES buffer for 5 min in a shaker (Stuart orbital incubator S150) then incubated with NHS and EDC solution (200 mM NHS (150 µL), 800 mM EDC (150 µL)) in an equal volume of MES buffer for 15 min at RT. Washing with MES buffer was repeated for 5 min and then in sodium acetate buffer (10 mM, pH 5.0) for 5 min. All washing steps were carried out on a shaker. A solution of streptavidin (250 µg/mL in sodium acetate buffer (10 mM, pH 5.0)) was spotted in test conditions and buffer spotted in control conditions. Spots were 2 µL in volume and pipetted directly onto the gold surface.

After 15 min, the spots were pipetted off and the slide washed with sodium acetate buffer (10 mM, pH 5.0) for 5 min. A solution of 1 M ethanolamine (pH 8.5) was pipetted over the entire surface of the slide and incubated for 10 min to cap unreacted sites on the monolayer. Washing with sodium acetate buffer was repeated then the buffer changed to PBST for 5 min. CD271-biotin (10 µg/mL in PBST) was spotted in the test conditions and buffer only spotted for control conditions. The substrate was incubated for 30 min before washing in PBST for 5 min. The slide was incubated in 1% bovine serum albumin (BSA, in PBST) for 30 min and then washed. Anti-biotin ALP (1 µg/mL, 0.5 µg/mL and 0.1 µg/mL in PBST) was spotted in test conditions and incubated for 45 min. The slide was washed in PBST twice, then three times in PBS for 5 min each.

After the last wash, the slide was placed in BCIP/NBT substrate (1 tablet dissolved in 10 mL distilled water) and incubated for 10 min. The slide was washed three times in water (2 min each) and dried. Photographs were taken using a Zeiss AX10 microscope and AxioCam MRc 5 camera with 10x magnification.

6.2.4 Design, fabrication and assembly of a prototype microfluidic device

6.2.4.1 Overall device design using Autodesk Fusion360 software

The initial design for a prototype microfluidic device was drawn in Autodesk Fusion360 software. The design consisted of a gold-coated substrate which could be functionalised with antibodies for specific cell capture. On top of the gold surface, four PDMS channels were designed to allow microfluidic flow, with inlets from the top side of the device and outlets from the bottom side of the device. This was designed so that the fluid flow would be in the direction of gravity to increase cell recovery. The gold substrate had four holes where the outlets were, and a bottom layer of PDMS was designed to secure the outlet tubing in place. The bottom layer of PDMS had four 1 mm cylinder protrusions so it would fit flush with the 1 mm gold substrate.

On top of the channels a Perspex clamp was designed to hold the channels in place, and a Perspex rig was designed to hold the PDMS, gold substrate, and clamp structure. The Perspex rig had indents where valves could sit to control the fluid flow before fluid entered the channels. The Autodesk Fusion360 design is shown in Figure 6.4.

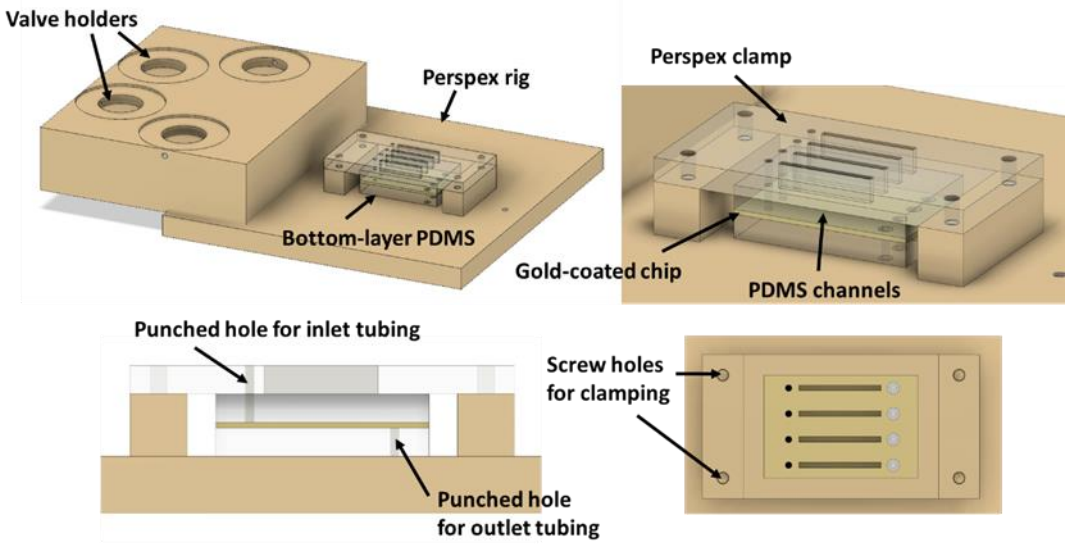

Figure 6.4 Autodesk Fusion360 design for a prototype microfluidic device

An overall device design was drawn using Autodesk Fusion360 software. The top left photo shows the full device, the top right photo shows a closer view of the microfluidic channels, the bottom left photo shows a side view of the channels and the bottom right photo shows the top view of the channels.

6.2.4.2 Fabrication of a gold-coated surface for antibody functionalisation

Once an overall design had been established, the individual parts were drawn in 2D in L-Edit v12.6 (Figure 6.5), and fabricated. Two different substrates were used as a basis for the gold-coated substrate – standard glass slides (Fisher Scientific, 12373118) and silicon wafers (650 – 700 micron thickness, 150 mm diameter). The glass slides were scribed in half and the silicon wafers were cut using a wafer saw to the same size as half a glass slide (25 mm x 37.5 mm). Four 3 mm-diameter holes were laser cut from the substrate to allow for the outlet tubing (see Figure 6.4 and Figure 6.5).

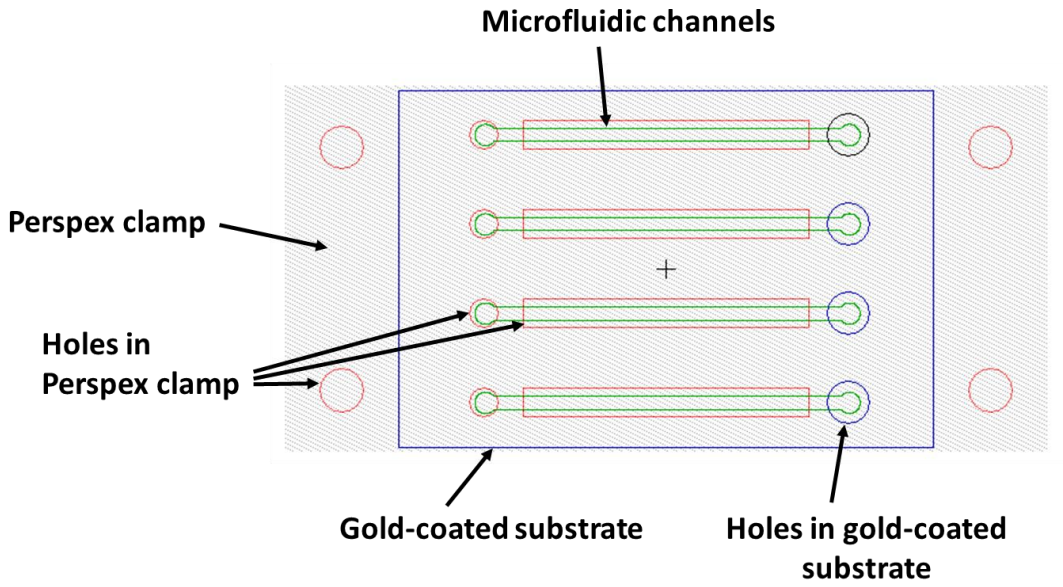

Figure 6.5 L-Edit drawing of the gold-coated substrate, microfluidic channels and clamp for fabrication

The Perspex clamp (grey), the gold substrate (blue), and the microfluidic channels (green) were drawn in 2D in L-edit. The red circles and rectangles show laser-cut holes in the Perspex clamp for screws (larger red circles), inlet tubing (smaller red circles) and to view the channels (red rectangles), and the blue circles show holes in the gold substrate for the outlet tubing. The channel dimensions were 25.5 mm in length and 900 µM in width.

Once the holes in the substrate had been laser cut, the substrates were coated with a 50 nm layer of gold using an e-beam evaporator (Leybold). The substrates were cleaned using piranha solution (70% sulphuric acid, 30% hydrogen peroxide) and placed in an oxygen plasma for 5 min, 50 W. The substrates were dehydrated on a hot plate for 5 min at 200 °C before placed in the evaporation chamber. A 5 nm layer of titanium was used as an adhesion layer. Figure 6.6 shows gold-coated substrates ready for antibody functionalisation.

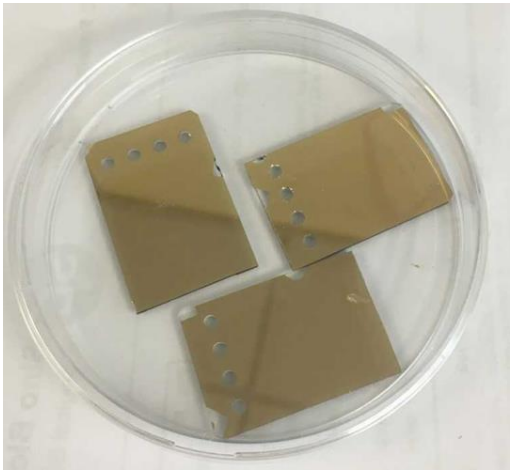

Figure 6.6 Gold-coated substrate for antibody functionalisation

Glass slides or silicon wafer were coated with a 5 nm titanium adhesion layer and a 50 nm gold layer using an e-beam evaporator.

6.2.4.3 Microfluidic channel design and fabrication of a PDMS mould using SU-8 photoresist

The microfluidic channel design was drawn in L-Edit v12.6 and consisted of four individual channels, 25.5 mm in length and 900 µM in width (shown in green in Figure 6.5). Four channels were designed so that each channel could be used for separate control experiments. The dimensions were designed so that the channels would fit on half a microscope slide, had a low aspect ratio, and were similar to a microfluidic device used by Qasaimeh *et al.* (2017)(253) to capture CD138-expressing cells.

A PDMS mould was made using standard soft lithography techniques (see Section 6.1.1). A silicon wafer (Nova Electronic Materials) was cleaned using piranha solution (70% sulphuric acid, 30% hydrogen peroxide) and placed in an oxygen plasma for 5 min, 50 W. The wafer was dehydrated on a hot plate for 5 min at 200 °C, then spin-coated with SU-8 photoresist (MicroChem formulations 50-100) according to the manufacturer's recommendations for 100 µM thickness. The spin-coated wafer was pre-baked for 5 min at 65 °C and soft-baked for a further 25 min at 95 °C. A Maskless Aligner (MLA-150) was used to pattern the microfluidic channels directly onto the resist-covered wafer (375 nm, dose 1600). The patterned wafer was post-baked for 1 min at 65 °C then the temperature ramped to 95 °C for 10 min. After post-exposure baking, SU-8 photoresist was developed in EC solvent (MicroChem) for 11 min with a solvent change after 6 min. The wafer was hard-baked at 200 °C for 5 min to reduce cracks in the mould.

The height of the ridges in the mould were measured using a surface profiler (Alpha-Step IQ) to estimate the height of the PDMS channels subsequently made

from the mould. A 5 mm PDMS gasket was laser cut from Perspex and attached to the wafer using double-sided sticky tape (3M™ VHB™). The finished PDMS mould is shown in Figure 6.7.

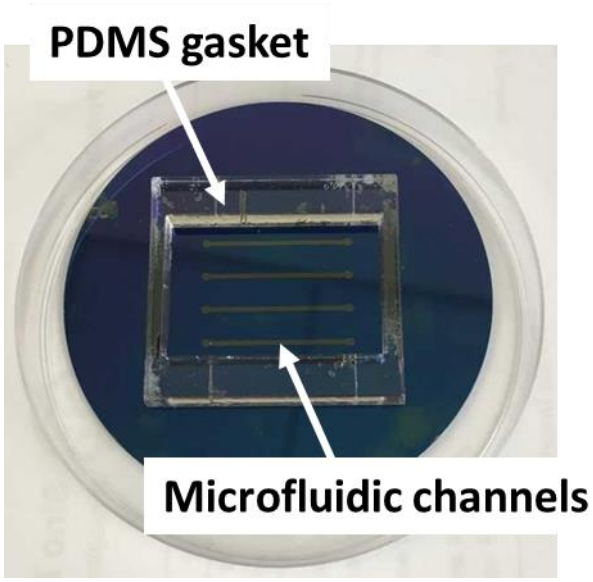

Figure 6.7 PDMS mould fabricated using photolithography techniques

A PDMS mould was fabricated using SU-8 negative photoresist and a maskless aligner. Four microfluidic channels were patterned onto the photoresist to create channels with height of 90-100 microns. A 5 mm PDMS gasket was made from Perspex and attached to the wafer using double-sided sticky tape.

PDMS (Sylgard 184, Dowsil) was mixed in a ratio of 10:1, siloxane: curing agent, and degassed in a vacuum chamber. The PDMS was poured into the mould and levelled using a glass slide to scrape away excess. The mould was placed in an oven at 65 °C for 24 h. The PDMS was released out of the mould using a scalpel and 1.5 mm holes punched at each inlet for inlet tubing.

6.2.4.4 Fabrication of a bottom-layer PDMS mould using a milling machine

The mould for the bottom layer of PDMS was required to have four 1 mm cylinder indentations so that the PDMS would have four 1 mm cylinder protrusions that would fit flush with the laser-cut holes in the gold substrate. The PDMS mould was drawn in 3D in Autodesk Fusion360 (Figure 6.8) and milled from 10 mm Perspex using a computer numerical control (CNC) milling machine (Roland). The PDMS was mixed and cured as described in Section 6.2.4.3.

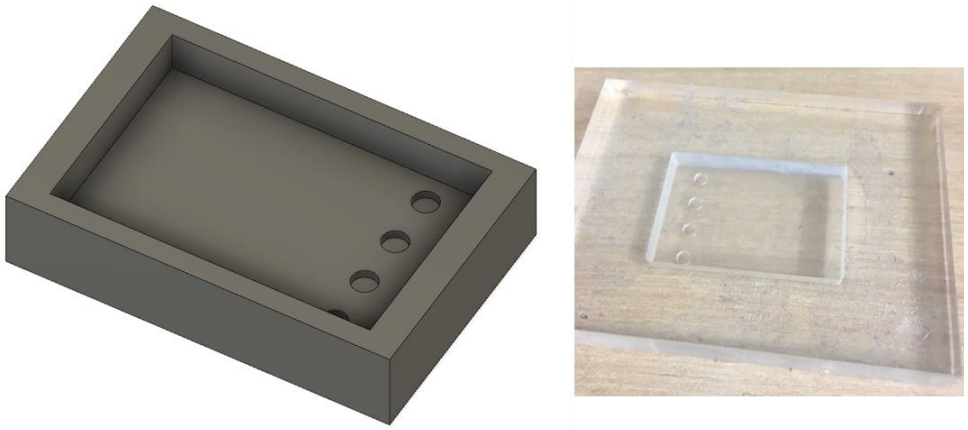

Figure 6.8 Bottom layer PDMS mould fabricated using a milling machine

The bottom layer PDMS mould was drawn in Autodesk Fusion360 (left-hand side) and fabricated using a CNC milling machine (right-hand side). The four 1 mm indentations were designed so that the PDMS had four 1 mm protrusions and would fit flush with the holes in the gold-coated substrate.

6.2.4.5 Assembly of a prototype device

The Perspex clamp and rig were laser cut and assembled using M3 and M6 screws. Acetone was used to solvent-weld the smaller pieces of Perspex. Polytetrafluoroethylene (PTFE) tubing (0.3 mm inner diameter, 1.6 mm outer diameter) was cut and assembled as inlet tubing, and 1 mm inner diameter, 1.6 mm outer diameter PTFE tubing was cut and assembled as outlet tubing. A larger diameter outlet tubing was used to reduce fluidic resistance at the outlet and prevent leaks in the channel. Four-way valves (IDEX Health & Science, V101L) were positioned so that buffer or cell suspension could be injected to waste before injection into the channels, thus reducing the possibility of air bubbles entering the channels. The assembled device is shown in Figure 6.9.

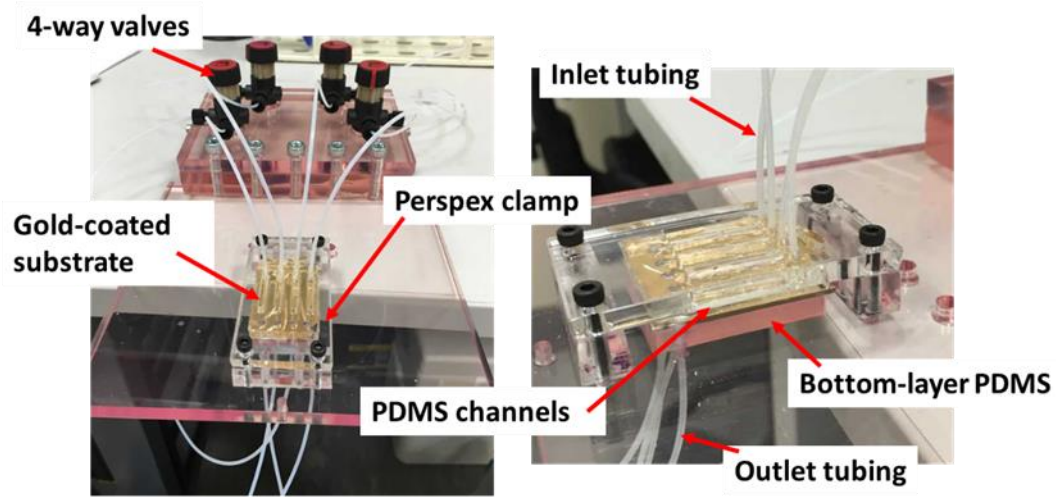

Figure 6.9 Fabricated and assembled prototype device

The prototype device was assembled using screws and solvent welding. PTFE tubing was used for inlet and outlet tubing. Four-way valves were positioned to control the fluid flow before fluid entered the channels.

6.2.5 Prototype device experiment protocols

For all experiments using the prototype device, the gold substrate was functionalised in the same way as for the colorimetry experiment (Section 6.2.3) using a PEG SAM and NHS/EDC crosslinking chemistry (Sections 4.3 and 4.4), streptavidin and a CD271-biotin antibody. Each solution was pipetted onto the substrate and incubated for 10 min. Between each solution the substrate was washed by pipetting buffer over the surface and for each buffer change the new buffer was incubated for 2 min before the subsequent solution. The substrate was incubated with 1% BSA for 30 min to help prevent non-specific adsorption of proteins to the substrate surface, then dried using a nitrogen gun, and assembled with the PDMS channels onto the Perspex rig. The channels were manually flushed with 1% BSA, then a syringe pump (PHD 2000 Programmable, Harvard Apparatus) was programmed at a low flow rate (1 µL/min) for 30-60 min. The buffer was changed to the running buffer for the experiment, and injected for 30-60 min before cell suspension injection.

The cells for each experiment were harvested using 3-5 mL trypsin-EDTA solution (Sigma, T4049), filtered through a 40 micron cell strainer (Corning, 352340) and counted using a haemocytometer. For each injection, buffer or cell suspension was injected to waste to purge the tubing of any air bubbles, then the four-way valve rotated to inject the medium into the channel. Cell suspensions were kept on ice before and after injection into the device.

6.2.5.1 Experiments using single cell populations

The initial experiments carried out using the prototype device used single cell populations to determine the specificity of cell capture. Channels were functionalised with either CD271-biotin antibody (Miltenyi Biotec, 130-113-419) or CD34-biotin antibody (Miltenyi Biotec, 130-113-177), both at 10 µg/mL. Three conditions were tested in total:

1. CD271+ SH-SY5Y cells in a CD271-biotin functionalised channel
2. CD271- fibroblast cells in a CD271-biotin functionalised channel
3. CD271+ SH-SY5Y cells in a CD34-biotin functionalised channel

Two running buffers were investigated during the initial experiments; serum-free alpha MEM culture medium with 0.005% Tween 20 and MACS buffer[9] with 0.005% Tween 20. Cells were suspended in running buffer at a concentration of 2.5 million cells/mL. Cell suspensions (50 µL) were injected into a channel using a syringe pump programmed at 100 µL/min. The cells were incubated in the channel for 5 min to allow sedimentation of the cells to the channel surface then unbound cells were washed away at 5 µL/min, until no more cells were moving.

Photos were taken at the same location of the channel before the cell injection, during the 5 min incubation and after the 5 µL/min buffer wash. Using ImageJ, the number of cells in each photo could be estimated as follows: for each photo the smooth continuous background was subtracted by setting a rolling ball radius (e.g. 6 pixels), the threshold was adjusted, and the number of particles above 25 pixels analysed. The same values were set for all associated images. The number of ‘cells’ before the cell injection (i.e. background fouling on the channel surface) was subtracted from both the ‘5 min incubation’ and ‘after 5 µL/min wash’ photos. The percentage of cells bound could then be calculated.

6.2.5.2 Experiments using mixed cell populations

To assess specific cell capture from mixed cell populations, SH-SY5Y cells and fibroblast cells were mixed in different ratios and the mixed populations injected into the device. The following ratios were evaluated (SH-SY5Y cells: fibroblast cells); 100: 0, 75: 25, 50: 50, 25: 75, 12: 88, 6: 94, 3: 97, 1.5: 98.5. The mixed cell populations were injected into the device using the same procedure as above (Section 6.2.5.1), using MACS buffer with 0.005% Tween 20 as the running buffer

[9] MACS buffer: PBS (Lonza, 17-516F), 2 mM EDTA (Sigma Aldrich, E7889), 0.5% BSA (Sigma Aldrich, A9647), filter sterilised

(see Section 6.3.2) and at a total cell concentration of 20 million cells/mL (see Section 6.3.3.2).

The results from the device were compared to the specificity of flow cytometry. For flow cytometry analysis, SH-SY5Y and fibroblast cells were mixed in the same ratios as described above and analysed using a Cytoflex S cytometer. The mixed populations were suspended in FACS buffer[10] and labelled with a CD271-PE antibody (Miltenyi Biotec, 130-113-421, 0.5 µg/mL) or an isotype-matched control antibody (IgG1-PE, BD Biosciences, 555749, 0.5 µg/mL). Unlabelled cells were also analysed for gating purposes. The cells were incubated with the antibody for 15 min at 4 °C in the dark. FACS buffer (2 mL) was added to each FACS tube and the cells washed by centrifugation for 5 min at 300 g and 4 °C. Cells were re-suspended in 350 µL FACS buffer and 20,000 events were collected for each sample. Flow cytometry events were gated for single cells using the gating strategy shown in Chapter 4: Section 4.5.

6.2.5.3 Fluorescent labelling of cells

To confirm the specificity of cell capture within the device, the two cell types were fluorescently labelled with different coloured cell trackers and analysed using a multiband filter set (Semrock, LF488/561-B-000) and a multichannel imaging system (Photometrics DV2™).

Cells were fluorescently labelled 24 hours prior to testing as it was found that fluorescent labelling affected the cell binding behaviour when carried out immediately prior to testing. SH-SY5Y cells were labelled with green cell tracker (Invitrogen, C7025) and fibroblast cells were labelled with red cell tracker (Invitrogen, C34552). The cell trackers were warmed to RT and re-suspended in filtered DMSO to make 10 mM solutions. The solutions were diluted to 10 µM in serum-free culture medium and warmed to 37 °C. Culture medium was removed from the cell culture flask, replaced with cell tracker solution and incubated for 30-45 min in the cell culture incubator. Cell tracker solution was removed and the cells incubated in their normal culture conditions until the following day.

The mixed cell population experiments with fluorescently-labelled cells were carried out in the same way as Section 6.2.5.2 but only 100% SH-SY5Y, 50% SH-SY5Y, 25% SH-SY5Y and 6% SH-SY5Y populations were evaluated.

---

[10] FACS buffer: PBS (Lonza, 17-516F), 0.5% BSA (Sigma Aldrich, A9647) and 0.05% sodium azide, filter sterilised (0.22 µm)

6.2.6 Post-enrichment analysis

6.2.6.1 Investigating the viability of cells post-enrichment

The viability of cells post-enrichment was investigated using flow cytometry. SH-SY5Y cells that had been captured and released in the device were collected and their viability compared to cells suspended in medium, on ice, for the same duration (medium control) and cells that had been injected into the device at different flow rates but with no incubation period (microfluidic controls). A new channel design with higher throughput (see Section 6.3.5) was used for viability, proliferation (Section 6.2.6.2), manipulation (Section 6.2.6.3) and cell recovery (Section 6.2.6.4) experiments.

The cell enrichment procedure in the new channels was carried out as follows; cells were injected into the device at a concentration of 20 million cells/mL at 100 µL/min and incubated with no flow for 5 min. Unbound cells were washed away at 20 µL/min for 100 µL to ensure cells reached the end of the outlet tubing (70 µL tubing volume). Bound cells were collected directly into a FACS tube at 320 µL/min for 200 µL. The flow rates used for the buffer wash and cell release were four times higher than previously used because the new channel design branched into four separate channels. Microfluidic controls were injected into the device at three different flow rates; 100 µL/min, 500 µL/min and 3000 µL/min for 200 µL, and collected directly into a FACS tube. Medium controls were kept on ice at the same cell concentration (20 million cells/mL, 50 µL) for the duration of the experiment.

All cells were centrifuged at 300 g, 4 °C for 5 min and re-suspended in ice-cold FACS buffer. A 7-amino-actinomycin D (7-AAD) Staining Solution (Miltenyi Biotec, 130-111-568, 0.525 µg/mL) was added to each tube and incubated in the dark for at least 5 min before analysis. A Cytoflex S flow cytometer was used for analysis and 20,000 events recorded for each sample.

Cells that had been through a MACS column were also analysed in the same way for comparison to a “gold standard” method of cell enrichment.

6.2.6.2 Investigating the proliferation of cells post-enrichment

To look at the longer-term viability and function of the cells, bound and released cells were seeded in 24-well plates and their proliferation assessed at two different time points using a Pico green assay for dsDNA quantification. The same controls were used as for viability testing (Section 6.2.6.1) – medium controls and microfluidic controls.

After the enrichment procedure in the device (carried out in the same way as Section 6.2.6.1), the cells were counted and seeded at 40,000 cells per well in normal SH-SY5Y cell culture medium (0.5 mL per well) in two 24-well plates (Corning, 3526). Each experimental condition was carried out in triplicate (with the exception of the captured and released population where 1-3 replicates were carried out depending on the number of cells collected) and the entire experiment carried out three times on different days with different cells and a new device. After 2 days in culture, the cells in one plate were washed twice with PBS and lysed with 0.1% Triton-X100 (200 µL per well) with repeated freeze/thaw cycles; the cell culture plate was frozen at -80 °C for 10 min then thawed at 37 °C for 10 min. After thawing, the cell suspension was mixed and the freeze/thaw cycle repeated twice more.

A Quant-iT™ PicoGreen™ dsDNA Assay Kit (Invitrogen, P11496) was used to quantify the dsDNA in each sample. A standard curve was prepared using lambda DNA supplied with the kit (100 µg/mL in TE buffer[11]) and lysed cells were diluted 20-fold in TE buffer. Quant-iT™ PicoGreen® dsDNA reagent (supplied with the kit) was diluted 200-fold and protected from light until ready to use. All standards and samples were pipetted in triplicate in a 96-well plate (Corning, 3599), 100 µL per well. Quant-iT™ PicoGreen® dsDNA reagent was added at 100 µL per well and incubated in the dark for 5 min. The samples were excited at 480 nm and the fluorescence emission intensity measured at 520 nm using a spectrofluorometer (Thermo Scientific Varioskan® flash).

The fluorescence mean value of the blank wells was subtracted from all standards and samples. A standard curve was plotted in Origin and the dsDNA content of the samples calculated using linear regression analysis.

The second 24-well plate was processed in the same way 5 days after seeding to assess cell proliferation between the two time points and the relative difference between samples.

6.2.6.3 Investigating the manipulation of cells during the enrichment process

In order to have significant advantages over current affinity-based enrichment technologies, the cells must be minimally manipulated during the procedure. For an initial analysis of the cell manipulation, flow cytometry was used to assess if any of the antibody immobilised on the channel surface was present on the cells

[11] TE buffer: 200 mM tris-HCl, 20 mM EDTA, pH 7.5 (supplied with Quant-iT™ PicoGreen™ dsDNA Assay Kit, Invitrogen, P11496)

after they had been captured and released. This was carried out by incubating the cells with an anti-biotin-PE conjugated secondary antibody (Miltenyi Biotec, 130-111-068) to detect if any of the CD271-biotin antibody was present. A further experimental condition using CD271-biotin and anti-biotin-PE as a secondary antibody was conducted alongside to ensure the CD271 antigen was not affected by the capture and release process.

Samples were processed through the device as described in Section 6.2.6.1. Two samples of captured and released cells were collected, one for incubation with anti-biotin-PE and one for incubation with CD271-biotin antibody (and subsequent labelling with anti-biotin-PE). Samples were centrifuged at 300 g at 4 °C for 5 min and re-suspended in 100 µL FACS buffer for antibody labelling. Labelling was carried out according to the manufacturer's recommendations; each antibody was used at a dilution of 1:50 (2 µL in 100 µL) and incubated for 10 min in the dark at 4 °C. Cells were washed by addition of 2 mL FACS buffer and centrifuged at 300 g and 4 °C for 5 min. Cells were re-suspended in 100 µL FACS buffer for secondary antibody labelling or 350 µL FACS buffer for analysis.

Control samples at a concentration of 20 million cells/mL were suspended in medium on ice for the duration of the cell enrichment experiment and labelled at the same time as test samples. Control samples were labelled with anti-biotin-PE and CD271-biotin for comparison, as well as a sample unlabelled for gating purposes.

A Cytoflex S Flow Cytometer was used to record data and at least 10,000 events were collected in the single cells gate (see Chapter 4: Section 4.5 for flow cytometry gating strategy).

6.2.6.4 Investigating cell recovery from the prototype device

The cell recovery from the device was calculated and compared to the recovery of cells from a MACS column.

A SH-SY5Y cell suspension (20 million cells/mL, 200 µL) was injected into the device at 100 µL/min and then immediately washed out with 400 µL buffer (at 100 µL/min). Cells were counted using a haemocytometer and a percentage calculated from the original volume of cells injected (4 million cells in a 200 µL injection, plus 210,000 cells in the tubing volume from the syringe to the valve after flushing out air bubbles). The percentage recovery was compared to cells which had been through a MACS column following the standard MACS protocol but with no microbead labelling; unlabelled cells were pipetted into the column in a 500 µL volume and the column was washed with 3x 3 mL MACS buffer. The

cells were centrifuged at 300 g for 5 min to re-suspend in a smaller volume for counting.

6.3 Results and Discussion

6.3.1 Immobilisation of a CD271 antibody to a gold substrate for specific cell capture

A prototype device was designed and the individual parts fabricated and assembled as described in Section 6.2.4. The design of the device relies upon the specific capture of cells on the surface of a functionalised microfluidic channel. The first step was to ensure that a CD271 antibody (for specific cell capture) could be immobilised to the channel surface in a uniform manner and via a controlled mechanism.

The proposed mechanism of immobilisation was the same method used in Chapter 5: Section 5.2.10 for SPR analysis, using a PEG monolayer (Section 4.3) and crosslinking chemistry (Section 4.4). The gold-coated wafer substrate prepared in Section 6.2.4.2 was first incubated with a SAM to help prevent non-specific binding to the channel surface, and carboxylic acid groups in the monolayer were activated by NHS and EDC chemistry.

Two CD271 antibodies were initially investigated; one conjugated to phycoerythrin dye (CD271-PE) and the other conjugated to biotin (CD271-biotin). The CD271-PE antibody was found to reliably bind to CD271+ cells during the work carried out in Chapter 5: Section 5.3.4. The CD271-biotin antibody was purchased from the same supplier (Miltenyi Biotec) and was produced by an identical clone. The CD271-PE antibody was immobilised directly to the SAM via NHS and EDC crosslinking, whereas in the case of the CD271-biotin antibody, streptavidin was immobilised to the SAM then CD271-biotin bound to the streptavidin (Section 6.2.2.2).

During the development of a prototype device, an established cell line was used to optimise cell capture and release rather than primary cells. This was because primary cells were of limited supply and were only used when the efficacy of the device had been recognised. Established cell lines are continuous which means they can divide indefinitely ensuring a good supply of cells for preliminary experiments. In Chapter 5: Section 5.3.4.6, it was shown that the SH-SY5Y cell line expresses the CD271 antigen and can therefore act as a positive cell line for specific cell capture. For a negative control, primary human dermal fibroblast cells

were purchased which do not express the CD271 antigen. This was confirmed by flow cytometry analysis as shown in Figure 6.10.

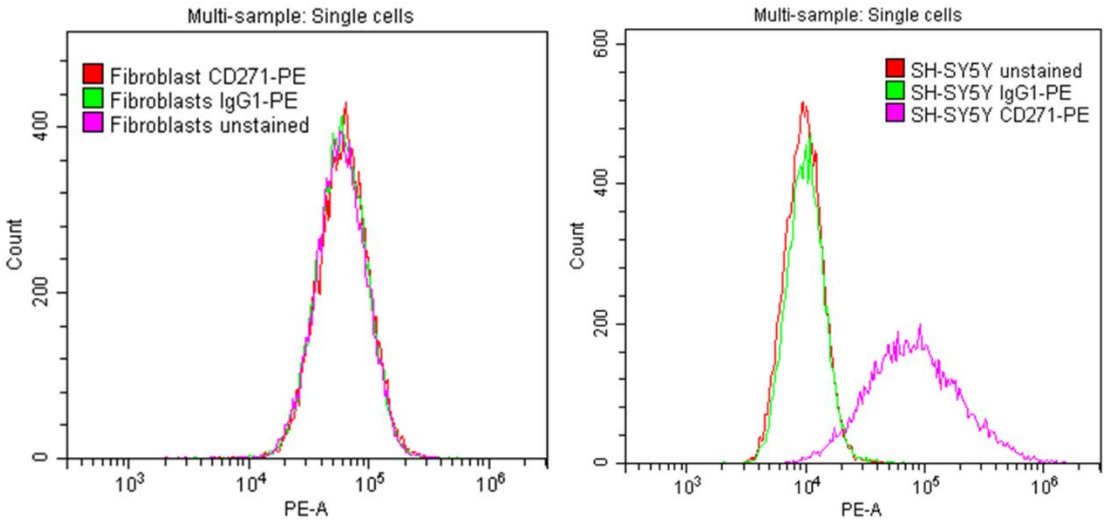

Figure 6.10 Flow cytometry histograms showing CD271- fibroblast cells and CD271+ SH-SY5Y cells used for optimisation of specific cell capture

The left panel shows fibroblasts analysed by flow cytometry either unlabelled (pink), labelled with an isotype-matched control antibody (IgG1-PE, green) or labelled with a CD271-PE antibody (red). All histograms are identical showing that fibroblasts do not express the CD271 antigen on their cell surface. The panel on the right shows the same analysis of SH-SY5Y cells for comparison. SH-SY5Y cells were either unlabelled (red), labelled with an isotype-matched control antibody (IgG1-PE, green) or labelled with a CD271-PE antibody (pink). The pink histogram shows a large percentage of SH-SY5Y cells are positive for anti-CD271-PE labelling compared to the negative controls, and therefore express the CD271 antigen on their cell surface.

6.3.1.1 Surface plasmon resonance analysis of specific cell capture

Initial analysis of specific cell capture on a surface functionalised with either CD271-PE or CD271-biotin was measured via SPR. The SPR experiments were carried out on an Autolab ESPIRIT SPR instrument which has sensor substrates almost identical to the channel surface in the prototype device. The SPR sensor discs were purchased from Xantec Bioanalytics and are glass discs with a gold layer of approximately 50 nm. In this work, gold-coated glass slides and gold-coated silicon wafers were used as a surface for antibody functionalisation - both with a gold layer of approximately 50 nm.

During SPR measurements it was found that using a layer of streptavidin and a CD271-biotin antibody reduced non-specific cell fouling to the gold surface compared to using a CD271-PE antibody alone (Figure 6.11). After the last cell

injection on the CD271-biotin functionalised surface, 411 response units were recorded in the flow cell where SH-SY5Y cells had been injected compared to 2.5 response units in the flow cell where fibroblast cells had been injected. After the last cell injection on the CD271-PE functionalised surface, 129 response units were recorded in the flow cell where SH-SY5Y cells had been injected compared to 29 response units in the flow cell where fibroblast cells had been injected. This means there was proportionally 37 times more non-specific binding on the CD271-PE functionalised surface.

This could be for a number of reasons; firstly, the protocols differed slightly in that the unreacted sites on the monolayer were blocked using ethanolamine after the immobilisation of streptavidin (and before the immobilisation of CD271-biotin antibody) whereas for the CD271-PE antibody, ethanolamine was not used as it was thought that any unreacted sites on the monolayer would no longer be active by the time cells were injected (at least 2 hours later due to the harvesting and transport of cells).

Further to this, the SPR results observed for both CD271-PE and CD271-biotin functionalised surfaces could not be repeated and therefore reliable conclusions could not be drawn. During repeats, SH-SY5Y cells bound to the functionalised surface during the injection (i.e. the SPR angle increased) however, when buffer was injected after the cells were bound, cells were immediately washed from the surface (the SPR angle decreased to the baseline level). In comparison, the SPR sensogram shown in Figure 6.11, shows that the SH-SY5Y cells remained bound to the surface until the pH of the running buffer was increased.

It was decided to investigate the CD271 antibody conjugated to biotin for cell capture in the prototype device. This was because the initial result indicated less non-specific binding using this antibody and it was also available at a higher concentration meaning it was more economical and there would be less batch-to-batch variation between experiments.

The initial results indicated that by using a pH 9.0 buffer, more than 70% of bound cells could be released from the functionalised surface. This is important because the cells need to be released from the surface post-enrichment in order to use them in cellular therapies. This preliminary result suggests a change in pH could be used as a mechanism for cell release.

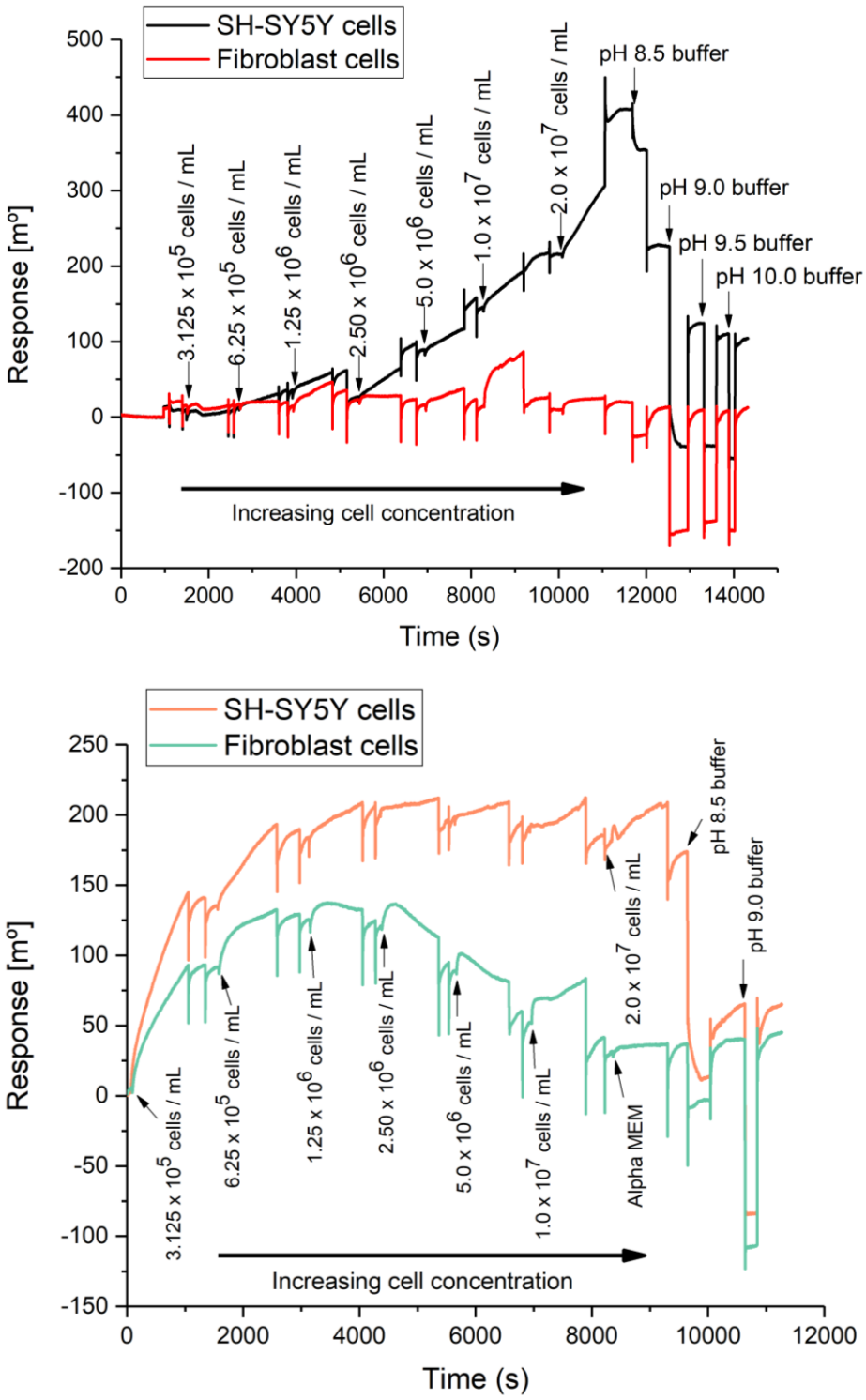

Figure 6.11 SPR sensograms showing CD271+ cells binding to CD271 antibodies immobilised to a gold surface

The upper panel shows SPR measurements recorded when SH-SY5Y cells and fibroblast cells were injected onto a CD271-biotin functionalised surface (310 - 330 units immobilised). The lower panel shows SPR measurements recorded when both cell types were injected onto a CD271-PE functionalised surface (170 - 200 units immobilised). More non-specific binding was observed on the CD271-PE functionalised surface compared to the CD271-biotin functionalised surface.

6.3.1.2 Colorimetry assessment of antibody immobilisation on the channel surface

During SPR measurements, the immobilisation of antibody on the surface can be measured by a change in the SPR angle (Section 4.2). However, for the immobilisation of an antibody on the microfluidic channel surface this information was not available. Instead, a colorimetry experiment was carried out to ensure that antibody was present and coating the surface in a uniform manner. A series of controls were also tested to ensure antibodies were immobilised via crosslinking chemistry and were not present through any other interaction with the surface.

An anti-biotin-ALP secondary antibody was used with BCIP/NBT substrate for detection of the CD271-biotin antibody on the gold surface (Section 6.2.3). It was found that where the correct biochemistry had been applied, antibody was present on the gold surface (Figure 6.12). There was a small amount of secondary antibody present when no CD271-biotin antibody was present (Figure 6.12 - panels 5a and 5b), however a clear difference was observed where antibody was present (Figure 6.12 - panels 1a and 1b). The pixel intensity of a 22x22 pixel square (drawn in the top right corner for each image) was quantified using ImageJ (Figure 6.13). The average pixel intensity for replicates 6a and 6b (where no secondary antibody was used) was subtracted from all other values and the result reported as the absolute value. There was an average difference of 22 pixel intensity units when CD271 antibody was present in test condition 1 to when no CD271 antibody was present in test condition 5. Altogether, this result provided confidence that the channel surface would be functionalised and antibodies would be available for specific cell capture within the prototype device.

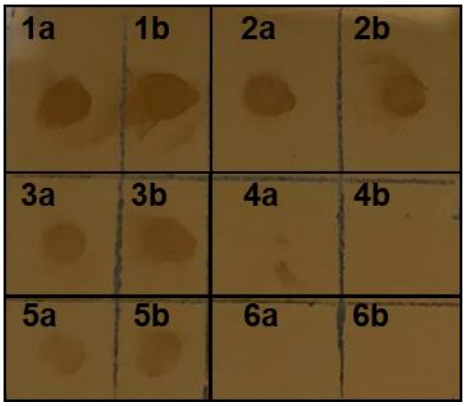

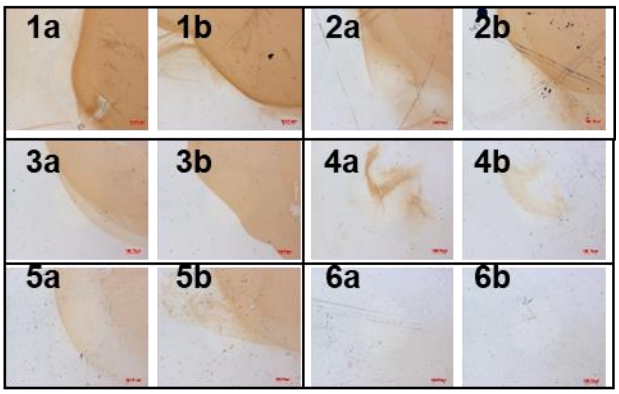

1. Full immobilisation (sAb – 1 µg/mL)	**2.** Full immobilisation (sAb – 0.5 µg/mL)
3. Full immobilisation (sAb – 0.1 µg/mL)	**4.** Immobilisation without streptavidin (sAb – 1 µg/mL)
5. Immobilisation without CD271-biotin antibody (sAb – 1 µg/mL)	**6.** Immobilisation without secondary antibody

Figure 6.12 Colorimetry experiment showing CD271-biotin was present on the gold channel surface

The upper left panel shows a macroscopic image of the gold substrate spotted with CD271-biotin antibody or relevant control condition. The upper right panel shows the same substrate microscopically imaged. The bottom table details each of the conditions tested, corresponding to the numbers displayed on the upper panels (two repeats of each condition – a and b). sAb=secondary antibody.

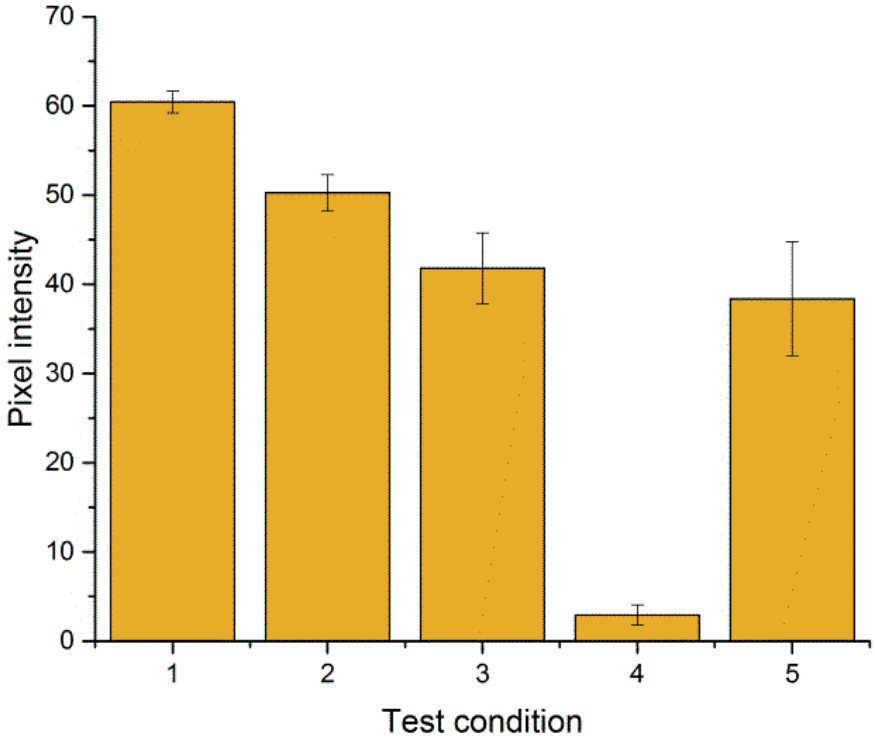

Figure 6.13 The pixel intensity of images from each test condition of the colorimetry experiment

ImageJ was used to quantify the pixel intensity of a square (22x22 pixels) in the top right corner of each of the microscope images shown in Figure 6.12. The test conditions correspond to the table shown in Figure 6.12. The background staining observed for test condition 5 (where no CD271 antibody was present) is comparable to test condition 3 (where secondary antibody was used at 10x lower concentration). There is a clear difference between test conditions 1 and 5 where the secondary antibody was used at the same concentration. No statistical analysis was carried out due to the low number of replicates. Bars represent the mean value and error bars represent the standard error of the mean (n=2 technical replicates).

6.3.2 Investigating specific cell capture and release in the prototype device using single cell populations

The aims of the first experiments using the prototype device were to assess the specificity of cell capture using single cell populations. Furthermore, the protocol of cell enrichment was refined including the buffer used for cell suspension and washes, and the procedure for injecting, capturing, releasing and collecting enriched cells.

Using the two cell populations described in Section 6.3.1, different combinations of specific and non-specific antibody were tested with different cells. The substrate was functionalised with either CD271-biotin antibody or CD34-biotin antibody. It was confirmed that SH-SY5Y cells did not express the CD34 antigen

on their cell surface and therefore should not bind to a channel functionalised with CD34-biotin antibody (Figure 6.14).

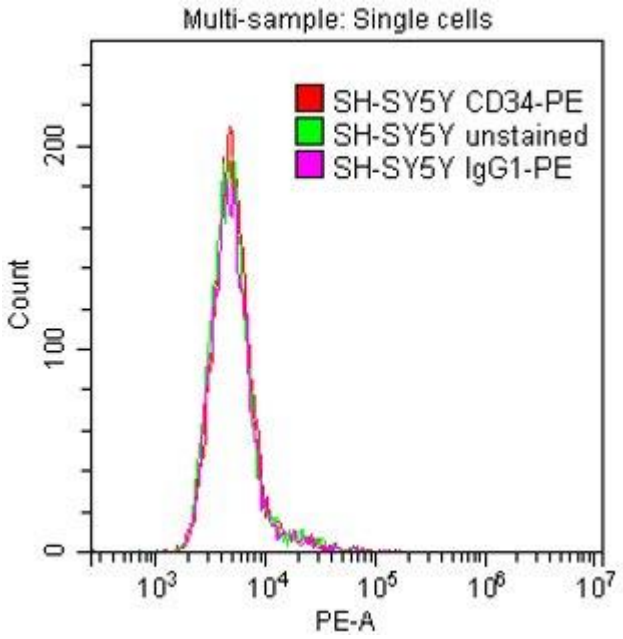

Figure 6.14 Flow cytometry analysis showing SH-SY5Y cells do not express the CD34 antigen

SH-SY5Y cells were labelled with CD34-PE antibody (red), an isotype-matched control antibody (IgG1-PE, pink), or unlabelled (green). The histograms show that SH-SY5Y cells do not express the CD34 antigen since there is no PE fluorescence detected for cells labelled with CD34-PE compared to the isotype control antibody and unlabelled cells.

Cell suspensions were injected into the device via a syringe pump at 100 µL/min flow rate and a 5 minute incubation period allowed cells to sediment and interact with the cell surface. Buffer washes at 5 µL/min were used to wash away unbound cells. Two buffers were trialled as running buffers in these experiments: Alpha MEM cell culture medium with 0.005% Tween 20 and MACS buffer[12] with 0.005% Tween 20. Each experiment was carried out in a single channel of the four-channel device (see Figure 6.5 for details of the channel design).

Figure 6.15 shows an example of a specific interaction in the device, where SH-SY5Y cells (CD271+) have been injected into a channel functionalised with a CD271-biotin antibody. Figure 6.16 shows an example of a non-specific interaction in the device, where fibroblast cells (CD271-) have been injected into a channel functionalised with CD271-biotin antibody. Figure 6.17 shows a non-

[12] MACS buffer: PBS, 2 mM EDTA and 0.5% BSA

specific interaction in the device where SH-SY5Y cells (CD271+) have been injected into a channel functionalised with CD34-biotin antibody.

Images were taken in the same location of the channel before a cell suspension injection, during the 5 minute incubation period and after a 5 µL/min buffer wash. Using ImageJ it was possible to analyse the number of 'particles' above a set number of pixels (25 pixels), and therefore using all three images it was possible to estimate the percentage of cells bound for each experiment (shown in Figure 6.18). There was a significant difference between specific interactions and non-specific interactions in the device.

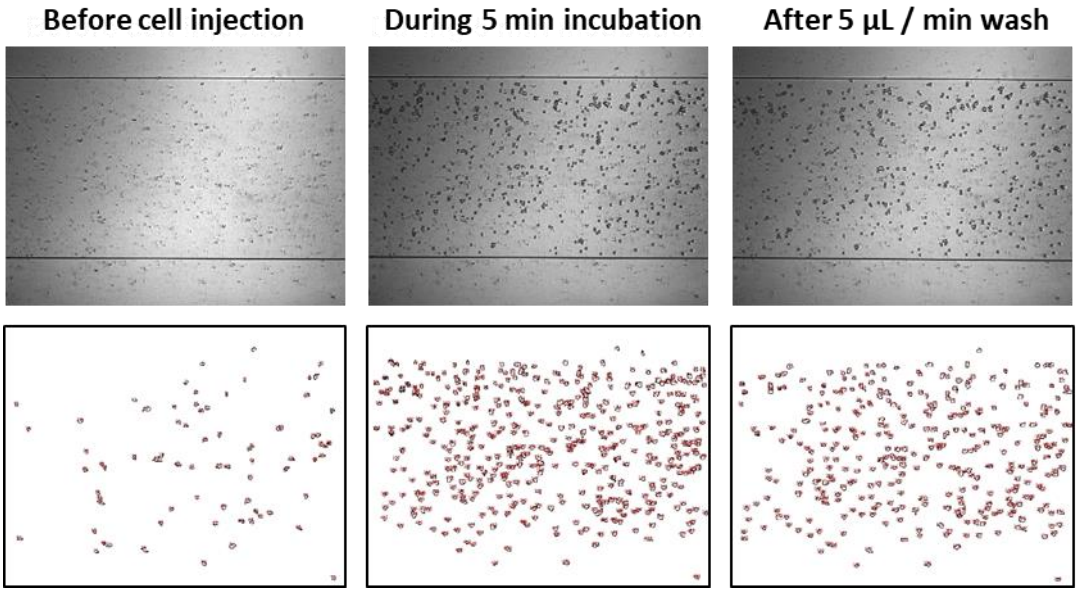

Figure 6.15 An example of a specific interaction in the prototype device using SH-SY5Y cells (CD271+) and a CD271 antibody-functionalised channel

Images were taken of the same section of channel before the cell suspension injection, during the 5 minute incubation period and after a 5 µL/min buffer wash. The top row shows images taken with a microscope camera, and the bottom row shows the same images analysed by ImageJ for particles above 25 pixels. These images show the injection of SH-SY5Y cells (CD271+) into a channel functionalised with a CD271-biotin antibody.

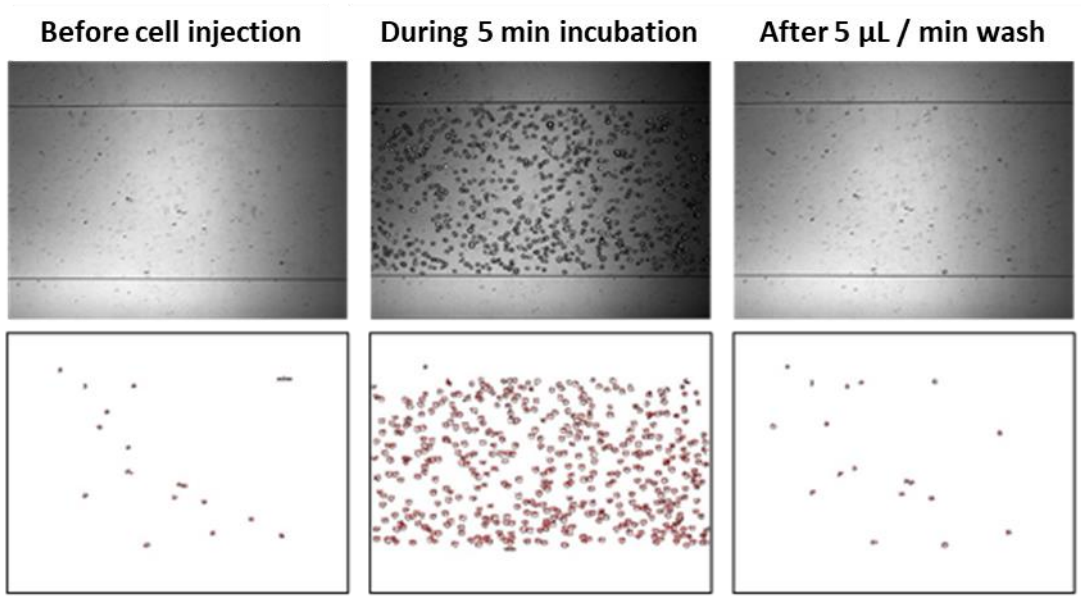

Figure 6.16 An example of a non-specific interaction in the prototype device using fibroblast cells (CD271-) and a CD271-biotin functionalised channel

Images were taken of the same section of channel before the cell suspension injection, during the 5 minute incubation period and after a 5 µL/min buffer wash. The top row shows images taken with a microscope camera, and the bottom row shows the same images analysed by ImageJ for particles above 25 pixels. These images show the injection of fibroblast cells (CD271-) into a channel functionalised with a CD271-biotin antibody.

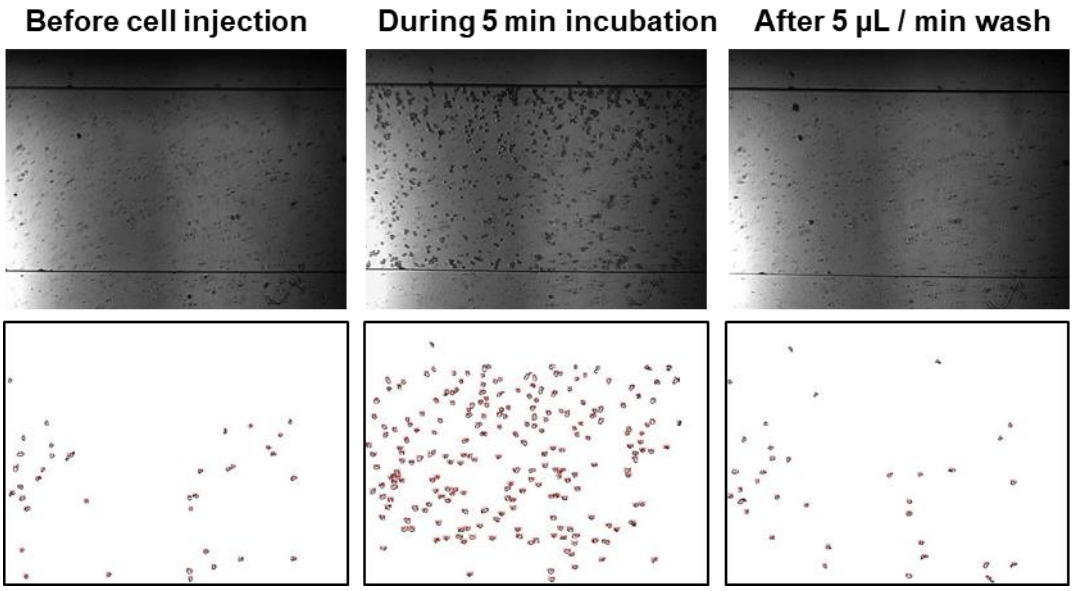

Figure 6.17 An example of a non-specific interaction in the prototype device using SH-SY5Y cells (CD271+) and a CD34-biotin functionalised channel

Images were taken of the same section of channel before the cell suspension injection, during the 5 minute incubation period and after a 5 µL/min buffer wash. The top row shows images taken with a microscope camera, and the bottom row shows the same images analysed by ImageJ for particles above 25 pixels. These images show the injection of SH-SY5Y cells (CD271+) into a channel functionalised with a CD34-biotin antibody.

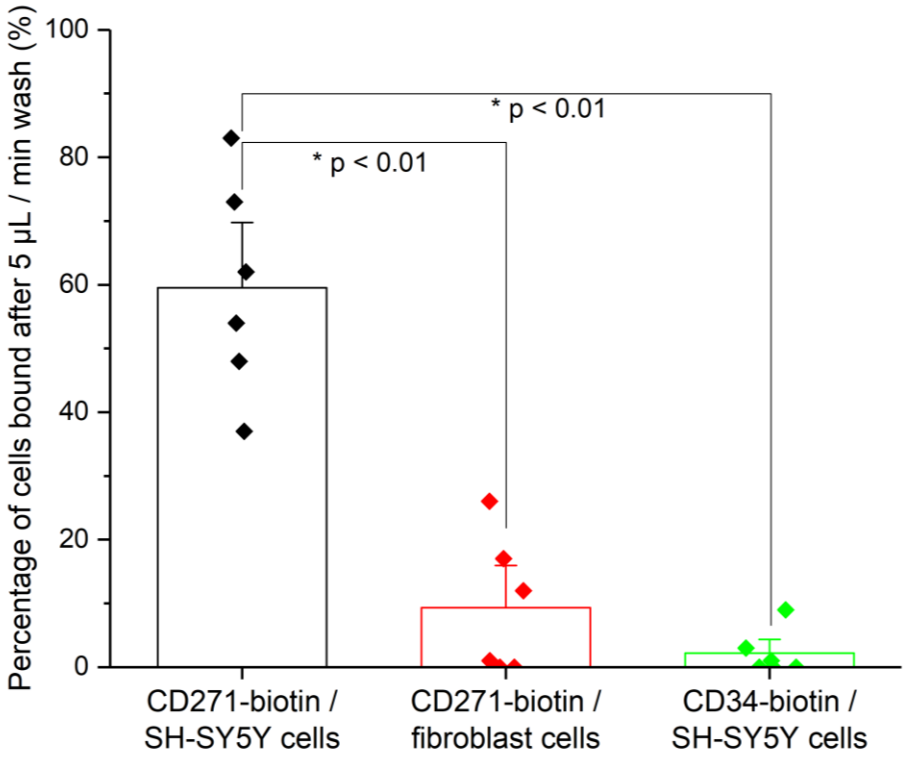

Figure 6.18 The percentage of cells bound in a prototype device for different antibody/cell interactions

The percentage of cells bound after a 5 µL/min buffer wash was estimated using ImageJ. Data shown here is data collated from experiments using both Alpha MEM culture medium and MACS buffer as running buffers. There was a significant difference between the specific interaction (CD271-biotin/SH-SY5Y cells) and non-specific interactions (CD271-biotin/fibroblast cells and CD34-biotin/SH-SY5Y cells), $p<0.01$, $n=6$. Statistical analysis was carried out using a Mann Whitney-U test since not all data was normally distributed according to the Shapiro Wilk test of normality. Bars represent the mean result and error bars represent the SEM.

Next, the percentage of cells bound using different running buffers was compared (Figure 6.19). It was found that there was no significant difference between the percentage of cells bound using either Alpha MEM or MACS buffer in any of the antibody/cell combinations.

However, it was assumed that there could be small advantages to using MACS buffer, for example; MACS buffer contains 0.5% BSA which could help prevent non-specific binding and it is not susceptible to pH change. On the other hand, Alpha MEM culture medium contains a carbonate buffering system and in atmospheric conditions the pH of the medium can rise due to carbon dioxide diffusing out. For these reasons, it was decided to use MACS buffer as the cell suspension buffer for future experiments.

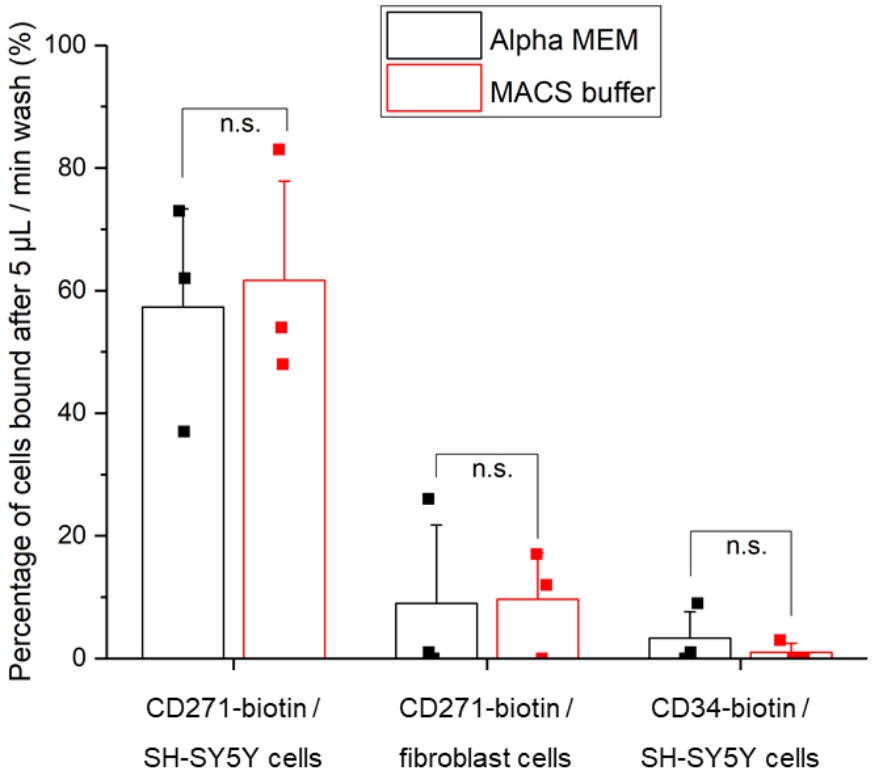

Figure 6.19 The percentage of cells bound in the prototype device using different running buffers

Alpha MEM culture medium with 0.005% tween 20 and MACS buffer with 0.005% Tween 20 were investigated as running buffers for cell enrichment experiments. It was found that there was no significant difference between the percentage of cells bound for any of the different antibody/cell interactions using either buffer. (n.s.=not significant, n=3). Statistical analysis was carried out using a Mann Whitney-U test since not all data was normally distributed according to the Shapiro Wilk test of normality. Bars represent the mean result and error bars represent the SEM.

It was also found that as the flow rate was increased, cells began to release from the cell surface with only 6 ± 3% of cells (mean value ± SEM, n=3) remaining bound after a buffer wash at 160 µL/min (Figure 6.20). Since releasing bound cells by increasing the flow rate was found to be effective, using buffer solutions with an increased pH was not investigated at this time. The impact of higher flow rates on cell viability was investigated and the results shown later in this chapter (Sections 6.3.6 and 6.3.7).

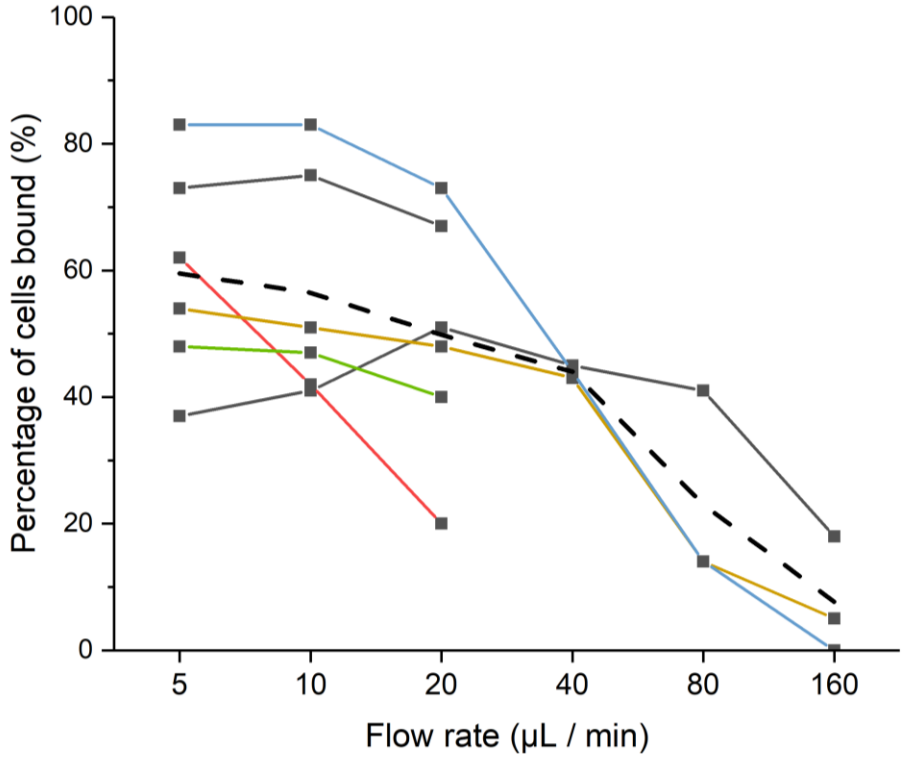

Figure 6.20 The percentage of bound cells when the flow rate was increased

The flow rate of buffer washes was increased from 5 µL/min to 160 µL/min and the number of cells bound after each wash was estimated using ImageJ. Each coloured line represents one experiment and the dashed line represents the mean value (n=6). As the flow rate was increased, bound SH-SY5Y cells (CD271+ cells) were released from the channel surface functionalised with CD271-biotin antibody.

6.3.3 Optimising cell capture and release in the prototype device

6.3.3.1 Reducing cell clumping

The initial experiments carried out with the prototype device showed that specific cell capture and release was achievable, however, there were still areas that required optimisation. For example in Figure 6.18 it can be seen that the percentage of bound cells was inconsistent between individual experiments. The reason for this was because cells in the small-diameter (0.3 mm) tubing during the 5 minute incubation period formed large cell clumps, and during the buffer wash the large cell clumps would “drag” bound cells from the channel surface. Therefore when the photo was taken after the buffer wash, the number of cells was diminished from the true value.

To overcome this issue a second inlet tubing was installed for the buffer wash (Figure 6.21). This allowed the cell suspension to be injected via one syringe pump (PHD 2000 Programmable, Harvard Apparatus) and inlet tubing, and the

buffer wash to be injected via a second syringe pump (NE-1000 Programmable, KF Technology) and inlet tubing. Adapting the protocol in this way meant that no cells incubated in the small-diameter tubing would flow across the cell surface when cells were bound, and the tubing could be flushed out before subsequent experiments. Using this protocol increased the consistency between experiments and ensured accurate data was being recorded (see Section 6.3.3.2).

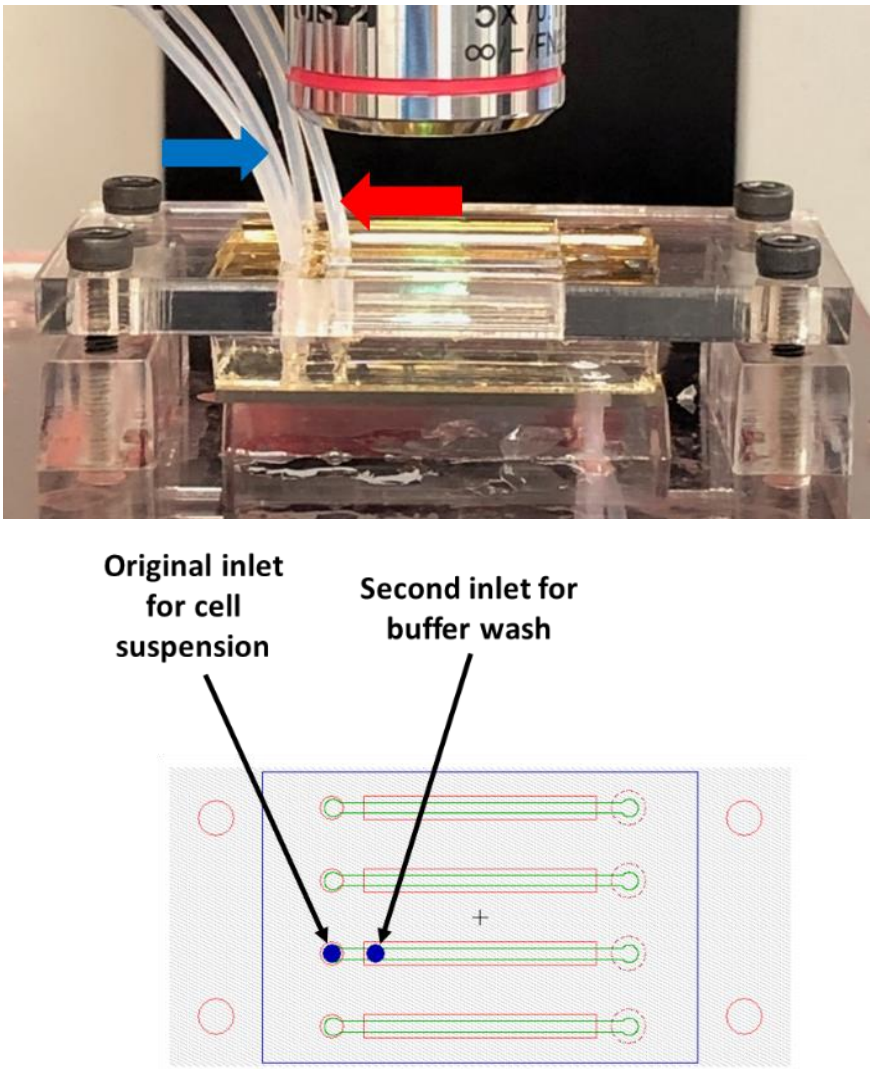

Figure 6.21 A second inlet tubing was installed for buffer washes

A second inlet tubing was installed in the second channel of the four-channel prototype device. This allowed the cell suspension to be injected via the first inlet tubing (indicated by the blue arrow and labelled in the schematic), and the buffer wash to be injected via the second inlet tubing (indicated by the red arrow and labelled in the schematic). Using the second channel only, meant cell clumps formed in the inlet tubing did not lead to inaccurate data collection. See Figure 6.5 for further description of this schematic.

6.3.3.2 Investigating the initial cell concentration

A further area of optimisation was to investigate the initial concentration of the cell suspension injected into the device. This was important in order to capture the maximum number of cells during one incubation period. Initial experiments were carried out at a concentration of 2.5 million cells/mL, to maximise the number of cells available for capture 5, 10 and 20 million cells/mL were trialled as initial cell concentrations.

It was found that increasing the initial cell concentration increased the number of cells bound during one 5 minute incubation (Figure 6.22) and that there was no significant difference between the percentage of cells bound at different cell concentrations (Figure 6.23). This meant it was beneficial to use the highest cell concentration of 20 million cells/mL. Although saturation of the channel surface was not observed, cell concentrations higher than 20 million cells/mL were not investigated because at the higher cell concentrations the cells began to clump together and caused more variable results.

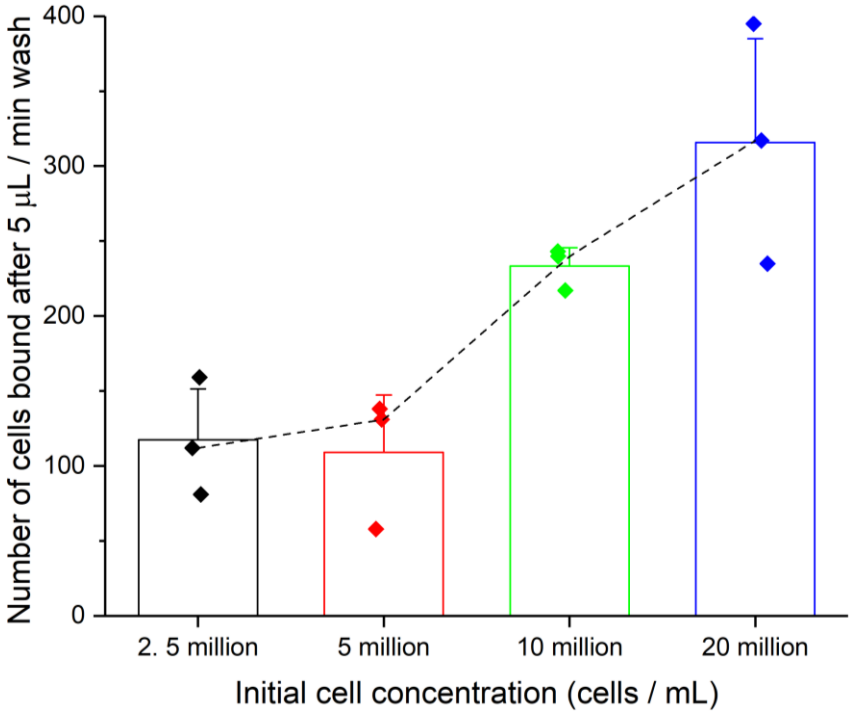

Figure 6.22 The number of cells bound increased when the initial cell concentration was increased

The initial cell suspension concentration was investigated with the aim to bind the maximum number of cells on the channel surface during one incubation. The number of cells bound to the channel surface increased as the initial concentration of the cell suspension was increased. The dashed line connects the median values, bars represent the mean values and the error bars represent the SEM.

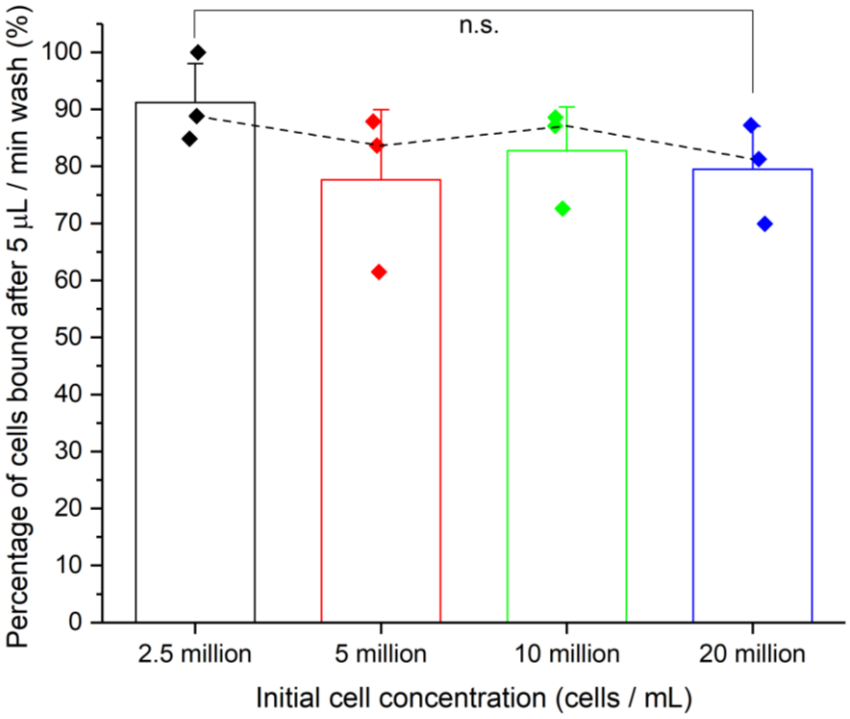

Figure 6.23 There was no difference in the percentage of cells bound when the initial cell concentration was increased

The initial cell suspension concentration was investigated with the aim to bind the maximum number of cells to the channel surface during one incubation. There was no significant difference between the percentage of cells bound to the channel surface as the initial concentration of the cell suspension was increased (n.s.=not significant, n=3). The dashed line connects the median values, bars represent the mean values and the error bars represent the SEM. Statistical analysis was carried using an independent samples t-test as the data was normally distributed according to the Shapiro-Wilk test of normality.

When comparing this data to the data recorded using the one-inlet device, it can be seen that the percentage of cells bound after the buffer wash was significantly higher and more consistent when using the second inlet tubing for buffer washes (Figure 6.24). Using the two-inlet device, the average percentage of cells bound in a 100% CD271+ population was 83 ± 3% (mean ± SEM, n=12), compared with 60 ± 7% (mean ± SEM, n=6) for the earlier data recorded using only one inlet tubing.

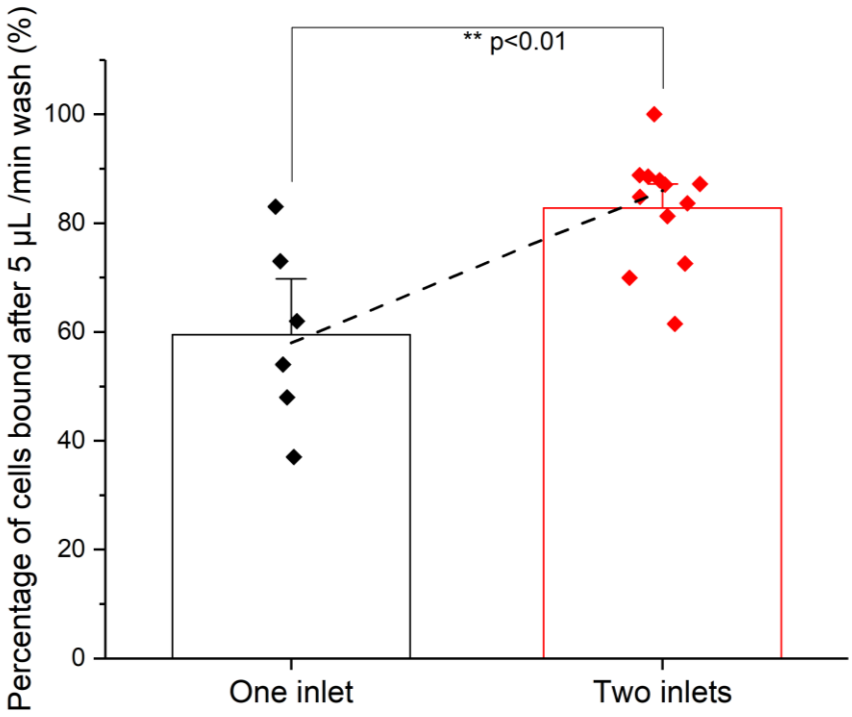

Figure 6.24 Comparison of data recorded using one-inlet device and two-inlet devices

For a 100 % SH-SY5Y population of cells, the percentage of cells bound after a 5 µL/min buffer wash was calculated using ImageJ. The percentage bound using a one-inlet device was compared to the percentage bound using a device with two inlets - designed to avoid large cell clumps distorting the percentage of cells bound to the channel surface. It was found that there was a significant difference in the percentage of cells bound using the two different device designs, with a higher and more consistent percentage of cells bound using a two-inlet device. Statistical analysis was carried out using an independent samples t-test as data was normally distributed according to the Shapiro Wilk test of normality (n=6 and n=12 respectively). Bars represent the mean values, the error bars represent the SEM and the dashed line connects the median values.

Further to this, the release of cells at higher flow rates was investigated using the optimised protocol. It was found that the profile of cell release was more consistent and predictable using the two-inlet device (Figure 6.25). SH-SY5Y cells reliably bound to the channel surface using flow rates of up to 20 µL/min and when flow rates were increased above 20 µL/min, cells were released. After buffer washes at 40 µL/min and 80 µL/min, only 1.7 ± 0.7% (mean ± SEM, n=12) of cells remained bound to the channel surface.

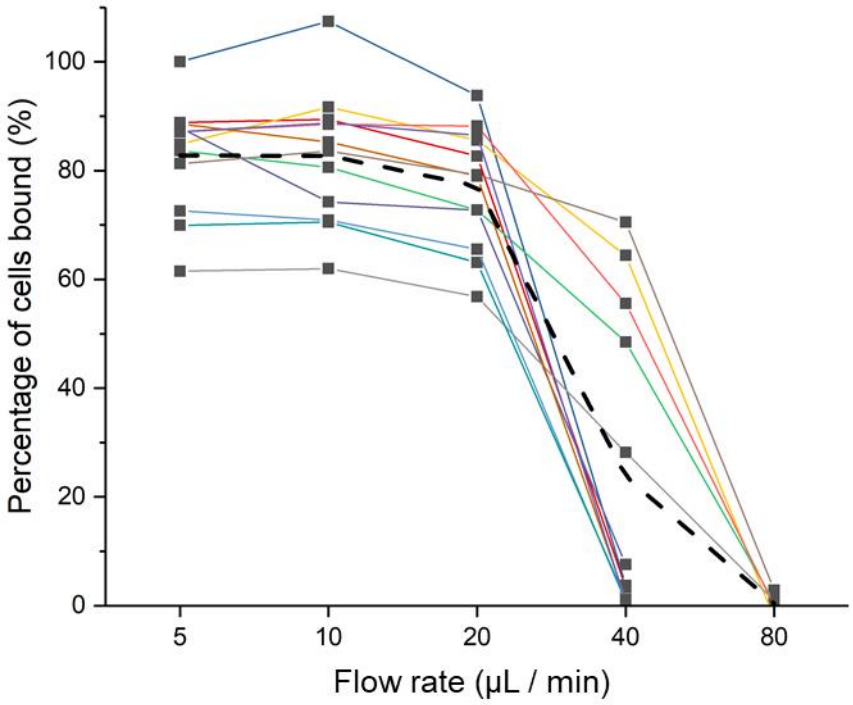

Figure 6.25 The percentage of bound cells remaining when the flow rate was increased using the two-inlet device

The flow rate of buffer washes was increased from 5 µL/min to 80 µL/min and the percentage of cells bound after each wash was calculated using ImageJ. Each coloured line represents one experiment and the dashed line represents the mean (n=12). SH-SY5Y cells reliably bound to the channel surface up to flow rates of 20 µL/min and released from the surface at flow rates above 20 µL/min.

6.3.4 Investigating specific cell capture and release in the prototype device using mixed cell populations

6.3.4.1 Analysis of mixed cell populations using the prototype device and flow cytometry

Once specific cell capture and release in the prototype device was optimised, the next aim was to increase the complexity of cell populations and assess specific cell capture from mixed cell populations. The fibroblast and SH-SY5Y cells were mixed together in different ratios and the mixed populations injected into the device using the protocol optimised in Section 6.3.3 (using one channel in the device only, with two inlets).

It was found that as the percentage of CD271+ SH-SY5Y cells in the initial cell population was decreased, the number of cells bound to the channel surface also decreased (Figure 6.26). This indicated that CD271+ cells were specifically

captured from mixed cell populations. The device performance was then compared to a gold standard method of cell enrichment – flow cytometry or FACS. Mixed cell populations of the same ratios were analysed by flow cytometry (Figure 6.27) and the number of CD271-expressing cells detected by flow cytometry compared to the number of cells bound to the channel surface (Figure 6.28).

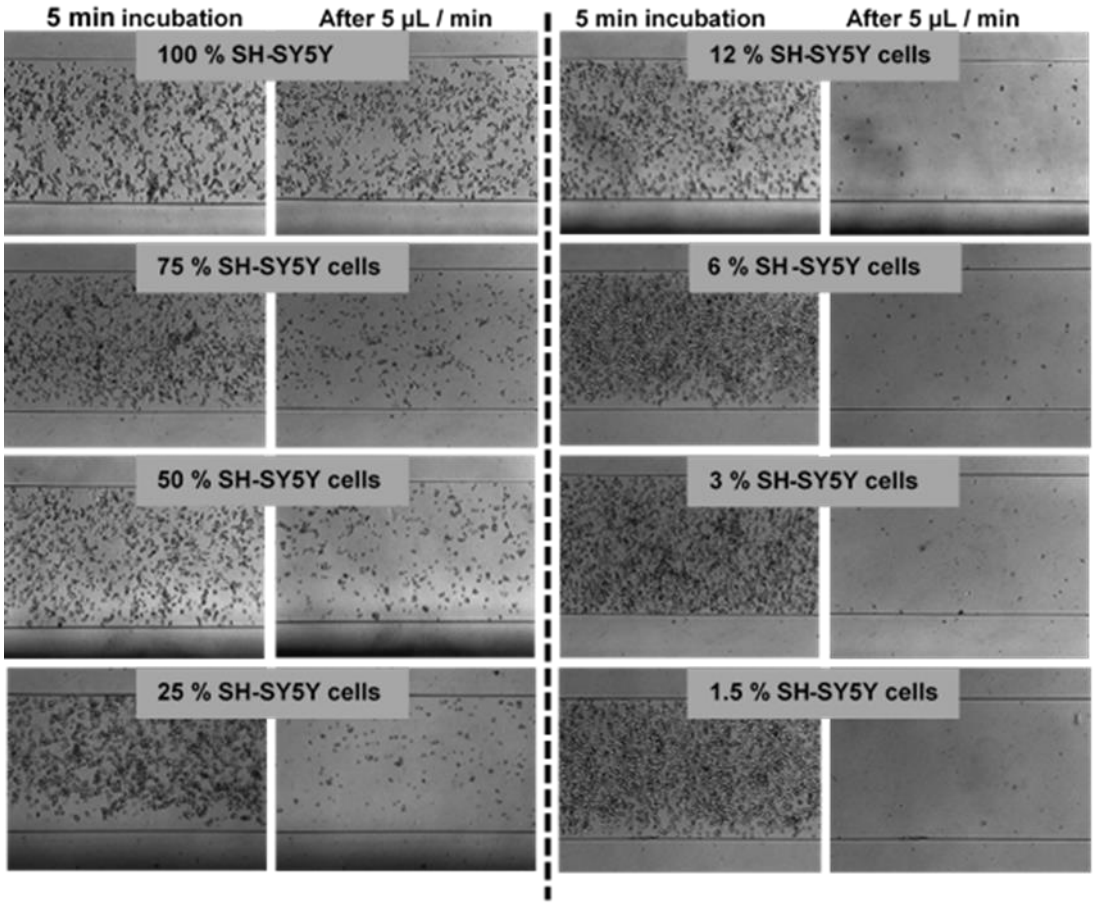

Figure 6.26 The percentage of cells bound to the channel surface decreased as the percentage of CD271+ cells in the population decreased

SH-SY5Y cells and fibroblast cells were mixed in different ratios and injected into the prototype device. Photos were taken during the 5 minute incubation period (shown on the left-hand side of each panel) and after a 5 µL/min buffer wash (shown on the right-hand side of each panel).The number of cells bound to the surface decreased as the percentage of SH-SY5Y cells in the initial population decreased.

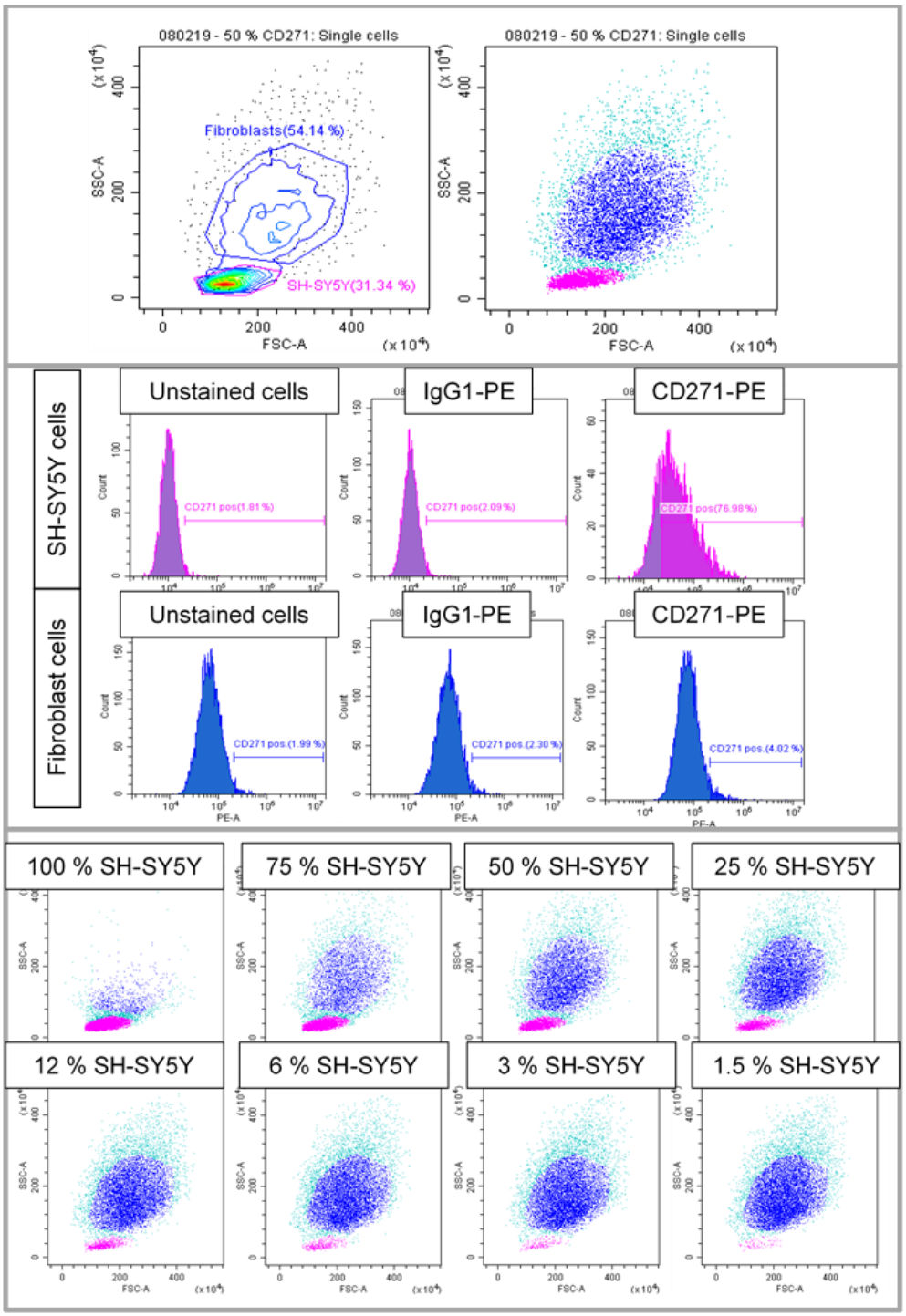

Figure 6.27 Flow cytometry analysis of mixed cell populations

SH-SY5Y cells and fibroblast cells were mixed in different ratios and analysed by flow cytometry. The top panel shows how the two different populations have been gated according to their forward and side scatter. The middle panel shows the CD271 expression of each population compared to an isotype control antibody (IgG1-PE) and unlabelled cells. The bottom panel shows how the number of cells in each population changes in the different mixed cell populations.

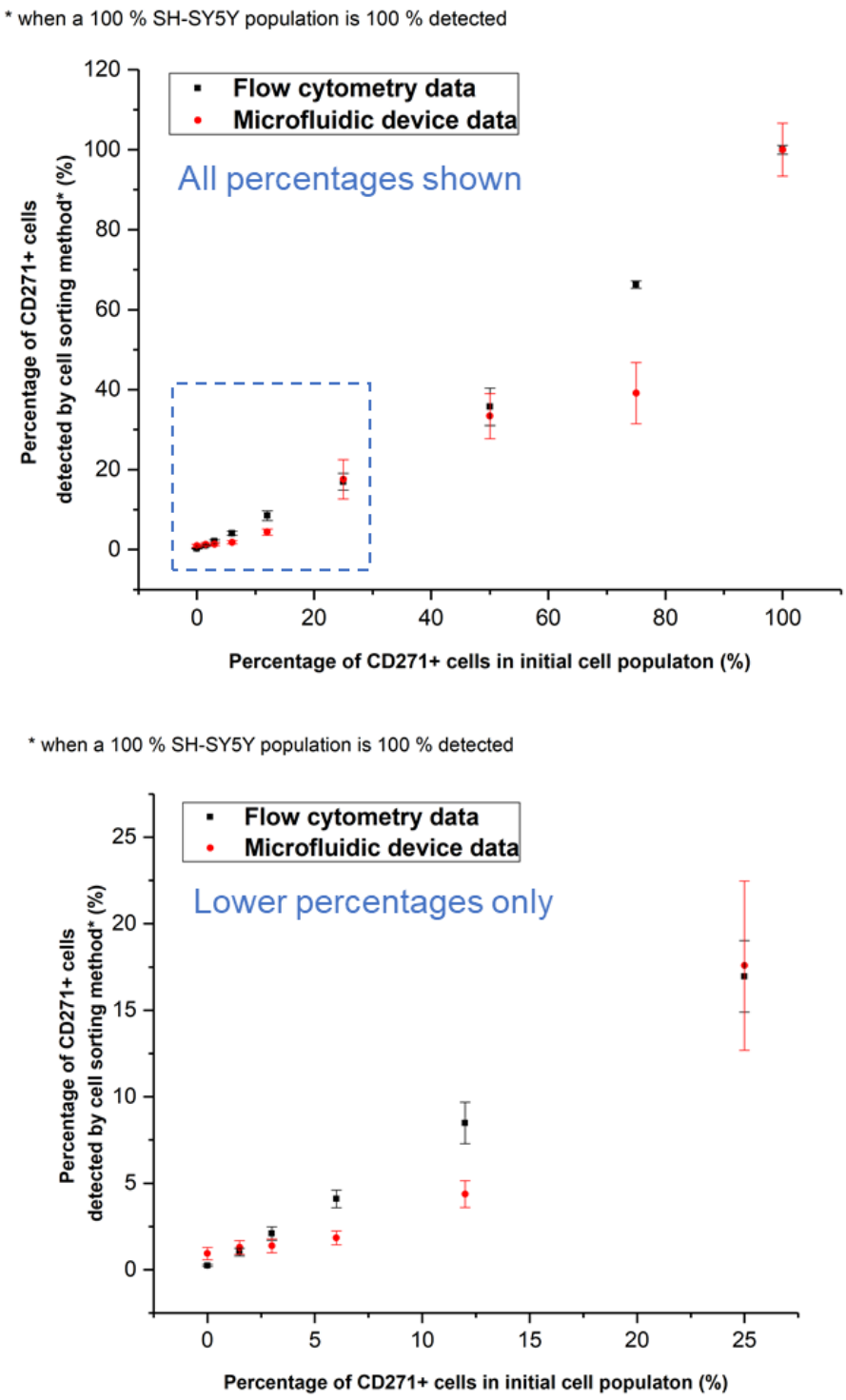

Figure 6.28 Microfluidic device and flow cytometry comparison using mixed cell populations

SH-SY5Y cells and fibroblast cells were mixed in different ratios and the percentage of CD271+ SH-SY5Y cells detected by the prototype device (red circles) compared to the number of CD271+ SH-SY5Y cells detected by flow cytometry (black squares). The data was normalised such that in an initial 100% SH-SY5Y population, 100% of CD271+ cells were detected by each method. The upper panel shows all percentages tested from 100% to 0% SH-SY5Y, the bottom panel shows the lower percentages only (25% to 0% SH-SY5Y – highlighted by the blue dashed box in the upper panel).

There was good overall agreement between the two methods of cell enrichment however by only analysing a small section of the channel at a time (approximately 1/12th), the device (or the method used for analysis) was not as sensitive as flow cytometry at detecting the lower percentages of CD271+ cells. Further to this, in a 75% population of CD271+ cells, there was a large discrepancy between the device data and the flow cytometry data. It could be that the relationship is non-linear and more complex than can be rationalised using this data only.

The cell capture efficiency of the device can be estimated by comparing the percentage of cells bound in the device to the percentage of cells in the initial cell population. For a more accurate analysis of the capture efficiency, the percentage of cells captured in a 0% CD271+ cell population was subtracted from all other populations to negate the effects of non-specific binding. By doing this, the capture efficiency of the device - taking into account all the different populations analysed - was calculated to be 45 ± 11% (mean ± SEM, n=8). Evidently, this value is relatively low.

As previously discussed, the sensitivity of the device (or analysis method) decreased as the percentage of CD271+ cells decreased, therefore subgroup analysis of the data may provide more useful information. The higher percentage populations (25-100% CD271+ cells) were analysed separately to the lower percentage populations (12.5-1.5% CD271+ cells) and from this analysis, the capture efficiency was calculated to be 70 ± 10% and 20 ± 3% respectively (mean ± SEM, n=4). These values emphasise the challenges involved in capturing cells present at low percentages, however this result could also be an artefact of the analysis method at lower percentages. Currently, the cells bound in only 1/12th of the device were analysed, this means that at lower percentages of CD271+ cells, there could have been greater inaccuracy in the result due to the smaller number of CD271+ cells present. In Chapter 7, different device protocols and methods of analysis are optimised to assess the binding of a low percentage of CD271+ cells.

For comparison, the detection efficiency according to the flow cytometry results was calculated. As before, the percentage of CD271+ cells detected in a 0% CD271+ population was subtracted from all other populations. The detection efficiency of the flow cytometry results was calculated to be 71 ± 5% (mean ± SEM, n=8). The capture efficiency of the device was therefore comparable to flow cytometry at higher percentages of CD271+ cells. The same subgroup analysis of the flow cytometry data revealed that the detection efficiency was 81 ± 8% for the higher percentage populations (25–100% CD271+ cells) and 62 ± 4% for the lower percentage populations (12.5–1.5% CD271+ cells), showing that the detection efficiency of the flow cytometry method also decreased at lower percentages, however it was still much greater than the device efficiency.

The capture efficiency of affinity-based microfluidic devices is often reported in the literature. Although there are no affinity-based microfluidic devices based on the capture of CD271+ cells (or any other MSC surface marker), there are many devices described for the capture of circulating tumour cells (CTCs) using anti-epithelial cell adhesion molecule (EpCAM) antibodies. These are discussed in detail in Chapter 8: Section 8.1.2. The possibility of using a hybrid microfluidic technology, with a high throughput pre-enrichment step, is also discussed in Chapter 8: Section 8.1.4. This could result in an increased percentage of CD271+ cells in a second stage of enrichment using this technology. Further development of the device to increase the throughput for clinical application and to allow analysis of the cells post-enrichment, is described in Section 6.3.5.

6.3.4.2 Analysis of mixed cell populations with fluorescent labelling

To further confirm the results of Section 6.3.4.1, and to assess the purity of captured cells, the two cell populations were fluorescently labelled with different coloured cell trackers. SH-SY5Y cells were labelled with green cell tracker and fibroblasts were labelled with red cell tracker (Section 6.2.5.3, Figure 6.29). Using a multiband filter set (Semrock, LF488/561-B-000) and a multichannel imaging system (Photometrics DV2™), spatially identical but spectrally distinct images were acquired simultaneously to determine if the CD271+ cells were the cells bound to the channel surface.

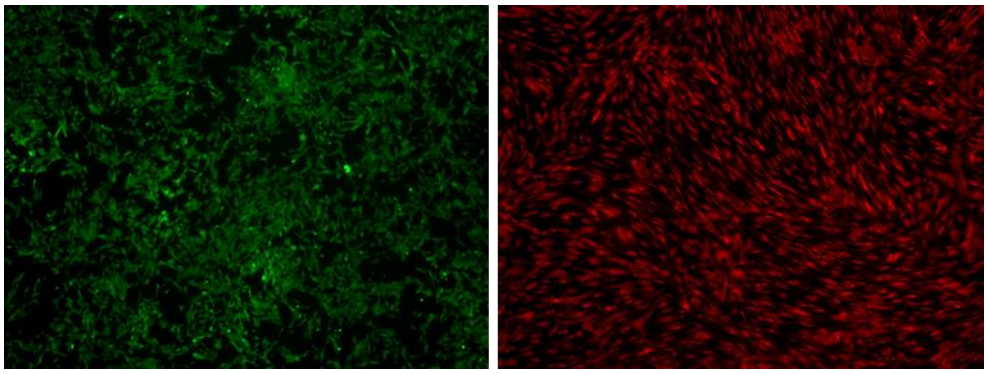

Figure 6.29 SH-SY5Y and fibroblast cells fluorescently labelled with green and red cell tracker respectively

On the left-hand side, SH-SY5Y cells are shown labelled with green cell tracker. On the right-hand side, fibroblast cells are shown labelled with red cell tracker. Labelling was carried out 24 h prior to testing in the device.

Four different populations were analysed; 100%, 50%, 25% and 6% SH-SY5Y populations, made up to a 100% with fibroblast cells. These experiments

confirmed the specificity of cell binding in the device as the majority of cells labelled with green cell tracker (CD271+ SH-SY5Y cells) bound to the functionalised surface, whereas the majority of cells labelled with red cell tracker (CD271- fibroblast cells) were washed away (Figure 6.30). A small percentage of fibroblasts bound to the channel in some cases, however, this was not of great concern since in all cases the CD271+ cells were significantly enriched from the initial cell population (approximately 13-fold enrichment observed from a 6% SH-SY5Y original population).

Using ImageJ, the purity of the enriched populations was estimated by counting the number of cells labelled with green cell tracker after the 5 µL/min buffer wash, and comparing with the number of cells labelled with red cell tracker. From the four different populations analysed – 6% SH-SY5Y, 25% SH-SY5Y and 50% SH-SY5Y the calculated purity was 80 ± 3% (mean ± SEM) after enrichment. The purity of enriched populations was therefore consistent at even the lowest percentage analysed.

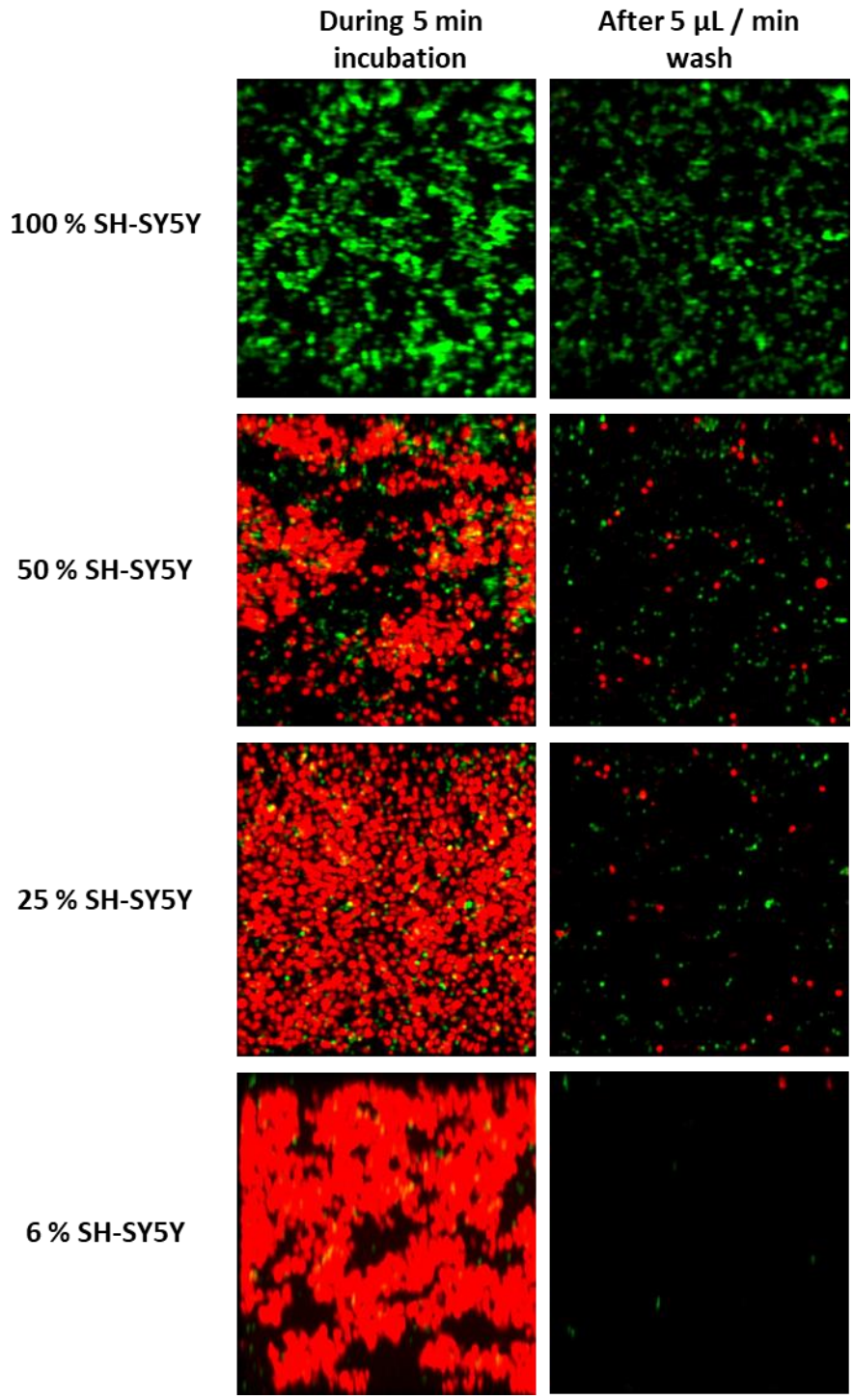

Figure 6.30 Specific cell capture confirmed using fluorescently-labelled mixed cell populations

SH-SY5Y cells were stained with green cell tracker and fibroblasts were stained with red cell tracker. The two cell types were mixed to make populations of 100% SH-SY5Y, 50% SH-SY5Y, 25% SH-SY5Y and 6% SH-SY5Y. Photos on the left-hand side were taken during the 5 minute incubation period. Photos on the right-hand side were taken after a 5 µL/min buffer wash. The majority of non-specific fibroblast cells were washed away whilst the majority of specific SH-SY5Y cells bound to the channel surface. ImageJ software was used to convert the images to RGB colour and the two spectrally distinct images were merged.

6.3.5 Increasing the surface area for cell capture and release

The worked carried out thus far demonstrated the efficacy of the device using a cell line that expressed the CD271 antigen and cells that did not express the CD271 antigen. To progress this work further and to show clinical utility, the number of cells processed and collected from the device needed to be increased further. This was for two reasons; firstly, clinical samples of bone marrow mononuclear cells typically contain less than 0.04% of CD271+ cells (Chapter 7: Section 7.3.1) and therefore large numbers of cells need to be processed to enrich (and visualise in the device) such a small percentage of cells. Secondly, to investigate the viability and manipulation of cells post-enrichment, a substantial number of cells needed to be collected to carry out post-enrichment analysis. Two device iterations were investigated to increase the surface area available for cell capture, detailed in the sections below.

6.3.5.1 Device iteration 1: using multiple-port manifolds

The prototype device was originally designed with four channels, however, it was only possible to operate one channel at a time due to the syringe pump and valve arrangement. Simultaneous use of the channels would therefore increase the throughput of the device by four times, allowing enough cells to be captured for post-enrichment analysis.

The first method trialled for simultaneous cell injection was using a 9-port manifold (IDEX Health & Science). Two manifolds were positioned so that all four channels were controlled by two valves (Figure 6.31), one valve and manifold for cell injection and one valve and manifold for buffer injection. The remaining 4 ports of each manifold were blocked with microfluidic plugs.

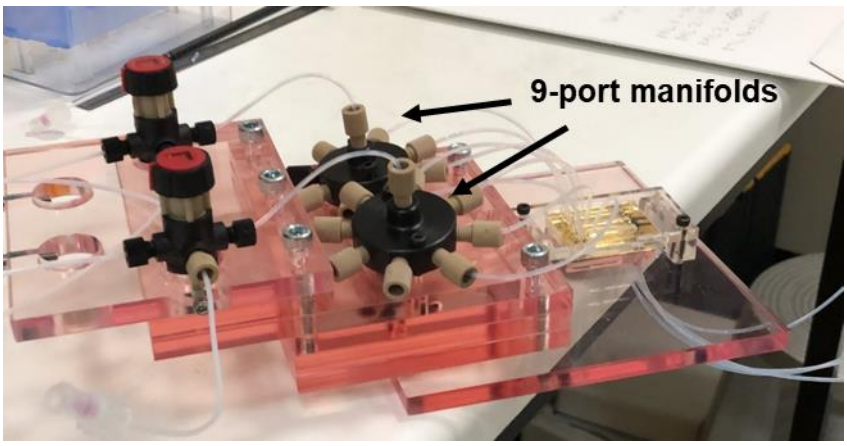

Figure 6.31 Manifolds incorporated into device design for simultaneous operation of four parallel channels

Two 9-port manifolds were positioned between the four-way valves and the channels so that each valve could operate four parallel channels simultaneously. One manifold was used for cell injection and the other manifold was used for buffer injection.

Using this design resulted in uneven cell distribution between the four channels, ranging from over 500 cells in channel 2 to less than 50 cells in channel 4 (Figure 6.32). This could have been due to the manifold itself, or the fact that having multiple inlets and outlets meant that microscopic differences in the channels led to less fluidic resistance in some channels than others. For example, the clamping of the PDMS could slightly favour channels on one side of the device compared to the other, or the position of outlet tubing could provide less resistance in one channel compared to another. Furthermore, the use of extra tubing exacerbated cell clumping issues (indicated in Figure 6.31) and it was considered that a simpler design would be more beneficial.

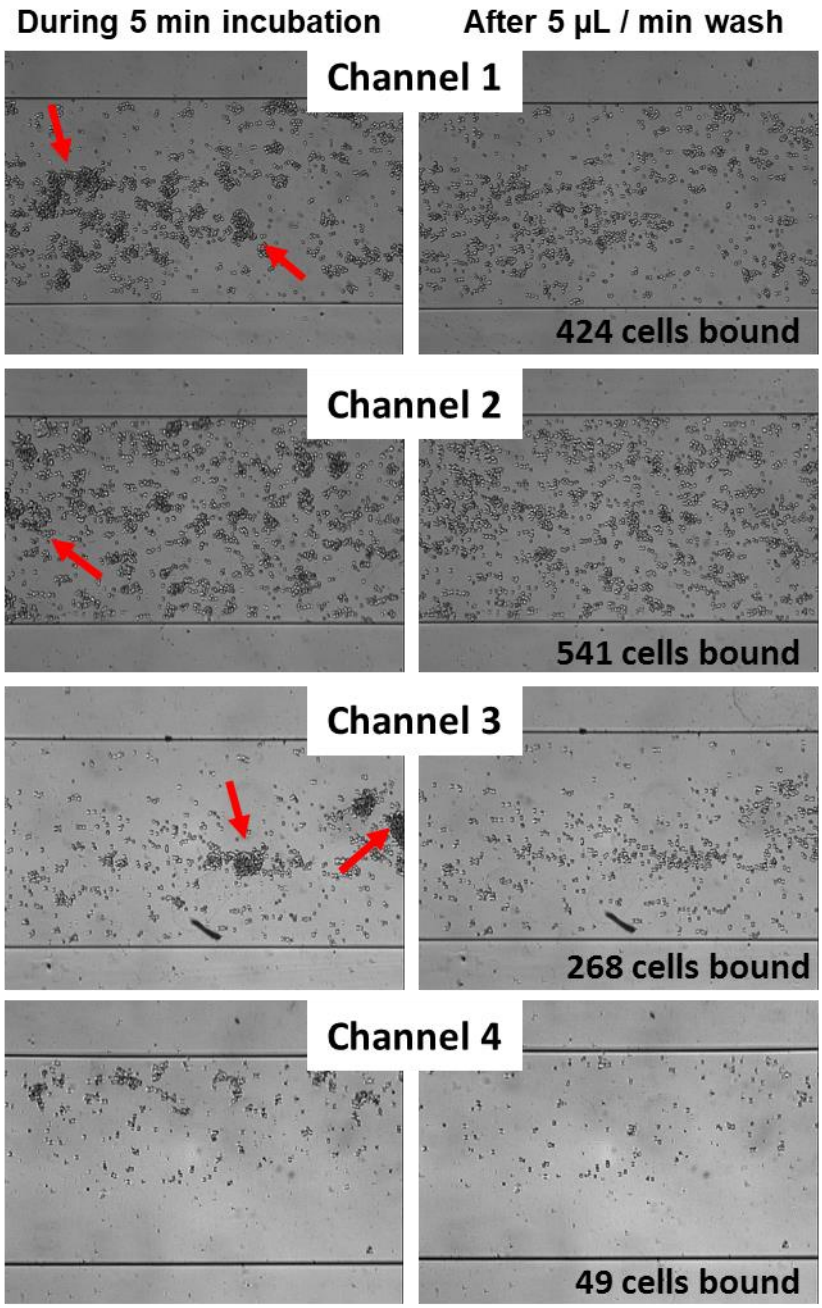

Figure 6.32 Distribution of cells in four parallel channels using 9-port manifolds for simultaneous operation

When 9-port manifolds were used for simultaneous operation of four parallel channels, the cells were unevenly distributed between the channels demonstrated by the vast difference in the number of cells bound (indicated in the bottom right corner of each image). In addition, using longer tubing before the cells entered the channels meant that large cell clumps formed (indicated by red arrows).

6.3.5.2 Device iteration 2: branched channel design

The second device iteration involved changing the channel design; rather than having four separate channels that required eight separate inlets and four

separate outlets, it was hypothesised that two inlets (one for cells and one for buffer) and just one outlet would provide more even flow, eradicating some of the complications introduced by the first device iteration. It was also hypothesised that having the channels closer together would reduce the effects of uneven clamping.

The design was first drawn in COMSOL in order to check the flow would be theoretically even in all channels (Figure 6.33). Once this was confirmed, the design was drawn in L-edit and a PDMS mould made using soft lithography techniques as previously described (Section 6.2.4.3). Using the new channel design, cells were more evenly distributed between all four channels, with the number of cells bound ranging from 900 to 1400 in all four channels (Figure 6.34). The more even cell distribution also led to an overall increased number of cells bound in the four channels during one incubation period, with an average of 320 cells bound per image using device iteration 1 compared to an average of 1198 cells bound per image using device iteration 2. It was therefore concluded that device iteration 2 would be suitable to collect enough cells for post-enrichment analysis, where the surface area available for cell capture was increased by 4.8 times compared to when using one single straight channel (see Figure 6.5) in previous experiments.

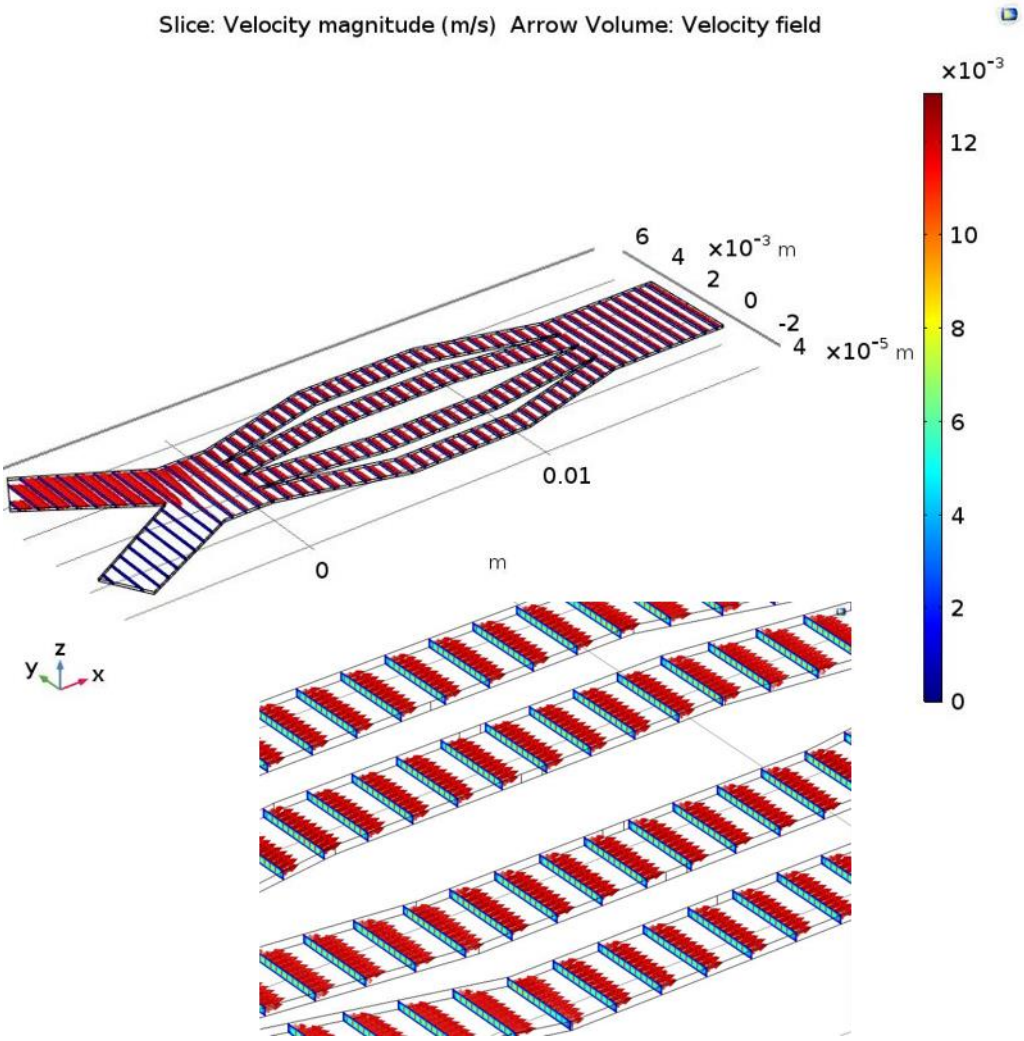

Figure 6.33 COMSOL simulation showing the theoretical flow in a two-inlet, one-outlet four-channel design

COMSOL simulations predicted the flow to be even in four parallel channels using a two-inlet, one outlet design. The top image shows the entire design and the bottom image is a closer view of the middle section of the four channels.

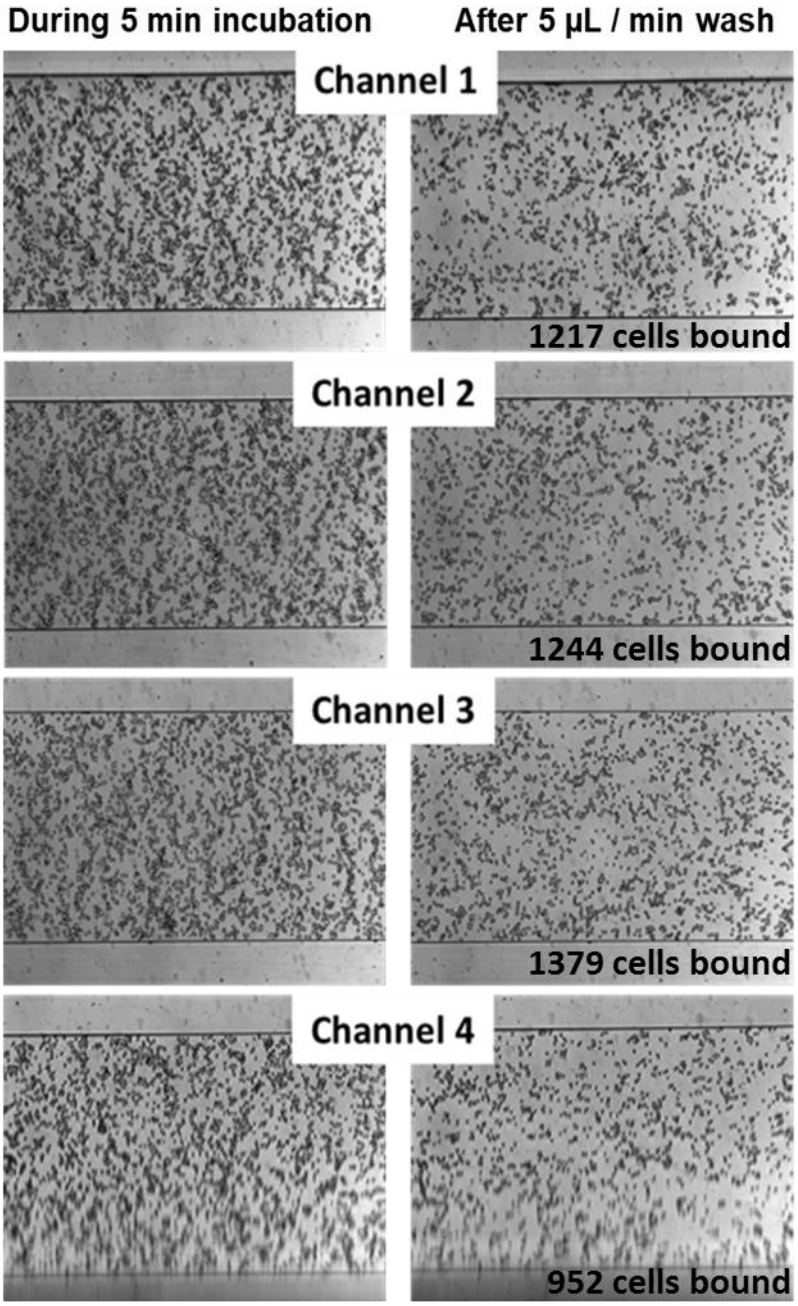

Figure 6.34 Cell distribution in four parallel channels using a two-inlet, one outlet channel design

When a two-inlet, one outlet channel design was used for simultaneous operation of four parallel channels, the cells were evenly distributed between the channels. There were no large cell clumps due to the shortened tubing length and the surface area available for cell capture was increased by 4.8 times.

6.3.6 Investigating the viability of cells post-enrichment

Due to the low percentage of CD271+ cells in clinical samples, post-enrichment analysis was carried out using SH-SY5Y cells that had been captured and

released in the prototype device. The first parameter analysed was the viability of cells, carried out via flow cytometry analysis using a 7-AAD viability stain (Section 6.2.6.1).

From the initial experiments, it was found that the number of intact cells was significantly decreased in control samples suspended in different medium. It was found that when cells were suspended in the buffer used for device experiments (MACS buffer with 0.005% Tween 20) the number of intact cells decreased dramatically compared to when cells were suspended in MACS buffer or Alpha MEM culture medium (Figure 6.35). It was therefore decided to carry out a controlled study into the effects of different buffers on the number of intact cells to ensure the buffer used for device experiments would not be detrimental to cells, since the loss of cell membrane integrity is a characteristic of cell death.

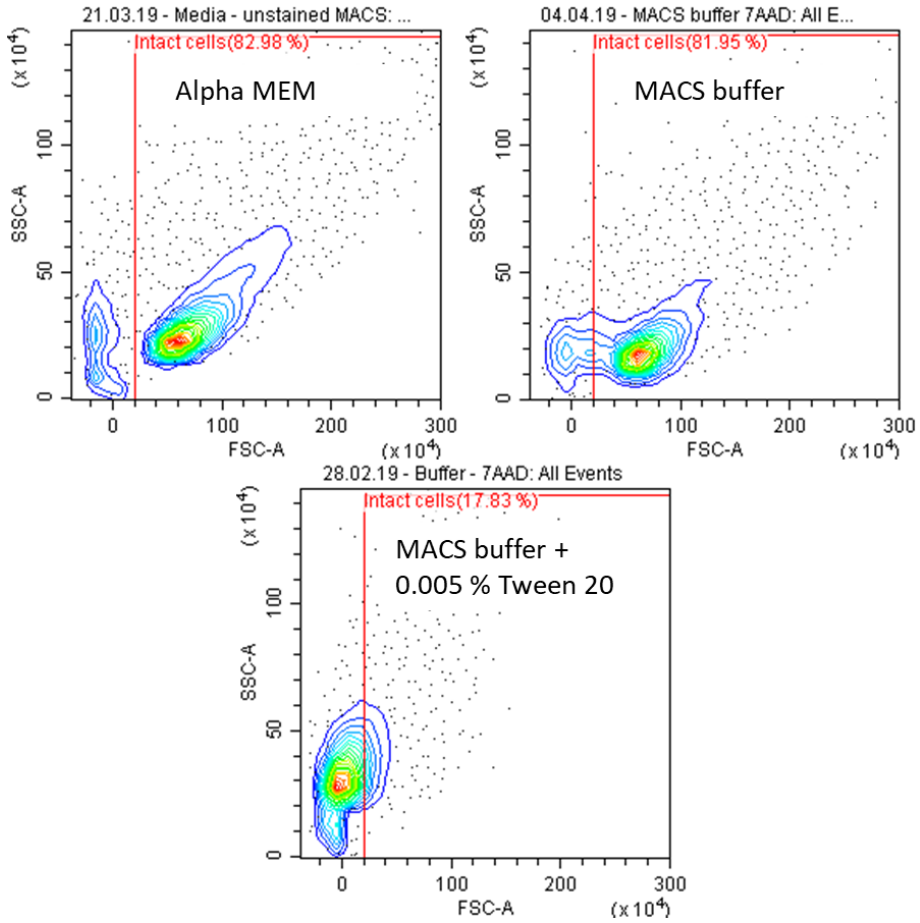

Figure 6.35 Variability in the percentage of intact cells when cells were suspended in different buffers

The upper panels show the forward/side scatter analysis of cells suspended in Alpha MEM culture medium and MACS buffer, and the lower panel shows the forward/side scatter analysis of cells suspended in MACS buffer with 0.005% Tween 20. The percentage of intact cells dramatically decreased when 0.005% Tween 20 was added to the buffer.

6.3.6.1 Investigating the viability of cells in different buffer solutions

To investigate the percentage of intact cells further, one million cells were either kept in serum-free cell culture medium, serum-free cell culture medium with 0.005% Tween 20, MACS buffer, or MACS buffer with 0.005% Tween 20. The volume of the medium was 50 µL replicating the cell concentration used during device experiments (20 million cells/mL).

It was found that after 2-3 hours in each medium, there was no significant difference in the percentage of intact cells when suspended in MACS buffer compared to serum-free cell culture medium (Figure 6.36). However, it was found that when 0.005% Tween 20 was added to either serum-free medium or MACS buffer the percentage of intact cells decreased significantly ($p<0.05$ and $p<0.01$ respectively).

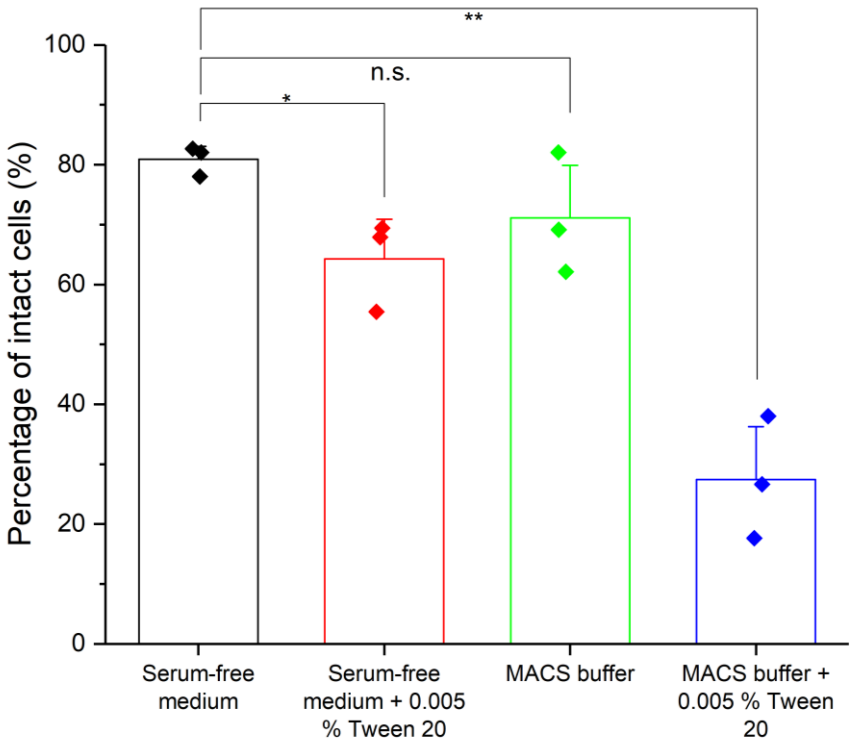

Figure 6.36 The percentage of intact cells when suspended in different medium

The percentage of intact cells was compared when cells were suspended in serum-free medium, serum-free medium with 0.005% Tween 20, MACS buffer or MACS buffer with 0.005% Tween 20. Cells were at a concentration of 20 million cells/mL in 50 µL for 2-3 hours before analysis via flow cytometry. Statistical analysis was carried out by an independent samples T-test as data was normally distributed according to the Shapiro Wilk test of normality. (n.s.= not significant, *p<0.05, **p<0.01, n=3). Bars represent the mean values and error bars represent the SEM.

Tween 20 was initially added to running buffer during device experiments to reduce non-specific binding (as was used for SPR experiments, Section 6.3.1.1) however even at low concentrations it was found to have a detrimental effect on the percentage of intact cells. Although there was no significant difference between culture medium and MACS buffer, it was noted that cells suspended in culture medium produced more consistent results than cells suspended in MACS buffer. It was therefore decided to carry out all future experiments in serum-free cell culture medium with no additional supplements to ensure the highest percentage of intact cells.

6.3.6.2 Investigating the viability of cells captured and released in the prototype device

Once the running buffer for device experiments had been optimised, the viability of cells bound and released in the device could be compared without any interfering factors. The viability of cells bound and released was compared to microfluidic controls (where the cells had been through the device at different flow rates with no incubation), and medium controls (where the cells had been kept in cell culture medium, on ice, for the duration of the experiment). Further to this, cells were also processed through a MACS column (in MACS buffer but without microbead labelling) and their viability analysed in the same way.

Repeats were carried out on different days using different cell cultures therefore natural biological variability was captured. The viability of cells according to the 7-AAD viability stain was reported from all the events recorded by the flow cytometer i.e. no gates were drawn around intact cells or single cells since cells damaged in the device may no longer be intact.

The results showed that there was no significant difference in the viability of cells between any of the conditions tested (Figure 6.37). It was observed that the results for the captured and released cells were more consistent than for any of the controls, this could be because only healthy viable cells are bound in the device (due to the specific antibody interaction for capture) and therefore intact and dead cells are washed away in the buffer wash. This result indicates that the cells were not harmed by the process of being captured and released in the device or by experiencing high flow rates (higher than those used for cell release) - as far as this limited analysis can show.

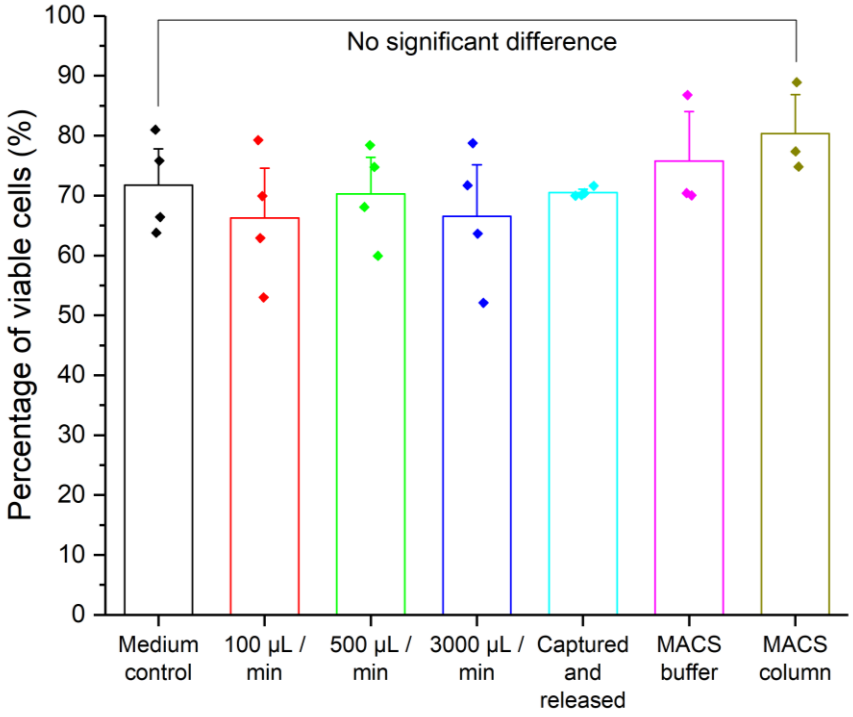

Figure 6.37 Cell viability after enrichment in the prototype device

The viability of cells which had been captured and released in the prototype device was compared to cells which had been through the device at different flow rates with no incubation (100 µL/min, 500 µL/min and 3000 µL/min) and cells which had not been through the device (medium control). Cells were also processed through a MACS column for comparison, or incubated in MACS buffer for the duration of the experiment. The viability of cells was evaluated using a 7-AAD viability stain and analysed using a flow cytometer. No significant difference was found between any of the conditions tested. Statistical analysis was carried out using an independent samples t-test or Mann Whitney U test to compare means depending on whether the data was normally distributed according to the Shapiro Wilk test of normality. Bars represent the mean values and error bars represent the SEM (n=4).

6.3.7 Investigating the proliferation of cells post-enrichment

For viability testing, the cells were analysed immediately after enrichment in the device. To establish if there were any adverse effects which may not be observed immediately, enriched cells were seeded at 40,000 cells/well in a 24-well plate and cultured for five days. On day two and day five, cell cultures were lysed and a Pico green dsDNA quantification kit (Invitrogen, P11496) was used to compare the quantity of dsDNA in each sample. The fold-increase in dsDNA content from day two to day five was calculated to negate differences in cell counting/cell seeding density, and the same medium and microfluidic controls were used as in previous experiments.

It was found that cells that had been captured and released in the device were able to proliferate at a comparable rate to cells that had not been through the device, and cells that had been through the device but not captured. There was no significant difference between any of the conditions tested (Figure 6.38). There are a number of potential sources of error associated with the experimental procedure for dsDNA quantification, including the human error associated with manual cell counting and the numerous pipetting steps in the dsDNA assay itself. Small differences in cell seeding density could lead to greater differences in the proliferation rate since cell density is a critical factor determining the proliferation of cells in culture (254). Although there was noticeable variation between replicates carried out on different days (each replicate series connected by a dashed line in Figure 6.38), in all experiments there was a minimum two-fold increase in the dsDNA present on day five compared to day two. The lowest fold-increase was observed from a medium control replicate suggesting that factors beside the microfluidic device had an effect on the rate of proliferation.

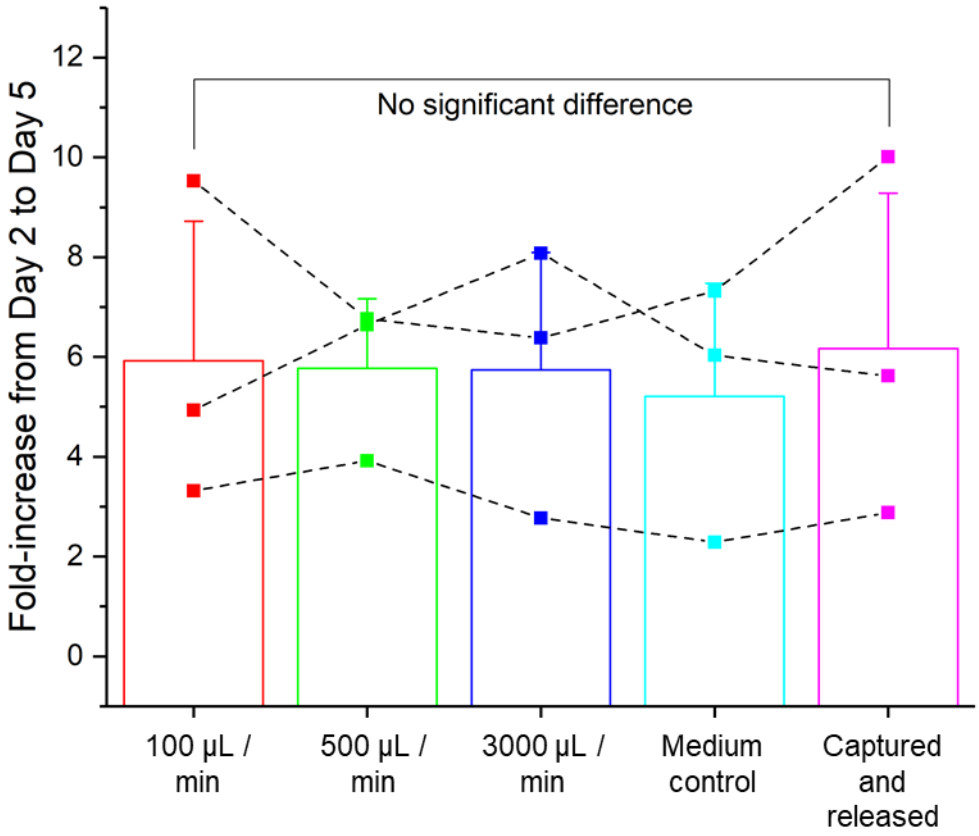

Figure 6.38 The fold-increase in dsDNA content between day two and day five of cells cultured post-enrichment

After enrichment in the microfluidic device, cells were seeded at 40,000 cells/well in a 24-well tissue culture plate. On day two and day five cells were lysed and the dsDNA content of each well quantified. The fold-increase between day two and day five was calculated to compare the proliferation rate of cells enriched in the device, to microfluidic and medium controls. There was no significant difference found between any of the conditions tested and there was a minimum 2-fold increase between day two and day five in all replicates. Statistical analysis was carried out using an independent samples t-test as the data was normally distributed according to the Shapiro-Wilk test of normality. Bars represent the mean result and error bars represent the SEM. The dashed lines connect the data points recorded in the same experiment.

6.3.8 Investigating the manipulation of cells post-enrichment

One of the key limitations of current affinity-based enrichment technologies is the need to pre-label cells with antibodies which remain attached to the cells post-enrichment. The enrichment technology developed here aims to be minimally manipulative and does not require any pre-labelling steps. The antibody interaction in the device is designed to be transient so that once cells are released from the antibody-functionalised surface they have no antibody attached to their cell surface. To evaluate whether this was the case, cells that had been captured

and released in the device were collected and labelled with anti-biotin-PE antibody to see if any of the CD271-biotin antibody on the functionalised surface remained attached to the cells post-release. The same antibody labelling was carried out on cells that had not been processed in the device.

As well as testing whether any antibody was attached to the cells, it was also necessary to check whether the CD271 antigen was still present on the cell surface and unaffected by the cell release process. For this, cells that had been captured and released were labelled with the CD271-biotin antibody and then anti-biotin-PE secondary antibody.

When analysed by a flow cytometer, it was found that less than 4% of cells that had been captured and released in the device were positive for anti-biotin-PE antibody, and there was no significant difference between the captured and released cells compared to cells that had not been through the device (Figure 6.39). Similarly, there was no significant difference in the percentage of positive cells labelled with CD271-biotin and anti-biotin-PE when captured and released compared to control cells. These results indicated that the antibody interaction in the device is only transient and no antibody remains attached to the cell surface post-release, nor is the antigen affected by the cell release process.

Although these results are encouraging, it is noted that further experiments are required to ensure that cells are truly minimally manipulated. For example, a transient interaction with an antibody may still affect downstream cell signalling processes and to assess this it would be necessary to carry out more in-depth gene expression analysis.

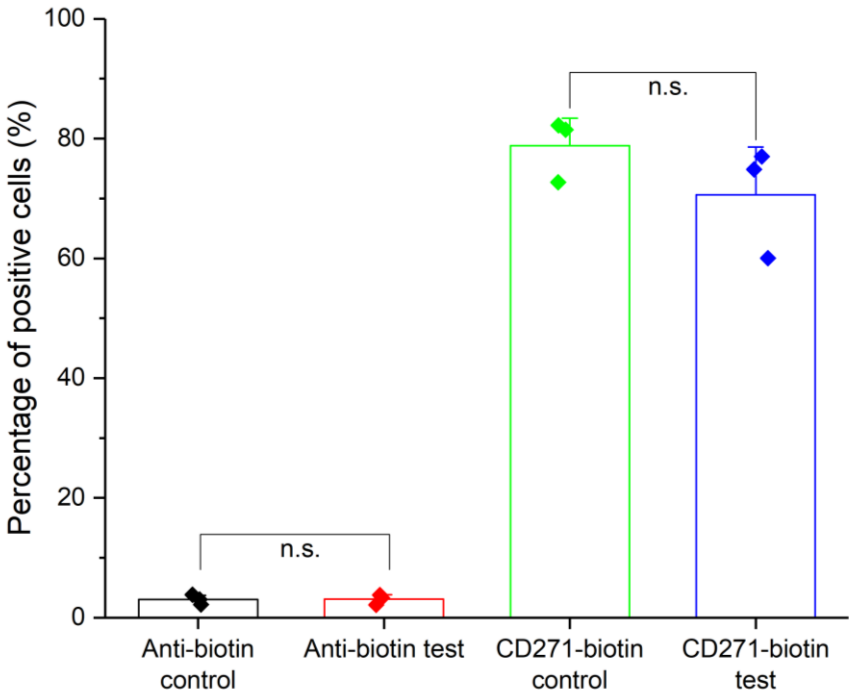

Figure 6.39 The percentage of antibody attached to the cell surface post-enrichment

To investigate whether any antibodies from the device were attached to the cells post-enrichment, captured and released cells were labelled with anti-biotin-PE (anti-biotin test, shown in red) and compared to cells that had not been processed in the device (anti-biotin control, shown in black). To investigate whether the CD271 antigen was still present on the cell surface after the cell release process, captured and released cells were labelled with CD271-biotin and anti-biotin-PE as a secondary antibody (CD271-biotin test, blue) and compared to cells that had not been processed in the device (CD271-biotin control, green). No significant difference was found between either of the test and control conditions (n.s.=not significant, n=3). Statistical analysis was carried out using an independent samples t-test since the data was normally distributed according to the Shapiro Wilk test of normality. Bars represent the mean values and the error bars represent the SEM.

6.3.9 Cell recovery from the device

Finally, the cell recovery from the device was calculated to ensure that cells were not lost in the microfluidic tubing during processing. A known volume and concentration of SH-SY5Y cells was injected into the device followed by a 400 µL buffer wash (100 µL/min flow rate) to flush cells out of the tubing and channels (Section 6.2.6.4). The recovered cells were counted using a haemocytometer. For comparison, cells were also processed through a MACS column using the standard protocol but without microbead labelling. The cells in the eluate from the column were counted and compared to the cells recovered from the microfluidic device.

It was found that there was no significant difference in the percentage of cells recovered using either method and that the percentage of cells recovered from the device was more than 80% for each replicate (Figure 6.40). This result demonstrates that there is no significant loss of cells in the microfluidic tubing compared to a gold standard method of cell enrichment.

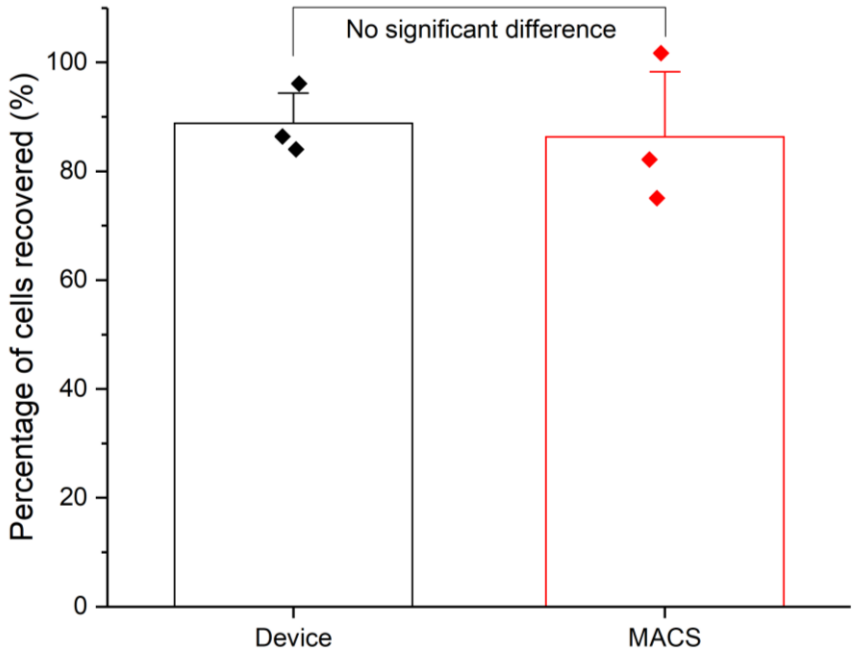

Figure 6.40 The percentage of cells recovered from the device compared to a MACS column

The cell recovery from the device was calculated and compared to the cell recovery from a MACS column. It was found that there was no significant difference in the cell recovery from both methods and the cell recovery from the device was above 80% in all replicates. Statistical analysis was carried out using an independent samples t-test since the data was normally distributed according to the Shapiro Wilk test of normality. Bars represent the mean values and the error bars represent the SEM (n=3).

6.4 Conclusions

This Chapter describes the design, fabrication and development of a microfluidic device capable of the specific cell capture of CD271+ cells. The specificity of the device was confirmed using different antibody-functionalised channels and different cell combinations, as well as using mixed cell populations to compare the device performance to a gold standard method of cell sorting. Moreover, it was shown that the enrichment process had no effect on the viability or

proliferation of cells and that according to the analysis carried out thus far, the cells could be classified as minimally manipulated.

For Human Cells, Tissues and Cellular and Tissue-Based Products (HCT/Ps), regulatory guidance from the FDA (section 1271.10(a)(1), (21 CFR 1271.10(a)(1))) states that a HCT/P must be minimally manipulated and defines this as 'processing that does not alter the relevant biological characteristics of cells or tissues' (255). The data described in this chapter showed no significant difference between cells processed in the device compared to non-processed cells, however, the experiments carried out here only demonstrate an initial assessment and more in-depth studies would be required to be certain. For example, analysis must be carried out using clinically-relevant cells rather than cell lines, and the therapeutic potential of the cells tested in relevant applications *in vitro* and *in vivo.*

The device has been shown to be comparable to FACS in terms of cell capture efficiency (for cell populations containing >25% of the target population) and comparable to MACS in terms of cell viability and recovery. The device has also been shown to enrich target populations with purities of approximately 80%. What is more, the device has significant advantages over both MACS and FACS in that no pre-labelling steps are required - which could lead to shorter processing times - and that no antibody is attached to the cells post-enrichment.

Currently, FACS is more suited to diagnostic applications due to the expense of instruments, and the expertise required for operation (256), whereas MACS provides a more cost-effective approach for clinical applications. However at this time the majority of MACS products are only certified for *in vitro* use (131), and there are varied reports on the safety of using iron-oxide containing nanoparticles for *in vivo* applications. There have been several reports indicating phenotypical alterations to cells labelled with iron-oxide containing particles for cell tracking purposes (257-259), however it has been shown that the iron levels used for magnetic resonance imaging and magnetic targeting of stem cells are typically several orders of magnitude higher than those used for microbead labelling (260).

The same study by Müller *et al.* (2017)(260) used MACS technology to enrich CD133+ HSCs and CD271+ MSCs and assessed the impact of the stem cells as well as the co-injected microbeads on the cardiac remodelling processes after myocardial infarction. The study was carried out in immunodeficient mice and it was found that 48 hours after transplantation no microbeads could be detected in the cells or surrounding heart tissue and improvements of cardiac function were reported.

Conversely, there is evidence to suggest that the ligation of receptors utilised for positive selection of cells has detrimental effects on downstream cellular processes. A study by Bhattacharjee *et al.* (2017)(261) found that monocytes isolated by positive selection using CD14 microbeads were impaired due to the microbead-blocked CD14 receptors. Stimulation by lipopolysaccharide led to activation and increased proliferation of monocytes isolated by negative selection however the response by positively selected cells was reduced and the cells did not proliferate. Similarly, in a comparison of FACS, positive selection by MACS and negative selection by MACS, Beliakova-Bethell *et al.* (2014)(262) reported changes in the gene expression of positively-selected cells compared to negative selection and FACS.

There are still insufficient studies exploring the effects of antibody-labelling on cellular processes for *in vivo* application and effects are likely to be dependent on the specific application of the cell therapy as well as the dose of cells required. Although the prototype device investigated in this chapter ligates CD271 cell surface receptors, the ligation is transient and no receptors remain blocked when the cells are collected from the device (i.e. before transplantation as a cellular therapy). Gene expression analysis of collected cells would elucidate whether the transient interaction affects any cell signalling processes and would further confirm if this novel enrichment method is advantageous over current affinity-based methods.

The work carried out in this chapter has provided proof-of-concept data for the use of a microfluidic device with affinity-based cell capture. In order to progress this technology further, the work in Chapter 7 investigates the feasibility of enriching CD271+ cells from clinical samples of bone marrow aspirate.

Chapter 7:
Enriching CD271+ cells from clinical samples of bone marrow aspirate

7.1 Introduction

In Chapter 6, a prototype cell enrichment device was developed for the specific capture of CD271+ cells, and optimised using a cell line known to constitutively express CD271. The work in this chapter aimed to establish the potential clinical utility of the device using cells derived from clinical bone marrow aspirates, typically with very low percentages of CD271+ cells. Initially, cells were characterised using existing cell enrichment technologies – MACS and FACS (Section 7.3.1) and the therapeutic potential of the enriched population investigated using a CFU-F assay (Section 7.1.1 and 7.3.4). Once critical information such as the typical number of CD271+ cells in BM-MNC populations had been established, enrichment of CD271+ cells was investigated using the prototype device (Section 7.3.6).

In Chapter 6, it was found that the capture efficiency of the device was low (~20%) when the target population was present at low concentrations of the total cell population. However, this could have been due to the analysis method where only a small section of the channel was analysed during one experiment. This would lead to greater inaccuracies where fewer CD271+ cells were present. In this chapter, different device protocols and methods of analysis were investigated (Section 7.3.7), as well as using a channel with greater surface area (developed in Chapter 6: Section 6.3.5) to gain a greater perspective of the binding of low percentage CD271+ populations typical of clinical samples.

7.1.1 Colony forming units-fibroblast (CFU-F) assay

A colony forming units-fibroblast (CFU-F) assay is an assay used to assess the number of MSCs present in a population of cells. When Friedenstein and colleagues first described MSCs in 1970 (263), their ability to generate colonies when plated at a low seeding density was a definitive property (264). To date, this remains one of the only accepted methods to identify MSCs. The method is relatively simple, cells are seeded at low densities, cultured in cell-culture medium and typically, adherent colonies are counted after 14 days. Unfortunately, several variables such as the initial seeding density, the medium used for culture and the colony counting method can make it difficult to compare results between different studies (265).

In this chapter of work, a CFU-F assay was performed after the enrichment and depletion of CD271+ cells from BM-MNC populations and the generation of CFU-Fs compared.

7.2 Materials and Methods

7.2.1 Bone marrow sample processing

Bone marrow aspirate samples from 15 different donors were used to carry out the experiments described in this chapter. All samples were taken intraoperatively following informed consent (REC reference number 06/Q1206/127 from the NRES Committee Yorkshire & the Humber–Leeds East) from patients admitted to Leeds General Infirmary for orthopaedic surgery. Patients did not have any known systemic illness, cancer, or metabolic diseases. Donor age ranged from 27 to 64 years. All bone marrow aspirates were consistently harvested from the same location (zone 6) of the posterior region of the iliac crest as previously described (266).

Samples were received as 4 mL volumes immediately following harvesting and were filtered through a 70 micron filter (Falcon, 352350). A 10x concentrate of red blood cell lysis buffer (BioLegend, 420301) was diluted to 1x with distilled water and warmed to RT. A 1 mL aliquot of bone marrow aspirate was added to 19 mL of lysis buffer, vortexed and incubated for 10 min at RT. Samples were centrifuged at 350 g for 5 min and the BM-MNCs re-suspended in 2 mL Alpha MEM culture medium (Lonza, BE12-169F). The centrifugation was repeated once more and the cells re-suspended in freezing medium (10% DMSO, 30% FBS, 60% Alpha MEM). BM-MNCs were frozen in 1 mL aliquots in specialised freezing containers (Sigma, C1562) which provided a cooling rate of 1 °C/min in a -80 °C freezer. After 24 h, the vials were transferred to a -180 °C cryotank.

7.2.2 Enrichment of CD271+ cells using MACS and FACS

BM-MNC populations were enriched for CD271+ cells using existing cell sorting methods – MACS and FACS. This was carried out in order to gain information with regards to the typical percentage and number of CD271+ cells in clinically-relevant populations.

Cryopreserved BM-MNCs, prepared as described in Section 7.2.1, were thawed at 37 °C and added dropwise to thawing medium[13] (4 mL per 1 mL vial thawed). Cells were washed by centrifugation for 10 min at 300 g and re-suspended in 10 mL thawing medium for 15 min for Deoxyribonuclease I (DNase I) treatment. Cells were then counted using a haemocytometer and a fraction of unseparated cells set aside on ice for FACS analysis.

The remaining cell suspension was centrifuged for 10 min at 300 g and re-suspended in 60 µL of MACS buffer[14] (with 0.1 mg/mL DNase I (Sigma, 11284932001)) per 10^7 cells. FcR blocking agent and CD271 microbeads (Miltenyi Biotec, 130-099-023) were added (40 µL per 10^7 cells) and incubated for 15 min at 4 °C (and mixed every 5 min). Cells were washed by adding 1-2 mL of MACS buffer (per 10^7 cells) and centrifuged for 5 min at 350 g. Cells were re-suspended in MACS buffer (500 µL for up to 10^8 cells) and passed through a cell strainer (Corning, 352350, 70 micron).

A LS column (Miltenyi Biotec, 130-042-401) was placed in the magnetic field of a MACS separator and prepared by rinsing with MACS buffer (3 mL). The cell suspension was applied to the column and the flow through collected (CD271-depleted population). The column was washed with MACS buffer (3x 3 mL) and the flow-through added to the CD271-depleted population of cells. The column was removed from the magnetic field and 5 mL MACS buffer added. The plunger supplied with the column was used to flush out CD271-enriched cells.

CD271-depleted and enriched populations were centrifuged (10 min, 350 g) and re-suspended in a smaller volume of MACS buffer for counting. Cells were aliquoted into Falcon™ round-bottom polypropylene tubes (FACS tubes, Corning, 352063; 1 million cells per tube for CD271-depleted and unseparated populations, all cells for CD271-enriched population) and labelled with antibodies according to Table 7.1. Human fibroblasts (known not to express the CD271 antigen – see Chapter 6: Figure 6.10) were added to the CD271-enriched cells to provide a final population of 1 million cells. This was to minimise the loss of CD271-enriched cells during processing, for example in centrifugation steps. Due to the much higher forward and side scatter of fibroblast cells, they were easily eliminated from all analyses. UltraComp eBeads™ Compensation Beads

---

[13] Thawing medium: MEM - Alpha Eagle with Earle's BSS (Lonza, BE12-169F) supplemented with 0.1 mg/mL Deoxyribonuclease I (DNase I, Sigma, 11284932001), 10% FBS (Sigma Aldrich, F7524), 1% L-Glutamine (200 mM, Sigma, G7513) and 1% P/S solution (Sigma, P4458)

[14] MACS buffer: PBS (Lonza, 17-516F), 2 mM EDTA (Sigma, E7889), 0.5% BSA (Sigma, A9647), filter sterilised

(Invitrogen, 01-2222-41) were used to compensate for fluorescence spectral overlap and the compensation matrix applied to all samples.

Antibody-labelled samples were incubated in the dark at 4 °C for 15 min. Cells were washed by addition of ice cold FACS buffer[15] (2 mL per tube) and centrifuged (5 min, 300 g). The supernatant was aspirated using Pasteur pipettes and the cells re-suspended in 350 µL for analysis. Propidium iodide (PI) or 7-AAD staining was carried out 5 min prior to analysis with no washing steps required. A Cytoflex S flow cytometer was used to record events or a BD Influx™ cell sorter for sterile FACS. Flow cytometry data was analysed using CytExpert software and gated for single cells (see Chapter 4: Section 4.5).

For sterile FACS, sorted cells were collected into 1.5 mL Eppendorf tubes with 0.5 mL Alpha MEM culture medium (Lonza, BE12-169F) supplemented with 20% FBS (Sigma Aldrich, F7524), 1% L-glutamine (200 mM, Sigma, G7513) and 1% P/S solution (Sigma, P4458). Sorted cells were seeded in 24-well plates for CFU-F analysis (Section 7.2.4).

[15] FACS buffer: FACS buffer: PBS (Lonza, 17-516F, 0.5% BSA (Sigma, A9647), 0.05% sodium azide, filter sterilised (0.22 µm)

Table 7.1 Antibody labelling for FACS

	Anti-CD271 antibody Monoclonal CD271-PE, human (Miltenyi Biotec, 130-113-983)	**Anti-CD45 antibody** Monoclonal CD45-FITC, human (Miltenyi Biotec, 130-110-679)	**Dead cell staining** **PI/7AAD** (BioLegend, 421301)/(Miltenyi Biotec, 130-111-568)	**Cells or beads**
Unseparated cells	N/A	N/A	N/A	Cells
Unseparated cells	N/A	N/A	14 µg/mL/0.525 µg/mL	Cells
Unseparated cells	N/A	7.5 µg/mL	N/A	Beads
Unseparated cells	0.5 µg/mL	N/A	N/A	Beads
Unseparated cells	**Isotype control** Monoclonal, mouse IgG1-PE (BD Biosciences, 555749) 0.5 µg/mL	**Isotype control** Monoclonal, mouse IgG2a-FITC (Miltenyi Biotec, 130-113-833) 7.5 µg/mL	14 µg/mL/0.525 µg/mL	Cells
Unseparated cells	0.5 µg/mL	7.5 µg/mL	14 µg/mL/0.525 µg/mL	Cells
CD271-depleted cells	0.5 µg/mL	7.5 µg/mL	14 µg/mL/0.525 µg/mL	Cells
CD271-enriched cells	0.5 µg/mL	7.5 µg/mL	14 µg/mL/0.525 µg/mL	Cells

7.2.3 Investigating the viability of cells in cryopreserved and fresh bone marrow aspirate samples

To study the effects of the cryopreservation and thawing process, a population of BM-MNCs was analysed without cryopreservation. The bone marrow aspirate sample was processed as described in Section 7.2.1, but after the cells were washed in Alpha MEM culture medium, the cells were re-suspended in FACS buffer and aliquoted into FACS tubes. Cells were labelled according to Table 7.1 (“unseparated cells”) using the same procedure as described in Section 7.2.2. Data was recorded using a Cytoflex S flow cytometer and analysed using CytExpert software (see Chapter 4: Section 4.5).

7.2.4 Investigating the clonogenic potential of enriched CD271+ cells

The cell populations sorted by MACS and FACS were seeded in well plates and cultured for 14 days. The original BM-MNC population (unseparated cells) and the CD271-depleted population were both seeded at 50,000 cells/cm^2 in a 6-well culture plate (Corning, 3516). The CD271-enriched population from MACS was further sorted by FACS into a population characterised by high CD271 expression and low CD45 expression (CD271bright/CD45low population). This population was seeded in a 24-well cell culture plate (Corning, 3526) at 200 - 1600 cells/cm^2 depending on the number of cells collected from FACS and the number of replicates carried out. Results were normalised to the cell seeding density. All populations were cultured in Alpha MEM culture medium supplemented with 20% FBS, 1% P/S and 1% L-glutamine (0.5 mL per well for 24-well plate cultures, 2 mL per well for 6-well plate cultures). Medium was changed on day seven and the colonies stained on day 14.

For colony staining, the medium was removed and the cultures were washed twice with PBS. The PBS was then removed and cultures were fixed with methanol for 5 min at RT. The methanol was removed and the culture plates air-dried in a sterile tissue culture hood. Giemsa staining solution (Sigma, GS500) was prepared by diluting 1: 20 in deionised water and added to each well for 30-45 min at RT. The stain was removed and the culture plates washed twice with deionised water. The culture plates were air-dried and colonies with more than 20 cells counted microscopically.

7.2.5 Estimating the number of CD271 molecules (antigens) on cell membranes of CD271+ cells

The number of CD271 antigens expressed on the cell membranes of different CD271+ populations was investigated using BD Quantibrite™ Beads (BD Biosciences, 340495). This experiment was carried out so that avidity effects could be taken into account when comparing the capture and release behaviour of the SH-SY5Y cell line compared to clinically-relevant populations.

SH-SY5Y cells were cultured and harvested as described in Chapter 4: Section 4.1.2. Cells were counted using a haemocytometer and 2.5 x 10^5 cells aliquoted per FACS tube. Cells in one tube were unlabelled, cells in a second tube were incubated with CD271-PE (Miltenyi Biotec, 130-113-421, 0.5 µg/mL) and cells in a third tube were incubated with an isotype-matched control antibody (IgG1-PE, BD Biosciences, 555749, 0.5 µg/mL). Cells were incubated in the dark for 10 min at 4 °C. Cells were washed by adding 2 mL FACS buffer and centrifuged (10 min, 300 g). The supernatant was aspirated and the cells re-suspended in 350 µL FACS buffer for analysis.

The BD Quantibrite™ Beads were re-suspended in 0.5 mL FACS buffer and vortexed. Beads and cell events were recorded using a Cytoflex S flow cytometer and analysed using CytExpert software. The beads were gated according to their forward and side scatter and 10,000 events collected. The singlet bead population was analysed using a histogram plot of PE fluorescence in linear values. The beads consisted of four levels of PE conjugation; low beads, med-low beads, med-high beads and high beads, producing four peaks in the histogram. Four gates were established around the four peaks (Figure 7.1, left panel) and the mean PE fluorescence value from each gate recorded. A linear regression was plotted of the Log_{10} value of the mean PE fluorescence and the Log_{10} value of the known amount of PE molecules per bead in each of the four categories (Figure 7.1, right panel). The mean PE fluorescence was then recorded for the SH-SY5Y cells and the number of PE molecules per cell calculated from the linear regression analysis. This method assumes there is a 1: 1 ratio of PE molecules to monoclonal antibody.

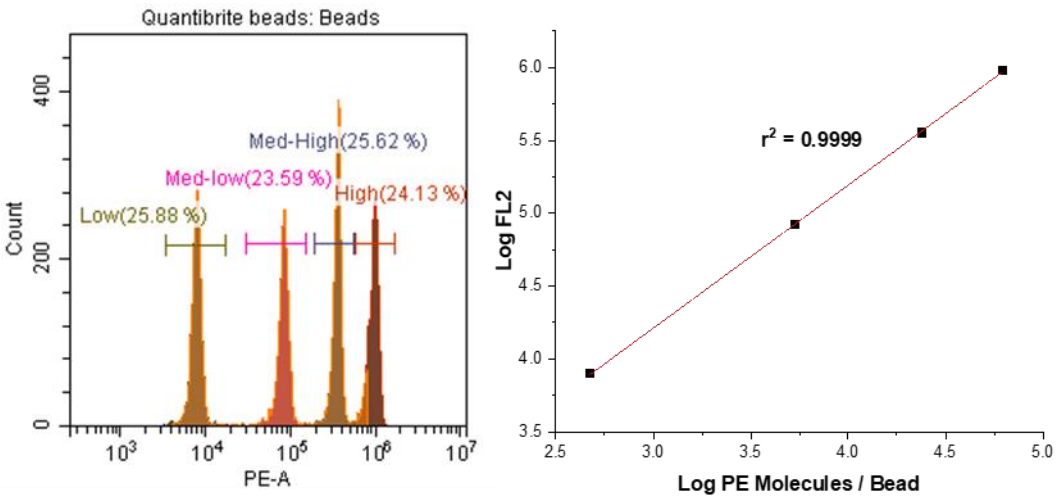

Figure 7.1 Flow cytometry analysis of BD Quantibrite™ Beads

The Quantibrite beads contained beads with four different levels of PE conjugation. A flow cytometry gate was drawn around the peak of each set of beads and the mean PE fluorescence value recorded (left panel). The Log_{10} value of the mean PE fluorescence was plotted against the Log_{10} value of PE molecules per bead (information supplied with the beads)(right panel). The linear regression was used to calculate the number of PE molecules per bead for different CD271+ populations (Section 7.3.5).

The same settings were applied to analyse a population of CD271bright/CD45low cells. The number of PE molecules per cell was also calculated for SH-SY5Y cells labelled with an isotype-matched control antibody and this number subtracted from antibody-labelled populations.

7.2.6 Investigating the enrichment of CD271+ cells from clinical bone marrow aspirate using the prototype microfluidic device

Using the current design of the prototype microfluidic device, BM-MNC populations required pre-enrichment before analysis. This was because the current processing capabilities of the device are limited and further device development is required before whole BM-MNC populations can be enriched.

The device was prepared as described in Chapter 6: Section 6.2.5. BM-MNC populations were pre-enriched using MACS as described in Section 7.2.2 but with a longer incubation with DNase I (60 min) prior to any centrifugation steps. The longer incubation before any centrifugation steps eliminated cell clumping observed previously. CD271-enriched and CD271-depleted cell populations were counted and stained with calcein AM (Biotium, 30002) to allow easier identification above the channel background. A staining solution of 2 µM calcein AM was prepared in MACS buffer. Cells were washed by centrifugation (10 min,

300 g) and re-suspended in the staining solution for 30 min at RT. The cells were washed by centrifugation (10 min, 300 g) and CD271-enriched cells re-suspended in 200 µL (the minimum loading volume of a 1 mL syringe used for cell suspension injection into the device). A fraction of the CD271-depleted population was diluted and prepared in the same volume for an equivalent comparison.

Cell suspensions were injected into the device using the same protocol as described in Chapter 6: Section 6.2.6.1. Briefly, the cell suspension was injected at 100 µL/min and incubated for 2 - 5 min. Unbound cells were washed away at 20 µL/min and the number of cells captured from each population compared. Photos were taken using a Hamamatsu ORCA-ER-1394 camera and analysed using ImageJ. For fluorescent images, the brightness and contrast were set at constant values for every image.

7.3 Results and Discussion

7.3.1 MACS and FACS analysis of clinical samples of bone marrow aspirate

Established cell enrichment technologies - MACS and FACS - were used to investigate the percentage of CD271+ cells typically present in clinical bone marrow aspirates in these initial experiments.

A commercially-available CD271 microbead kit (Miltenyi Biotec) was used to enrich CD271+ cells and the enriched population analysed using a flow cytometer (Section 7.2.2). An unseparated population was also analysed for comparison alongside the population of cells eluted from the MACS column (CD271-depleted population). All populations were labelled with a CD271-PE antibody (Miltenyi Biotec) - compatible with the CD271 microbead kit - and a CD45-FITC antibody (Miltenyi Biotec). A CD45 antibody was used in combination with a CD271 antibody in order to recognise a population of CD271bright/CD45low cells which have been well characterised in the literature (Chapter 2: Section 2.6.2.2). UltraComp eBeads™ Compensation Beads (Invitrogen) were used to compensate for fluorescence spectral overlap and the compensation matrix applied to all samples. Unlabelled samples and samples labelled with isotype-matched control antibodies were analysed alongside test samples for gating purposes (see Chapter 4: Section 4.5 for an example of flow cytometry gating of single cells).

The CD271 microbead kit bound 0.38 ± 0.08% of BM-MNCs with a total cell recovery of 46 ± 8% from the MACS column (mean ± SEM, n=3). When analysed by flow cytometry, it was found that an average of 4.7 ± 1.6% of the CD271-enriched population was the desired CD271bright/CD45low cell phenotype (mean ± SEM, n=3), enriched on average 125-fold from the unseparated population (range 84-fold to 193-fold, n=3). It was also found that the CD271bright/CD45low population was entirely depleted from the CD271-depleted population in all experiments. Representative flow cytometry plots from one experiment are shown in Figure 7.2.

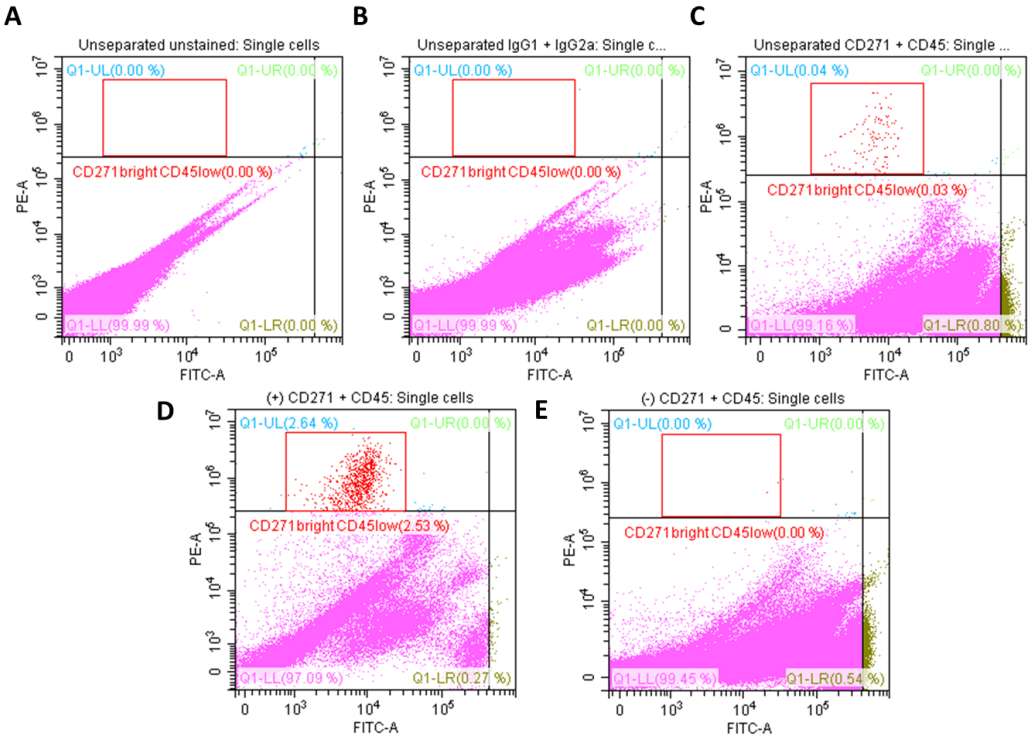

Figure 7.2 Flow cytometry dot plots showing MACS separated BM-MNC populations

Dot plots A-C show unseparated BM-MNC populations either unlabelled (A), labelled with isotype-matched controls (B), or labelled with CD271-PE and CD45-FITC antibodies (C). Dot plot D shows the MACS BM-MNC CD271-enriched population and dot plot E shows the MACS BM-MNC CD271-depleted population labelled with the same CD271-PE and CD45-FITC antibodies. A red box gate has been drawn around the CD271bright/CD45low population according to the unlabelled and isotype control samples. In the unseparated population, 0.03% of total single cells are in the box, in the CD271-enriched population, 2.53% of total single cells are in the box and in the CD271-depleted population, 0.00% of total single cells are in the box (as with the unlabelled and isotype-matched controls). 500,000 events were collected for unseparated and CD271-depleted populations, 200,000 events were collected for CD271-enriched populations.

When considering the actual number of CD271bright/CD45low cells rather than the percentage of the total single cell population, the average number of CD271bright/CD45low cells in an unseparated BM-MNC sample was 50 ± 15 cells recorded from 200,000 total events, and 2500 ± 1500 cells in the MACS BM-MNC CD271-enriched populations (mean ± SEM, n=3 (three separate experiments using BM-MNCs pooled from multiple donors). This is an average enrichment of 50-fold. Both the percentage and number of cells must be considered since the number of therapeutic cells is ultimately important for a cell therapy however the percentage demonstrates the purity of the population. The

large variation in the number of CD271bright/CD45low cells between experiments is expected since bone marrow aspirate samples were collected from different donors and factors such as the total aspiration volume were not controlled. It has been shown that the number of CD271bright/CD45low cells decreases 7-fold in a second draw of bone marrow aspirate compared to the first (aspirated from the same location)(180). The percentages and number of CD271bright/CD45low cells are summarised in Table 7.2.

Table 7.2 Summary of results from the initial characterisation of BM-MNCs using MACS enrichment and subsequent flow cytometry analysis

Data shown represents the mean ± SEM (n=3).

	Unseparated population	**CD271-enriched population**	**CD271-depleted population**	**Average enrichment factor**
Percentage of CD271bright/CD45low cells (%)	0.04 ± 0.02	4.7 ± 1.6	0.0 ± 0.0	118-fold
Number of CD271bright/CD45low cells (per 200,000 events)	50 ± 15	2500 ± 1500	1 ± 1	50-fold

The percentage of CD271bright/CD45low events reported by Cuthbert *et al.* (2012)(180) was in the range 0.001 – 0.100% with a median value of 0.026%. This is in good agreement with the percentage of CD271bright/CD45low events recorded in this work (0.04 ± 0.02%, range 0.02 – 0.08%). Furthermore, Jones *et al.* (2006)(184) used CD271-based positive selection and reported 0.3 ± 0.1% of cells were in the enriched fraction with 5.2 ± 1.5% MSC purity assessed by flow cytometry. Again, these results are comparable to the results found in this work where 0.38 ± 0.08% of cells were in the enriched fraction with 4.7 ± 1.6% MSC purity. Interestingly, Jones *et al.* experienced much improved recovery rates compared with those achieved in this work (77 ± 17% compared to 46 ± 8%) which could be caused by differences in the experimental procedure such as incubation times, centrifugation parameters and cell counting methods.

7.3.2 Investigating the impact of cryopreservation on the percentage and number of CD271bright/CD45low cells in clinical samples of bone marrow aspirate

The flow cytometry results described above confirmed that the CD271 microbead kit successfully enriched CD271+ cells from BM-MNCs, however, it was also found that the percentage of viable cells was less than 21% when analysed by flow cytometry (Figure 7.3, upper right panel). It was hypothesised that the reason for this was because the cells were thawed immediately prior to analysis with no *in vitro* culture. To test this hypothesis, a fresh sample of bone marrow aspirate was analysed without cryopreservation.

It was found that when the BM-MNCs were not cryopreserved, the viability increased to 74% according to PI viability staining (Figure 7.3, lower right panel). However the increase in viability was due to the shift of one population in particular (marked by a red box in Figure 7.3) which appeared to become apoptotic after cryopreservation and thawing. Fortunately the desired CD271bright/CD45low population are small cells that reside in the population marked by an orange box in Figure 7.3, therefore the viability of CD271bright/CD45low cells should be largely unaffected by the cryopreservation process. Previous research supports this data, demonstrating that the surface to volume ratio of a cell has an impact on its viability after cryopreservation (267). This is because larger cells have a smaller transfer surface for heat and mass transfer, and cryopreservation with high viability depends on the ability of water to flow out of the cell faster than the thermal flow. If the thermal flow is equal to the water flow, the freezing rate will induce intracellular water crystallisation during the osmotic exit of water leading to cell death.

In further support of this, the percentage of CD271bright/CD45low cells in the fresh sample was analysed and it was found that 0.05% of cells were the desired CD271bright/CD45low cells (Figure 7.4), which is within the SEM recorded from the thawed samples (0.04 ± 0.02%, mean ± SEM, n=3, Section 7.3.1). In contrast, the total number of desired cells was greater in the fresh sample compared to the thawed samples since there was an overall greater number of single cells in the fresh sample (500,000 total events collected, then gated for single cells (see Chapter 4: Section 4.5)). In the fresh sample there were 84 CD271bright/CD45low cells recorded from 200,000 events compared to an average of 50 ± 15 from three thawed samples. This data is summarised in Table 7.3.

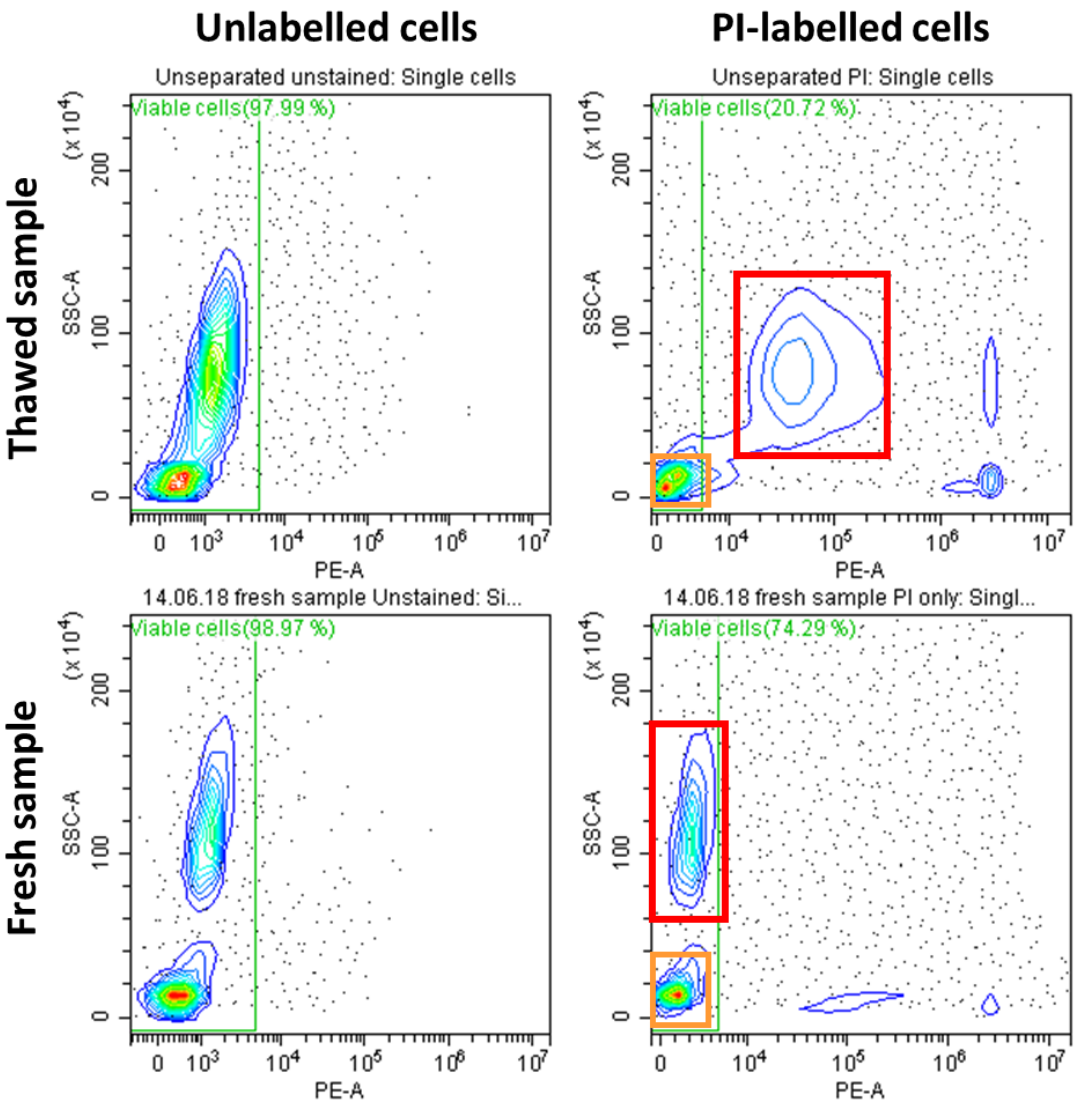

Figure 7.3 Flow cytometry analysis of the viability of BM-MNCs in fresh and thawed samples

Flow cytometry was used to assess the percentage of viable cells in samples of BM-MNCs when samples had been thawed or were analysed fresh. A gate was set according to an unlabelled sample (left-hand side) and compared to a sample labelled with propidium iodide (PI) viability stain (right-hand side). It was found that the percentage of viable cells was less than 21% when samples had been cryopreserved and then thawed, compared to 74% when samples were analysed fresh. 500,000 events were collected for the thawed sample and 100,000 events were collected for the fresh sample. The red box indicates a population of cells that became apoptotic after cryopreservation whereas cells in the orange box appeared to be unaffected by cryopreservation.

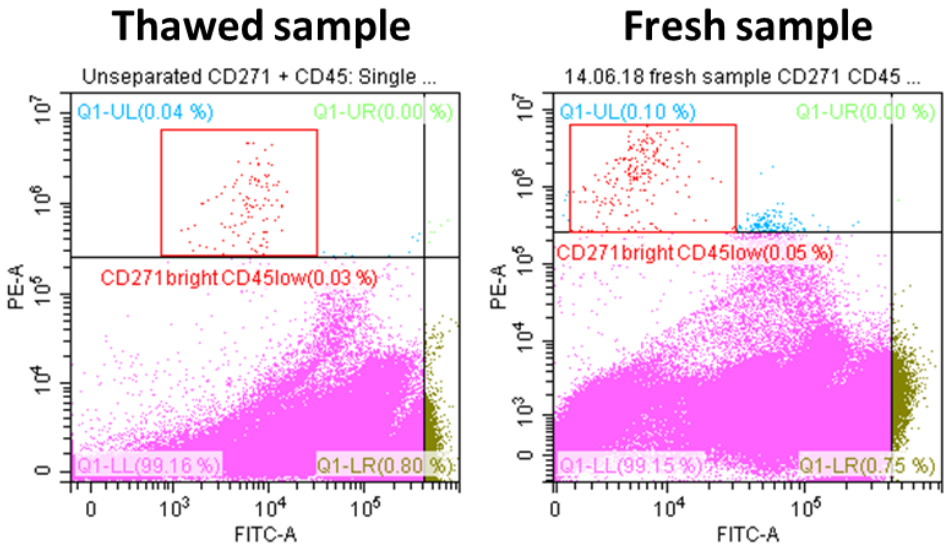

Figure 7.4 The percentage and number of CD271bright/CD45low cells in a thawed sample compared to a fresh sample of BM-MNCs

The percentage and number of CD271bright/CD45low cells in a thawed sample was compared to the percentage and number in a fresh sample. Samples were labelled with CD271-PE antibody and CD45-FITC antibody and 500,000 total events were collected. There were 0.03% cells in the CD271bright/CD45low gate in the thawed sample shown here and 0.05% in the fresh sample. As well as this, due to the higher percentage of single cells in the fresh sample the actual number of CD271bright/CD45low cells was greater. The fresh sample was analysed using the same template and therefore the same CD271bright/CD45low gate as for the data shown in Figure 7.2.

Table 7.3 Summary of results from fresh and thawed samples of BM-MNCs

Data shown represents the mean ± SEM for thawed samples (n=3). Only one replicate was carried out with a fresh sample due to limited sample availability.

	Thawed samples	Fresh sample
Percentage of CD271bright/CD45low cells (%)	0.04 ± 0.02	0.05
Number of CD271bright/CD45low cells (per 200,000 events)	50 ± 15	84

In order to draw accurate conclusions from this data, further analysis of fresh samples would be necessary to see if there was a significant difference between

the percentage and number of CD271bright/CD45 low cells in thawed and fresh samples from a range of different donors or using donor-matched samples. However due to limited sample availability, further repeats with fresh samples were not carried out and the information gathered from this experiment is taken as an indication only.

Despite this, there is evidence in the literature that supports this preliminary data to suggest that cryopreservation does in fact decrease the viability of BMNCs but does not affect their function. Yang et al. (2016)(268) observed an overall significant decrease in the viability of the BM-MNC population after cryopreservation but no significant difference in the progenitor subpopulations before and after cryopreservation. Moreover the beneficial effect of fresh and frozen BM-MNCs was comparable in an ischemic stroke model. This study and further studies (269, 270) verify that cryopreserved BM-MNCs maintain their bioactivity *in vitro* and *in vivo* and support the data shown here which suggests that the functional population are somewhat resistant to cryopreservation – possibly due to the small size of the cells.

Although this information is important for the design of further experiments, in the desired application cells would be processed within the same surgery and therefore not cryopreserved. The fact that there may be a greater number of CD271bright/CD45low cells in fresh samples is beneficial for the final application and must be considered as this technology is progressed further.

7.3.3 Comparison of the total cell recovery from MACS and FACS and the impact on the number of CD271bright/CD45low cells

In the first instance, the characterisation of BM-MNCs was carried out by pre-enriching CD271+ cells using MACS and then analysing or sorting using flow cytometry/FACS. However, it was noted that the percentage recovery of total cells from the MACS column was low (46 ± 8%) and therefore direct sorting via FACS could lead to a greater total cell recovery and consequently a greater number of CD271bright/CD45low cells collected from one experiment (avoiding the potential loss of cells in the MACS column).

A direct comparison of two experiments processing a similar number of BM-MNCs found that there was no apparent advantage of using FACS directly (Table 7.4). The main reason for this was the fact that cell clumping hindered both methods equally. When cells have been exposed to freeze/thawing, environmental stresses can accelerate the rate of death resulting in the release of ‘sticky’ DNA molecules from dying cells (271). This causes the cells to clump.

To counteract this, endonuclease DNase I was used at a concentration of 0.1 mg/mL in the thawing medium (with a 15 min incubation prior to MACS processing) and in the MACS buffer to minimise cell clumping from free DNA molecules.

Although DNase I treatment reduced cell clumping, the problem was not eradicated entirely and filtering through a 70 micron filter was required immediately prior to FACS. This led to a large loss of cells from the initial cell count and equated to a similar final cell count to the recovered cell population from the MACS column (also filtered through a 70 micron filter before application to the MACS column; numbers highlighted in red in Table 7.4). It is therefore unsurprising that a similar number of CD271bright/CD45 low cells were collected from the two methods. If cell clumping could be eradicated further, it is possible that directly sorting by FACS could lead to a greater number of CD271bright/CD45low cells, however, at this point there was no advantage of sorting cells via FACS directly. For the final experiments described in this Chapter (Sections 7.3.6 and 7.3.8), the DNase I protocol was optimised further to include a longer incubation time before any centrifugation steps which eradicated cell clumping entirely. It would therefore be interesting to repeat this comparison with the optimised protocol, however this was outside the scope of this work.

In contrast, at this time, there were several disadvantages to using FACS directly; to label and sort the entire population of BM-MNCs required 20 times more antibody and took four times longer cell sorting time compared to labelling and sorting a MACS pre-enriched sample. The longer processing times also exacerbated cell clumping issues. It was therefore decided to continue pre-enriching CD271+ cells using MACS prior to cell sorting using FACS.

Table 7.4 MACS and FACS comparison for BM-MNC processing

A comparison of two experiments processing a similar number of BM-MNCs using either MACS and FACS or FACS only.

Process	MACS and FACS	FACS only
Initial cell count	96,900,000	92,400,000 (40,249,993 counted by flow cytometer*)
Calculated cell recovery from MACS	37% (35,853,000)	N/A
Percentage of captured cells (%)	0.40	N/A
Total number of CD271bright CD45low cells collected from FACS	3524	3222
Number of CD271bright CD45low cells collected from FACS (per 10^6 cells)	983	800
Antibody required	8 µL	160 µL
Time required	1 h	4 h

*cells filtered through a 70 micron filter immediately prior to FACS causing large cell loss

7.3.4 The clonogenic potential of CD271-enriched and depleted BM-MNC populations

Once a protocol had been established to enrich CD271+ cells from clinical samples of bone marrow aspirate, the clonogenic potential of the different populations was assessed via a CFU-F assay (Sections 7.1.1 and 7.2.4). The samples were processed in the same way as described in Section 7.2.1 then pre-enriched using CD271 microbeads (Section 7.2.2). The enriched population was sorted using FACS under sterile conditions and the CD271bright/CD45low population collected. The CD271bright/CD45low population, the CD271-depleted population from the MACS column, and an unseparated population of cells were seeded at low densities in well plates and cultured for 14 days. On the 14th day,

colonies were stained with Giemsa stain and counted microscopically (Section 7.2.4).

It was found that in all but one case, there were no colonies present in the CD271-depleted cell populations (n=6, where two separate experiments were carried out, with three technical replicates for each experiment)(Figure 7.5). This was significantly different to an unseparated population of cells which contained a low percentage of CD271+ cells (n=6 (same replicates as above); $p<0.005$, Figure 7.7). In the CD271bright/CD45low population, three out of five replicates were enriched for CFU-F (Figure 7.6) and it was proposed that the two replicates with no colonies could be outliers. This was because in the first and second experiments (wells 1 and 2 in Figure 7.6) all the CD271bright/CD45low cells collected from FACS were seeded in one well and produced several colonies. However in the third experiment, the collected CD271bright/CD45low cells were seeded in triplicate (wells 3, 4 and 5 in Figure 7.6) and colonies were only visible in one well – the well seeded first (well 3). This could suggest that the cells were unevenly distributed between the wells leading to anomalous results.

The outlying results were excluded from statistical analysis and it was found that CFU-F were significantly enriched in the CD271bright/CD45low population compared to the unseparated populations of BM-MNCs ($p<0.05$, n=3). On average, CFU-F were enriched 220-fold in the CD271high/CD45low populations compared to the unseparated populations. Furthermore, from a qualitative perspective, colonies from the CD271bright/CD45low population were typically larger and more dense than those from the unseparated populations (Figure 7.5 and Figure 7.6).

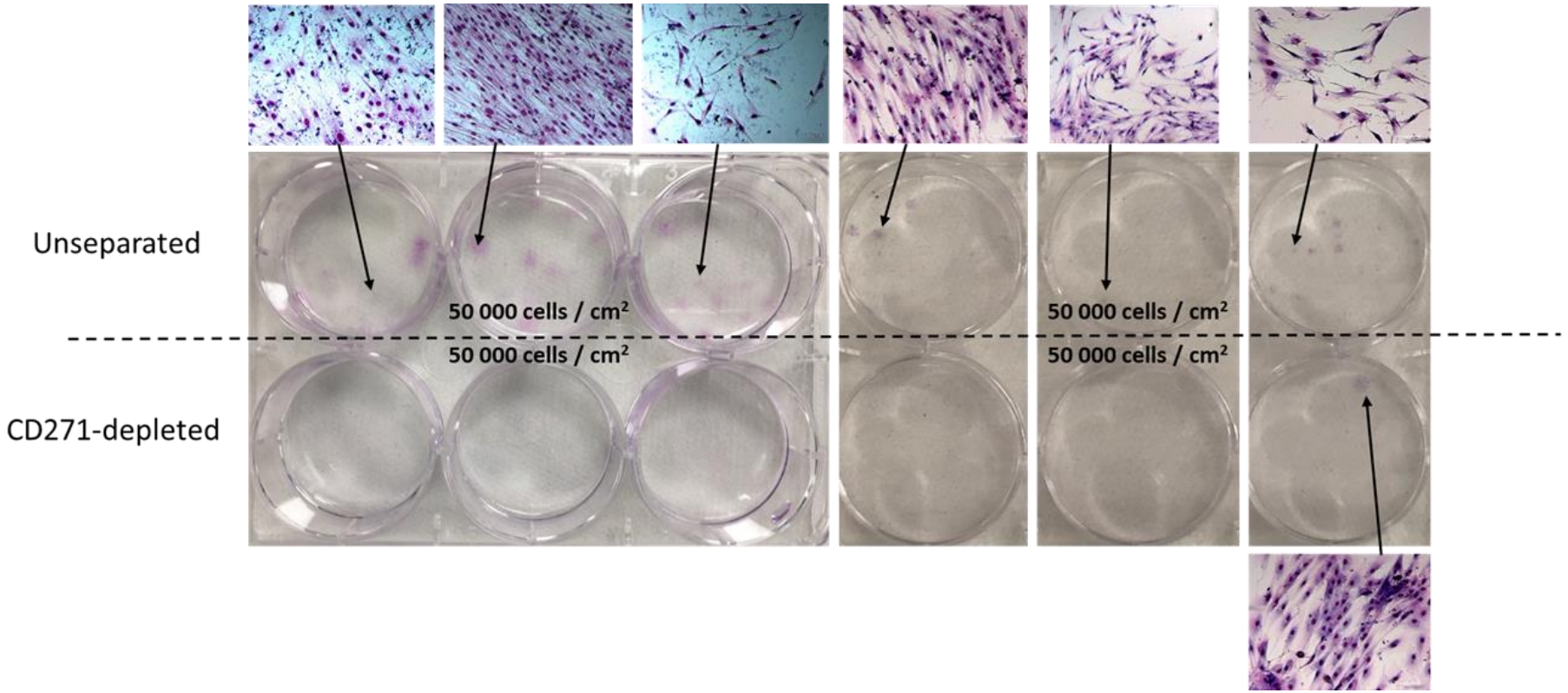

Figure 7.5 Macroscopic and microscopic images of colonies formed by unseparated and CD271-depleted BM-MNC populations after 14 days

A CFU-F assay was carried out to assess the clonogenic potential of the different cell populations sorted by MACS and FACS. The original BM-MNC population (unseparated cells) and CD271-depleted cells from the MACS column were seeded at 50 000 cells/cm^2. After 14 days in culture, colonies were stained with Giemsa stain and counted microscopically. Three technical replicates were carried out for each experiment, with two separate experiments carried out in total. BM-MNC samples from multiple donors were combined for each experiment.

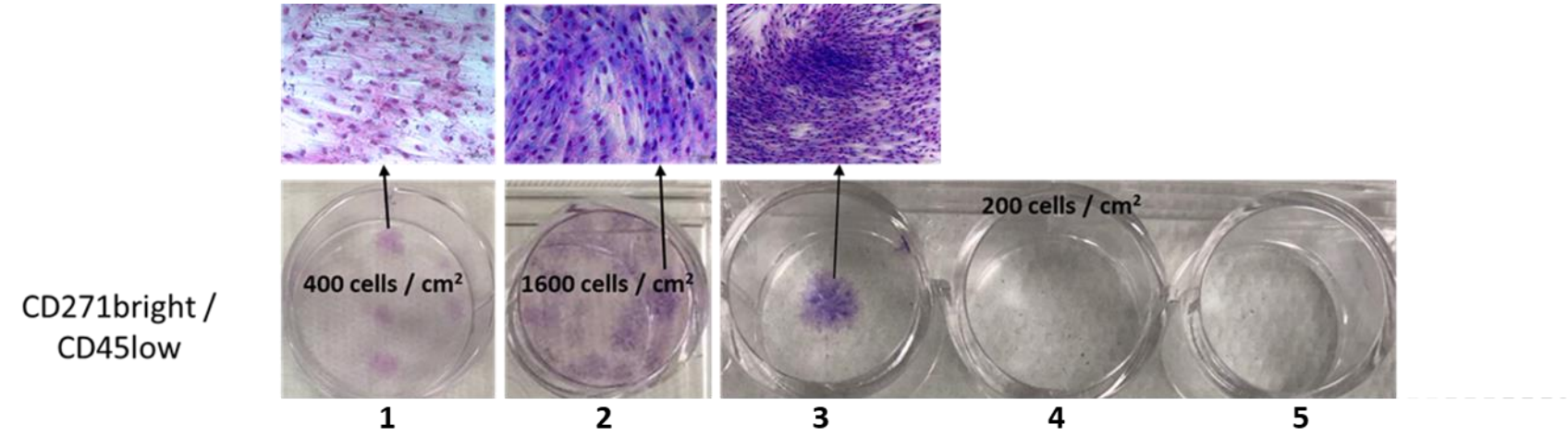

Figure 7.6 Macroscopic and microscopic images of colonies formed by CD271bright/CD45low cells after 14 days

A CFU-F assay was carried out to assess the clonogenic potential of the different cell populations sorted by MACS and FACS. CD271bright/CD45low cells were seeded at 200 - 1600 cells/cm^2. After 14 days in culture, colonies were stained with Giemsa stain and counted microscopically. Between one and three technical replicates were carried out for each experiment, with three separate experiments carried out in total. BM-MNC samples from multiple donors were combined for each experiment.

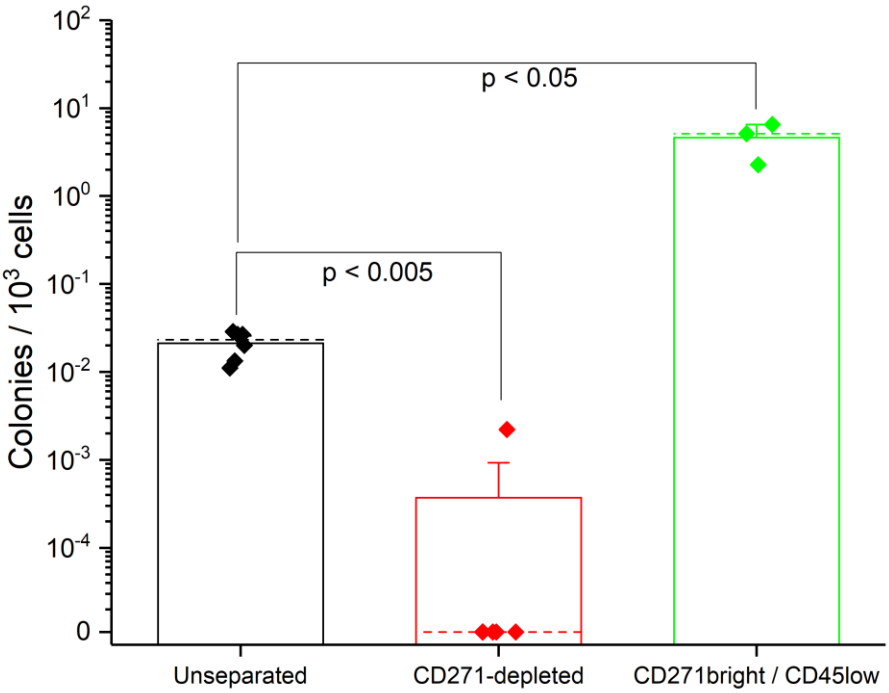

Figure 7.7 The number of colony-forming units in enriched and depleted populations of CD271+ cells

The number of colonies formed by different populations of cells sorted by MACS and FACS were counted microscopically and normalised according to cell seeding density. Significantly less colonies were found in CD271-depleted populations compared to populations of unseparated cells (where CD271+ cells were present at a low percentage)($p<0.005$, $n=6$). Significantly more colonies were found in CD271-enriched populations (CD271bright/CD45low) compared to unseparated populations of cells ($p<0.05$, $n=3$). Statistical analysis was carried out using a Mann Whitney U test since data was not normally distributed according to the Shapiro Wilk test of normality. Bars represent the mean values, dashed lines represent median values and error bars represent the SEM.

This data is supported by Cuthbert *et al.* (2012)(180), who investigated the clonogenic potential of CD271bright/CD45low cells and found that there was a linear relationship between the number of CD271bright/CD45low cells and the number of CFU-F. In their study, bone marrow aspirates were examined using a single-platform, lyse-no-wash protocol with 25 different donor samples, providing a robust analysis of CD271-enriched populations. In addition, Tormin *et al.* (2011)(193) reported that CFU-Fs were exclusively enriched in CD271+ populations when compared to CD45+ and CD271- populations.

In this work, the availability of samples limited the number of replicates carried out, and cells in the CD271bright/CD45low population were seeded at densities as low as 200 cells/cm^2. It was previously discussed that seeding at low densities could have lead to inaccuracies between replicates if samples were not homogenous, which resulted in what were assumed to be outlier results. In the unseparated and CD271-depleted populations, cells were consistently seeded at a higher density of 50,000 cells/cm^2 which could be why these populations demonstrated more reliable results. There was one result in the CD271-depleted population that could be suggested as an outlier, however there was no rationale to exclude this result and it was still found that the number of colonies in CD271-depleted populations was significantly different to the number of colonies in an unseparated population. In addition to the different seeding densities, increased uncertainty arises from the fact that CFU-F counting is subjective and does not take into account the different sizes of colonies. In the paper described above (180), digital measurements of total colony area were used alongside manual counting for a more accurate representation.

7.3.5 Estimating the number of CD271 molecules (antigens) on the cell membranes of CD271+ cells

Once the typical number of CD271+ cells in clinical samples of bone marrow aspirate had been estimated and their clonogenic potential determined, the aim was to investigate the feasibility of enriching these cells using the prototype device. One consideration before doing this was to compare the number of CD271 molecules (antigens) on the cell membranes of SH-SY5Y cells (used in Chapter 6 to optimise cell capture and release in the device) to the number of CD271 molecules (antigens) on the cell membranes of cells in the CD271-enriched populations of BM-MNCs. This was important because the number of antigens on each cell surface could affect how the cells bind and release in the device. For example, a high number of antigens on the cell surface may cause cells to be bound more tightly to the immobilised antibody due to avidity effects.

To estimate the number of CD271 antigens on the different cell surfaces, BD Quantibrite™ Beads (BD Biosciences) were used according to the manufacturer's protocol described in Section 7.2.5.

It was found that cells in the CD271bright/CD45low population of cells had over 75,000 CD271 antigens per cell assuming a 1:1 binding ratio of monoclonal antibody and conjugated PE molecules (Table 7.5). Assuming an average cell diameter of 16 µM (272), this estimates the density of antigens to be 93 molecules per μM^2. The number of CD271 antigens on SH-SY5Y cells was an order of magnitude lower than for the CD271bright/CD45low cells, and assuming an average cell diameter of 12 µM (272), only 8 molecules per μM^2. Although these numbers are only estimates, this data would appear logical since the CD271bright/CD45low cells display a higher fluorescence signal than SH-SY5Y cells. This experiment has helped provide quantitative data in this respect. To further confirm these estimates, additional analysis could be carried out using ELISA or quantitative real-time PCR, however these methods would also be indirect measurements of the number of CD271 molecules.

Since the number of CD271 antigens reported here is an order of magnitude higher for CD271bright/CD45low cells, and 12 times more dense on the cell surface, it must be considered that the binding behaviour of these cells could be different to SH-SY5Y cells in the device and it is possible different release mechanisms may need to be explored.

Table 7.5 The number of PE molecules per cell when labelled with a CD271-PE conjugated monoclonal antibody

The number of PE molecules per cell was estimated using Quantibrite™ Beads and flow cytometry analysis. The CD271bright/CD45low population of cells had comparable numbers of PE molecules to the 'high' beads. The SH-SY5Y cells were comparable to the 'med-low' beads. The number of PE molecules per cell of SH-SY5Y cells labelled with an isotype control antibody has been subtracted from both cell populations.

Population of cells	PE molecules/cell
CD271bright/CD45low	75861
SH-SY5Y	3686
Low beads	474
Med-low beads	5359
Med-high beads	23843
High beads	62336

7.3.6 Investigating the enrichment of CD271+ cells from clinical samples using the prototype device

In order to assess the capture of CD271+ cells in the prototype device, BM-MNCs were first enriched by MACS. This was necessary due to the low numbers of CD271+ cells in whole BM-MNC populations and the current processing capabilities of the device. At this stage, the aim was to carry out proof-of-concept experiments with cells from clinically relevant samples, however the technology would need further development before being capable of processing whole bone marrow samples with no pre-enrichment.

BM-MNCs were pre-enriched for CD271+ cells as described in Section 7.2.2. The CD271-enriched and depleted populations from MACS were both fluorescently labelled with a live cell stain (calcein AM) so that the low number of captured cells could be easily detected above background. The populations were injected into the device using the same protocol as described for previous experiments (Section 7.2.6) and a photo was taken at four different locations in the centre of each branched channel. The number of cells captured at each location for each population was compared.

From this initial trial, no significant difference could be detected between the CD271-enriched and CD271-depleted populations (data not shown). This could

be because one image only captures the activity in approximately 1/60th of the channel and therefore four images still only captures the activity in approximately 7% of the channel. Further to this, the total volume of the channels is 11 µL and the sample loading requires a minimum volume of 200 µL – this means that the population is significantly diluted and only a small proportion of the cells can be captured in one incubation.

It was also noted that more non-specific binding was observed when the CD271-depleted population was used compared to when non-specific fibroblast populations were used previously (Chapter 6: Section 6.3.2). Moreover, the cell concentrations of CD271-enriched and CD271-depleted populations were considerably different as the CD271-enriched population from MACS typically consisted of between 200,000 and 400,000 cells whereas the CD271-depleted population consisted of between 60 million and 80 million cells. In these initial experiments the CD271-depleted population was diluted to a concentration of 20 million cells/mL according to the optimised protocol in Chapter 6: Section 6.3.3.2. However, if non-specific binding is proportional to the number of cells present, having considerably different cell concentrations could obscure results. In further trials, the CD271-depleted population was diluted to a cell concentration comparable to that of the CD271-enriched population (Section 7.3.8).

7.3.7 Optimising a device protocol for the enrichment of CD271+ cells from clinical samples using a cell line model

To develop a protocol which may be able to show a more accurate representation of CD271-enriched and CD271-depleted populations in the device, modelling of CD271-enriched and CD271-depleted populations was carried out using mixtures of SH-SY5Y (CD271+) and fibroblast (CD271-) cells used during the optimisation of cell capture and release (Chapter 6: Section 6.3.4). From previous experiments carried out in Section 7.3.1, it was expected that in a pre-enriched population of BM-MNC CD271+ cells from MACS, there would be between 1000 and 6000 CD271+ cells and approximately 200,000 non-specific cells (see Figure 7.2, panel D for flow cytometry analysis of a pre-enriched population of BM-MNC CD271+ cells). Therefore 1000 – 6000 SH-SY5Y cells were mixed with 200,000 fibroblast cells and compared to CD271-depleted populations of 200,000 fibroblast cells only.

Two trials were carried out using the model populations; the first used repeat injections of the cell suspension to enable analysis of a greater total volume of the sample, and the second approach involved taking images of the entire

channel surface area to gain a more accurate assessment of the number of captured cells. The results from these trials are described in Section 7.3.7.1 and 7.3.7.2.

7.3.7.1 Trial one: model CD271-enriched and CD271-depleted populations with repeat injections

The model CD271-enriched population in trial one had 5000 SH-SY5Y cells and 195,000 fibroblast cells. The model CD271-depleted population had 200,000 fibroblast cells. The model populations were loaded into a 1 mL syringe in 200 µL volumes and injected 10 µL at a time. Each injection was incubated for 2 minutes before unbound cells were washed away at 20 µL/min. The subsequent cell suspension injections were also injected at 20 µL/min to ensure that already captured cells were not released from the channel surface. Photos were taken at four different locations (in the centre of each branched channel, as in Section 7.3.6) after each buffer wash, and the number of cells compared after one injection with images acquired after subsequent injections.

For the model CD271-enriched population, it was found that the cells captured in each image ranged from zero to three cells after one injection (Figure 7.8, top panel). If the cell suspension was truly homogenous, the number of SH-SY5Y cells in one image would be expected to be four or five cells after one incubation (25,000 SH-SY5Y cells/mL, 275 SH-SY5Y cells in 11 µL injection volume, four or five cells in 1/60th of the channel). Since cells at low concentrations are unlikely to be homogenous and due to the inherent error associated with manual cell counting, it would be reasonable to suggest the cells observed were in the expected range.

After seven injections, the number of cells captured in each image ranged from two to four cells. Although there was a slight increase observed after seven injections it was not of the order expected. The largest increase was observed in channel 1 – from zero to four cells. This was because after the first incubation, the cell suspension of the subsequent cell injection was no longer evenly distributed between the four channels. Using the current design of the prototype device, a short incubation period is necessary for cells to interact with the channel surface. In these circumstances, the incubation with no flow causes cells to also sediment in the inlet tubing which affects the distribution of cells when injected into the channels. For these reasons, it was decided that repeat injections were not an efficient way to analyse CD271-enriched populations in the device at this time.

For the model CD271-depleted population, it was found that after seven injections no cells were captured in the four locations of the channel analysed (Figure 7.8, bottom panel). In contrast to the initial trials using BM-MNC CD271-enriched and depleted populations, there was a difference observed between model CD271-enriched and depleted populations with respect to the number of cells captured. This supported the hypothesis that the greater amount of non-specific binding observed originally (described in Section 7.3.6), could have been obscured due to the higher cell concentrations of CD271-depleted populations.

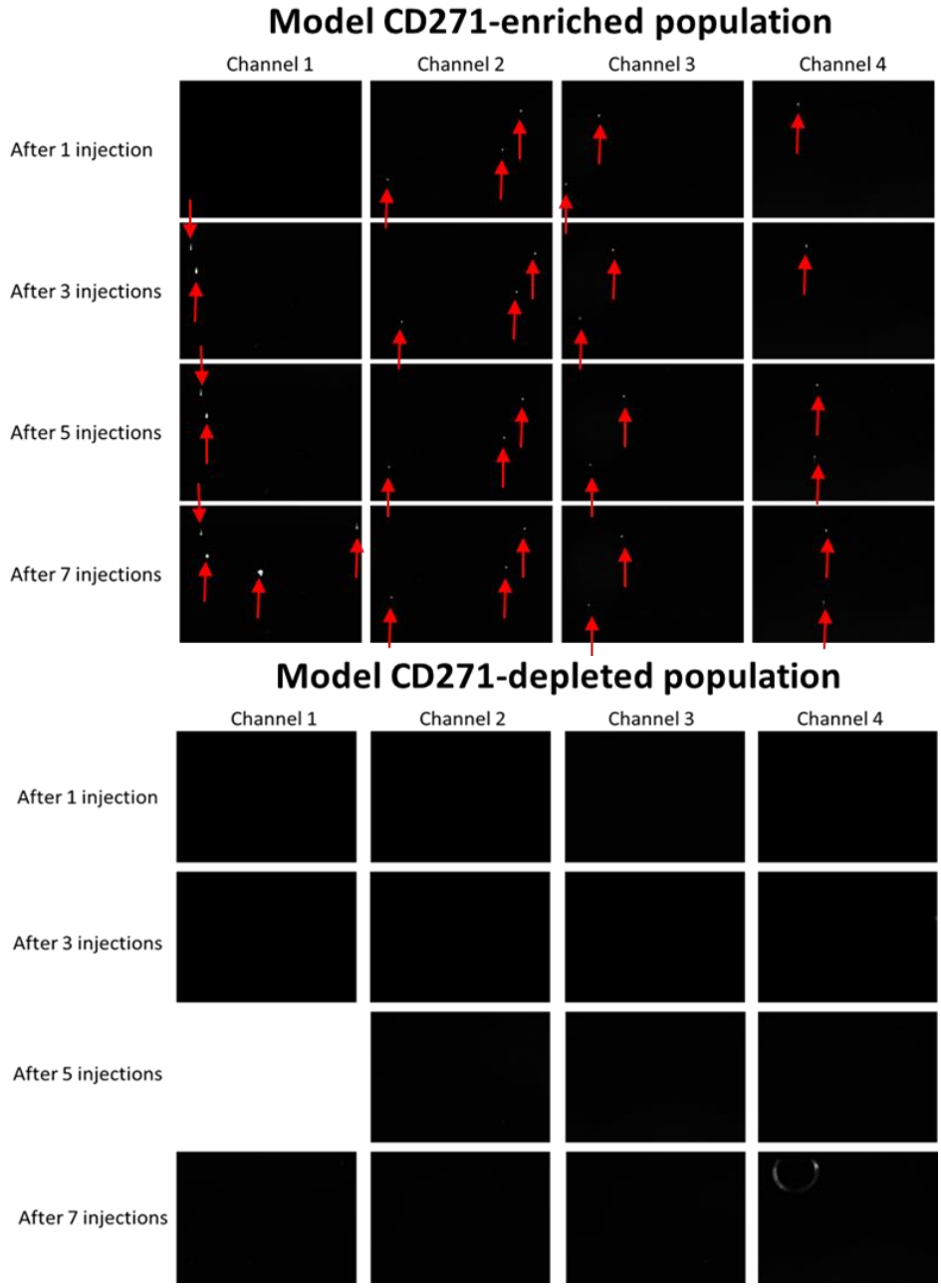

Figure 7.8 Model CD271-enriched and CD271-depleted populations were analysed using repeated injections into the prototype device

Model CD271-enriched and CD271-depleted populations were mixed using SH-SY5Y cells as CD271+ cells and fibroblasts as non-specific cells. The model populations were injected 10 µL at a time for the total available volume of sample. In the CD271-enriched population, several cells were captured and remained bound to the channel surface throughout repeated injections. In channels 1 and 4, the number of cells captured increased with the number of injections however this was not observed in channels 2 and 3. No cells were observed to be captured in the CD271-depleted population. All cells are indicated by a red arrow and one image is missing due to experimental error.

7.3.7.2 Trial two: model CD271-enriched and CD271-depleted populations with assessment of entire channel surface area

The results from trial one (described above) suggested that repeated injections were not feasible using the current device design due to cell sedimentation. An alternative approach to assess a larger volume of sample was therefore used, which was to take photos of the entire surface area of the channel after one incubation period. This allowed a more accurate assessment of cell numbers given that only 7% of the channel was assessed in previous protocols.

Two model CD271-enriched populations were investigated in trial two; one with 2500 SH-SY5Y cells and 200,000 fibroblast cells, and a second with 4000 SH-SY5Y cells and 200,000 fibroblast cells. These numbers were chosen according to the mean and SEM values recorded from three experiments carried out in Section 7.3.1, and should result in approximately 138 and 220 cells in the channel after one incubation, respectively. The model CD271-depleted population comprised of 200,000 fibroblast cells only. Model populations were fluorescently labelled as previously described for trial one. The populations were injected into the device at 100 µL/min, incubated for 5 min and then unbound cells washed away at 20 µL/min. Once all unbound cells had been washed away, photos were taken of the entire channel surface area.

For the CD271-enriched population with 2500 SH-SY5Y cells, it was found that ten cells were captured after one incubation (Figure 7.9). For the CD271-enriched population with 4000 SH-SY5Y cells it was found that 45 cells were captured after one incubation. This means there was a factor of 4.5 difference between the number of cells captured from the two model CD271-enriched populations where in theory there should have only been a factor of 1.6 difference. In addition, the number of cells bound was 14-fold and 5-fold lower than expected according to the initial cell concentration injected. It was discussed previously that there are inherent issues with manual cell counting and the accuracy of processing low numbers of cells that could lead to unexpected results. Further repeats and a range of different cell concentrations would need to be analysed to gather more reliable quantitative data.

Importantly, as in trial one, there was a difference observed between the model CD271-enriched populations and the model CD271-depleted population. For the CD271-depleted population there were five cells in total captured, however three of the cells were attached to debris present in the channel (indicated by a red dashed box in Figure 7.11). It was therefore decided to use the protocol from trial two to analyse clinical samples of BM-MNC CD271-enriched and depleted populations.

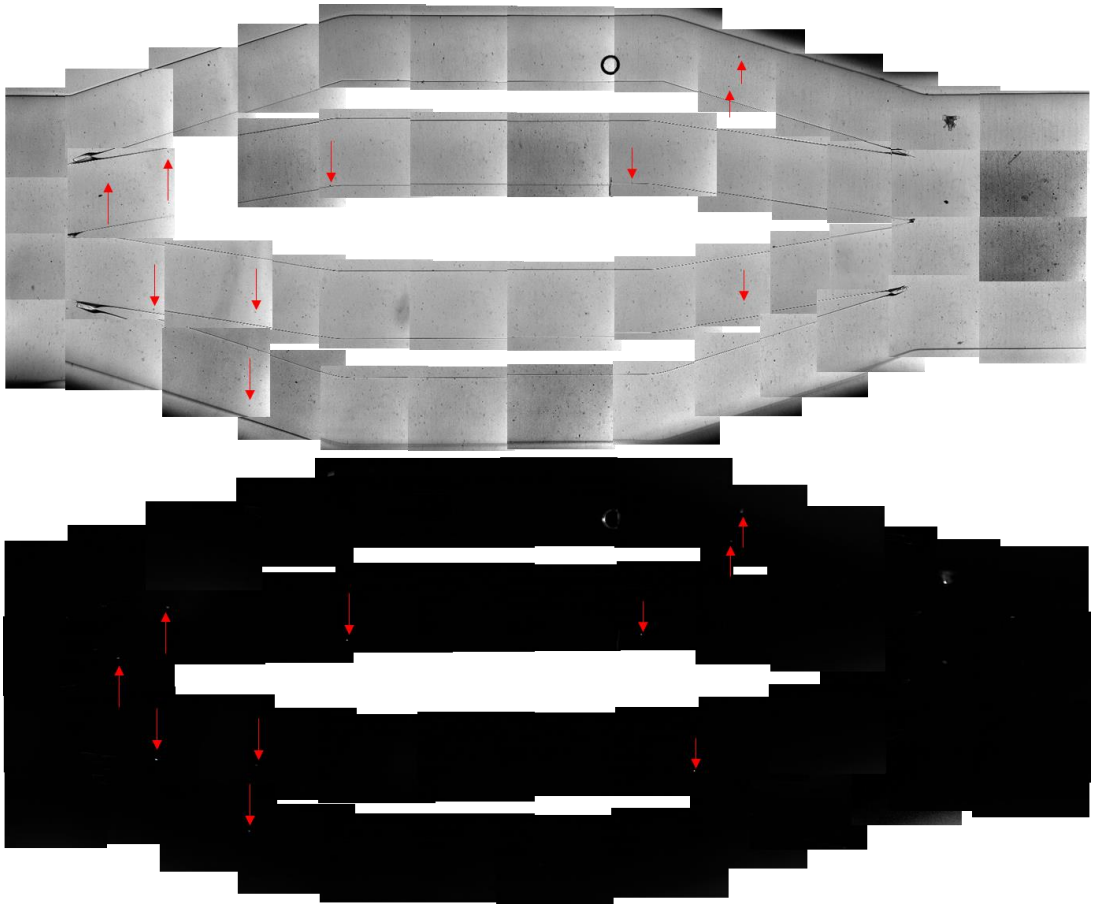

Figure 7.9 Assessment of entire channel surface area after injection of a model CD271-enriched population with 2500 SH-SY5Y cells

A model CD271-enriched population was mixed using 2500 SH-SY5Y cells and 200,000 fibroblast cells. Ten microlitres of cell suspension was injected and incubated for 5 minutes. After the unbound cells were washed away, photos were taken of the entire channel surface area. 10 cells were captured in total, marked by red arrows. The top image shows the channel using bright field microscopy and the bottom image shows the same view using fluorescence microscopy. Cells were stained with a live cell stain (calcein AM) to allow easier identification.

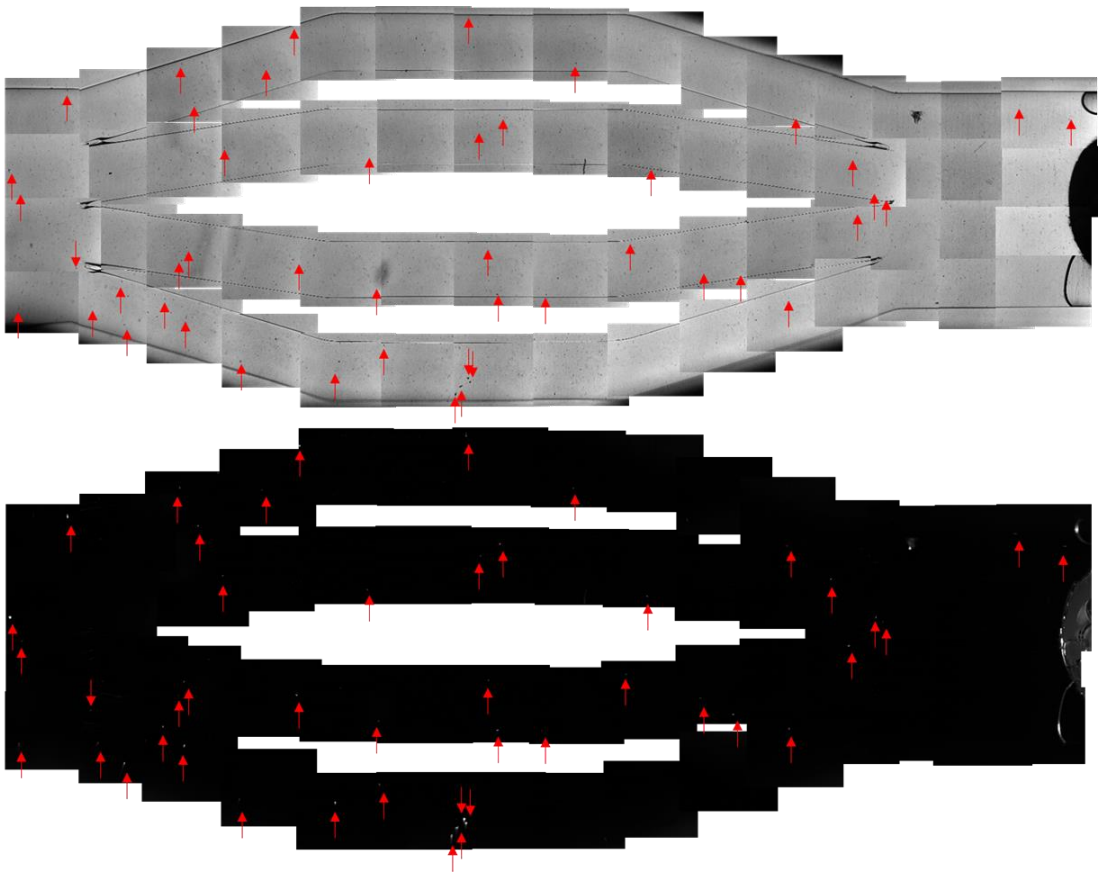

Figure 7.10 Assessment of entire channel surface area after injection of a model CD271-enriched population with 4000 SH-SY5Y cells

A model CD271-enriched population was mixed using 4000 SH-SY5Y cells and 200,000 fibroblast cells. Ten microlitres of cell suspension was injected and incubated for 5 minutes. After the unbound cells were washed away, photos were taken of the entire channel surface area. 45 cells were captured in total, marked by red arrows. The top image shows the channel using bright field microscopy and the bottom image shows the same view using fluorescence microscopy. Cells were stained with a live cell stain (calcein AM) to allow easier identification.

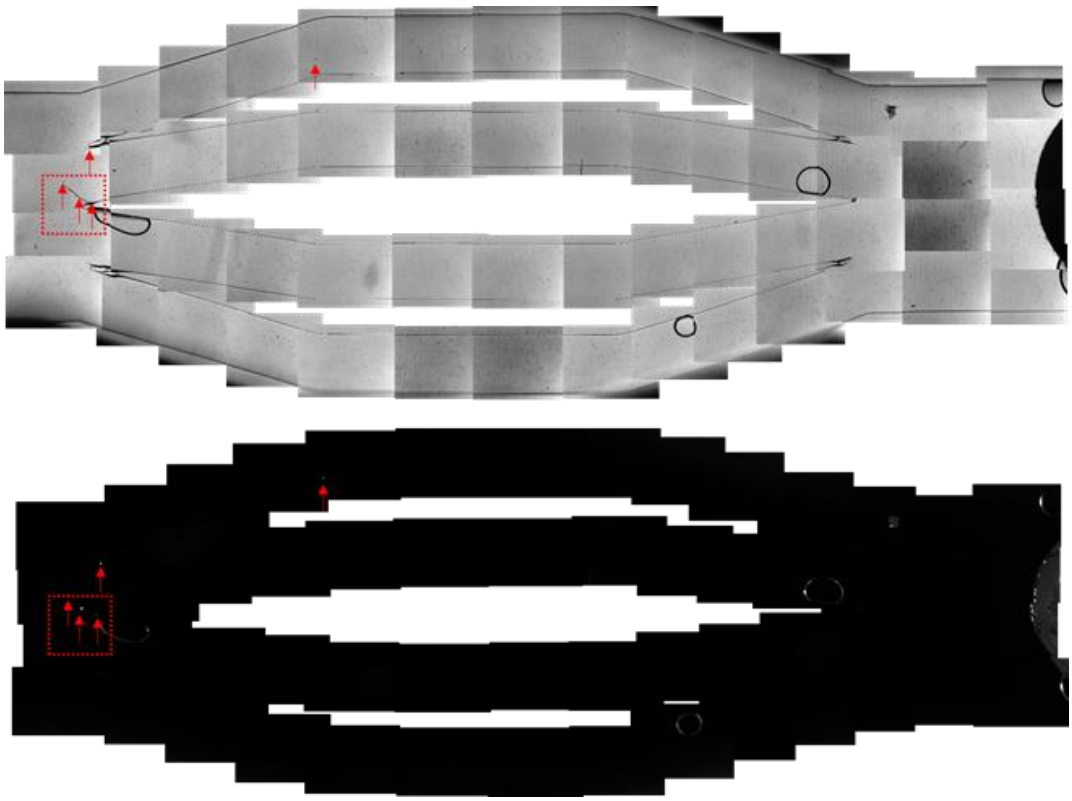

Figure 7.11 Assessment of entire channel surface area after injection of a model CD271-depleted population

The model CD271-depleted population consisted of 200,000 fibroblast cells. Ten microlitres of cell suspension was injected and incubated for 5 minutes. After the unbound cells were washed away, photos were taken of the entire channel surface area. Five cells were captured in total however three cells were attached to debris in the channel – marked by the dashed red box. Captured cells are marked by a red arrow. The top image shows the channel using bright field microscopy and the bottom image shows the same view using fluorescence microscopy. Cells were stained with a live cell stain (calcein AM) to allow easier identification.

7.3.8 Using the optimised device protocol to assess BM-MNC CD271-enriched and CD271-depleted populations

BM-MNCs were processed as described in Section 7.2.6 and the CD271-enriched population obtained using MACS. The CD271-enriched population was centrifuged, counted and re-suspended in a volume of 200 µL for injection into the prototype device. The CD271-depleted population (after MACS separation) was centrifuged, counted and diluted to a concentration of 1 million cells/mL in 200 µL (200,000 cells in 200 µL – comparable to the number of cells in the CD271-enriched population from MACS). A third population was prepared in which 4000 SH-SY5Y cells were spiked into 200,000 cells from the CD271-depleted population. This population represented the model CD271-enriched population used in Section 7.3.7.2 however with a more accurate representation

of non-specific cells. Of course it is important to remember that the model populations may not behave in the same way as the BM-MNC populations due to the differing number of CD271 molecules on the cell surface (Section 7.3.5). However, the model populations provide additional data required since the availability of clinical samples was limited.

It was found that there was a greater number of cells captured in the SH-SY5Y spiked population (Figure 7.12) and the BM-MNC CD271-enriched population (Figure 7.13) than the BM-MNC CD271-depleted population (Figure 7.14). As was previously observed, there was more non-specific binding than when using fibroblast cells however when the cell concentrations were normalised there was still a clear difference between BM-MNC CD271-enriched and depleted populations. The result from trial two (Section 7.3.7.2) and the results from this experiment are summarised and compared in Table 7.6.

The percentage of cells captured in each population was estimated by approximating the total number of cells in the channel during the five minute incubation period, and comparing this to the number of cells captured after the 20 µL/min buffer wash. The total number of cells in the channel during the incubation period was calculated by:

1. Counting the number of cells in four representative images from each repeat (12 images in total)
2. Calculating an average from the 12 images (17 ± 2, mean ± SEM)
3. Multiplying the average by 60 (60 images taken for entire surface area of the channel)

This calculation resulted in an approximation of 1000 ± 90 cells in the channel during the five minute incubation period (mean ± SEM, n=12). The percentage of cells captured after a 20 µL/min buffer wash could then be estimated. From three repeats including two model CD271-enriched populations and one BM-MNC CD271-enriched population, the percentage of cells captured was 5.9 ± 1.0%. When the number of ‘non-specific’ cells captured from the model CD271-depleted and BM-MNC CD271-depleted populations was subtracted from the CD271-enriched populations, the percentage of cells captured was 4.1 ± 0.6%. These numbers are in good agreement with the percentage of CD271bright/CD45low cells identified in three sterile FACS repeats (4.7 ± 1.6%)(Table 7.6).

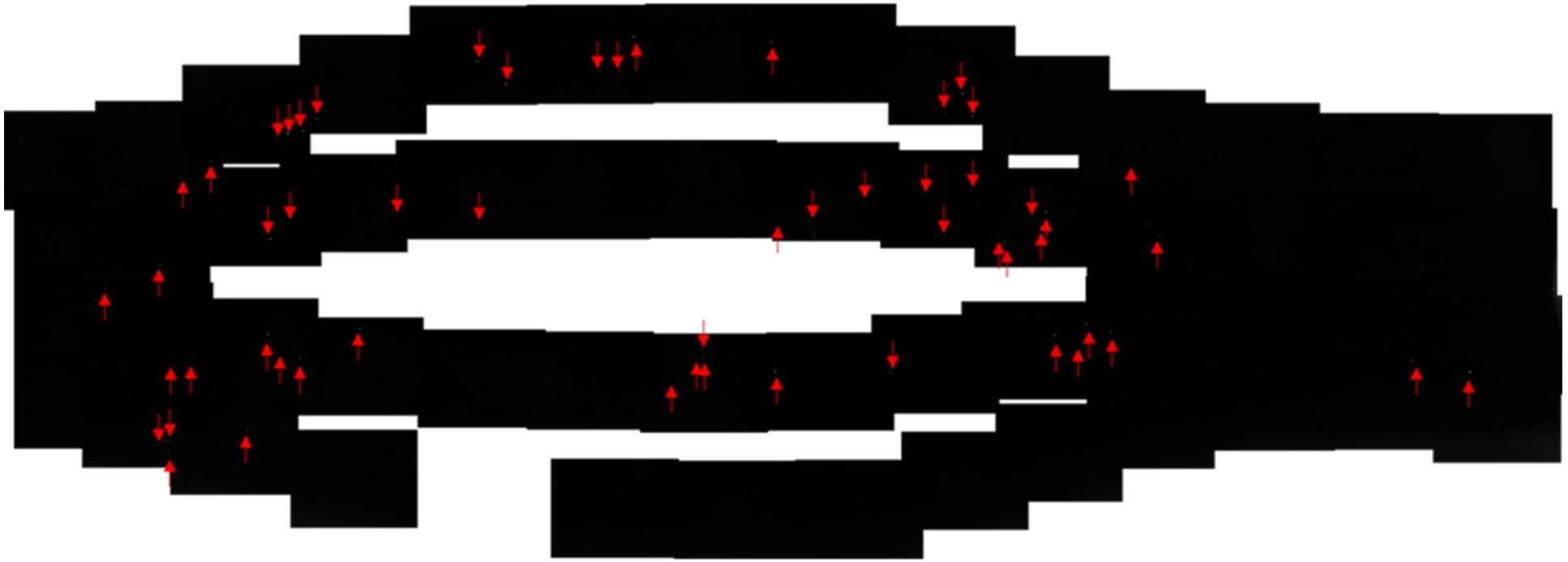

Figure 7.12 Assessment of entire channel surface area when a BM-MNC CD271-depleted population spiked with 4000 SH-SY5Y cells was injected into the prototype device

A MACS separated BM-MNC CD271-depleted population was spiked with 4000 SH-SY5Y cells and injected into the prototype device. After a 5 min incubation, unbound cells were washed away at 20 µL/min and photos were taken of the entire channel surface area. Cells were stained with a live cell stain (calcein AM) to enable detection above the channel background and bound cells are marked with red arrows. The BM-MNC CD271-depleted population spiked with 4000 SH-SY5Y cells was injected at 1 million cells/mL and the number of cells captured (normalised to cell concentration) is reported in Table 7.6.

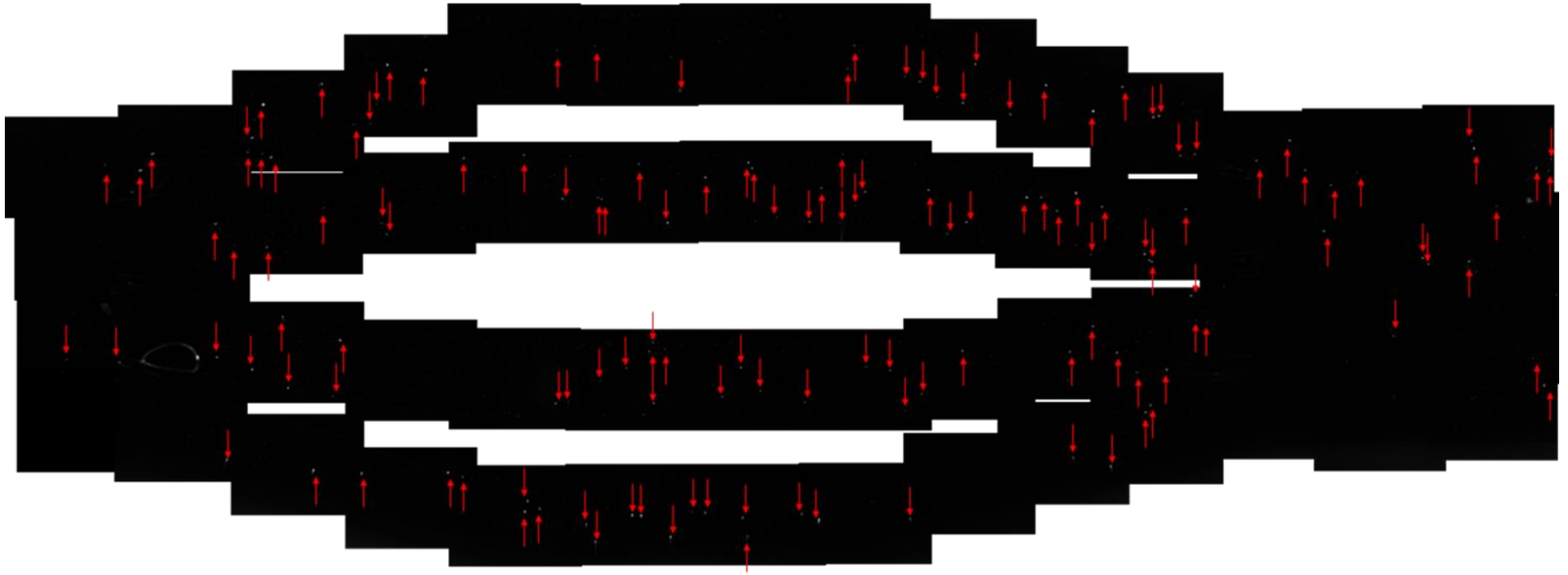

Figure 7.13 Assessment of entire channel surface area when a BM-MNC CD271-enriched population of cells was injected into the prototype device

A MACS separated BM-MNC CD271-enriched population was injected into the prototype device. After a 5 min incubation, unbound cells were washed away at 20 µL/min and photos were taken of the entire channel surface area. Cells were stained with a live cell stain (calcein AM) to enable detection above the channel background and bound cells are marked with red arrows. The BM-MNC CD271-enriched population was injected at 1.9 million cells/mL and the number of cells captured (normalised to cell concentration) is reported in Table 7.6.

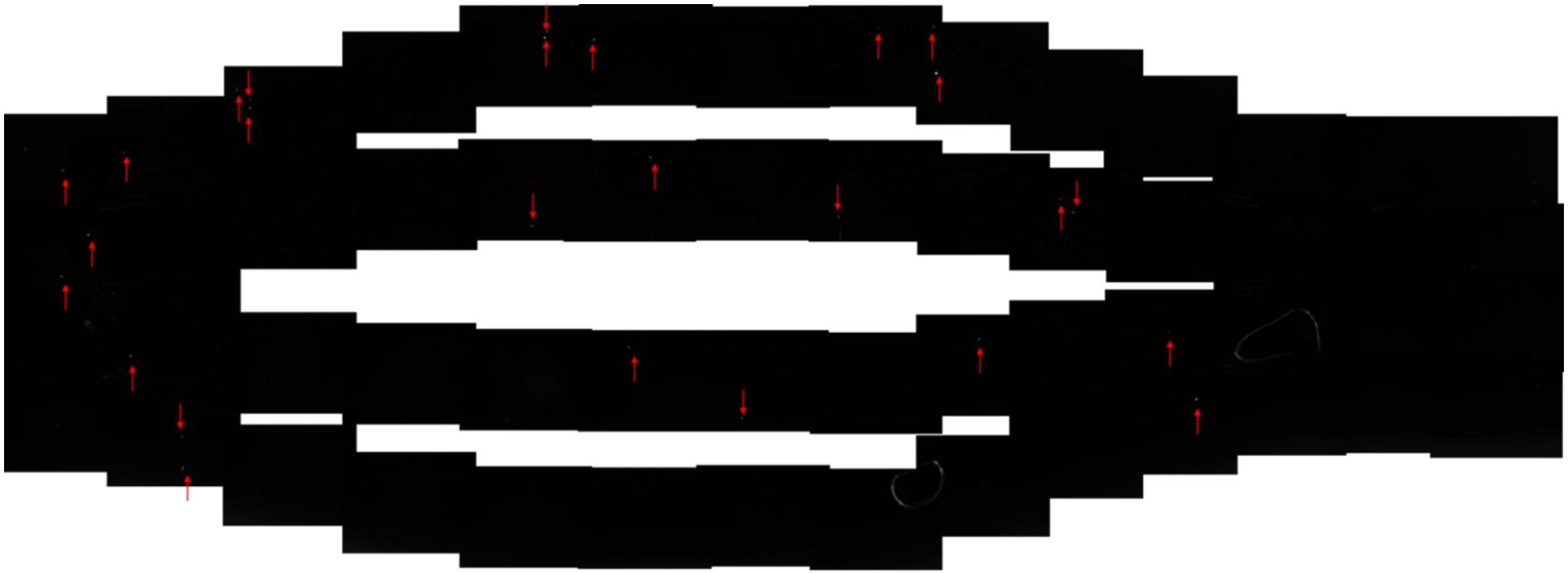

Figure 7.14 Assessment of entire channel surface area when a BM-MNC CD271-depleted population was injected into the prototype device

A MACS separated BM-MNC CD271-depleted population was injected into the prototype device. After a 5 min incubation, unbound cells were washed away at 20 µL/min and photos were taken of the entire channel surface area. Cells were stained with a live cell stain (calcein AM) to enable detection above the channel background and bound cells are marked with a red arrow. The BM-MNC CD271-depleted population was injected at 1 million cells/mL and the number of cells captured (normalised to cell concentration) is reported in Table 7.6.

Table 7.6 Summary of results using model CD271-enriched and depleted populations and BM-MNC CD271-enriched and depleted populations in the prototype device and compared with FACS

Row		Repeat 1: model CD271-enriched population (Section 7.3.7.2)	Repeat 2: SH-SY5Y spiked BM-MNC CD271-depleted population (Section 7.3.8)	Repeat 3: BM-MNC CD271-enriched population (Section 7.3.8)	Mean ± SEM (n=3)
1	Number of cells captured from enriched population*	44	55	77	N/A
2	Number of cells captured from depleted population*	2	26		N/A
3	Row 1 – Row 2	42	29	51	41 ± 6
5	Percentage of cells captured including all cells (%)	4.4	5.5	7.7	5.9 ± 1.0
4	Percentage of cells captured excluding ‘non-specific’ cells (%)	4.2	2.9	5.1	4.1 ± 0.6
5	Percentage of CD271bright/CD45low cells sorted by sterile FACS				4.7 ± 1.6

* Number of cells normalised to cell concentration of 1 million cells/mL

Although the data presented here is based on cell counts only, it has provided an early indication of the efficacy of the prototype device using clinically relevant populations. From this data it appears that the prototype device captures a similar percentage of cells to the percentage of CD271bright/CD45low cells identified by

sterile FACS from pre-enriched BM-MNC populations. It must however be noted that the method has made multiple assumptions and does not include the errors associated with these assumptions. The numbers processed by the prototype device need to be greatly increased for a more accurate assessment and to allow collection of cells post-enrichment.

From this preliminary experiment it was found that the cells could be released from the antibody-functionalised surface by increasing the flow rate (as previously found in Chapter 6: Section 6.3.2 for SH-SY5Y CD271+ cells) however it was not possible to elucidate what flow rate would be most suitable with the small number of cells captured. In Section 7.2.5, it was estimated that the number of CD271 antigens on the surface of CD271bright/CD45low cells was an order of magnitude higher than for SH-SY5Y cells and therefore higher flow rates may be required for the release of cells. Some of the cells captured in this experiment released at lower flow rates (<1 mL/min), however to release all cells higher flow rates were required (>1 mL/min). Analysis of a greater number of cells is required to optimise the release of CD271bright/CD45low cells in the prototype device.

Post-enrichment analysis of CD271bright/CD45low cells would also need to be carried out to ensure that if higher flow rates are required, it does not affect the viability or function of cells. Fluidic force has been commonly used for cell detachment however there are concerns that the shear stress involved could result in cell damage (273). The effects of flow acceleration on cancer cell lines adhered to functionalised surfaces was explored by Cheung *et al.* (2009)(274). They found that low acceleration resulted in significant cell deformation, however there was negligible deformation under high flow acceleration. It has also been found that shear stress can change the cell microenvironment; Wang *et al.* (2005)(275) investigated the relationship between shear stress and endothelial differentiation of an murine embryonic cell line, and Chowdhury *et al.* (2010)(276) demonstrated that cell softness dictates the stress-induced spreading of mouse embryonic stem cells and could drive the differentiation of cells.

In this work, post-enrichment analysis was carried out on a SH-SY5Y neuroblastoma cell line (Chapter 6: Section 6.3.6) which included assessing the viability and proliferation capacity of cells enriched in the device. Here it was found that there were no detrimental effects of cell detachment via increased flow rates, however, it was previously discussed that more in-depth analysis is required to confirm this. Whilst utilising shear stress to detach cells has the advantages of being simple and inexpensive, more sophisticated methods could result in less harmful methods of detachment.

Alternative methods have been explored for MSC detachment including; temperature-sensitive polymers (277), light-sensitive polymers (278) and

electrochemical harvesting and bulk pH decrease on polyelectrolyte monolayers (279). Some of the data reported in Chapters 5 and 6 suggested pH-mediated release could be used as a release mechanism; pH mediated release was observed in SPR analysis of SH-SY5Y cells on a CD271 antibody-functionalised surface (Chapter 6: Section 6.3.1.1) and pH-mediated release of Affimers was used during phage display selection of CD271-specific Affimers (Chapter 5: Section 5.3.1.2). Although there were no CD271-specific Affimers established in this work, aptamers such as Affimers have the potential to be selected with specific properties which could aid the detachment of cells. Zhu *et al.* (2012)(280) used surface-immobilised aptamers to capture a leukaemia cell line which could then be released by a moderate increase in temperature.

At this time, increased flow rates were used to detach cells from the channel surface however as the device is developed further, more work will be required to assess if this is the most suitable method of detachment.

7.4 Conclusions

In this chapter of work, the previously optimised prototype device has been evaluated with clinical samples of bone marrow aspirate. The overall aim of the device is to be able to enrich a population of cells that could be used in cell therapies. A CD271bright/CD45low population of cells has been well characterised in the literature and has been shown to have high clonogenic and multipotent potential (see Chapter 2: Section 2.6.2.2). The device was therefore designed to capture CD271+ cells in an antibody-functionalised microfluidic channel. This concept allows controlled fluid flow to wash away undesired cells resulting in a therapeutic population of cells with higher purity.

Clinical bone marrow aspirates were supplied with informed consent from patients undergoing orthopaedic surgery, and MACS and FACS were used to characterise the CD271bright/CD45low cell population. The percentage and number of CD271bright/CD45low cells in BM-MNC populations was very low and therefore different protocols were investigated to demonstrate the efficacy of the prototype device. At this stage, only preliminary data has been collected, limited by the availability of clinical samples and the low number of CD271+ cells. To progress this technology further, a number of considerations must be taken into account; the number of cells required for cell therapies, the throughput capabilities of the device, different sources of MSCs and the possibility of a hybrid microfluidic technology. Each of these considerations are discussed in detail in Chapter 8.

Chapter 8: Future work and thesis conclusions

8.1 Considerations for future work

8.1.1 The number of cells required for MSC therapies

To progress this technology further, the total number of cells required to have a clinically beneficial effect in any MSC therapy must be considered, and currently, this number is largely unknown. Chapter 2: Section 2.2 summarises the results from recent clinical trials to treat a number of different diseases in which the number of MSCs used varies from 10^6 to 10^8 million cells/mL with no consensus on what constitutes an effective dose. Furthermore, these trials use cells that have been expanded *in vitro* or have been concentrated using density gradient centrifugation. They therefore comprise of a heterogeneous population of cells with unknown therapeutic effect.

Hernigou *et al.* (2005)(3) used density gradient centrifugation to concentrate bone marrow aspirate for treatment of non-union fractures in 60 patients. They found that successful treatments contained an average of 55,000 MSCs (calculated by extrapolation of CFU-F results) compared to an average of 19,000 MSCs for patients where bone union was not obtained. This study provided an indication of the number of MSCs required for the treatment of non-union bone fractures, however, a large volume of aspirate was taken from patients (300 mL) and only a small fraction of this was assessed for CFU-F potential. This method could therefore inaccurately predict the number of MSCs injected into the fracture site.

In 2018, two studies were published by Petters *et al.* (4, 5) investigating the use of CD271-selected MSCs as a single stage treatment (without prior *in vitro* expansion of cells) for cartilage repair. Recognising the potential of intraoperative therapies, Petters first investigated different biomarkers for isolating CFU-Fs from ovine bone marrow and then used the population isolated by the defined marker to generate a cartilage graft consisting of clinically approved collagen type I hydrogel and the non-expanded MSC population (4). They found that CD271 was the most effective marker and that CD271-selected cells were capable of producing a cartilage graft comparable to a heterogeneous population of unseparated BM-MNCs - despite the fact that the CD271-selected cells were seeded at a significantly reduced volume (6.25% of the volume used for unseparated BM-MNCs). The actual number of CD271-positive MSCs seeded in the graft was reported as 4207, demonstrating that a minimal number of CD271+ cells were able to populate the graft with viable cells with adequate chondrogenic potential. The authors discussed that enriching the CD271 subset of MSCs

depletes non-chondrogenic differentiable cells and results in a usable volume of cells (4).

In the second study, the same cartilage grafts were investigated however using human bone marrow rather than ovine bone marrow (5). Here it was found that at the final time point (day 35) the number of cells in the CD271+ graft was 2.2-fold higher than in grafts with unseparated BM-MNCs, even though the CD271+ grafts were originally seeded with 4% of the cells that were seeded for unseparated BM-MNCs (9000 cells per graft vs. 225,000 cells per graft). The sulphated glycosaminoglycan (sGAG) content (present in cartilage tissue) was also higher in CD271+ grafts compared to unseparated BM-MNC grafts. The greater chondrogenic potential of CD271-selected MSCs was also reported by Mifune *et al.* (2013)(281) in both *in vitro* and *in vivo* studies however these cells were culture-expanded after CD271-selection.

The studies suggest that if pre-enriched, non-expanded cells are used for MSC therapies, the number of cells required is in the thousands rather than the millions. Further *in vivo* proof of concept studies are required for CD271-selected cell therapies which could clarify the ideal cell dose.

8.1.2 Increasing the throughput of the device for clinical application

Evidently, to enrich cell numbers on this scale, the throughput of the device must be increased. Currently only a small fraction of the cell suspension was able to be analysed in the device due to the laborious methods involved. The most effective way to analyse the number of cells captured was to photograph the entire surface area of the channel which still resulted in the identification of less than 150 cells. The volume of the current channel is 11 µL in total and the minimum reliable loading volume (due to sample injection from a 1 mL syringe) is ~200 µL. Therefore in one incubation, only ~5% of the cell suspension was being analysed. If repeat injections could be successfully employed then the number of cells captured could be increased to 1000’s rather than 100’s.

The current limitation of repeated injections was the fact that the cells sedimented during the incubation period in the absence of flow. This meant that the cell distribution was not homogenous and led to an inefficient method of cell capture. If a mixing mechanism was incorporated into the device, repeat injections would become feasible and allow for easier methods of analysis. A mixing mechanism could be incorporated where the flow continued in a sample loop away from the microfluidic channel so cells remained in a homogenous suspension and were available for repeat injections.

Moreover, if cell capture could be achieved under continuous flow conditions it would be of even greater benefit. Chueng *et al.* (2009)(274) reported that 'although difficult', it was possible to capture moving cancer cells at low flow rates (1 µL/min) in an N-cadherin antibody-functionalised channel, however the capture efficiency was ~50% compared to almost 100% when a 5 min incubation with no flow was used. Cell capture at low flow rates was not observed in this work however with some channel modifications this could become a possibility. To improve the capture efficiency of microfluidic devices, microstructures such as microposts, micropillar and herringbones mixer have been designed such that the flow is changed from streamlined to chaos or vortex (282). This increases the contact frequency between cells and the functionalised substrates leading to a higher capture efficiency. It must however be noted that increasing contact frequency between cells and functionalised substrates could also compromise purity due to a greater amount of non-specific binding. The efficiency and purity of various devices with incorporated microstructures are discussed below.

Nagrath and colleagues (283) describe the capture of circulating tumour cells (CTCs) on a chip with an array of microposts functionalised with anti-epithelial-cell-adhesion-molecule (EpCAM) antibodies. At a flow rate of 1-2 mL/hour the capture efficiency was 65% with a purity of approximately 50%. Improved capture efficiencies have been reported in similar devices – Gleghorn *et al.* (2010)(284) used staggered obstacle arrays that optimised CTC-wall interactions and reported a capture efficiency of 85% with 68% purity. Finally, a capture efficiency as high as 98% was found by Sheng *et al.* (2012)(285) who also investigated properties such as channel depth as a factor of capture efficiency. They found that as the channel depth was increased the capture efficiency decreased, however a decreased channel depth compromised purity.

The decreased capture efficiency was observed to be due to the reduced interactions between the cells and the aptamer-functionalised channel top and bottom, and the decreased purity was observed to be due to the geometric trapping of non-specific cells in channels with a smaller channel depth. For example, the channel with the greatest depth (44 µM) had a capture efficiency of ~92% and a purity of ~80% compared with the smallest channel depth (24 µM) which had a capture efficiency of ~98% with a purity of ~20% - clearly demonstrating the compromise between capture efficiency and purity with increased contact frequency, either due to non-specific capture or trapping of cells.

In devices comprising of herringbones mixers; a study compared the capture efficiency of CTCs using a flat device or a herringbones mixer device and found that the capture efficiency was <8% in the flat device at 0.48 mL/hour and a

maximum of ~30% at the lowest flow rate applied (0.12 mL/hour), compared with ~40% and ~80% for the herringbones device respectively (286). The herringbones device was then enlarged for use with clinical samples and compared to a micropost-based device. The herringbones device was still found to have superior capture efficiency - ~26% higher than the micropost-based device – however both devices achieved purities of <15%. Another herringbones device reported 90-92% capture efficiency of CTCs at flow rates as high as 3.6 mL/hour (287). In this study a high purity of 84% was achieved whilst maintaining the capture efficiency of ~90% by increasing the width of herringbone grooves to avoid cell trapping. To avoid the complicated microfabrication steps involved in the above devices, Cheng *et al.* (2016)(288) created a 3D scaffold chip fabricated from PDMS and found that at flow rates less than 6 mL/hour there was more than 90% capture efficiency but there was no information on the population purity.

Affinity-based capture in microfluidic devices has been widely explored for the capture of CTCs due to the fact that CTCs ubiquitously express EpCAM and blood cells do not, providing a specific biomarker for CTC isolation. There are no reports of microfluidic devices with antibody-based capture for MSCs perhaps owing to the fact that there is no consensus on a specific biomarker for MSCs. In this work CD271 was chosen due to a significant amount of literature evidence showing that this biomarker isolates a subset of MSCs with high clonogenic potential (Chapter 2: Section 2.6.2.2). However different strategies could be explored using this platform technology and the most effective population of MSCs for MSC therapies is not yet known.

A device developed to capture circulating plasma cells (CPCs) in multiple myeloma used the plasma cell biomarker CD138 (253). Using a herringbones mixer device it was reported that the capture efficiency was between 40–70% depending on parameters such as flow rate, antibody concentration and cell suspension. The purity was also low at 1–5% necessitating CD138 staining after capture for an accurate analysis of CPCs present. This demonstrates the challenges involved using different biomarkers and the requirement for optimisation in each case. The capture efficiency of the device described in this thesis was found to be ~70% for target populations greater than 25% however ~20% for target populations less than 25% (Chapter 6: Section 6.3.4.1). The purity was consistently high at 80 ± 3% for populations higher than 6% initial target cell concentration (lower percentage target populations were not assessed). With further optimisation of the capture efficiency at lower target cell concentrations, this device shows great potential for enriching a high purity MSC subpopulation.

If the device and protocols could be developed to capture a greater number of cells, the throughput could be further optimised by increasing the number of parallel channels. In this work the throughput was increased 4.8-fold by changing the channel design (Chapter 6: Section 6.3.5.2) therefore this is a relatively simple way to reduce the time taken for enrichment, with the final aim to enrich cells within an intraoperative timeframe.

8.1.3 Investigating different sources of MSCs to increase the number of CD271+ cells available for capture

Whilst increasing the throughput of the device is essential, the percentage of CD271bright/CD45low cells in BM-MNC populations is inherently low. To gain a larger therapeutic population of cells, different sources of MSC could be explored. Adipose tissue has been suggested as a rich source of MSCs where 1–10% of the stromal fraction are MSCs (289). In a comparison of bone marrow and adipose tissue it was found that approximately 11% of the stromal vascular fraction of adipose tissue (AT-SVF) was CD271+ compared to 2% in BM-MNCs (290). However, CFU-Fs were only enriched in the CD271-enriched BM-MNCs not the CD271-enriched AT-SVF population. On further analysis it was established that a subset of cells with high proliferative and clonogenic abilities could be isolated by CD271 selection from adipose tissue however only from lipoaspiration samples not abdominoplasty samples.

Another study investigated the relationship between donor age and CD271 expression of adipose tissue-derived mesenchymal stem cells (AT-MSCs) from cosmetic liposuction patients (191). Here it was found that there was a negative correlation with age however even the average lowest proportion of CD271+ cells (1.8% for ages 51-65) was higher than that typically found in BM-MNC populations. No CFU-F assessment was carried out in the study. In a comparison of foetal and adult MSCs from different sources, there was an average of 8.4% CD271+ cells from AT-MSCs and 3.7% in BM-MNCs (291). Unfortunately, CFU-F analysis was reported as adult versus foetal MSCs therefore no direct comparison between BM-MNCs and AT-MSCs. Altogether, the evidence does suggest a higher proportion of CD271+ cells in adipose tissue removed by lipoaspiration, however whether these cells have the same clonogenic potential as CD271+ cells from BM-MNCs needs to be confirmed.

Furthermore, the cryopreservation process was not optimised in this work, which was speculated to cause a significant decrease in viability of BM-MNCs (Chapter 7: Section 7.3.2). The detrimental effects were not able to be fully established however it was hypothesised that immediate processing of cells would lead to a

higher number of CD271+ cells in BM-MNC populations. Differences in membrane permeability and surface to volume ratio causes cells to have varying responses to cryopreservation leading to differences in viability when thawed (292). This highlights the necessity of protocol optimisation for different cell types.

8.1.4 Developing a hybrid microfluidic technology

Finally, a microfluidic device based on affinity capture to enrich a specific population of MSCs is likely to always require pre-processing steps. In this work, the red blood cells were lysed to obtain a mononuclear cell fraction and CD271+ cells were pre-enriched from the mononuclear cell fraction using MACS technology. The aim of this novel device is to overcome limitations associated with MACS such as the attachment of magnetic microbeads and lengthy pre-labelling steps, therefore this would not suffice as a pre-processing step.

Instead, the aim is to develop a hybrid microfluidic technology incorporating a high throughput, less specific pre-processing step in the first stage of the device and a highly specific, affinity-based capture in the second stage of the device. A hybrid technology such as this would provide a high purity population of MSCs in an enclosed and portable device suitable for use within an operating theatre.

The proposed technology for the first stage of the device is currently being developed within this research group. Smith *et al.* (2017)(293) describe the development of surface acoustic wave–dielectrophoresis (SAW-DEP) technology which combines acoustophoresis (a density-based separation method) and dielectrophoresis (a separation method based on the dielectric properties of a cell) in order to overcome the limitations of each individual method and provide a rapid, label-free cell separation method. In the publication the separation of viable and non-viable dental pulp stem cells was demonstrated using a SAW-DEP device with throughput of 10^4 cells/minute (293). Current work has increased this throughput further and is working towards the separation of individual cell types from whole blood. This technology would provide an ideal method of pre-enrichment in the first stage of a hybrid microfluidic device.

8.2 Thesis conclusions and summary

In conclusion to this thesis, each of the objectives described in Chapter 3 have been completed and the research aim has been achieved. During the completion of objective 1 (Section 3.2.1), an appropriate binding molecule for affinity-capture of CD271+ cells was established, as well as the identification of a cell line model

for use during the proof-of-concept stages of development. These aspects were essential to achieving the research aim; reliable and highly specific binding of CD271+ cells is fundamental to enriching a population of cells with high purity, and since the number of CD271+ cells in clinical samples is extremely low, optimising cell capture and release in the device using clinical samples would have posed an extraordinary challenge.

During the completion of objective 2 (Section 3.2.2), a prototype microfluidic device was designed and fabricated, and it was discovered that the device could effectively capture CD271+ cells from mixed cell populations. Through several device iterations, cell capture and release was optimised and allowed the collection of enriched CD271+ cell line populations. Post-enrichment analysis suggested that cells remained viable, able to proliferate under normal cell culture conditions, and had no antibody attached to the cell surface post-release – a significant advantage compared to current affinity-based cell sorting methods.

Finally, the completion of objective 3 (Section 3.2.3) evaluated the feasibility of capturing CD271+ cells from clinical samples of bone marrow aspirate. It was found that the device captured a comparable number of cells to the number of CD271+ cells found in typical bone marrow aspirates analysed using established cell sorting methods. This was a significant step towards demonstrating clinical utility and progressing the device towards commercialisation.

In summary, this technology is in the early stages of the development process, initial proof-of-concept has been demonstrated using a cell line, and preliminary data with clinical samples indicates it is a viable method to enrich CD271+ cells. Further development of the device to enable repeat injections into the device, or capture under continuous flow, would allow a clinically relevant number of cells to be collected for MSC therapies. This technology could be combined with a high-throughput microfluidic technology to provide a novel, rapid, highly specific and minimally manipulative method of stem cell enrichment.

List of References

1. Wei, X. et al. Mesenchymal stem cells: a new trend for cell therapy. *Acta Pharmacol Sin.* 2013, **34**(6), pp.747-54.
2. Pittenger, M.F. et al. Multilineage potential of adult human mesenchymal stem cells. *Science.* 1999, **284**(5411), pp.143-7.
3. Hernigou, P. et al. Percutaneous autologous bone-marrow grafting for nonunions. Influence of the number and concentration of progenitor cells. *J Bone Joint Surg Am.* 2005, **87**(7), pp.1430-7.
4. Petters, O. et al. Point-of-care treatment of focal cartilage defects with selected chondrogenic mesenchymal stromal cells-An in vitro proof-of-concept study. *J Tissue Eng Regen Med.* 2018, **12**(7), pp.1717-1727.
5. Oliver, P. et al. Single-Stage Preparation of Human Cartilage Grafts Generated from Bone Marrow-Derived CD271+ Mononuclear Cells. *Stem Cells and Development.* 2018, **27**(8), pp.545-555.
6. Diogo, M.M. et al. Separation technologies for stem cell bioprocessing. *Biotechnology and Bioengineering.* 2012, **109**(11), pp.2699-2709.
7. Bocelli-Tyndall, C. et al. Fibroblast growth factor 2 and platelet-derived growth factor, but not platelet lysate, induce proliferation-dependent, functional class II major histocompatibility complex antigen in human mesenchymal stem cells. *Arthritis Rheum.* 2010, **62**(12), pp.3815-25.
8. Friedenstein, A.J. et al. The development of fibroblast colonies in monolayer cultures of guinea-pig bone marrow and spleen cells. *Cell Tissue Kinet.* 1970, **3**(4), pp.393-403.
9. Xu, W. et al. Mesenchymal stem cells from adult human bone marrow differentiate into a cardiomyocyte phenotype in vitro. *Exp Biol Med (Maywood).* 2004, **229**(7), pp.623-31.
10. Oswald, J. et al. Mesenchymal stem cells can be differentiated into endothelial cells in vitro. *Stem Cells.* 2004, **22**(3), pp.377-84.
11. Chen, L.B. et al. Differentiation of rat marrow mesenchymal stem cells into pancreatic islet beta-cells. *World J Gastroenterol.* 2004, **10**(20), pp.3016-20.
12. Barzilay, R. et al. Induction of human mesenchymal stem cells into dopamine-producing cells with different differentiation protocols. *Stem Cells Dev.* 2008, **17**(3), pp.547-54.
13. Oryan, A. et al. Role of Mesenchymal Stem Cells in Bone Regenerative Medicine: What Is the Evidence? *Cells Tissues Organs.* 2017, **204**(2), pp.59-83.
14. Bagno, L. et al. Mesenchymal Stem Cell-Based Therapy for Cardiovascular Disease: Progress and Challenges. *Mol Ther.* 2018, **26**(7), pp.1610-1623.
15. Lukomska, B. et al. Challenges and Controversies in Human Mesenchymal Stem Cell Therapy. *Stem Cells International.* 2019, **2019**, p.10.
16. Briggs, A.M. et al. Reducing the global burden of musculoskeletal conditions. *Bulletin of the World Health Organization.* 2018, **96**(5), pp.366-368.
17. Tsang, A. et al. Common Chronic Pain Conditions in Developed and Developing Countries: Gender and Age Differences and Comorbidity With Depression-Anxiety Disorders. *The Journal of Pain.* 2008, **9**(10), pp.883-891.

18. United Nations, D.o.E.a.S.A., Population Division. *World Population Ageing 2017 - Highlights.* https://www.un.org/en/development/desa/population/publications/pdf/ageing/WPA2017_Highlights.pdf, 2017.
19. Grayson, W.L. et al. Stromal cells and stem cells in clinical bone regeneration. *Nature reviews. Endocrinology.* 2015, **11**(3), pp.140-150.
20. Huang, S. et al. Systemic and Local Administration of Allogeneic Bone Marrow-Derived Mesenchymal Stem Cells Promotes Fracture Healing in Rats. *Cell Transplant.* 2015, **24**(12), pp.2643-55.
21. Connolly, J.F. and Shindell, R. Percutaneous marrow injection for an ununited tibia. *Nebr Med J.* 1986, **71**(4), pp.105-7.
22. Hernigou, P. et al. Percutaneous autologous bone-marrow grafting for nonunions. Surgical technique. *J Bone Joint Surg Am.* 2006, **88 Suppl 1 Pt 2**, pp.322-7.
23. Park, S.-H. et al. Calcium phosphate combination biomaterials as human mesenchymal stem cell delivery vehicles for bone repair. *Journal of biomedical materials research. Part B, Applied biomaterials.* 2011, **97**(2), pp.235-244.
24. Lee, G.S. et al. Direct deposited porous scaffolds of calcium phosphate cement with alginate for drug delivery and bone tissue engineering. *Acta Biomater.* 2011, **7**(8), pp.3178-86.
25. Kim, J. et al. Bone regeneration using hyaluronic acid-based hydrogel with bone morphogenic protein-2 and human mesenchymal stem cells. *Biomaterials.* 2007, **28**(10), pp.1830-7.
26. Horwitz, E.M. et al. Transplantability and therapeutic effects of bone marrow-derived mesenchymal cells in children with osteogenesis imperfecta. *Nat Med.* 1999, **5**(3), pp.309-13.
27. Fischer, U.M. et al. Pulmonary passage is a major obstacle for intravenous stem cell delivery: the pulmonary first-pass effect. *Stem Cells Dev.* 2009, **18**(5), pp.683-92.
28. Walczak, P. et al. Dual-modality monitoring of targeted intraarterial delivery of mesenchymal stem cells after transient ischemia. *Stroke.* 2008, **39**(5), pp.1569-74.
29. Togel, F. et al. Administered mesenchymal stem cells protect against ischemic acute renal failure through differentiation-independent mechanisms. *Am J Physiol Renal Physiol.* 2005, **289**(1), pp.F31-42.
30. Togel, F. et al. Bioluminescence imaging to monitor the in vivo distribution of administered mesenchymal stem cells in acute kidney injury. *Am J Physiol Renal Physiol.* 2008, **295**(1), pp.F315-21.
31. Janowski, M. et al. Cell size and velocity of injection are major determinants of the safety of intracarotid stem cell transplantation. *J Cereb Blood Flow Metab.* 2013, **33**(6), pp.921-7.
32. Connolly, J.F. et al. Autologous marrow injection as a substitute for operative grafting of tibial nonunions. *Clin Orthop Relat Res.* 1991, (266), pp.259-70.
33. Liebergall, M. et al. Stem cell-based therapy for prevention of delayed fracture union: a randomized and prospective preliminary study. *Molecular therapy : the journal of the American Society of Gene Therapy.* 2013, **21**(8), pp.1631-1638.
34. Kaigler, D. et al. Stem cell therapy for craniofacial bone regeneration: a randomized, controlled feasibility trial. *Cell Transplant.* 2013, **22**(5), pp.767-77.

35. Pelegrine, A.A. et al. Clinical and histomorphometric evaluation of extraction sockets treated with an autologous bone marrow graft. *Clin Oral Implants Res.* 2010, **21**(5), pp.535-42.
36. Rickert, D. et al. Maxillary sinus floor elevation with bovine bone mineral combined with either autogenous bone or autogenous stem cells: a prospective randomized clinical trial. *Clin Oral Implants Res.* 2011, **22**(3), pp.251-8.
37. Sauerbier, S. et al. Bone marrow concentrate and bovine bone mineral for sinus floor augmentation: a controlled, randomized, single-blinded clinical and histological trial--per-protocol analysis. *Tissue Eng Part A.* 2011, **17**(17-18), pp.2187-97.
38. Sauerbier, S. et al. In vivo comparison of hard tissue regeneration with human mesenchymal stem cells processed with either the FICOLL method or the BMAC method. *Tissue Eng Part C Methods.* 2010, **16**(2), pp.215-23.
39. Hermund, N.U. et al. Reimplantation of cultivated human bone cells from the posterior maxilla for sinus floor augmentation. Histological results from a randomized controlled clinical trial. *Clin Oral Implants Res.* 2012, **23**(9), pp.1031-7.
40. Jin, Y.-Z. and Lee, J.H. Mesenchymal Stem Cell Therapy for Bone Regeneration. *Clinics in orthopedic surgery.* 2018, **10**(3), pp.271-278.
41. Koga, H. et al. Mesenchymal stem cell-based therapy for cartilage repair: a review. *Knee Surg Sports Traumatol Arthrosc.* 2009, **17**(11), pp.1289-97.
42. Goldberg, A. et al. The use of mesenchymal stem cells for cartilage repair and regeneration: a systematic review. *Journal of Orthopaedic Surgery and Research.* 2017, **12**(1), p.39.
43. Lo Monaco, M. et al. Stem Cells for Cartilage Repair: Preclinical Studies and Insights in Translational Animal Models and Outcome Measures. *Stem cells international.* 2018, **2018**, pp.9079538-9079538.
44. Palazzo, C. et al. Risk factors and burden of osteoarthritis. *Annals of Physical and Rehabilitation Medicine.* 2016, **59**(3), pp.134-138.
45. Giannini, S. et al. One-step bone marrow-derived cell transplantation in talar osteochondral lesions. *Clin Orthop Relat Res.* 2009, **467**(12), pp.3307-20.
46. Freitag, J. et al. Mesenchymal stem cell therapy in the treatment of osteoarthritis: reparative pathways, safety and efficacy – a review. *BMC Musculoskeletal Disorders.* 2016, **17**(1), p.230.
47. Wakitani, S. et al. Mesenchymal cell-based repair of large, full-thickness defects of articular cartilage. *J Bone Joint Surg Am.* 1994, **76**(4), pp.579-92.
48. Nejadnik, H. et al. Autologous bone marrow-derived mesenchymal stem cells versus autologous chondrocyte implantation: an observational cohort study. *Am J Sports Med.* 2010, **38**(6), pp.1110-6.
49. Emadedin, M. et al. Intra-articular injection of autologous mesenchymal stem cells in six patients with knee osteoarthritis. *Arch Iran Med.* 2012, **15**(7), pp.422-8.
50. Erickson, I.E. et al. High mesenchymal stem cell seeding densities in hyaluronic acid hydrogels produce engineered cartilage with native tissue properties. *Acta Biomater.* 2012, **8**(8), pp.3027-34.

51. Koga, H. et al. Comparison of mesenchymal tissues-derived stem cells for in vivo chondrogenesis: suitable conditions for cell therapy of cartilage defects in rabbit. *Cell Tissue Res.* 2008, **333**(2), pp.207-15.
52. Muschler, G.F. et al. Spine fusion using cell matrix composites enriched in bone marrow-derived cells. *Clinical orthopaedics and related research.* 2003, (407), pp.102-118.
53. Roth, G.A. et al. Global, Regional, and National Burden of Cardiovascular Diseases for 10 Causes, 1990 to 2015. *J Am Coll Cardiol.* 2017, **70**(1), pp.1-25.
54. Mathiasen, A.B. et al. Bone marrow-derived mesenchymal stromal cell treatment in patients with severe ischaemic heart failure: a randomized placebo-controlled trial (MSC-HF trial). *European Heart Journal.* 2015, **36**(27), pp.1744-1753.
55. Teerlink, J.R. et al. Benefit of cardiopoietic mesenchymal stem cell therapy on left ventricular remodelling: results from the Congestive Heart Failure Cardiopoietic Regenerative Therapy (CHART-1) study. *European Journal of Heart Failure.* 2017, **19**(11), pp.1520-1529.
56. Florea, V. et al. Dose Comparison Study of Allogeneic Mesenchymal Stem Cells in Patients With Ischemic Cardiomyopathy (The TRIDENT Study). *Circulation Research.* 2017, **121**(11), pp.1279-1290.
57. Hare, J.M. et al. Comparison of Allogeneic vs Autologous Bone Marrow–Derived Mesenchymal Stem Cells Delivered by Transendocardial Injection in Patients With Ischemic Cardiomyopathy: The POSEIDON Randomized TrialMesenchymal Stem Cells and Ischemic Cardiomyopathy. *JAMA.* 2012, **308**(22), pp.2369-2379.
58. Heldman, A.W. et al. Transendocardial Mesenchymal Stem Cells and Mononuclear Bone Marrow Cells for Ischemic Cardiomyopathy: The TAC-HFT Randomized TrialMesenchymal and Bone Marrow Cell InjectionMesenchymal and Bone Marrow Cell Injection. *JAMA.* 2014, **311**(1), pp.62-73.
59. Global, regional, and national burden of neurological disorders during 1990-2015: a systematic analysis for the Global Burden of Disease Study 2015. *Lancet Neurol.* 2017, **16**(11), pp.877-897.
60. Singh, A. et al. Global prevalence and incidence of traumatic spinal cord injury. *Clinical epidemiology.* 2014, **6**, pp.309-331.
61. Volkman, R. and Offen, D. Concise Review: Mesenchymal Stem Cells in Neurodegenerative Diseases. *STEM CELLS.* 2017, **35**(8), pp.1867-1880.
62. Karussis, D. et al. Safety and immunological effects of mesenchymal stem cell transplantation in patients with multiple sclerosis and amyotrophic lateral sclerosis. *Arch Neurol.* 2010, **67**(10), pp.1187-94.
63. Oh, K.W. et al. Phase I trial of repeated intrathecal autologous bone marrow-derived mesenchymal stromal cells in amyotrophic lateral sclerosis. *Stem Cells Transl Med.* 2015, **4**(6), pp.590-7.
64. Mazzini, L. et al. Autologous mesenchymal stem cells: clinical applications in amyotrophic lateral sclerosis. *Neurol Res.* 2006, **28**(5), pp.523-6.
65. Petrou, P. et al. Safety and Clinical Effects of Mesenchymal Stem Cells Secreting Neurotrophic Factor Transplantation in Patients With Amyotrophic Lateral Sclerosis: Results of Phase 1/2 and 2a Clinical Trials. *JAMA Neurol.* 2016, **73**(3), pp.337-44.

66. Lee, J.S. et al. A long-term follow-up study of intravenous autologous mesenchymal stem cell transplantation in patients with ischemic stroke. *Stem Cells.* 2010, **28**(6), pp.1099-106.
67. Lee, P.H. et al. A randomized trial of mesenchymal stem cells in multiple system atrophy. *Ann Neurol.* 2012, **72**(1), pp.32-40.
68. Xu, P. and Yang, X. The Efficacy and Safety of Mesenchymal Stem Cell Transplantation for Spinal Cord Injury Patients: A Meta-Analysis and Systematic Review. *Cell Transplant.* 2019, **28**(1), pp.36-46.
69. Yu, D. et al. [Effects of bone marrow mesenchymal stem cells transplantation on expression of vascular endothelial growth factor gene and angiogenesis after spinal cord injury in rats]. *Zhongguo Xiu Fu Chong Jian Wai Ke Za Zhi.* 2011, **25**(7), pp.837-41.
70. Chiba, Y. et al. Transplanted bone marrow stromal cells promote axonal regeneration and improve motor function in a rat spinal cord injury model. *Neurosurgery.* 2009, **64**(5), pp.991-9; discussion 999-1000.
71. Kurtzberg, J. et al. Allogeneic human mesenchymal stem cell therapy (remestemcel-L, Prochymal) as a rescue agent for severe refractory acute graft-versus-host disease in pediatric patients. *Biol Blood Marrow Transplant.* 2014, **20**(2), pp.229-35.
72. Le Blanc, K. et al. Mesenchymal stem cells for treatment of steroid-resistant, severe, acute graft-versus-host disease: a phase II study. *Lancet.* 2008, **371**(9624), pp.1579-86.
73. Amer, M.E. et al. Clinical and laboratory evaluation of patients with end-stage liver cell failure injected with bone marrow-derived hepatocyte-like cells. *Eur J Gastroenterol Hepatol.* 2011, **23**(10), pp.936-41.
74. Duijvestein, M. et al. Autologous bone marrow-derived mesenchymal stromal cell treatment for refractory luminal Crohn's disease: results of a phase I study. *Gut.* 2010, **59**(12), pp.1662-9.
75. Hu, J. et al. Safety and therapeutic effect of mesenchymal stem cell infusion on moderate to severe ulcerative colitis. *Exp Ther Med.* 2016, **12**(5), pp.2983-2989.
76. Ciccocioppo, R. et al. A Refractory Celiac Patient Successfully Treated With Mesenchymal Stem Cell Infusions. *Mayo Clin Proc.* 2016, **91**(6), pp.812-9.
77. Dietz, A.B. et al. Autologous Mesenchymal Stem Cells, Applied in a Bioabsorbable Matrix, for Treatment of Perianal Fistulas in Patients With Crohn's Disease. *Gastroenterology.* 2017, **153**(1), pp.59-62.e2.
78. Squillaro, T. et al. Clinical Trials With Mesenchymal Stem Cells: An Update. *Cell Transplant.* 2016, **25**(5), pp.829-48.
79. Mahmood, A. et al. Treatment of Traumatic Brain Injury in Adult Rats with Intravenous Administration of Human Bone Marrow Stromal Cells. *Neurosurgery.* 2003, **53**(3), pp.697-703.
80. Forte, A. et al. Mesenchymal stem cells effectively reduce surgically induced stenosis in rat carotids. *J Cell Physiol.* 2008, **217**(3), pp.789-99.
81. Son, B.R. et al. Migration of bone marrow and cord blood mesenchymal stem cells in vitro is regulated by stromal-derived factor-1-CXCR4 and hepatocyte growth factor-c-met axes and involves matrix metalloproteinases. *Stem Cells.* 2006, **24**(5), pp.1254-64.
82. Shi, M. et al. Regulation of CXCR4 expression in human mesenchymal stem cells by cytokine treatment: role in homing efficiency in NOD/SCID mice. *Haematologica.* 2007, **92**(7), pp.897-904.

83. Kitaori, T. et al. Stromal cell–derived factor 1/CXCR4 signaling is critical for the recruitment of mesenchymal stem cells to the fracture site during skeletal repair in a mouse model. *Arthritis & Rheumatism.* 2009, **60**(3), pp.813-823.
84. Schmidt, A. et al. Mesenchymal stem cells transmigrate over the endothelial barrier. *European Journal of Cell Biology.* 2006, **85**(11), pp.1179-1188.
85. Ruster, B. et al. Mesenchymal stem cells display coordinated rolling and adhesion behavior on endothelial cells. *Blood.* 2006, **108**(12), pp.3938-44.
86. Ries, C. et al. MMP-2, MT1-MMP, and TIMP-2 are essential for the invasive capacity of human mesenchymal stem cells: differential regulation by inflammatory cytokines. *Blood.* 2007, **109**(9), pp.4055-63.
87. Barbash, I.M. et al. Systemic delivery of bone marrow-derived mesenchymal stem cells to the infarcted myocardium: feasibility, cell migration, and body distribution. *Circulation.* 2003, **108**(7), pp.863-8.
88. Lee, R.H. et al. Intravenous hMSCs improve myocardial infarction in mice because cells embolized in lung are activated to secrete the anti-inflammatory protein TSG-6. *Cell stem cell.* 2009, **5**(1), pp.54-63.
89. Sasaki, M. et al. Mesenchymal stem cells are recruited into wounded skin and contribute to wound repair by transdifferentiation into multiple skin cell type. *J Immunol.* 2008, **180**(4), pp.2581-7.
90. Li, K. et al. Not a process of simple vicariousness, the differentiation of human adipose-derived mesenchymal stem cells to renal tubular epithelial cells plays an important role in acute kidney injury repairing. *Stem Cells Dev.* 2010, **19**(8), pp.1267-75.
91. Nanes, M.S. Tumor necrosis factor-alpha: molecular and cellular mechanisms in skeletal pathology. *Gene.* 2003, **321**, pp.1-15.
92. Pereira, R.F. et al. Marrow stromal cells as a source of progenitor cells for nonhematopoietic tissues in transgenic mice with a phenotype of osteogenesis imperfecta. *Proc Natl Acad Sci U S A.* 1998, **95**(3), pp.1142-7.
93. Crisostomo, P.R. et al. Human mesenchymal stem cells stimulated by TNF-alpha, LPS, or hypoxia produce growth factors by an NF kappa B- but not JNK-dependent mechanism. *Am J Physiol Cell Physiol.* 2008, **294**(3), pp.C675-82.
94. Xu, G. et al. The role of IL-6 in inhibition of lymphocyte apoptosis by mesenchymal stem cells. *Biochemical and biophysical research communications.* 2007, **361**(3), pp.745-750.
95. Grote, K. et al. Toll-like receptor 2/6-dependent stimulation of mesenchymal stem cells promotes angiogenesis by paracrine factors. *Eur Cell Mater.* 2013, **26**, pp.66-79; discussion 79.
96. Park, J.H. et al. Human umbilical cord blood-derived mesenchymal stem cells prevent diabetic renal injury through paracrine action. *Diabetes Research and Clinical Practice.* 2012, **98**(3), pp.465-473.
97. Lee, M.J. et al. Proteomic analysis of tumor necrosis factor-alpha-induced secretome of human adipose tissue-derived mesenchymal stem cells. *J Proteome Res.* 2010, **9**(4), pp.1754-62.
98. Galderisi, U. and Giordano, A. The gap between the physiological and therapeutic roles of mesenchymal stem cells. *Med Res Rev.* 2014, **34**(5), pp.1100-26.

99. Liechty, K.W. et al. Human mesenchymal stem cells engraft and demonstrate site-specific differentiation after in utero transplantation in sheep. *Nat Med.* 2000, **6**(11), pp.1282-6.
100. Han, Z. et al. The role of immunosuppression of mesenchymal stem cells in tissue repair and tumor growth. *Cell & bioscience.* 2012, **2**(1), pp.8-8.
101. Uccelli, A. et al. Mesenchymal stem cells in health and disease. *Nature Reviews Immunology.* 2008, **8**, p.726.
102. Maccario, R. et al. Interaction of human mesenchymal stem cells with cells involved in alloantigen-specific immune response favors the differentiation of CD4+ T-cell subsets expressing a regulatory/suppressive phenotype. *Haematologica.* 2005, **90**(4), pp.516-25.
103. Bernardo, Maria E. and Fibbe, Willem E. Mesenchymal Stromal Cells: Sensors and Switchers of Inflammation. *Cell Stem Cell.* 2013, **13**(4), pp.392-402.
104. Olsen, T.R. et al. Peak MSC—Are We There Yet? *Frontiers in Medicine.* 2018, **5**(178).
105. Galipeau, J. and Sensebe, L. Mesenchymal Stromal Cells: Clinical Challenges and Therapeutic Opportunities. *Cell Stem Cell.* 2018, **22**(6), pp.824-833.
106. Coelho, M.B. et al. Intraoperative stem cell therapy. *Annu Rev Biomed Eng.* 2012, **14**, pp.325-49.
107. Kern, S. et al. Comparative analysis of mesenchymal stem cells from bone marrow, umbilical cord blood, or adipose tissue. *Stem Cells.* 2006, **24**(5), pp.1294-301.
108. Perry, B.C. et al. Collection, cryopreservation, and characterization of human dental pulp-derived mesenchymal stem cells for banking and clinical use. *Tissue Eng Part C Methods.* 2008, **14**(2), pp.149-56.
109. Usas, A. and Huard, J. Muscle-derived stem cells for tissue engineering and regenerative therapy. *Biomaterials.* 2007, **28**(36), pp.5401-6.
110. De Coppi, P. et al. Isolation of amniotic stem cell lines with potential for therapy. *Nat Biotechnol.* 2007, **25**(1), pp.100-6.
111. Zhang, J. et al. The challenges and promises of allogeneic mesenchymal stem cells for use as a cell-based therapy. *Stem cell research & therapy.* 2015, **6**, pp.234-234.
112. Eliopoulos, N. et al. Allogeneic marrow stromal cells are immune rejected by MHC class I- and class II-mismatched recipient mice. *Blood.* 2005, **106**(13), pp.4057-65.
113. Sbano, P. et al. Use of donor bone marrow mesenchymal stem cells for treatment of skin allograft rejection in a preclinical rat model. *Arch Dermatol Res.* 2008, **300**(3), pp.115-24.
114. Berglund, A.K. et al. Immunoprivileged no more: measuring the immunogenicity of allogeneic adult mesenchymal stem cells. *Stem cell research & therapy.* 2017, **8**(1), pp.288-288.
115. *Good manufacturing practice and good distribution practice.* [Online]. 2019. [Accessed 20.08.19].
116. Zhu, B. and Murthy, S.K. Stem Cell Separation Technologies. *Curr Opin Chem Eng.* 2013, **2**(1), pp.3-7.
117. Lennon, D.P. and Caplan, A.I. Isolation of human marrow-derived mesenchymal stem cells. *Experimental Hematology.* 2006, **34**(11), pp.1604-1605.

118. Gothard, D. et al. In search of the skeletal stem cell: isolation and separation strategies at the macro/micro scale for skeletal regeneration. *Lab on a Chip.* 2011, **11**(7), pp.1206-1220.
119. Apel, A. et al. Suitability of human mesenchymal stem cells for gene therapy depends on the expansion medium. *Experimental Cell Research.* 2009, **315**(3), pp.498-507.
120. Posel, C. et al. Density gradient centrifugation compromises bone marrow mononuclear cell yield. *PLoS One.* 2012, **7**(12), p.e50293.
121. Gudleviciene, Z. et al. Quick and effective method of bone marrow mesenchymal stem cell extraction. *Open medicine (Warsaw, Poland).* [Online]. 2015, **10**(1), pp.44-49. [Accessed 2015]. Available from: http://europepmc.org/abstract/MED/28352676

http://europepmc.org/articles/PMC5152963?pdf=render

http://europepmc.org/articles/PMC5152963

https://doi.org/10.1515/med-2015-0008
122. Hermann, P.C. et al. Concentration of bone marrow total nucleated cells by a point-of-care device provides a high yield and preserves their functional activity. *Cell Transplant.* 2008, **16**(10), pp.1059-69.
123. Hegde, V. et al. A prospective comparison of 3 approved systems for autologous bone marrow concentration demonstrated nonequivalency in progenitor cell number and concentration. *J Orthop Trauma.* 2014, **28**(10), pp.591-8.
124. Assmus, B. et al. Red blood cell contamination of the final cell product impairs the efficacy of autologous bone marrow mononuclear cell therapy. *J Am Coll Cardiol.* 2010, **55**(13), pp.1385-94.
125. Mouquet, F. et al. The presence of apoptotic bone marrow cells impairs the efficacy of cardiac cell therapy. *Cell Transplant.* 2011, **20**(7), pp.1087-97.
126. van Beem, R.T. et al. Recovery and functional activity of mononuclear bone marrow and peripheral blood cells after different cell isolation protocols used in clinical trials for cell therapy after acute myocardial infarction. *EuroIntervention.* 2008, **4**(1), pp.133-8.
127. Brown, M. and Wittwer, C. Flow cytometry: principles and clinical applications in hematology. *Clin Chem.* 2000, **46**(8 Pt 2), pp.1221-9.
128. Thiel, A. et al. Immunomagnetic cell sorting—pushing the limits. *Immunotechnology.* 1998, **4**(2), pp.89-96.
129. Grützkau, A. and Radbruch, A. Small but mighty: How the MACS®-technology based on nanosized superparamagnetic particles has helped to analyze the immune system within the last 20 years. *Cytometry Part A.* 2010, **77A**(7), pp.643-647.
130. Andrade, P.Z. et al. Initial CD34+ cell-enrichment of cord blood determines hematopoietic stem/progenitor cell yield upon Ex vivo expansion. *Journal of Cellular Biochemistry.* 2011, **112**(7), pp.1822-1831.
131. Biotec, M. *Regulatory notes.* [Online]. [Accessed]. Available from: https://www.miltenyibiotec.com/GB-en/regulatory-notes.html
132. Biotec, M. *Clinical-scale isolation of mesenchymal stromal cells from bone marrow according to their CD271 expression.* 2012. [Accessed 21.08.19].
133. Wang, X. et al. Enhanced cell sorting and manipulation with combined optical tweezer and microfluidic chip technologies. *Lab Chip.* 2011, **11**(21), pp.3656-62.

134. Adams, J.D. et al. Multitarget magnetic activated cell sorter. *Proceedings of the National Academy of Sciences of the United States of America.* 2008, **105**(47), pp.18165-18170.
135. Srisa-Art, M. et al. Identification of rare progenitor cells from human periosteal tissue using droplet microfluidics. *Analyst.* 2009, **134**(11), pp.2239-2245.
136. Baret, J.-C. et al. Fluorescence-activated droplet sorting (FADS): efficient microfluidic cell sorting based on enzymatic activity. *Lab on a Chip.* 2009, **9**(13), pp.1850-1858.
137. Pethig, R. et al. Dielectrophoresis: A Review of Applications for Stem Cell Research. *Journal of Biomedicine and Biotechnology.* 2010, **2010**.
138. Abd Rahman, N. et al. Dielectrophoresis for Biomedical Sciences Applications: A Review. *Sensors (Basel, Switzerland).* 2017, **17**(3), p.449.
139. Yoshioka, J. et al. Label-Free Rapid Separation and Enrichment of Bone Marrow-Derived Mesenchymal Stem Cells from a Heterogeneous Cell Mixture Using a Dielectrophoresis Device. *Sensors (Basel, Switzerland).* 2018, **18**(9).
140. Flanagan, L.A. et al. Unique dielectric properties distinguish stem cells and their differentiated progeny. *Stem Cells.* 2008, **26**(3), pp.656-65.
141. Song, H. et al. Continuous-flow sorting of stem cells and differentiation products based on dielectrophoresis. *Lab on a Chip.* 2015, **15**(5), pp.1320-1328.
142. González-González, M. et al. Current strategies and challenges for the purification of stem cells. *Journal of Chemical Technology & Biotechnology.* 2012, **87**(1), pp.2-10.
143. Reschiglian, P. et al. Field-flow fractionation and biotechnology. *Trends Biotechnol.* 2005, **23**(9), pp.475-83.
144. Roda, B. et al. A novel stem cell tag-less sorting method. *Stem Cell Rev.* 2009, **5**(4), pp.420-7.
145. Vykoukal, J. et al. Enrichment of putative stem cells from adipose tissue using dielectrophoretic field-flow fractionation. *Lab Chip.* 2008, **8**(8), pp.1386-93.
146. Roda, B. et al. Field-flow fractionation in bioanalysis: A review of recent trends. *Analytica Chimica Acta.* 2009, **635**(2), pp.132-143.
147. Lee, L.M. Label-free mesenchymal stem cell enrichment from bone marrow samples by inertial microfluidics. *Analytical methods.* 2018, **v. 10**(no. 7), pp.pp. 713-721-2018 v.10 no.7.
148. Wu, H.W. et al. A microfluidic device for separation of amniotic fluid mesenchymal stem cells utilizing louver-array structures. *Biomed Microdevices.* 2009, **11**(6), pp.1297-307.
149. Jung, H. et al. Sorting of human mesenchymal stem cells by applying optimally designed microfluidic chip filtration. *Analyst.* 2015, **140**(4), pp.1265-74.
150. Gossett, D.R. et al. Label-free cell separation and sorting in microfluidic systems. *Analytical and bioanalytical chemistry.* 2010, **397**(8), pp.3249-3267.
151. Nery, A.A. et al. Recognition of biomarkers and cell-specific molecular signatures: aptamers as capture agents. *J Sep Sci.* 2009, **32**(10), pp.1523-30.
152. Ng, E.W. et al. Pegaptanib, a targeted anti-VEGF aptamer for ocular vascular disease. *Nat Rev Drug Discov.* 2006, **5**(2), pp.123-32.

153. Guo, K.T. et al. A new technique for the isolation and surface immobilization of mesenchymal stem cells from whole bone marrow using high-specific DNA aptamers. *Stem Cells.* 2006, **24**(10), pp.2220-31.
154. Hou, Z. et al. Characterization and target identification of a DNA aptamer that labels pluripotent stem cells. *Cell research.* 2015, **25**(3), pp.390-393.
155. Hu, X. et al. A Difunctional Regeneration Scaffold for Knee Repair based on Aptamer-Directed Cell Recruitment. *Advanced Materials.* 2017, **29**(15), p.1605235.
156. Tiede, C. et al. Adhiron: a stable and versatile peptide display scaffold for molecular recognition applications. *Protein Engineering Design and Selection.* 2014, **27**(5), pp.145-155.
157. Reverdatto, S. et al. Peptide aptamers: development and applications. *Current topics in medicinal chemistry.* 2015, **15**(12), pp.1082-1101.
158. Tiede, C. et al. Affimers proteins are versatile and renewable affinity reagents. *Elife.* 2017, **6**.
159. Sharma, R. et al. Label-free electrochemical impedance biosensor to detect human interleukin-8 in serum with sub-pg/ml sensitivity. *Biosens Bioelectron.* 2016, **80**, pp.607-613.
160. KGaA, M. *Antibody Basics.* [Online]. 2019. [Accessed 09.11.19].
161. Caplan, A.I. Mesenchymal stem cells. *J Orthop Res.* 1991, **9**(5), pp.641-50.
162. Caplan, A.I. Mesenchymal Stem Cells: Time to Change the Name! *Stem Cells Transl Med.* 2017, **6**(6), pp.1445-1451.
163. Sipp, D. et al. Clear up this stem-cell mess. *Nature.* 2018, **561**(7724), pp.455-457.
164. Dominici, M. et al. Minimal criteria for defining multipotent mesenchymal stromal cells. The International Society for Cellular Therapy position statement. *Cytotherapy.* 2006, **8**(4), pp.315-7.
165. Horwitz, E.M. et al. Clarification of the nomenclature for MSC: The International Society for Cellular Therapy position statement. *Cytotherapy.* 2005, **7**(5), pp.393-5.
166. Le Blanc, K. and Davies, L.C. MSCs—cells with many sides. *Cytotherapy.* 2018, **20**(3), pp.273-278.
167. Lv, F.-J. et al. Concise Review: The Surface Markers and Identity of Human Mesenchymal Stem Cells. *STEM CELLS.* 2014, **32**(6), pp.1408-1419.
168. Simmons, P.J. and Torok-Storb, B. Identification of stromal cell precursors in human bone marrow by a novel monoclonal antibody, STRO-1. *Blood.* 1991, **78**(1), pp.55-62.
169. Psaltis, P.J. et al. Enrichment for STRO-1 expression enhances the cardiovascular paracrine activity of human bone marrow-derived mesenchymal cell populations. *J Cell Physiol.* 2010, **223**(2), pp.530-40.
170. Gronthos, S. et al. Molecular and cellular characterisation of highly purified stromal stem cells derived from human bone marrow. *J Cell Sci.* 2003, **116**(Pt 9), pp.1827-35.
171. Martens, T.P. et al. Mesenchymal lineage precursor cells induce vascular network formation in ischemic myocardium. *Nat Clin Pract Cardiovasc Med.* 2006, **3 Suppl 1**, pp.S18-22.
172. Kolf, C.M. et al. Mesenchymal stromal cells. Biology of adult mesenchymal stem cells: regulation of niche, self-renewal and differentiation. *Arthritis research & therapy.* 2007, **9**(1), pp.204-204.

173. Lin, G. et al. Tissue distribution of mesenchymal stem cell marker Stro-1. *Stem cells and development.* 2011, **20**(10), pp.1747-1752.
174. Fitter, S. et al. The Mesenchymal Precursor Cell Marker Antibody STRO-1 Binds to Cell Surface Heat Shock Cognate 70. *Stem Cells.* 2017, **35**(4), pp.940-951.
175. Ning, H. et al. Mesenchymal stem cell marker Stro-1 is a 75 kd endothelial antigen. *Biochemical and biophysical research communications.* 2011, **413**(2), pp.353-357.
176. Lee, R.H. et al. The CD34-like protein PODXL and alpha6-integrin (CD49f) identify early progenitor MSCs with increased clonogenicity and migration to infarcted heart in mice. *Blood.* 2009, **113**(4), pp.816-826.
177. Gronthos, S. et al. Surface protein characterization of human adipose tissue-derived stromal cells. *J Cell Physiol.* 2001, **189**(1), pp.54-63.
178. Sarugaser, R. et al. Human Umbilical Cord Perivascular (HUCPV) Cells: A Source of Mesenchymal Progenitors. *STEM CELLS.* 2005, **23**(2), pp.220-229.
179. Quirici, N. et al. Isolation of bone marrow mesenchymal stem cells by anti-nerve growth factor receptor antibodies. *Experimental Hematology.* 2002, **30**(7), pp.783-791.
180. Cuthbert, R. et al. Single-platform quality control assay to quantify multipotential stromal cells in bone marrow aspirates prior to bulk manufacture or direct therapeutic use. *Cytotherapy.* 2012, **14**(4), pp.431-440.
181. El-Jawhari, J.J. et al. The CD45lowCD271high Cell Prevalence in Bone Marrow Samples May Provide a Useful Measurement of the Bone Marrow Quality for Cartilage and Bone Regenerative Therapy. *J Bone Joint Surg Am.* 2017, **99**(15), pp.1305-1313.
182. Ganguly, P. et al. The Analysis of In Vivo Aging in Human Bone Marrow Mesenchymal Stromal Cells Using Colony-Forming Unit-Fibroblast Assay and the CD45lowCD271+ Phenotype. *Stem Cells International.* 2019, **2019**, p.14.
183. Jones, E. et al. Large-scale extraction and characterization of CD271+ multipotential stromal cells from trabecular bone in health and osteoarthritis: implications for bone regeneration strategies based on uncultured or minimally cultured multipotential stromal cells. *Arthritis Rheum.* 2010, **62**(7), pp.1944-54.
184. Jones, E.A. et al. Optimization of a flow cytometry-based protocol for detection and phenotypic characterization of multipotent mesenchymal stromal cells from human bone marrow. *Cytometry B Clin Cytom.* 2006, **70**(6), pp.391-9.
185. Jones, E.A. et al. Isolation and characterization of bone marrow multipotential mesenchymal progenitor cells. *Arthritis Rheum.* 2002, **46**(12), pp.3349-60.
186. Jones, E. and McGonagle, D. Human bone marrow mesenchymal stem cells in vivo. *Rheumatology (Oxford).* 2008, **47**(2), pp.126-31.
187. Kuçi, S. et al. CD271 antigen defines a subset of multipotent stromal cells with immunosuppressive and lymphohematopoietic engraftment-promoting properties. *Haematologica.* 2010, **95**(4), pp.651-659.
188. Hermida-Gomez, T. et al. Bone marrow cells immunomagnetically selected for CD271+ antigen promote in vitro the repair of articular cartilage defects. *Tissue Eng Part A.* 2011, **17**(7-8), pp.1169-79.

189. Flores-Torales, E. et al. The CD271 expression could be alone for establisher phenotypic marker in Bone Marrow derived mesenchymal stem cells. *Folia Histochem Cytobiol.* 2010, **48**(4), pp.682-6.
190. Biotec, M. *Mesenchymal stem cells (MSCs) for cell therapy.* [Online]. [Accessed].
191. Cuevas-Diaz Duran, R. et al. Age-related yield of adipose-derived stem cells bearing the low-affinity nerve growth factor receptor. *Stem Cells Int.* 2013, **2013**, p.372164.
192. Zeddou, M. et al. The umbilical cord matrix is a better source of mesenchymal stem cells (MSC) than the umbilical cord blood. *Cell Biology International.* 2010, **34**(7), pp.693-701.
193. Tormin, A. et al. CD146 expression on primary nonhematopoietic bone marrow stem cells is correlated with in situ localization. *Blood.* 2011, **117**(19), pp.5067-77.
194. Russell, K.C. et al. In vitro high-capacity assay to quantify the clonal heterogeneity in trilineage potential of mesenchymal stem cells reveals a complex hierarchy of lineage commitment. *Stem Cells.* 2010, **28**(4), pp.788-98.
195. Sacchetti, B. et al. Self-Renewing Osteoprogenitors in Bone Marrow Sinusoids Can Organize a Hematopoietic Microenvironment. *Cell.* 2007, **131**(2), pp.324-336.
196. Maijenburg, M.W. et al. The composition of the mesenchymal stromal cell compartment in human bone marrow changes during development and aging. *Haematologica.* 2012, **97**(2), pp.179-83.
197. Gang, E.J. et al. SSEA-4 identifies mesenchymal stem cells from bone marrow. *Blood.* 2007, **109**(4), pp.1743-51.
198. The Mesenchymal Stem Cell Antigen MSCA-1 is Identical to Tissue Non-specific Alkaline Phosphatase. 2010, **19**(5), pp.669-677.
199. Yu, K.-R. et al. CD49f Enhances Multipotency and Maintains Stemness Through the Direct Regulation of OCT4 and SOX2. 2012, **30**(5), pp.876-887.
200. Kuroda, Y. et al. Unique multipotent cells in adult human mesenchymal cell populations. *Proceedings of the National Academy of Sciences of the United States of America.* 2010, **107**(19), pp.8639-8643.
201. Delorme, B. et al. Specific plasma membrane protein phenotype of culture-amplified and native human bone marrow mesenchymal stem cells. *Blood.* 2008, **111**(5), pp.2631-5.
202. Martinez, C. et al. Human bone marrow mesenchymal stromal cells express the neural ganglioside GD2: a novel surface marker for the identification of MSCs. *Blood.* 2007, **109**(10), pp.4245-4248.
203. Khan, W.S. et al. Bone marrow-derived mesenchymal stem cells express the pericyte marker 3G5 in culture and show enhanced chondrogenesis in hypoxic conditions. *J Orthop Res.* 2010, **28**(6), pp.834-40.
204. Shi, S. and Gronthos, S. Perivascular niche of postnatal mesenchymal stem cells in human bone marrow and dental pulp. *J Bone Miner Res.* 2003, **18**(4), pp.696-704.
205. Sivasubramaniyan, K. et al. Prospective Isolation of Mesenchymal Stem Cells from Human Bone Marrow Using Novel Antibodies Directed Against Sushi Domain Containing 2. *Stem Cells and Development.* 2013, **22**(13), pp.1944-1954.

206. Battula, V.L. et al. Isolation of functionally distinct mesenchymal stem cell subsets using antibodies against CD56, CD271, and mesenchymal stem cell antigen-1. *Haematologica.* 2009, **94**(2), pp.173-184.
207. Sobiesiak, M. et al. The mesenchymal stem cell antigen MSCA-1 is identical to tissue non-specific alkaline phosphatase. *Stem Cells Dev.* 2010, **19**(5), pp.669-77.
208. Estève, D. et al. Multiple Functions of MSCA-1/TNAP in Adult Mesenchymal Progenitor/Stromal Cells. *Stem cells international.* 2016, **2016**, pp.1815982-1815982.
209. Suila, H. et al. Are globoseries glycosphingolipids SSEA-3 and -4 markers for stem cells derived from human umbilical cord blood? *J Mol Cell Biol.* 2011, **3**(2), pp.99-107.
210. Scientific, T. *Introduction to Cell Culture.* [Online]. [Accessed 17.05.19]. Available from: https://www.thermofisher.com/uk/en/home/references/gibco-cell-culture-basics/introduction-to-cell-culture.html
211. Xiong, Z.Y.a.H.-R. *Culture Conditions and Types of Growth Media for Mammalian Cells.* 2011.
212. Tang, Y. et al. Surface Plasmon Resonance: An Introduction to a Surface Spectroscopy Technique. *J Chem Educ.* 2010, **87**(7), pp.742-746.
213. Vericat, C. et al. Self-assembled monolayers of thiols and dithiols on gold: new challenges for a well-known system. *Chem Soc Rev.* 2010, **39**(5), pp.1805-34.
214. Cerruti, M. et al. Poly(ethylene glycol) monolayer formation and stability on gold and silicon nitride substrates. *Langmuir.* 2008, **24**(19), pp.10646-53.
215. Scientific, T. *Crosslinking Technical Handbook.* 2012.
216. BioLabs, N.E. *Phage Display.* [Online]. 2019. [Accessed].
217. Bazan, J. et al. Phage display--a powerful technique for immunotherapy: 1. Introduction and potential of therapeutic applications. *Hum Vaccin Immunother.* 2012, **8**(12), pp.1817-28.
218. Scientific, T. *Overview of ELISA.* [Online]. [Accessed 23.04.19]. Available from: https://www.thermofisher.com/uk/en/home/life-science/protein-biology/protein-biology-learning-center/protein-biology-resource-library/pierce-protein-methods/overview-elisa.html
219. Scientific, T. *Avidin-Biotin Interaction.* [Online]. [Accessed 23.04.19]. Available from: https://www.thermofisher.com/uk/en/home/life-science/protein-biology/protein-biology-learning-center/protein-biology-resource-library/pierce-protein-methods/avidin-biotin-interaction.html
220. Academy, K. *DNA sequencing.* [Online]. 2019. [Accessed 23.04.19]. Available from: https://www.khanacademy.org/science/high-school-biology/hs-molecular-genetics/hs-biotechnology/a/dna-sequencing
221. Structural Genomics, C. et al. Protein production and purification. *Nature methods.* 2008, **5**(2), pp.135-146.
222. Information, N.C.f.B. *Polymerase Chain Reaction (PCR).* [Online]. [Accessed 23.04.19]. Available from: https://www.ncbi.nlm.nih.gov/probe/docs/techpcr/
223. Campus, W.G. *What is PCR (polymerase chain reaction)?* [Online]. [Accessed 23.04.19]. Available from: https://www.yourgenome.org/facts/what-is-pcr-polymerase-chain-reaction
224. Struhl, K. Gene regulation. A paradigm for precision. *Science.* 2001, **293**(5532), pp.1054-5.

225. education, N. *Gel electrophoresis.* [Online]. [Accessed 23.04.19]. Available from: https://www.nature.com/scitable/definition/gel-electrophoresis-286
226. Leeds, U.o. *Ion Mobility Spectrometry-Mass Spectrometry.* [Online]. 2019. [Accessed 17.05.19]. Available from: https://biologicalsciences.leeds.ac.uk/facilities/doc/mass-spectrometry/page/4
227. Biotec, M. *CD271 Microbead Kit.* [Online]. 2013. [Accessed]. Available from: https://www.miltenyibiotec.com/upload/assets/IM0007186.PDF
228. abcam. *KD value: a quantitative measurement of antibody affinity.* [Online]. [Accessed].
229. Ferlemann, F.C. et al. Surface marker profiling of SH-SY5Y cells enables small molecule screens identifying BMP4 as a modulator of neuroblastoma differentiation. *Scientific reports.* 2017, **7**(1), pp.13612-13612.
230. Alfaleh, M.A. et al. Strategies for Selecting Membrane Protein-Specific Antibodies using Phage Display with Cell-Based Panning. *Antibodies.* 2017, **6**(10).
231. Jones, M.L. et al. Targeting membrane proteins for antibody discovery using phage display. *Scientific reports.* 2016, **6**, pp.26240-26240.
232. Carpenter, E.P. et al. Overcoming the challenges of membrane protein crystallography. *Current opinion in structural biology.* 2008, **18**(5), pp.581-586.
233. Crepin, R. et al. Whole-cell biopanning with a synthetic phage display library of nanobodies enabled the recovery of follicle-stimulating hormone receptor inhibitors. *Biochem Biophys Res Commun.* 2017, **493**(4), pp.1567-1572.
234. Wang, J. et al. Selection of phage-displayed peptides on live adherent cells in microfluidic channels. *Proc Natl Acad Sci U S A.* 2011, **108**(17), pp.6909-14.
235. Sorensen, M.D. et al. Microselection--affinity selecting antibodies against a single rare cell in a heterogeneous population. *J Cell Mol Med.* 2010, **14**(7), pp.1953-61.
236. Pavoni, E. et al. Optimized selection of anti-tumor recombinant antibodies from phage libraries on intact cells. *Mol Immunol.* 2014, **57**(2), pp.317-22.
237. Gerstenbruch, S. et al. Analysis of cross-reactive and specific anti-carbohydrate antibodies against lipopolysaccharide from Chlamydophila psittaci. *Glycobiology.* 2009, **20**(4), pp.461-472.
238. Eisenhardt, S.U. et al. Subtractive single-chain antibody (scFv) phage-display: tailoring phage-display for high specificity against function-specific conformations of cell membrane molecules. *Nat Protoc.* 2007, **2**(12), pp.3063-73.
239. Giordano, R.J. et al. Biopanning and rapid analysis of selective interactive ligands. *Nat Med.* 2001, **7**(11), pp.1249-53.
240. Hoogenboom, H.R. et al. Selection-dominant and nonaccessible epitopes on cell-surface receptors revealed by cell-panning with a large phage antibody library. *Eur J Biochem.* 1999, **260**(3), pp.774-84.
241. Pruitt, K.D. et al. NCBI Reference Sequences: current status, policy and new initiatives. *Nucleic acids research.* 2009, **37**(Database issue), pp.D32-D36.

242. Ducret, M. et al. Immunophenotyping Reveals the Diversity of Human Dental Pulp Mesenchymal Stromal Cells In vivo and Their Evolution upon In vitro Amplification. *Frontiers in physiology.* 2016, **7**, pp.512-512.
243. Tomlinson, M.J. et al. Negative Human Dental Pulp Cells Yield Significantly More Adherent Colony Forming Cells than the Positive Phenotype

International Journal of Stem Cell Research & Therapy. 2016, **3**(1).
244. Pan, W. et al. Characterization of p75 neurotrophin receptor expression in human dental pulp stem cells. *Int J Dev Neurosci.* 2016, **53**, pp.90-98.
245. Alvarez, R. et al. Single CD271 marker isolates mesenchymal stem cells from human dental pulp. *Int J Oral Sci.* 2015, **7**(4), pp.205-12.
246. Houssin, G.V.C.a.T. *INTRODUCTION ABOUT PDMS SOFT-LITHOGRAPHY AND POLYMER MOLDING FOR MICROFLUIDICS.* [Online]. 2019. [Accessed].
247. Whitesides, G.M. and Stroock, A.D. Flexible methods for microfluidics. *Phys. Today.* 2001, **54**(6), pp.42-48.
248. Friend, J. and Yeo, L. Fabrication of microfluidic devices using polydimethylsiloxane. *Biomicrofluidics.* 2010, **4**(2), p.026502.
249. Ogura, T. et al. Whole cell-based surface plasmon resonance measurement to assess binding of anti-TNF agents to transmembrane target. *Analytical Biochemistry.* 2016, **508**, pp.73-77.
250. Mizuguchi, T. et al. Intact-cell-based surface plasmon resonance measurements for ligand affinity evaluation of a membrane receptor. *Analytical Biochemistry.* 2012, **420**(2), pp.185-187.
251. Technologies, R. *Streptavidin/NeutrAvidin Coupling to mSAM or Dextran Surface.* [Online]. [Accessed].
252. Wirtz, R. et al. High-sensitivity colorimetric detection of DNA hybridization on a gold surface with high spatial resolution. *Nanotechnology.* 2002, **14**(1), pp.7-10.
253. Qasaimeh, M.A. et al. Isolation of Circulating Plasma Cells in Multiple Myeloma Using CD138 Antibody-Based Capture in a Microfluidic Device. *Scientific Reports.* 2017, **7**, p.45681.
254. Piedimonte, G. et al. Effect of cell density on growth rate and amino acid transport in simian virus 40-transformed 3T3 cells. *Cancer Res.* 1982, **42**(11), pp.4690-3.
255. *Regulatory Considerations for Human Cells, Tissues, and Cellular and Tissue-Based Products: Minimal Manipulation and Homologous Use 2017*. https://www.fda.gov/regulatory-information/search-fda-guidance-documents/regulatory-considerations-human-cells-tissues-and-cellular-and-tissue-based-products-minimal:
256. Plouffe, B.D. et al. Fundamentals and application of magnetic particles in cell isolation and enrichment: a review. *Rep Prog Phys.* 2015, **78**(1), p.016601.
257. Mahmoudi, M. et al. Effect of Nanoparticles on the Cell Life Cycle. *Chemical Reviews.* 2011, **111**(5), pp.3407-3432.
258. Farrell, E. et al. Effects of iron oxide incorporation for long term cell tracking on MSC differentiation in vitro and in vivo. *Biochem Biophys Res Commun.* 2008, **369**(4), pp.1076-81.
259. Kostura, L. et al. Feridex labeling of mesenchymal stem cells inhibits chondrogenesis but not adipogenesis or osteogenesis. *NMR Biomed.* 2004, **17**(7), pp.513-7.

260. Müller, P. et al. Intramyocardial fate and effect of iron nanoparticles co-injected with MACS® purified stem cell products. *Biomaterials.* 2017, **135**, pp.74-84.
261. Bhattacharjee, J. et al. Monocytes isolated by positive and negative magnetic sorting techniques show different molecular characteristics and immunophenotypic behaviour. *F1000Res.* 2017, **6**, p.2045.
262. Beliakova-Bethell, N. et al. The effect of cell subset isolation method on gene expression in leukocytes. *Cytometry A.* 2014, **85**(1), pp.94-104.
263. Friedenstein, A.J. et al. Stromal cells responsible for transferring the microenvironment of the hemopoietic tissues. Cloning in vitro and retransplantation in vivo. *Transplantation.* 1974, **17**(4), pp.331-40.
264. Pochampally, R. Colony forming unit assays for MSCs. *Methods Mol Biol.* 2008, **449**, pp.83-91.
265. Veyrat-Masson, R. et al. Mesenchymal content of fresh bone marrow: a proposed quality control method for cell therapy. *Br J Haematol.* 2007, **139**(2), pp.312-20.
266. Hernigou, J. et al. Understanding bone safety zones during bone marrow aspiration from the iliac crest: the sector rule. *Int Orthop.* 2014, **38**(11), pp.2377-84.
267. Dumont, F. et al. Cell Size and Water Permeability as Determining Factors for Cell Viability after Freezing at Different Cooling Rates. *Applied and Environmental Microbiology.* 2004, **70**(1), pp.268-272.
268. Yang, B. et al. Cryopreservation of Bone Marrow Mononuclear Cells Alters Their Viability and Subpopulation Composition but Not Their Treatment Effects in a Rodent Stroke Model. *Stem Cells Int.* 2016, **2016**, p.5876836.
269. Xie, X.H. et al. Promotion of bone repair by implantation of cryopreserved bone marrow-derived mononuclear cells in a rabbit model of steroid-associated osteonecrosis. *Arthritis Rheum.* 2012, **64**(5), pp.1562-71.
270. Casado-Diaz, A. et al. Cryopreserved human bone marrow mononuclear cells as a source of mesenchymal stromal cells: application in osteoporosis research. *Cytotherapy.* 2008, **10**(5), pp.460-8.
271. Inc., S.T. *DNase I Treatment for Clumpy Cell Suspensions.* [Online]. 2019. [Accessed]. Available from: https://www.stemcell.com/dnase-i-treatment-for-clumpy-cell-suspensions.html
272. Millipore, E. *Sizes of various cells.* [Online]. [Accessed].
273. Plouffe, B.D. and Murthy, S.K. Perspective on microfluidic cell separation: a solved problem? *Anal Chem.* 2014, **86**(23), pp.11481-8.
274. Cheung, L.S. et al. Detachment of captured cancer cells under flow acceleration in a bio-functionalized microchannel. *Lab Chip.* 2009, **9**(12), pp.1721-31.
275. Wang, H. et al. Shear stress induces endothelial differentiation from a murine embryonic mesenchymal progenitor cell line. *Arterioscler Thromb Vasc Biol.* 2005, **25**(9), pp.1817-23.
276. Chowdhury, F. et al. Material properties of the cell dictate stress-induced spreading and differentiation in embryonic stem cells. *Nat Mater.* 2010, **9**(1), pp.82-8.
277. Shi, D. et al. Proliferation and multi-differentiation potentials of human mesenchymal stem cells on thermoresponsive PDMS surfaces grafted with PNIPAAm. *Biosci Rep.* 2009, **30**(3), pp.149-58.

278. Higuchi, A. et al. Photon-Modulated Changes of Cell Attachments on Poly(spiropyran-co-methyl methacrylate) Membranes. *Biomacromolecules.* 2004, **5**(5), pp.1770-1774.
279. Guillaume-Gentil, O. et al. Electrochemically switchable platform for the micro-patterning and release of heterotypic cell sheets. *Biomed Microdevices.* 2011, **13**(1), pp.221-30.
280. Zhu, J. et al. Specific capture and temperature-mediated release of cells in an aptamer-based microfluidic device. *Lab Chip.* 2012, **12**(18), pp.3504-13.
281. Mifune, Y. et al. Therapeutic superiority for cartilage repair by CD271-positive marrow stromal cell transplantation. *Cell Transplant.* 2013, **22**(7), pp.1201-11.
282. Cheng, S.-B. et al. Current techniques and future advance of microfluidic devices for circulating tumor cells. *TrAC Trends in Analytical Chemistry.* 2019, **117**, pp.116-127.
283. Nagrath, S. et al. Isolation of rare circulating tumour cells in cancer patients by microchip technology. *Nature.* 2007, **450**(7173), pp.1235-9.
284. Gleghorn, J.P. et al. Capture of circulating tumor cells from whole blood of prostate cancer patients using geometrically enhanced differential immunocapture (GEDI) and a prostate-specific antibody. *Lab Chip.* 2010, **10**(1), pp.27-9.
285. Sheng, W. et al. Aptamer-enabled efficient isolation of cancer cells from whole blood using a microfluidic device. *Anal Chem.* 2012, **84**(9), pp.4199-206.
286. Stott, S.L. et al. Isolation of circulating tumor cells using a microvortex-generating herringbone-chip. *Proc Natl Acad Sci U S A.* 2010, **107**(43), pp.18392-7.
287. Sheng, W. et al. Capture, release and culture of circulating tumor cells from pancreatic cancer patients using an enhanced mixing chip. *Lab Chip.* 2014, **14**(1), pp.89-98.
288. Cheng, S.-B. et al. High-Efficiency Capture of Individual and Cluster of Circulating Tumor Cells by a Microchip Embedded with Three-Dimensional Poly(dimethylsiloxane) Scaffold. *Analytical Chemistry.* 2016, **88**(13), pp.6773-6780.
289. Camilleri, E.T. et al. Identification and validation of multiple cell surface markers of clinical-grade adipose-derived mesenchymal stromal cells as novel release criteria for good manufacturing practice-compliant production. *Stem Cell Res Ther.* 2016, **7**(1), p.107.
290. Busser, H. et al. Isolation and Characterization of Human Mesenchymal Stromal Cell Subpopulations: Comparison of Bone Marrow and Adipose Tissue. *Stem Cells Dev.* 2015, **24**(18), pp.2142-57.
291. Barilani, M. et al. Low-affinity Nerve Growth Factor Receptor (CD271) Heterogeneous Expression in Adult and Fetal Mesenchymal Stromal Cells. *Scientific Reports.* 2018, **8**(1), p.9321.
292. Hunt, C.J. Technical Considerations in the Freezing, Low-Temperature Storage and Thawing of Stem Cells for Cellular Therapies. *Transfusion Medicine and Hemotherapy.* 2019, **46**(3), pp.134-150.
293. Smith, A.J. et al. Rapid cell separation with minimal manipulation for autologous cell therapies. *Scientific Reports.* 2017, **7**, p.41872.

Appendix A: KingFisher Flex Protocol "Phage_Display_Competition"

Protocol Step	Plate	Volume (µL)	Settings
Tipcomb	96 deep well tip comb		
Pick-Up: Tipcomb	KingFisher 96 KF plate		
Collect Beads	Plate: Binding Microtiter deep well 96 plate		Collect count 1 Collect time (s) 1
Binding	Plate: Binding Microtiter deep well 96 plate	300	Beginning of Step Release beads [hh:mm:ss]: 00:00:00 Mixing/Heating Parameters Mix time [hh:mm:ss]: 00:00:10 Speed: fast Mix time [hh:mm:ss]: 01:00:00 Speed: slow End of step Collect beads, count: 5 Collect time (s): 30
Wash 1	Plate: Wash 1 Microtiter deep well 96 plate	950	Beginning of Step Release beads [hh:mm:ss]: 00:00:00 Mixing/Heating Parameters Mix time [hh:mm:ss]: 00:01:00 Speed: slow

			End of step **Collect beads, count: 5** **Collect time (s): 30**
Wash 2	**Plate: Wash 2** **Microtiter deep well 96 plate**	**950**	**Beginning of Step** **Release beads [hh:mm:ss]: 00:00:00** **Mixing/Heating Parameters** **Mix time [hh:mm:ss]: 00:01:00** **Speed: slow** **End of step** **Collect beads, count: 5** **Collect time (s): 30**
Wash 3	**Plate: Wash 3** **Microtiter deep well 96 plate**	**950**	**Beginning of Step** **Release beads [hh:mm:ss]: 00:00:00** **Mixing/Heating Parameters** **Mix time [hh:mm:ss]: 00:01:00** **Speed: slow** **End of step** **Collect beads, count: 5** **Collect time (s): 30**
Wash 4	**Plate: Wash 4** **Microtiter deep well 96 plate**	**950**	**Beginning of Step** **Release beads [hh:mm:ss]: 00:00:00** **Mixing/Heating Parameters** **Mix time [hh:mm:ss]: 00:01:00** **Speed: slow** **End of step**

			Collect beads, count: 5 **Collect time (s): 30**
Particle Release	**Plate: pH elution** **KingFisher 96 KF plate**	**100**	**Beginning of Step** **Release beads [hh:mm:ss]: 00:00:10** **Speed: Fast**
Leave: Tipcomb	**96 deep well tip comb**		

Appendix B: KingFisher Flex Protocol "Phage_Display_Wash_Elute"

Protocol Step	Plate	Volume (µL)	Settings
Tipcomb	96 deep well tip comb		
Pick-Up: Tipcomb	KingFisher 96 KF plate		
Collect Beads	Plate: Binding Microtiter deep well 96 plate		Collect count 1 Collect time (s) 1
Binding	Plate: Binding Microtiter deep well 96 plate	300	Beginning of Step Release beads [hh:mm:ss]: 00:00:00 Mixing/Heating Parameters Mix time [hh:mm:ss]: 00:00:10 Speed: fast End of step Collect beads, count: 5 Collect time (s): 30
Wash 1	Plate: Wash 1 Microtiter deep well 96 plate	950	Beginning of Step Release beads [hh:mm:ss]: 00:00:00 Mixing/Heating Parameters Mix time [hh:mm:ss]: 00:01:00 Speed: slow End of step Collect beads, count: 5 Collect time (s): 30

Wash 2	**Plate: Wash 2** **Microtiter deep well 96 plate**	**950**	**Beginning of Step** **Release beads [hh:mm:ss]: 00:00:00** **Mixing/Heating Parameters** **Mix time [hh:mm:ss]: 00:01:00** **Speed: slow** **End of step** **Collect beads, count: 5** **Collect time (s): 30**
Wash 3	**Plate: Wash 3** **Microtiter deep well 96 plate**	**950**	**Beginning of Step** **Release beads [hh:mm:ss]: 00:00:00** **Mixing/Heating Parameters** **Mix time [hh:mm:ss]: 00:01:00** **Speed: slow** **End of step** **Collect beads, count: 5** **Collect time (s): 30**
Wash 4	**Plate: Wash 4** **Microtiter deep well 96 plate**	**950**	**Beginning of Step** **Release beads [hh:mm:ss]: 00:00:00** **Mixing/Heating Parameters** **Mix time [hh:mm:ss]: 00:01:00** **Speed: slow** **End of step** **Collect beads, count: 5** **Collect time (s): 30**
pH Elution	**Plate: pH elution**	**100**	**Beginning of Step**

	KingFisher 96 KF plate		**Release beads [hh:mm:ss]: 00:00:00** **Mixing/Heating Parameters** **Mix time [hh:mm:ss]: 00:07:30** **Speed: slow** **Post mix[hh:mm:ss]: 00:00:05** **Speed: Bottom mix** **End of step** **Collect beads, count: 5** **Collect time (s): 30**
Triethylamine Elution	**Plate: Triethylamine** **KingFisher 96 KF plate**	**100**	**Beginning of Step** **Release beads [hh:mm:ss]: 00:00:00** **Mixing/Heating Parameters** **Mix time [hh:mm:ss]: 00:03:30** **Speed: slow** **Post mix[hh:mm:ss]: 00:00:05** **Speed: Bottom mix** **End of step** **Collect beads, count: 5** **Collect time (s): 30**
Leave: Tipcomb	**96 deep well tip comb**		

Appendix C: KingFisher Flex Protocol "Phage_Display_Standard"

Protocol Step	Plate	Volume (ul)	Settings
Tipcomb	96 deep well tip comb		
Pick-Up: Tipcomb	KingFisher 96 KF plate		
Collect Beads	Plate: Binding Microtiter deep well 96 plate		Collect count 1 Collect time (s) 1
Binding	Plate: Binding Microtiter deep well 96 plate	300	Beginning of Step Release beads [hh:mm:ss]: 00:00:00 Mixing/Heating Parameters Mix time [hh:mm:ss]: 00:00:10 Speed: fast Mix time [hh:mm:ss]: 01:00:00 Speed: slow End of step Collect beads, count: 5 Collect time (s): 30
Wash 1	Plate: Wash 1 Microtiter deep well 96 plate	950	Beginning of Step Release beads [hh:mm:ss]: 00:00:00 Mixing/Heating Parameters Mix time [hh:mm:ss]: 00:01:00 Speed: slow

			End of step **Collect beads, count: 5** **Collect time (s): 30**
Wash 2	**Plate: Wash 2** **Microtiter deep well 96 plate**	**950**	**Beginning of Step** **Release beads [hh:mm:ss]: 00:00:00** **Mixing/Heating Parameters** **Mix time [hh:mm:ss]: 00:01:00** **Speed: slow** **End of step** **Collect beads, count: 5** **Collect time (s): 30**
Wash 3	**Plate: Wash 3** **Microtiter deep well 96 plate**	**950**	**Beginning of Step** **Release beads [hh:mm:ss]: 00:00:00** **Mixing/Heating Parameters** **Mix time [hh:mm:ss]: 00:01:00** **Speed: slow** **End of step** **Collect beads, count: 5** **Collect time (s): 30**
Wash 4	**Plate: Wash 4** **Microtiter deep well 96 plate**	**950**	**Beginning of Step** **Release beads [hh:mm:ss]: 00:00:00** **Mixing/Heating Parameters** **Mix time [hh:mm:ss]: 00:01:00** **Speed: slow** **End of step**

			Collect beads, count: 5 **Collect time (s): 30**
pH Elution	**Plate: pH elution** **KingFisher 96 KF plate**	**100**	**Beginning of Step** **Release beads [hh:mm:ss]: 00:00:00** **Mixing/Heating Parameters** **Mix time [hh:mm:ss]: 00:07:30** **Speed: slow** **Post mix[hh:mm:ss]: 00:00:05** **Speed: Bottom mix** **End of step** **Collect beads, count: 5** **Collect time (s): 30**
Triethylamine Elution	**Plate: Triethylamine** **KingFisher 96 KF plate**	**100**	**Beginning of Step** **Release beads [hh:mm:ss]: 00:00:00** **Mixing/Heating Parameters** **Mix time [hh:mm:ss]: 00:03:30** **Speed: slow** **Post mix[hh:mm:ss]: 00:00:05** **Speed: Bottom mix** **End of step** **Collect beads, count: 5** **Collect time (s): 30**
Leave: Tipcomb	**96 deep well tip comb**		